The potential of Sentinel-2 data for detecting grassland management intensity to support monitoring of meadow bird populations

MSc. THESIS

Marijke Elisabeth Bekkema

Submitted in part fulfillment of the requirements for the degree of Master of Science in Geographical Information Systems (UNIGIS)
Faculty of Economics and Business Administration
Vrije Universiteit Amsterdam
The Netherlands

June 2017

vrije Universiteit amsterdam

Abstract

From the 1970s onwards, the population of meadow birds in the Netherlands has dramatically declined. Disappearance of meadow birds is mainly attributed to agricultural changes; especially the shift from extensively managed, herb-rich meadows to intensively managed monocultures of ryegrass causes high mortality of juvenile birds. There is a positive correlation between the occurrence of stable bird populations and presence of extensive, herb-rich grassland. Remote Sensing may contribute to mapping the distribution of extensive meadows to support monitoring of meadow bird populations. This thesis assesses the potential of open source high-resolution, multi-temporal, multi-spectral Sentinel-2A satellite data to detect differences in grassland management intensity (fertilizing, mowing, grazing) at parcel level in Friesland, the Netherlands.

A rule-based classification method was developed using the Sentinel-2 Red Edge Position (S2REP), Normalized Difference Vegetation Index (NDVI) and Mean Absolute Spectral Dynamics (MASD) for nine observation dates in 2016. Decision rules were based on thresholds determined by See5 univariate decision tree software. Monoculture grassland could reliably be differentiated from extensive grassland on both clay and peat soils. After the first mowing date, spectral response shows strong overlap. Therefore, availability of springtime imagery, preferably from the second half of April, is essential for accurate classification. Good classification results were achieved using a contextual rule-based classification approach based on the S2REP and NDVI values for April 21st in combination with knowledge on first mowing date. The S2REP was found to be the most important attribute for classification (100%) followed by NDVI (50%) whilst the MASD parameter did not contribute to the classification. The contextual rule-based classification achieved an overall accuracy of 84.3% and a KHAT of 0.65 compared to 82.5% and a KHAT of 0.59 for a statistical rule-based classification based on decision rules for four observation dates.

According to the contextual rule-based classification for Littenseradiel, Friesland, 31% of the total grassland area is classified as extensive vs. 69% as monoculture. 69% of the registered nests of Black-tailed godwit, Common redshank, Northern lapwing and Oystercatcher are found on extensive grassland vs. 20% on monoculture grassland and 11% on other/arable land.

Change in NDVI between two consecutive observation dates can be used to detect first mowing dates at parcel level. However, for accurate mowing detection, temporal resolution should be 10-15 days. For the 2016 growing season, the gaps between cloud free acquisition dates were too large. With the launch of Sentinel-2B, temporal resolution will increase to 5 days. Combining Sentinel-2 with Sentinel-1 SAR data may also improve detection of mowing.

Table of contents

Disclaimer

The results presented in this thesis are based on my own research at the Faculty of Economics and Business Administration of the Vrije Universiteit Amsterdam.
All assistance received from other individuals and organizations has been acknowledged and full reference is made to all published and unpublished sources.
This thesis has not been submitted previously for a degree at any institution.

Signed:

Marijke Bekkema
Itens, June 12th 2017

Name:	Marijke Elisabeth Bekkema
Adress:	Hearedyk 46
	8735 HS Itens
Telephone:	0515 333636
Email:	m_e_bekkema@hotmail.com
Student nr.:	2088886
Study programme:	UNIGIS MSc. in Geographical Information Science, intake January 2014
Supervisors:	Niels van Manen & Marieke Eleveld

Acknowledgements

To many people, grassland may not seem to be a very ground-breaking research subject; after all, all grass looks green to the less interested observer. But in the municipality where I live, Littenseradiel Friesland, 83% of the ground surface area consists of grassland; it determines the landscape every day and every season. Changes to this unique meadow landscape will not go unnoticed. Since the summer of 2016, grassland has become a hot topic in Friesland. In regional newspapers, discussions appear about ongoing industrialization of agriculture. Concerns are expressed about intensively managed monoculture grasslands and associated loss of biodiversity, especially meadow bird decline. Also, documentaries on grassland have been broadcasted on regional television. Introduction of the word 'landscape-ache' (*landschapspijn*), which signifies the sadness people feel about the loss of our small-scale agricultural landscape with its herb-rich meadows, insects, butterflies and birds, has led to emotional discussions between farmers and citizens. I will not deny that I am also worried about loss of biodiversity. Nevertheless, I have approached this research with an open mind. But I have found that there is reason for concern; according to my model, 69% of the grassland area in Littenseradiel currently consists of monoculture grassland. However, not all extensive grassland is lost. Now that people are becoming more aware of the importance of these remaining patches of herb-rich land, I hope that they will be protected for the future.

I would like to thank the people that helped me with this thesis. First of all, thanks to my supervisors, Niels van Manen en Marieke Eleveld. Thanks to Prof. Jan-Peter Mund for commenting on my first results. I am also grateful to Marco Hoekstra of the Bond Friese Vogelwachten who kindly provided GIS data of nesting sites for meadow birds in Littenseradiel. And thanks to Jelle de Boer and Simon de Winter of Natuurmonumenten for providing meadow bird data for Skrins and Skrok. Finally, I would like to thank my partner Fedde Bloemhof, who kept me company during many bicycle tours and walks during my field surveys.

Marijke Bekkema, Itens, June 2017.

Black-tailed Godwit in herb-rich grassland, Lionserpolder, Littenseradiel April 2017.

1.0 Introduction

1.1 Grassland management and meadow bird decline

In the municipality Littenseradiel in Friesland, the Northern Netherlands, the landscape has changed rapidly over the last two decades. In springtime, one could enjoy colorful grasslands buzzing with insects and the sounds of godwits and lapwings. Today, most farmers' fields are without flowers, bees, butterflies and meadow birds. This problem does not only occur in Friesland. From the 1970s onwards, the population of migratory meadow birds in the entire Netherlands has drastically declined (Teunissen et al. 2012). Since 1960, 75% of the breeding population has disappeared (Koffijberg et al. 2012). For example, in 1975 there were 120.000 godwit breeding pairs in the Netherlands; in 2008 their numbers had decreased to 55.000 (Jensen et al. 2008; Sovon 2017). Despite ongoing efforts to protect the meadow birds, their decline seems to speed up during the last decade (Teunissen and Plate 2011; Teunissen et al. 2012)(Figure 1.1). Unfortunately, this trend is visible throughout Europe (CLO 2015)(Figure 1.2). Loss of meadow birds and decreasing biodiversity are important problems and therefore part of the Dutch National Research Agenda (see inset below).

The Dutch National Research Agenda Chapter 1: Man, the environment and the economy (p. 23)

Question 003: Why is biodiversity important and how do we protect it.
Sub questions: Why is biodiversity declining so rapidly in the Netherlands, specifically **migratory birds**, insects, amphibians and reptiles and soil organisms. What sustainable solutions are there for halting this decline.

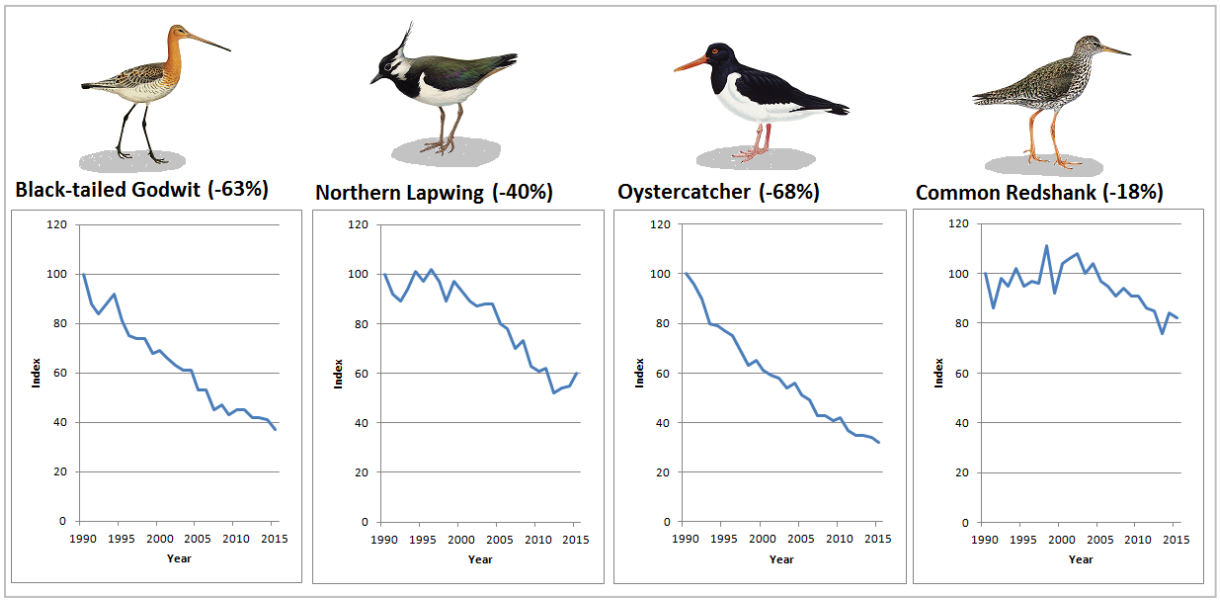

Figure 1.1: Decline of four important meadow bird species in the Netherlands from 1990 to 2015 (Index breeding population 1990 = 100%)(CLO 2017 (=CBS, Sovon, Netwerk Ecologische Monitoring)).

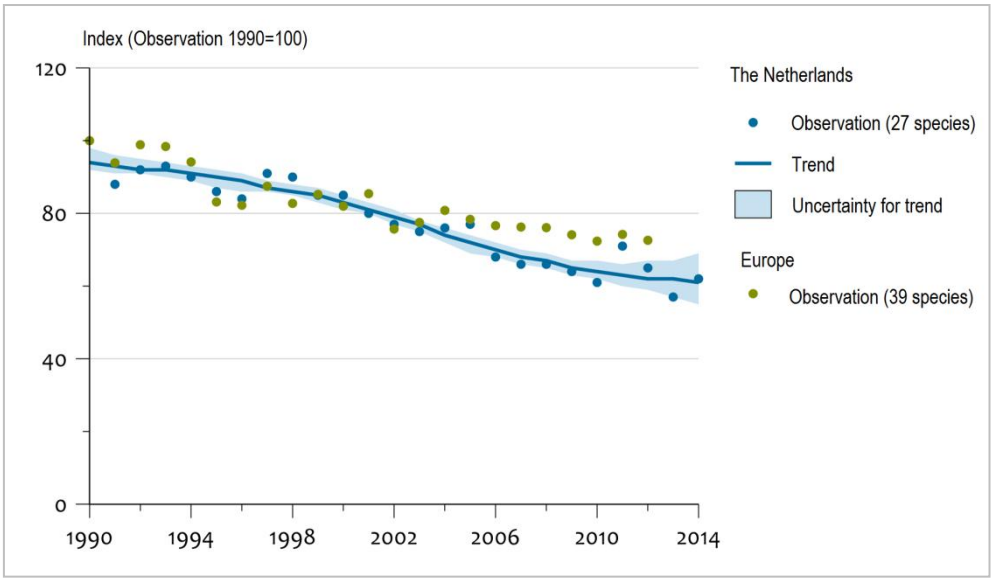

Figure 1.2: Decline of Farmland Bird Indicator from 1990 to 2014; the Netherlands vs. Europe (Netwerk Ecologische Monitoring (Sovon, CBS), European Bird Census Council 2015).

Grasslands cover 28% of the land surface of the Netherlands (CBS 2016); most of these grasslands have an agricultural function, serving as the main source of forage for livestock, nevertheless they are also of high nature value as ecological habitat of meadow birds, wild bees, roe deer and other animals (Carlier et al. 2009). Changes in agricultural grassland management are high on the list of causes of meadow bird decline (CLO 2017; CLO 2015; Groen et al. 2012; Kentie et al. 2013a; Kleijn et al. 2010). Dairy farmers strive to maximize productivity through intensification of grassland use (CLO 2017). Meadows are frequently re-seeded with protein-rich, high produce perennial ryegrass (*Lolium perenne*). Stimulated by the application of high amounts of liquid manure and artificial fertilizer, this fast growing grass produces dense swards and fields can be mown for silage production more frequent (almost once a month) and earlier in spring, ca. end of April, beginning of May (Groen et al. 2012; Kleijn et al. 2010; Koffijberg et al. 2012; Verhulst et al. 2008).

In this thesis, these intensively managed 'improved' grasslands are referred to as monoculture grasslands, emphasizing their uniformity and monotonous appearance (Figure 1.3). The term extensive grasslands is used for extensively managed fields that contain various species of grasses and herbs. In this context, extensive management means: no application of artificial fertilizer or liquid manure and sparingly application of dry manure, grazing by small herds of cattle or sheep (usually after the breeding season), first mowing date after June 15th, high groundwater levels and presence of foot drains (=narrow ditches within the field). This type of grasslands has become rare and is usually only found within nature reserves and at organic farmers.

New bird protection schemes, developed from 2012 onwards, focus on so-called meadow bird core areas (*weidevogel kerngebieden*) (Teunissen et al. 2012). Here, suitable environmental conditions should be created or preserved to maintain a healthy population. Required environmental conditions are: openness of the landscape, large interconnected breeding areas, presence of clay- and/or peat soils, high groundwater levels in spring (20-40 cm below surface), a delayed first mowing date (not before June 15th), no liquid manure injection and the presence of herb-rich grassland (Teunissen et al. 2012; van 't Veer et al. 2008). These conditions are typically found in areas with extensively managed grasslands.

Conservation efforts are now also aimed at protection of herb-rich grassland. *'Red de rijke weide'*, an initiative of the Dutch *Vogelbescherming* strives to achieve 200.000 ha herb-rich farmland

in 2020; 94 farmers have already joined this initiative (Vogelbescherming 2017). In August 2015, *LandschappenNL*, a partnership of twelve Dutch provincial landscape organizations has pleaded to subsidize farmers in order to stimulate development of herb-rich grasslands (LandschappenNL 2015). They argue that it is highly desirable to map the distribution of herb-rich meadows. To this date, no such dataset is available.

Grassland use intensity is spatio-temporally variable, surveying the large area of grasslands would be time-consuming and expensive (Franke et al. 2012). Thanks to their ability to gain detailed information on large areas at relatively high temporal resolution, Remote Sensing (RS) techniques have been increasingly used for nature conservation monitoring. For example, to assess baseline habitat condition and extent as well as changes in habitat condition, species diversity and threats (Nagendra et al. 2012; Toivonen and Luoto 2003). RS may therefore also be suitable to map the presence of herb-rich meadows and support monitoring of meadow bird populations and their habitat. A prerequisite for this is that different grassland types can be distinguished and that images are available that allow assessment at parcel scale. Currently, just a few examples of this type of grassland RS research exist (Asam et al. 2015; Courault et al. 2010; Franke et al. 2012; Sibanda et al. 2017). This thesis explores the potential of free open source, multi-temporal, high resolution, multi-spectral Sentinel-2 satellite data for detecting agricultural grassland management intensity and herb-richness at parcel level in a study area in Friesland, the Netherlands.

1.2 Research aim & objectives

Main aim of this research is to develop a Remote Sensing-based method that allows to detect differences in grass types and grassland use intensity, using free open source satellite imagery and free open source GIS software. If extensively managed, herb-rich meadows can be recognized on high resolution Sentinel-2 imagery, the method can be used to create distribution maps of herb-rich grassland to support monitoring of the Dutch meadow bird populations. If, in the nearby future, farmers will be subsidized for creating herb-rich grasslands, the method may also be used to assess changes in total area of herb-rich meadows through time and to monitor the effect of the subsidies. Because open source data and software is used, the method will also be affordable for non-profit nature conservation organizations.

To achieve this aim, spectral separability for monoculture and extensive grasslands on both clay and peat soils is assessed. Two vegetation index time series are generated and used for rule-based classification: the Normalized Difference Vegetation Index (NDVI) and the Sentinel-2 Red-Edge Position (S2REP), utilizing information from the two Sentinel-2 red-edge bands. Also, the Mean Absolute Change Dynamic (MASD) parameter (Franke et al. 2012) is calculated and its usefulness for classification of grassland management intensity is investigated. Two related classification methods are applied and validated through ground truthing: 1) statistical rule-based classification based on a decision-tree (DT) generated using the See5 (C5.0) algorithm, and 2) contextual rule-based classification, which uses simplified decision rules derived from the See5 DT in combination with knowledge of local grassland management, specifically the 1st mowing date. To demonstrate its potential with regard to meadow bird conservation, the most accurate grassland management map will be compared with the distribution of meadow bird nests in the municipality Littenseradiel, Friesland. Possibilities for detecting mowing and grazing at parcel level are also examined, since these are important aspects in meadow bird conservation (Jensen et al. 2008). Spectral heterogeneity will be tested as a proxy for biodiversity, since this parameter may be useful to examine differences in herb-richness between monoculture and extensive grasslands, as well as variations in herb-richness between extensive grasslands.

1.3 Research questions

The overall research question is:
Can multi-spectral Sentinel-2 satellite imagery be used to differentiate between extensively managed, herb-rich grasslands and intensively managed, monoculture grasslands at parcel level in Friesland, the Netherlands?

Sub-questions:
1: Is there a significant difference between spectral response curves of extensively managed grasslands and monoculture grasslands?
2: Which Sentinel-2 spectral bands are the most suitable for mapping grassland management intensity?
3: Is there a significant difference in spectral response for monoculture and extensive grasslands on peat soils compared to clay soils?
4: What is the optimal time of year to discriminate between extensive and monoculture grasslands?
5: Is it necessary to use a combination of images acquired at different times of the growing season to achieve accurate classification of grassland management?
6: What are the benefits of the S2REP vegetation index compared to the NDVI?
7: Is the Mean Absolute Spectral Dynamic (MASD) parameter useful for classification of grassland use intensity?
8: Which classification method yields the best results in terms of classification accuracy?
9: Can spectral heterogeneity be used as an indicator of species richness/biodiversity?
10: Can mowing and grazing be detected at parcel level?
11: Based on the results for the current study area, is it possible to map grassland management intensity and herb-richness for the entire Netherlands?

1.4 Thesis outline

Chapter 2.0 contains background information on grassland; general importance of grasslands is discussed and the seasonal grass production curve is explained, since this will help to understand spectral response curves and NDVI and S2REP time series. A literature review of causes of meadow bird decline is presented as well as a literature review on remote sensing of grasslands. Chapter 3.0 describes the data that were used. It gives background information on the Sentinel-2 mission and the capabilities of the Sentinel-2 red-edge bands for vegetation analysis. Data processing steps, such as atmospheric correction, are explained. Chapter 4.0 describes the South-Central Friesland study area and Littenseradiel and Grouw field survey areas. It contains additional information on local weather conditions and a timeline for agricultural grassland management activities for 2016, essential background knowledge for interpreting NDVI and S2REP time series. Chapter 5.0 discusses the methods that were used. Results can be found in Chapter 6.0, which contains spectral response curves, vegetation index time series, MASD maps, classification results and accuracy assessment. In Chapter 7.0 potential applications of the grassland management intensity map for meadow bird conservation are given. The output map is compared with the distribution of meadow bird nest sites in Littenseradiel. Also, a model for detecting mowing and grazing, is presented and discussed. Chapter 8.0 gives the final conclusion/discussion followed by the references in Chapter 9.0. The Appendices contain additional maps and tables with results for statistical tests.

Extensive grassland at Skrok, Littenseradiel, clay soil area (March 3rd 2017).

Monoculture grassland near Easterein, Littenseradiel, clay soil area (March 10th 2017).

Extensive grassland at Lionserpolder, Littenseradiel, clay soil area (April 17th 2017).

Monoculture grassland near Lionserpolder, Littenseradiel, clay soil area (April 17th 2017).

Extensive, herb-rich grassland at De Burd, near Grouw, peat soil area (April 22nd 2017).

Monoculture grassland near De Veenhoop, peat soil area (April 22nd 2017).

Figure 1.3: Differences between extensive and monoculture grassland in March and April.

2.0 Background information

2.1 Grasslands

2.1.1 Importance of grasslands

Grasslands cover 31.5% of the global landmass (Ali et al. 2016). Extensive grasslands, e.g. hay pastures in Europe, support plant and animal biodiversity and have high nature value (Carlier et al. 2009; Halabuk et al. 2015). As the second largest terrestrial carbon sink, grasslands are also an essential part of the global carbon cycle and grassland use intensity and grassland degradation influence greenhouse gas emissions (Ali et al. 2016; Franke et al. 2012). In the Netherlands, 956.000 ha (28%) of the land surface consists of improved, intensively used agricultural grassland. 90% of this grassland is used for the production of silage to feed dairy cattle during wintertime, 3% for production of hay, 4% for fresh grass to feed cattle that are kept indoors during the summer and 3% is used for other purposes (CBS 2016). It is estimated that grasslands in the Netherlands contain 148 million tonnes of carbon (Schils 2012).

2.1.2 Grass production curve

Seasonal grass production curves typically display two peaks (Figure 2.1). Grass growth begins in March, speeds up in April and reaches its first, and highest, peak in May. In June and July, growth slows down due to slower re-growth after the first (or second) cut but this is also related to the flowering season for grass vegetation, ca. half May to half June (Visscher 2010). In August, grass growth reaches a second peak. The two-peaked production curve is found for grass species on different soil types and in all climates (Alberda 1959).

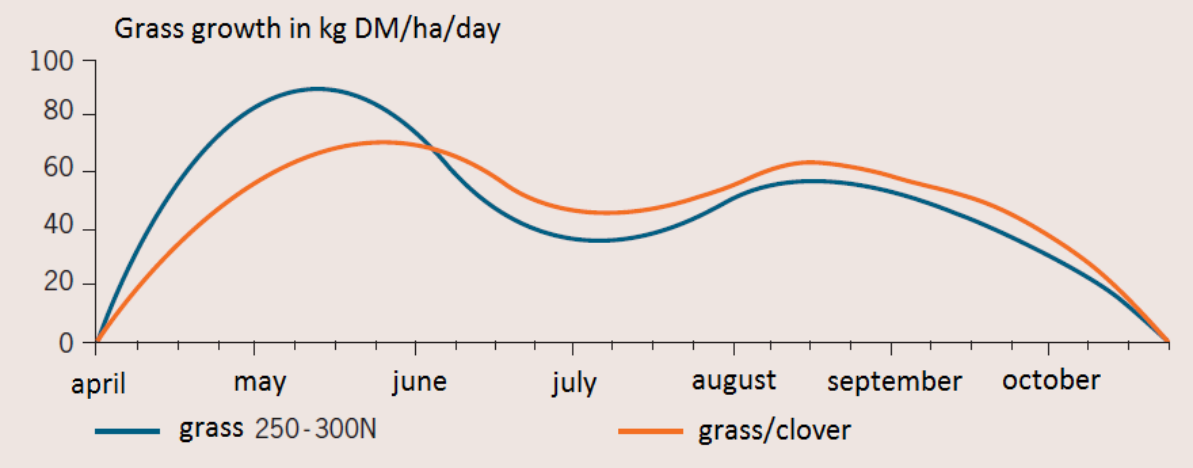

Figure 2.1: Seasonal grass production curve for grass with application of 250 kg N and a grass/clover mixture (from: Visscher 2010).

2.1.3 Factors that influence grass growth

The five factors that are most important for grass growth are: light, temperature, air (CO_2 and O_2), moisture (rain and soil moisture) and availability of nutrients (nitrogen). Grassland use, e.g. grazing or mowing, and management intensity also influence grass production and grass nutritional quality (Visscher 2010). Grass, as all plants, uses light as energy source for photosynthesis; from March onwards the amount of daylight is adequate to initiate vegetation growth. Onset of grass growth is found at soil temperatures between 5 and 8 °C, measured at a depth of 10 cm below ground surface.

In the Netherlands, optimal air temperature for grass growth is between 15 and 25 °C; above 25 °C, grass ceases to grow (Gollenbeek and Hoving 2016). Availability of water is also essential for photosynthesis. During periods of drought, leaf stomata close, reducing CO_2 uptake and reducing leaf growth. The natural decrease of grass growth in June/July will be enhanced during dry summers (Visscher 2010). Presence of too much moisture, e.g. very wet soils due to high groundwater levels, will slow down grass growth because these soils require more time to warm up in spring (Gollenbeek and Hoving 2016). In extensive grasslands in spring, water levels are usually higher than on intensive grasslands, therefore the onset of grass growth will be delayed.

Nitrogen (N) is an important element in chlorophyll and in enzymes required for photosynthesis (Clevers and Gitelson 2013). Besides N, other nutrients that are important for building proteins are minerals such as phosphorus, sodium, potassium, calcium, molybdenum and iron. Local soil type influences the amount of minerals that is available for the grass vegetation. Peat soils contain high amounts of organic matter and hence more N than sandy soils (Visscher 2010). Clay soils have a high cation exchange capacity which increases soil fertility; the clay minerals attract e.g. sodium, potassium, magnesium and calcium (Schils 2012).

The amount of available nutrients is regulated by application of fertilizers. General rule of thumb is that the more N applied, the higher the grass production (Visscher 2010). Grass growth in monoculture meadows is mainly stimulated by application of liquid manure, this is allowed from February 15th onwards. European member states allow farmers to apply a maximum of 170 kg N/ha; however, in the Netherlands, farmers that own at least 70% grassland are allowed to apply 250 kg N/ha (derogation) (Hooijboer et al. 2014). Compared to intensively managed grasslands, grass growth in April is much slower on extensive grassland because little or no fertilizer is applied. (Visscher 2010).

Finally, grass production also depends on grass species. Nowadays, in the Netherlands, ryegrass (*Lolium perenne*) is the most important grass type used for dairy farming. Quality of grassland, in terms of nutritional value for dairy cattle, is measured in the amount of ryegrass that is present: the more ryegrass the better. Therefore, most intensively managed fields contain monocultures of ryegrass. A disadvantage of ryegrass is that it is sensitive to dry and very wet conditions. To ensure high production levels, intensively managed meadows are frequently re-seeded. Mixtures of ryegrass with smooth-meadow grass (*Poa pratensis*) and clover also occur because these are more suitable for grazing. Organic farmers often use mixtures of different grass types and clover. Clover acts as a natural fertilizer, it enhances N availability of soils (Visscher 2010).

2.2 Meadow birds

In the Netherlands, the term 'meadow birds' is used for migratory birds that breed on agricultural grasslands or arable lands (Groen et al. 2012). This thesis focuses on four meadow bird species, the Black-tailed Godwit (Grutto, *Limosa l. limosa*), the Northern Lapwing (Kievit, *Vanellus vanellus*), the Oystercatcher (Scholekster, *Haematopus ostralegus*) and the Common Redshank (Tureluur, *Tringa totanus*) and their habitats. The Netherlands have an international conservation responsibility for the Godwit because 40% of the European population breeds here (Hooijmeijer et al. 2011; Kleijn et al. 2010).

2.2.1 Causes of meadow bird decline

Over the last 50 years, the population of meadow birds in the Netherlands has dramatically declined despite ongoing agri-environmental and other conservation schemes (Kentie et al. 2013a; Teunissen and Plate 2011; Teunissen et al. 2012). The most important factors that explain this decline are:
1) Habitat loss caused by expanse of urban areas and infrastructure, combined with the increase of traffic (CLO 2017; CLO 2015; Teunissen and Plate 2011).
2) Loss of habitat quality due to changes in agricultural management aimed at increased efficiency and to maximize productivity of dairy cattle:

- Use of larger and faster tractors for mowing and for manure injection (Teunissen and Plate 2011).
- Intensification of grassland use (CLO 2017; CLO 2015; Groen et al. 2012; Kentie et al. 2013a; Kleijn et al. 2010); this causes:
  - A shift from herb-rich grassland to structurally uniform monocultures of protein-rich, fast growing grass types such as ryegrass (*Lolium perenne*), which leads to earlier and more frequent mowing (Verhulst et al. 2008).
  - Increased use of pesticides (CLO 2015) and use of anti-helminthic drugs (avermectins and ivermectins) in cattle and sheep; residues of these drugs excreted in faeces of treated animals are insecticidal, reducing the amount of food for juvenile birds (Vickery et al. 2001).
  - Increased use of fertilizer and manure injection; earthworm numbers decrease under high fertilizer application rates, reducing the amount of food for adult birds (Vickery et al. 2001).
  - Removal of (micro) relief through dragging or rolling of meadows (Kleijn et al. 2010).
  - Higher stocking densities (Kentie et al. 2013a).
- A decrease in the total area of grassland caused by a shift from grass to crops, e.g. maize and biofuels (Franke et al. 2012; Koffijberg et al. 2012). Between 1950 and 2013 the total area of grassland in the Netherlands decreased from 1.317.000 ha to 932.000 ha, although the last few years it has slightly increased to 956.000 ha, which is mainly due to increase in temporary grassland (CBS 2017).

3) Changes in water management: increased and deeper drainage to maintain low groundwater levels (Koffijberg et al. 2012). Foot drains are replaced by underground drainage. Because of drier conditions in the fields, farmers can start to inject liquid manure early in spring (Groen et al. 2012).
4) Climate change, leading to increased winter and spring temperatures; since the 1980s median mowing dates have been advanced 15 days due to early warming of soils in spring, whilst hatching of e.g. godwit eggs has not advanced. Nowadays more chicks are exposed to agricultural activities (Kleijn et al. 2010).
5) Increased predation pressure; numbers of predators have increased and places where juveniles can hide from predators are lacking due to removal of relief, removal of foot drains and early mowing (Kentie et al. 2013a).

2.2.2 The importance of herb-rich grasslands

The factors stated above especially contribute to the loss of juvenile meadow birds, which is the main reason for population decline (Verhulst et al. 2008). Godwit and redshank chicks cannot survive in monoculture grasslands, the juveniles require long (but not too long), herb-rich vegetation that contains enough insects for feeding. The dense ryegrass vegetation lacks (large) insects, it also inhibits movement of the juveniles and many birds get killed during mowing and manuring (Kentie et al. 2013a; Verhulst et al. 2008). Extensively managed grasslands with a high concentration of herbs, e.g. dandelions, cuckoo-flowers and buttercups, are required for the survival of juvenile birds (Groen et al. 2012; Verhulst et al. 2008). It was found that apparent survival during the first year of life is 2.5 times higher for godwit chicks that hatched on herb-rich fields than chicks hatched on intensively managed, monoculture fields (Kentie et al. 2013a; 2013b).

Groen et al. (2012) investigated habitat selection of godwits in South West Friesland. In total 8480 ha grassland was investigated of which 80% consisted of intensively managed grassland with low groundwater levels. It was found that vegetation herb-richness, presence of foot drains and high groundwater level are the most important landscape characteristics influencing the quality of godwit habitat. Moist, herb-rich fields with foot drains attracted highest densities of godwits (Groen et al. 2012). Influence of soil type was also investigated; it was found that adult godwits preferred sandy clay loam and sandy clay. Soil texture affects the number of earthworms and penetrability of the soil and therefore the availability of earthworms, the most important prey for adult godwits (Groen et al. 2012).

In this thesis a similar definition of herb-richness is used as in the research of Groen et al. (2012) and Kentie et al. (2013b). Three categories of herb-richness can be discerned:

1) **Herb-poor**: fields dominated by high-productive ryegrass types, 1 to 3 plant species including some Dandelions (Paardebloem, *Taraxacum* species), Nettle (Brandnetel, *Urtica dioica*) or Stitchwort (Muur, *Stellaria* species), mostly on parcel edges. Intensively used (monoculture) grasslands belong to this category.

2) **Moderate herb-rich**: high produce grass types but with higher amount of herbs, e.g. Dandelion, Stitchwort, Buttercup (Boterbloem, *Ranunculus* species), Sorrel (Veldzuring, *Rumex acetosa*), Cuckoo flower (Pinksterbloem, *Cardamine pratensis*) and Daisy (Madeliefje, *Bellis perennis*).

3) **Herb-rich**: meadows with over 10 species of herbs and various grass types e.g. Sweet Vernal Grass (Reukgras, *Anthaxanthum odoratum*), Crested Dog's tail (Kamgras, *Cynosurus cristatus*) and Tufted Grass (Gestreepte Witbol, *Holcus lanatus*) and beside the herbs of category 2, also other herbs such as Ragged Robin (Echte Koekoeksbloem, *Silene floscuculi*), Yellow Rattle (Kleine Ratelaar, *Rhinanthus minor*), Water Forget-me-not (Moerasvergeet-mij-nietje, *Myosotis scorpioides*). In the Netherlands, this type of fields is usually only found within grassland reserves managed by nature conservation organizations.

The indirect effects of grassland management on meadow birds are summarized in Figure 2.2.

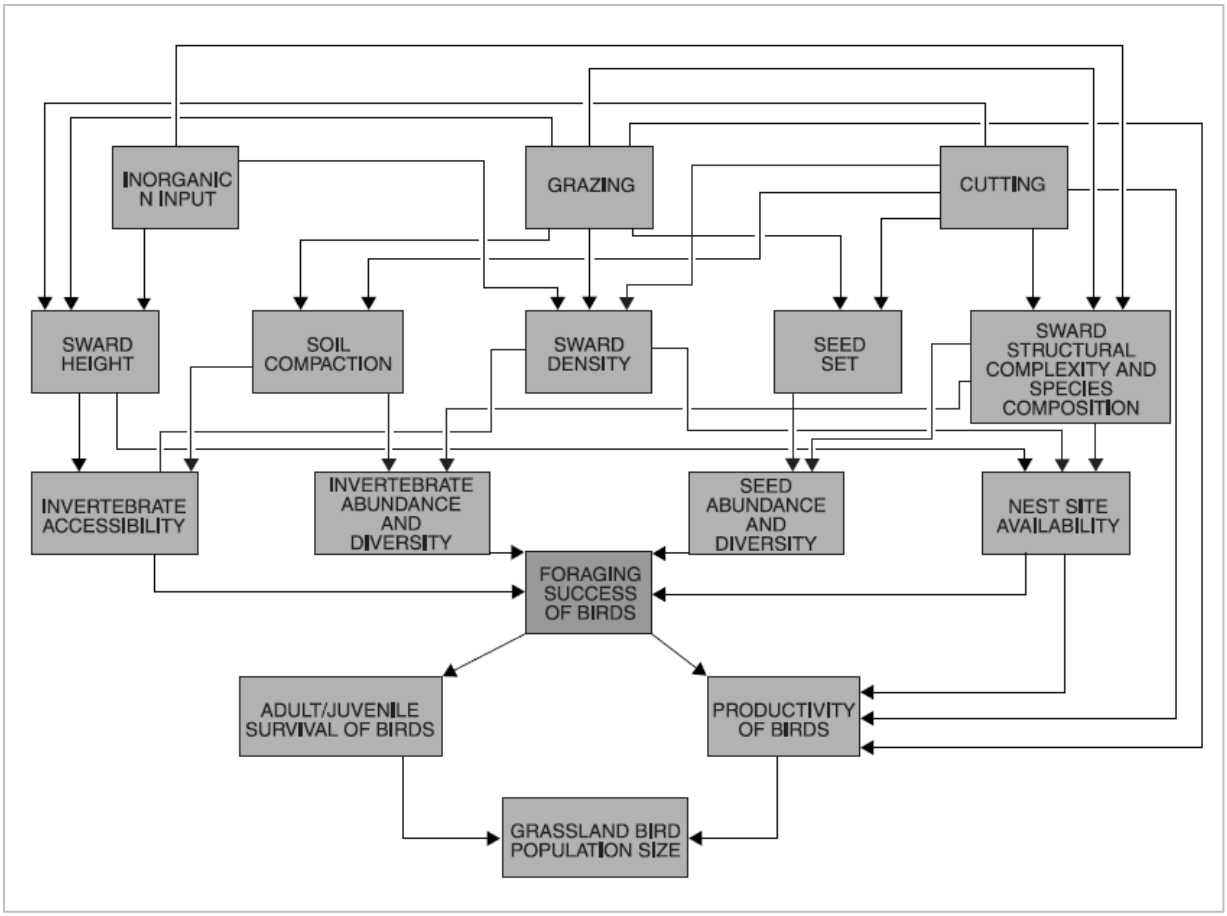

Figure 2.2: Diagram of the indirect effects of grassland management on birds (Vickery et al. 2001).

2.3 Meadow bird conservation in Friesland

2.3.1 Meadow bird landscapes

Since 2011, joint meadow bird conservation organizations in Friesland, e.g. '*BoerenNatuur*', *'It Fryske Gea*', *Natuurmonumenten* and '*Staatsbosbeheer*', have focused on conservation of meadow bird landscapes, specifically aimed at the protection of godwits. These landscapes should consist of quiet, very open, moist to wet grassland areas of at least 250 ha in size with few roads, built-up areas and shrubs. They should contain at least 10 godwit pairs per 100 ha (Oosterveld & Hoekema 2012). Within meadow bird landscapes, meadow bird core areas can be discerned that should provide a safe place for breeding and a suitable habitat for juvenile birds. The intention is that bird populations in these areas are able to maintain themselves. Conservation in core areas comprises bird reserves and meadows with agricultural nature management; together, these areas form a 'meadow bird management mosaic' (Oosterveld & Hoekema 2012). Besides conservation by professional organizations, nest protection and protection of chicks is also performed by volunteers, usually members of the Bond Friese Vogelwachten (BFVW). The environment that surrounds core areas should function as a buffer area between bird reserves and areas with intensive agricultural management. To achieve this, in Friesland, also so-called *'Skriezekrites'* exist; this may be groups that focus on protection of godwits on parcels without agricultural nature management that lie outside the reserves. These groups are often joint efforts of various conservation organizations in combination with volunteers of BFVW. In other cases it may be groups of farmers, working together to protect godwits and other meadow birds on their farmland (e.g. *Skriezekrite Idzegea*) (Skriezekrite

Idzegea 2008).

Landscape management in bird reserves is optimized to sustain high numbers of meadow birds. In some reserves 30 godwit pairs per 100 ha can be found; birds in these areas form the source population (Oosterveld & Hoekema 2012). Bird reserves consist of open herb-rich fields with foot drains. Groundwater levels are kept high, dry manure is applied every few years (Figure 2.3) and mowing is postponed until at least June 15th. These areas resemble traditional breeding habitats of meadow birds (Kentie et al. 2013a).

2.3.2 Agricultural nature management

To halt meadow bird decline, several agri-environment schemes for conservation of meadow birds have been implemented in the Netherlands since 1981. Agreements within these schemes generally prohibit changes in drainage and require protection of nests by mowing around the nests or by applying a resting period. In such fields no agricultural activities are allowed between April 1st and specific dates in June/July (Kleijn et al. 2004). Unfortunately, research has shown that these schemes have not led to an increase in meadow birds (Kleijn et al. 2004). Reason for this may be that the number of parcels with agricultural nature management is too small compared to the large area with intensive management (Kleijn et al. 2004). It may also be that these parcels lie too close to infrastructure and built-up areas or that their soil type and moisture level is not suitable for meadow birds (Teunissen et al. 2012). Furthermore, postponed mowing in intensively used fields with high produce grass types creates dense swards that inhibit movement of chicks and these fields may also not contain enough (large) insects (Kentie et al. 2013a).

From 2016 onwards, individual agricultural nature management organizations are required to work together as management collectives within the new agri-environment scheme *'Agrarisch Natuur en Landschaps Beheer 2016'* (ANLb2016) (Melman et al. 2016). In Friesland, seven overarching collectives exist that coordinate the nature management activities of ca. 2000 farmers that operate within smaller collectives; in total these farmers manage 15.000 ha. The seven collectives are united in *'Kollektivenberied Fryslân'* (KBF). Farmers take part on a voluntary base but are compensated for loss of income (KBF 2017). Before a collective of farmers is allowed to join the new scheme, they have to develop a sound management plan. It is hoped that this new, more balanced scheme will lead to better results than previous schemes (Melman et al. 2016).

Figure 2.3: Dry manure on extensive fields, Skrok, Littenseradiel (March 2017).

Liquid manure injection on monoculture field, Itens, Littenseradiel (March 2017).

2.4 Remote Sensing of grassland

2.4.1 Principles of Remote Sensing

Remote Sensing (RS) can be defined as: "*the acquisition of information about an object without being in physical contact with it*" (Elachi 1987). This broad definition includes acquisition of various data types using many different types of sensors. Focus of this thesis is on RS data collected by electromagnetic energy sensors operated from the Sentinel-2A satellite. The principle of this form of RS is that electromagnetic waves emitted by an energy source, e.g. the sun, interact in different ways with earth surface features. The incident energy can be either absorbed, reflected or transmitted depending on material type and condition of the features. Also, the proportion of absorbed, reflected and transmitted energy varies at different wavelengths. Satellite sensors measure the amount of incident energy that is reflected by the earth surface. Spectral reflectance (ρ) is measured as a function of the wavelength and is the ratio between the energy at wavelength λ reflected from the object and the energy of wavelength λ incident upon the object (Lillesand et al. 2015).

2.4.2 Spectral reflectance of vegetation

Spectral response of features and objects on the earth surface can be plotted as a function of wavelength, creating spectral reflectance curves (Lillesand et al. 2015). Because features respond very differently to irradiance, these curves are often called spectral signatures. The difference in response makes it possible to distinguish vegetation from e.g. water or built-up areas and to recognize different types of vegetation. Figure 2.4 shows the average spectral reflectance curves, measured by a spectrometer, for fresh green lawn grass and dry grass (USGS 2017). Satellite-based sensors only collect data for parts of the spectrum. This means that some of the information and subtle features in the curve will inevitably be lost (Kumar et al. 2001).

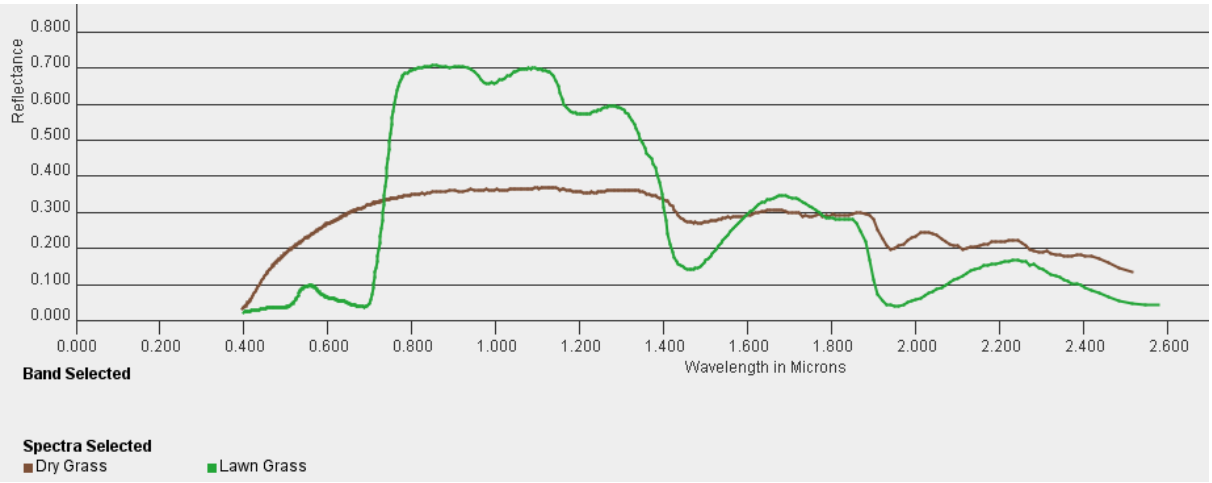

Figure 2.4: Spectral reflectance curve for dry grass and lawn grass (from: USGS Spectral characteristics viewer; USGS 2017).

Spectral response curves of vegetation display a very characteristic configuration that depends on: 1) the concentration, distribution and type of plant pigments; 2) the internal leaf structure; 3) surface roughness of the leafs and 4) water content (Kumar et al. 2001). In the visible light range (~400-700 nm), vegetation shows low reflectance for violet-blue and red light because chlorophyll pigments in plants absorb red light for photosynthesis. Green light is not used for photosynthesis, hence the appearance of a small reflectance peak for green visible light. Different types of plant pigments, e.g. chlorophyll, carotene and xanthophyll, have their own absorption maxima (Kumar et al. 2001).

In senescing vegetation and in stressed plants, chlorophyll pigment degrades; plant color changes from green to yellow because carotene and xanthophyll become the dominant pigments, reflecting both green and red light. Dead vegetation appears brown because brown pigments, tannins, replace carotene and xanthophyll, hence reflectance values in the visible light range increase. This effect can be seen in the spectral response curve of dry grass (Figure 2.4).

The reflectance red-edge, a steep increase in reflectance, is a characteristic feature of spectral response of vegetation that lies between ~690 and 740 nm. The red-edge can be used for assessment of biophysical parameters such as leaf chlorophyll content (LCC) and leaf area index (LAI) (Frampton et al. 2013; Kumar et al. 2001; Schuster et al. 2012). The amount of chlorophyll per unit area is an indicator of plant photosynthesis capacity. The point of maximum slope on the red to infrared curve is called the red-edge inflection point. This point is different for different types of vegetation. To accurately determine the inflection point, it is required to measure reflectance in a high number of very narrow bands (Kumar et al. 2001). An increase in leaf chlorophyll content leads to a shift in the red-edge position towards longer wavelengths (Delegido et al. 2013). The point of maximum reflectance usually lies at ~800 nm and is called the red-edge shoulder.

In the Near Infra Red (NIR) region (~700-1000 nm), reflectance is high because the energy levels of NIR are too low to be used for photosynthesis. Variation in spectral response in NIR is caused by differences in internal leaf structure and water content (Kumar et al. 2001). In senescing vegetation, interior cell walls break down, changing the optical properties of the leaf, which causes a decrease in NIR reflectance. Hence, the NIR response for dry grass is lower than for green grass (Figure 2.4) (Kumar et al. 2001).

The Short Wave Infra Red (SWIR) (~1000-3000 nm) is characterized by water absorption bands at ~1200, 1450 and 1940 nm. Lignine, cellulose, starch, proteins and nitrogen are leaf biochemicals that also have absorption bands in the SWIR range, but in fresh leaves these are usually masked by the presence of water. High water content will decrease reflectance in the water absorption bands (Kumar et al. 2001). In the SWIR range between the water absorption bands, reflectance of leaves increases during drought (Liew 2001). Dry vegetation contains less water than fresh green vegetation and therefore shows less variation in reflectance for the SWIR region; reflectance is higher compared to green vegetation (Figure 2.4).

Chemical and physical plant characteristics respond to management treatments, e.g. application of fertilizer increases chlorophyll content which in turn influences the plants' spectral characteristics, making it possible to discriminate between untreated fields and fields that have been fertilized (Sibanda et al. 2017; Sibanda et al. 2015).

2.4.3 Remote Sensing of grassland

2.4.3.1 Applications of RS for grassland research

Because of the large surface area, it is time-consuming and expensive to survey and monitor grasslands worldwide using ground-based methods (Ali et al. 2016; Franke et al. 2012). However, over the last two decades, RS is increasingly used to study grasslands and their properties, thanks to the emergence of advanced techniques in geoinformatics (Gao 2006). Many studies have effectively used optical RS data for monitoring, mapping and quantifying different grassland types and biophysical parameters (Ali et al. 2016). However, research that uses RS for assessing agricultural grassland management intensity at parcel level is rare (Asam et al. 2015; Franke et al. 2012; Sibanda et al. 2017). Current availability of high temporal and spatial resolution imagery from e.g. RapidEye and Sentinel-2, offers new perspectives for this type of research (Asam et al. 2015). Applications of RS for grassland research can be classified into three main groups (Clerici et al. 2012):

1) Grassland mapping; usually as a part of global or regional land cover mapping.
2) Grassland type classification and monitoring; for areas where the location of grasslands is already known.
3) Grassland change analysis; this includes studies of grassland degradation due to overgrazing, overgrowth or climate change.
Since this thesis belongs to the 2nd group, the literature review will focus on the second purpose: RS for grassland type classification and monitoring.

2.4.3.2 Time series of vegetation indices

Characteristics of grassland vary throughout the growing season depending on temperature, soil moisture, fertilization and other management activities such as mowing and grazing (See section 2.1). To get a complete picture of these variations, it is essential to analyze data acquired at different observation dates. Within RS there is usually a trade-off between spatial and temporal resolution (Ali et al. 2016). Satellites that deliver high-resolution data, tend to have a limited temporal resolution, e.g. Landsat 8 (30 m spatial resolution) has a revisit time of 16 days and Sentinel-2A (10 m spatial resolution) has a revisit time of 10 days. But, when Sentinel-2B becomes operational, imagery will be available every 5 days. In contrary, satellites with high temporal resolution, often have a low spatial resolution; e.g. MODIS with a 1 day revisit time, has a maximum spatial resolution of 250 m. Unfortunately, 250 m pixel size is too coarse to assess grassland use intensity and management practices at parcel level.

Most RS-based grassland studies use one or more vegetation indices (VI) to discriminate between different grassland types or assess grassland management characteristics. In a VI, reflectance values at two or more wavelengths are combined to accentuate specific features of the spectral signature for vegetation (Ali et al. 2016). VI's are useful for spatial and temporal inter-comparison of photosynthetic activity and health condition of vegetation (Huete et al. 2002). The most often used VI is the Normalized Difference Vegetation Index, first proposed by Rouse et al. (1974); it is the normalized ratio between reflected energy in the red chlorophyll absorption range and reflectance in the NIR range, providing an indication of vegetation 'greenness' (Delegido et al. 2013; Frampton et al. 2013; Lillesand et al. 2015). NDVI time series have shown to be be useful for estimating primary grass production; it was found that they provide good estimates for dry green biomass and clearly show seasonal changes for vegetation growth and senescence (Nestola et al. 2016). Therefore, it is likely that the NDVI seasonal curve will be comparable to the grassland production curve (Figure 2.1). Drawbacks of the NDVI are that it is susceptible to soil and atmospheric influences and that it often saturates for areas with dense vegetation cover (Mutanga and Skidmore 2004; Sakowska et al. 2016).

The Enhanced Vegetation Index (EVI) has been developed specifically for the Moderate Resolution Imaging Spectroradiometer (MODIS) satellite sensor. The EVI is also a ratio between reflectance in NIR and red visible light, but with additional use of coefficients, such as the canopy background adjustment and use of the blue spectral band to correct for aerosol influences in the red band (Huete et al. 2002).

VI time series can be affected by noise caused by atmospheric variability and cloud contamination, as well as bi-directional effects that result from the angular relationship between the sun, the object and the sensor (Lillesand et al. 2015; Nitze et al. 2015). To reduce this noise, various smoothing techniques/filtering methods have been applied, e.g. curve-fitting functions (Jönson and Eklundh 2004). However, small fluctuations in time series can also be attributed to e.g. mowing and grazing; by applying a filter, this information may be lost or reduced (Halabuk et al. 2015).

For the Netherlands, Lips (2011) has used MODIS 16 and 8 days composite EVI time series to study grassland management intensity in the context of meadow bird conservation. It was found that the MODIS data did not allow direct classification of intensively and extensively used grassland due to noise. However, based on the 16-day EVI time series, a model was developed to detect the 1st mowing date for two study areas in Arkenheem-Eemland and Laag-Holland. Mowing causes a sudden drop in EVI value that can be detected by studying the EVI change between two consecutive observation dates. This model performed well and it was concluded that grassland use intensity can be derived indirectly by detecting the 1st mowing date, because extensive grasslands are not mown before June. Due to the coarse spatial resolution of MODIS imagery (250 m), grassland management could not be detected at parcel level.

Halabuk et al. (2015) used MODIS 16 day NDVI and EVI composite time series in combination with decision rules derived from a simple decision tree algorithm, to detect grass cutting in hay meadows in Slovakia. They found that classification based on NDVI series yielded slightly better results than EVI for discriminating between uncut and cut meadows. Also, if noise reduction was applied by using Fourier filtering methods, classification accuracy decreased.

Courault et al. (2010) successfully detected mowing events and irrigation dates at parcel level in the Mediterranean Crau region in France, using NDVI and LAI time series derived from Formosat-2 imagery (8 m spatial resolution, 4 spectral bands, 3-4 days revisit time).

Nitze et al. (2015) used a Feature Importance measure within the Random Forest machine learning method (based on Classification And Regression Tree (CART) classifiers) to determine optimal image acquisition periods for grassland classification in Ireland. The Feature Importance measure represents the contribution of a specific variable/attribute to classification accuracy. In Random Forest methods, multiple decision trees are used to improve classification rate. EVI and NDVI data derived from MODIS Terra 16-day composites (MOD13Q1) over a 9 year period were used to discriminate between improved and semi-improved grasslands. They found that the months April and November showed the most optimal separability for both VI's. EVI outperformed NDVI in classification accuracy. However, inter-annual variations occurred due to differences in weather conditions. Overall classification accuracies varied between 80 and 95% (Nitze et al. 2015).

Asam et al. (2015) studied agricultural grassland management intensity in south Bavaria using Leaf Area Index (LAI) time series derived from 9 RapidEye images for 2011. The RS based LAI was compared with in-situ LAI measurements. Asam et al. (2015) state that grassland biomass is better represented by the biophysical parameter LAI than by other VI's (e.g. NDVI) that are developed to assess relative vegetation abundance and vegetation health; LAI is calculated using the PROSAIL inverted radiation transfer model in which local viewing and illumination conditions are also taken into account. LAI was found to be suitable for discrimination at parcel level between very intensively managed fields (that are mown 4 times per year or more), intensively managed fields (that are mown 2-3 times), intensively managed pastures (that are alternately grazed and cut) and extensively managed meadows and moorland (cut at most once a year). Decision tree software was used to derive decision rules based on LAI statistics. E.g. LAI standard deviation was used to investigate LAI variability; extensively managed meadows showed low LAI variability because they are not frequently mown. Unfortunately, not all mowing events were detected due to gaps in the time series.

Dussaux et al. (2014) also successfully used LAI, derived from SPOT imagery, to detect mowing and grazing in grasslands in France. They found that LAI was a better predictor for these activities than NDVI.

2.4.3.3 Advantages of using the red-edge spectral bands

Because grasslands in general display a very similar spectral signature, information from specific wavelengths is required to be able to discriminate between different grassland types (Ali et al. 2016). Several high-resolution earth observation satellites now collect data in the red-edge wavelengths, e.g. RapidEye, WorldView-3 and Sentinel-2. This part of the spectrum is related to vegetation chlorophyll content (Clevers and Gitelson 2013; Frampton et al. 2013; Kumar et al. 2001; Schuster et al. 2012) and is also suitable for estimating leaf nitrogen content (Clevers and Gitelson 2013; Ramoelo et al. 2015). Using red-edge bands reduces the saturation effect which is often found in NDVI; in the red-edge region, absorption by chlorophyll is lower than in the red visible light region (Clevers and Gitelson 2013; Mutanga and Skidmore 2004). Seasonal variation in chlorophyll content was found to be related to gross primary production in maize and soybean crops (Gitelson et al. 2006). Therefore for grassland, seasonal variability for VI's related to chlorophyll content, such as the Sentinel-2 Red-Edge Position (Frampton et al. 2013), may display a similar pattern as the grassland production curve (Figure 2.1).

As the research of Franke et al. (2012) illustrates (See section 2.4.3.5), RapidEye data with its additional red-edge spectral band can be successfully used for classification of grasslands. Schuster et al. (2012) have also shown that the inclusion of data from a red-edge spectral band can improve land use classification results; they found the RapidEye red-edge band particularly useful for discriminating between vegetation classes in open landscapes.

Sibanda et al. (2017) used the red-edge band in the commercial WorldView-3 satellite (8 multispectral bands, 1.24 m spatial resolution, average revisit time < 1 day) to discriminate and map complex grassland management treatments in southern Africa. They were able to detect grazing, burning, mowing and fertilizer treatment using discriminant analysis (= comparable to Principal Component Analysis). Incorporating the red-edge band improved classification accuracy from 65 to 70%.

2.4.3.4 Image classification methods

Image classification procedures are used to automatically categorize each image pixel into separate land cover classes or themes. Classification is usually based on spectral patterns, e.g. pixels with similar spectral characteristics are grouped together into specific land cover classes (Lillesand et al. 2015). Classification methods that are used to discriminate between grassland types can be divided into statistical, object-oriented and machine learning approaches (including decision-trees), although hybrid strategies have also been applied. All methods have been successfully used for different regions and using different earth observation satellites.

Until the 1990s, maximum likelihood classification was the most often used statistical classification method (Ali et al. 2016). The maximum likelihood classifier evaluates variance and covariance of spectral response patterns of different land use classes, and classifies pixels based on their probability of belonging to a class; the assumption is made that training data follows a normal (Gaussian) distribution (Ali et al. 2016; Lillesand et al. 2015). For example, Toivonen and Luoto (2003) used supervised classification with the maximum likelihood classifier to detect semi-natural grasslands in Finland, using Landsat TM imagery. In general, for grassland studies, overall maximum likelihood classification accuracies range from 70-90% (Ali et al. 2016). Drawback of this classification method is that Gaussian distribution is required and that it can be computationally slow if a large number of spectral channels are used and pixels have to be discriminated into a large number of spectral classes (Lillesand et al. 2015).

Nowadays, data driven machine learning approaches are more popular than maximum likelihood classification. E.g. artificial neural networks are computational models that resemble the structure and functions of biological neural networks. Based on input information that flows through the network and produces particular outputs, the network itself changes or 'learns' (Lillesand et al. 2015). Disadvantages are that for this approach, availability of large amounts of data for multiple years is required and choice of design of network architecture and choice of assigning learning parameter values are not straightforward (Pal and Mather 2003). From 2000 onwards, decision trees (DT's) have also been increasingly used for image classification. DT's apply a sequential approach in assigning attributes to specific classes. Advantages of DT's are that they are computationally fast, they do not make statistical assumptions concerning frequency distributions and analysts can easily interpret their outcome in contrary to neural networks, which are more like a 'black box' (Pal and Mather 2003). An example of DT software is See5 (Rulequest Research 2015) (See section 5.5.1). Compared to Maximum likelihood classification, DT classification achieved slightly higher overall accuracies for multi-spectral data. Accuracies were slightly lower than those achieved by Artificial Neural Networks (Pal and Mather 2003).

Object-based image analysis combines both spectral and spatial pattern recognition. Spatial pattern recognition involves pixel classification based on aspects as image texture, feature size and shape, repetition and context. Imagery is segmented into discrete objects before the objects are classified. In general, object-based approaches produce classifications that look more smooth than per-pixel based methods (Lillesand et al. 2015). Object-based classification was successfully used in combination with statistical DT classifiers by Franke et al. (2012) to classify different grassland types (See section 2.4.3.5). Also, Brenner et al. (2012) used vector-based image segmentation to map the presence of invasive Buffelgrass in Northern America.

2.4.3.5 Assessing grassland use intensity at parcel level

The number of studies that assess grassland use intensity and management at parcel level is still very limited (Asam et al. 2015; Sibanda et al. 2017). An important example of this type of research is the study performed by Franke et al. (2012). Since their work is used as main guide for the methodology applied in this thesis, a summary of their methods and results is given in this paragraph.

High spatial resolution (5 m), multi-spectral (5 bands: blue, green, red, red-edge, NIR), multi-temporal imagery (5 observation dates) acquired by the commercial RapidEye satellite was used to assess grassland use intensity for a research area in the Bavarian Alps, southern Germany. The researchers found that demand for this type of information was very high amongst ecology researchers and environmental protection agencies. Intensively used grasslands were defined as grasslands that are mown three to six times per year with a first mowing date between mid-April and beginning of May; these grasslands contain a low number of vascular plant species. Tilled grasslands consist of bare soil at the beginning of the growing season and are often used for producing maize. Extensively used grasslands are relatively species rich; the first mowing date is not before the end of May/beginning of June. Semi-natural grasslands are often found on wet or very dry sites, they contain a high number of species and are not used to produce hay.

To study vegetation dynamics, two VI's were calculated for 1500 sample points: the Normalized Difference Vegetation Index (NDVI) and the Normalized Red-edge Vegetation Index (NREVI), using the red-edge band available in RapidEye imagery. Also, a new indicator for grassland use intensity was developed, the Mean Absolute Spectrum Dynamic (MASD), representing spectral dynamics of the land surface over time (See section 5.4.2).

It was found that in April, extensively used grasslands displayed a wide NDVI range with a median of 0.6, whilst for intensively used grasslands the NDVI range was narrow with a median of ~0.81. After June, NDVI values for both intensive and extensively used grasslands showed the same fluctuation pattern that is mainly driven by mowing (Figure 2.5). The MASD parameter was found to be useful for identification of grassland use intensity at parcel level, because extensively used grasslands display low MASD values whereas intensively used grasslands have high spectral dynamics and therefore high MASD values.

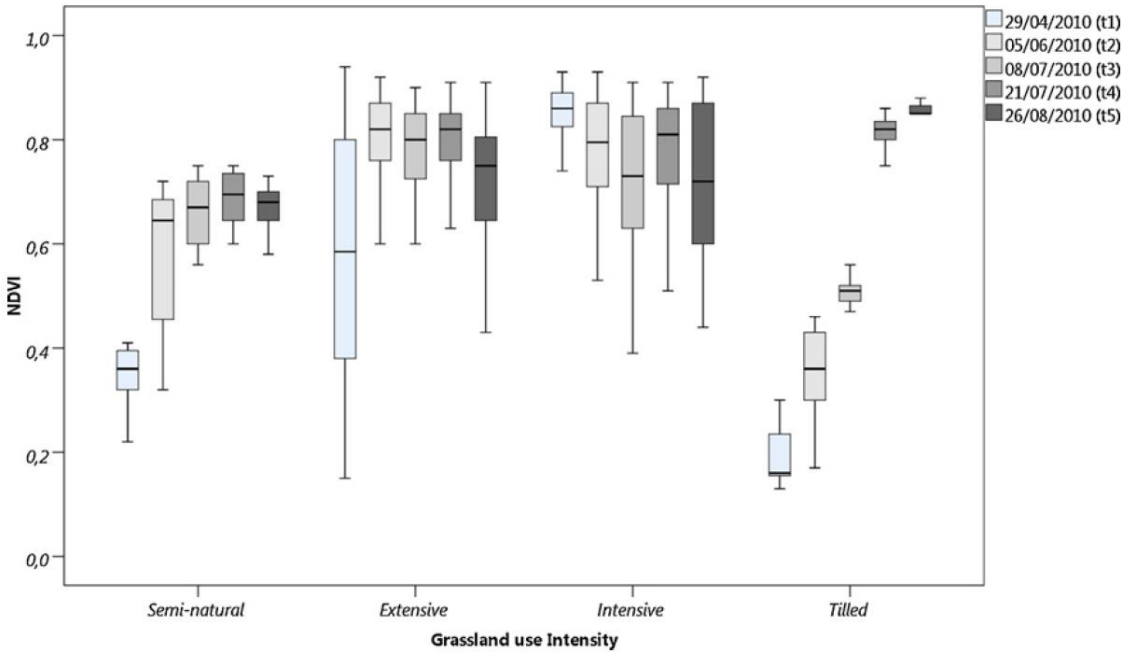

Figure 2.5: Box plots representing NDVI time series for grasslands with different use intensities. An early observation date allows accurate differentiation between intensively and extensively used grassland (from: Franke et al. 2012).

Two methods of grassland classification were used. First, a statistical classifier approach in which See5 decision tree software was used to generate a DT based on input of NDVI, NREVI and MASD values for 5 observation dates for 400 sample points (the training data). The DT can be translated into decision rules used for classification of RapidEye satellite imagery. The method was validated using the 1100 remaining sample points as test data.

The second approach is a context-based classification, incorporating knowledge on seasonal aspects of management practices in the study area for which a simple rule set was developed. E.g. it is assumed that mowing of grassland causes spectral changes and can therefore be used as an indicator of grassland use intensity. Both rule sets were implemented in eCognition, software for object-based classification. Combinations of different observation dates were tested. High overall accuracies were achieved using all 5 observation dates, with 85.7% for the statistical method and 82.7% for the context-based approach. Reduction to 3 observation dates led to decrease in overall accuracy to 82.2% for the statistical method and 74.8% for the context-based approach.

In conclusion, semi-natural grasslands, extensively used grasslands, intensively used grasslands and tilled grassland could be reliably distinguished at parcel level, however, influence of seasonal aspects should be taken into account for selection of adequate observation dates. Early observation is necessary because after the 1st mowing date, intensively and extensively used grasslands may reveal similar spectral characteristics.

2.4.4 The Spectral Variation Hypothesis

The Spectral Variation Hypothesis (SVH), posed by Palmer et al. in 2000, states that spatial variability in spectral reflectance, or spectral heterogeneity, is correlated to spatial variation in the environment and that objective measures of spectral variability can be used as a proxy for biodiversity (Palmer 2000; 2002; Rocchini et al. 2007; 2016). If this holds true, than RS can be used to gather information on biodiversity at a large scale. Instead of using classification methods to create discrete landcover/habitat classes, whereby a lot of information is lost, the original spatial pattern of reflectance is used to assess spectral heterogeneity (Palmer 2002). The SVH has been tested by various researchers. Gould (2000) calculated the variation in NDVI (using standard deviation), derived from Landsat TM imagery, for 17 plots of 0.5 km^2 in size with known species richness. Regression analysis was performed between measured species richness, NDVI variability and weighted vegetation type abundance. It was found that variation in NDVI and weighted abundance of vegetation types were significantly correlated to vascular species richness for all study sites.

Besides standard deviation of NDVI or the coefficient of variation (CV), various other measures of spectral heterogeneity have been proposed and used to predict species richness for different types of environments: e.g. variance of spectral response within a (pixel) neighborhood to predict woody-plant species richness in tropical dry forests (Gillespie 2005), the mean distance from the spectral centroid to predict species richness in the Tallgrass Prairie Preserve in Oklahoma, USA (Palmer et al. 2002) and the mean distance from the spectral centroid in a principal component space for grasslands in Sweden (Möckel et al. 2016), for savannah vegetation in Central Namibia (Oldeland et al. 2010), and Italian wetlands (Rocchini et al. 2007). These measures have been successfully used to predict species richness at local scale (Rocchini et al. 2016). However, there are some spatial scale related pitfalls in using RS data for species diversity estimation. If imagery with high spatial resolution is used (1-5 m), spatial heterogeneity may be contaminated by shadows whilst low resolution imagery may not be suitable for detection of fine-grained patterns (Rocchini et al. 2016). Viedma et al. (2012) investigated species richness and spectral heterogeneity at three scales, 1 m^2, 25 m^2 and 100 m^2. They found that the strength of the relationship between plant species richness and spectral heterogeneity increased with the size of spectral and vegetation sample areas. Total species richness could be satisfactory modeled at 100 m^2 scale using high spatial resolution Quickbird (4 m^2) imagery.

Scale related pitfalls are also illustrated by the research of Möckel et al. (2016) who tested the SVH for assessing species richness in grasslands. They used airborne hyperspectral data (415 - 2345 nm; 1 m spatial resolution) to predict fine scale plant species richness in grazed dry grasslands on the island of Öland, Sweden. Plant vascular species were recorded for 104 4x4 m plots and compared with a 245-waveband hyperspectral data set. Two modeling approaches to predict within plot diversity were used, 1) a spectral response approach, based on reflectance information for all bands and 2) a spectral heterogeneity approach based on mean distance to spectral centroid for the first five principal components. The spectral response approach successfully predicted species richness, but the spectral heterogeneity approach did not. The researchers suspect that the size of the plots was too small to establish a relationship between spectral heterogeneity and local plant species diversity (Möckel et al. 2016).

In conclusion, variability in spectral reflectance may be useful for assessing biodiversity, however, it is important to be aware of the influence of spatial and spectral scale and occurrence of e.g. shadows that will increase spectral heterogeneity.

3.0 Data

3.1 Sentinel-2 satellite data

3.1.1 The Sentinel-2 mission

The Sentinel-2 mission is part of six Sentinel missions, developed by ESA for the European Copernicus program. Aim of this program is effective environmental monitoring to help respond to the challenges of global change; e.g. to monitor land use change, to provide information for risk mapping and to support relief efforts in case of natural disasters or other humanitarian crises (ESA 2015a). Data acquired by the Sentinel missions will be made available free of charge to users all over the world (ESA 2015a).

The Sentinel-2 mission consists of two identical polar-orbiting satellites in the same sun-synchronous orbit phased at 180° to each other at a mean altitude of 786 km. Their revisit time is five days at the equator. The orbit inclination is 98.62° and the Mean Local Solar Time (MLST) at the descending node is 10:30 (am), similar to the overpass time of LANDSAT and SPOT (Satellite Pour l'Observation de la Terre) satellites. The first Sentinel satellite, Sentinel-2A was launched on June 23rd 2015 and its twin, Sentinel-2B was launched on March 7th 2017 (ESA 2017b). Geographical coverage comprises land and coastal areas from 56° South (Isla Hornos, Cape Horn, South America) to 83° North (above Greenland). Lifespan of the satellites is 7.25 years (ESA 2015b). The satellites are monitored and controlled through the Sentinel Core ground segment, which is also responsible for systematically processing, archiving and distribution of Sentinel data and monitoring of data quality; actual data is usually available within 3 to 24 hours (ESA 2015b).

Sentinel-2A and 2B are designed for multispectral high-resolution imaging of the earth in the tradition of NASA's LANDSAT program and the French SPOT missions. Both Sentinel-2 satellites carry a passive Multi Spectral Instrument (MSI) that collects sunlight reflected by the earth using a pushbroom sensor. The MSI collects data for 13 spectral bands in the Very Near Infra Red (VNIR) and Short Wave Infra Red (SWIR) spectra at 10, 20 or 60 m spatial resolution (Figure 3.1; Table 3.1). The orbital swath width is 290 km (ESA 2017a). Compared to the LANDSAT missions, the width of Sentinel-2 spectral bands is more narrow to reduce the influence of atmospheric constituents, e.g. water vapor (ESA 2015b) (Figure 3.1).

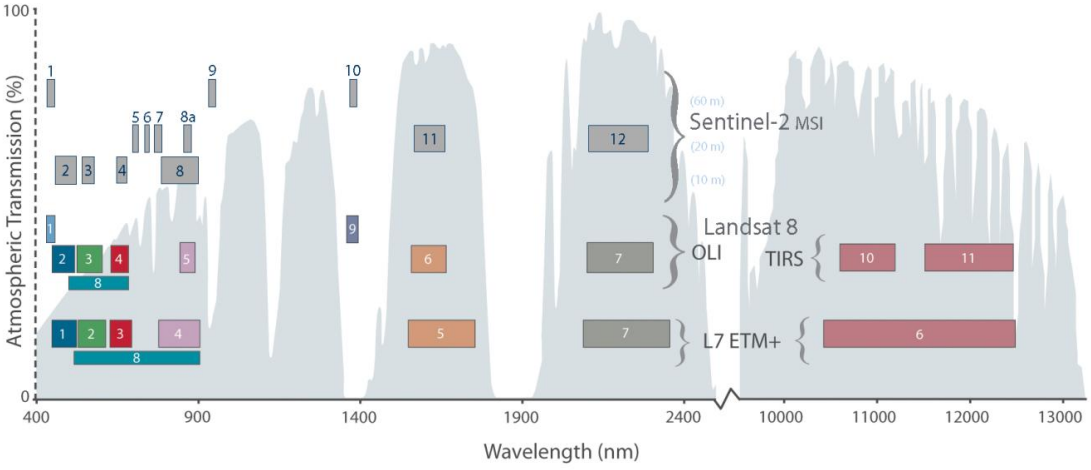

Figure 3.1: Comparison of LANDSAT 7 and 8 bands with Sentinel-2 (NASA 2017).

Table 3.1: Overview of spatial resolution, wavelengths, bandwidths and purposes of the Sentinel-2 Spectral bands (ESA 2017d; Lillesand et al. 2015). (VIS = visible light; NIR = Near Infrared; SWIR = Shortwave Infrared).

Spatial Res. (m)	Band Nr & Part of Spectrum	Central Wave-length (nm)	Band-width (nm)	Purpose
10	2 VIS Blue	490	65	Sensitive to vegetation senescing, carotenoid, browning and soil background; atmospheric correction (aerosol scattering).
	3 VIS Green	560	35	Green peak, sensitive to total chlorophyll in vegetation.
	4 VIS Red	665	30	Maximum chlorophyll absorption; calculation of NDVI, S2REP.
	8 NIR	842	115	Vegetation analysis; calculation of Leaf Area Index (LAI), NDVI.
20	5 Vegetation Red Edge	705	15	Position of red-edge S2REP; vegetation classification; consolidation of atmospheric corrections; fluorescence baseline.
	6 Vegetation Red Edge	740	15	Position of red-edge S2REP; vegetation classification; atmospheric correction, retrieval of aerosol load.
	7 Vegetation Red Edge	783	20	Is the edge of the Near-Infrared (NIR) plateau; vegetation classification; calculation of Leaf Area Index (LAI), S2REP.
	8a Narrow NIR	865	20	Vegetation classification; NIR plateau, sensitive to total chlorophyll, biomass, LAI and protein; water vapor absorption reference; retrieval of aerosol load and type; NDWI.
	11 SWIR	1610	90	Assessment of soil moisture/vegetation water content; calculation of NDWI (Normalized Difference Water Index). Also sensitive to lignin, starch and forest above ground biomass. Snow/ice/cloud separation.
	12 SWIR	2190	180	Assessment of Mediterranean vegetation conditions. Distinction of clay soils for the monitoring of soil erosion. Distinction between live biomass, dead biomass and soil, e.g. for burn scars mapping.
60	1 VIS Blue Aerosol	443	20	Atmospheric correction (aerosol scattering).
	9 Water vapor	945	20	Water vapor absorption, atmospheric correction.
	10 SWIR	1380	30	Detection of thin cirrus for atmospheric correction.

3.1.2 Capabilities of Sentinel-2 for vegetation analysis

Figure 3.2 shows the spectral response curves for dry grass and lawn grass in combination with the Sentinel-2 spectral bands. Noteworthy are bands 5 and 6 in the red-edge part of the spectrum, band 7 on the NIR edge and bands 8 and 8A on the NIR plateau. E.g. the Landsat 8 mission did not provide any reflectance measurements for the red-edge region (Figure 3.1). As explained in Chapter 2.0, the red-edge is the prominent increase in reflectance between the red absorption maximum and high reflectance in the NIR. The combination of band 5 and 6 therefore offers opportunities for improved characterization of the vegetation red-edge. First evaluations of the capabilities of Sentinel-2 for quantitative estimation of biophysical variables in vegetation have shown that the Sentinel-2 MSI sensor can successfully be used for estimating canopy chlorophyll content, leaf chlorophyll concentration and leaf area index (Frampton et al. 2013) as well as nitrogen content (Clevers and Gitelson 2013; Ramoelo et al. 2015). A new VI has been developed for Sentinel-2, the Sentinel-2 Red-edge Position index (S2REP). This VI uses the Sentinel-2 red-edge bands 5 and 6 combined with NIR band 7 and red band 4 (Frampton et al. 2013). SWIR band 11 can be used in combination with B8A to calculate the Normalized Difference Water Index (NDWI) and assess differences in soil/vegetation moisture content (Demonceau 2016).

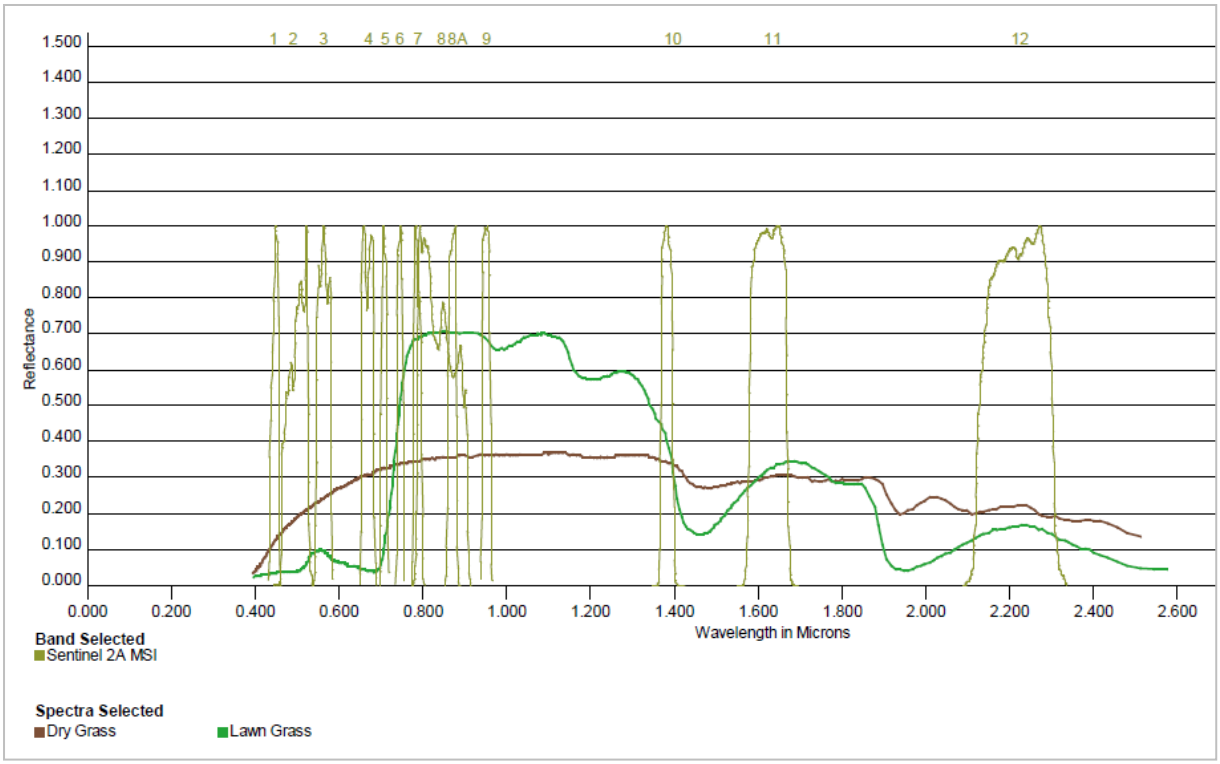

Figure 3.2: Spectral response curves of dry grass and lawn grass vs. distribution of Sentinel-2A spectral bands (USGS 2017).

3.1.3 Sentinel-2 data products

Five different product levels exist: Level-0, Level-1A, Level-1B, Level-1C and Level-2A (Table 3.2). Currently, only Level-1C tiles are available for download through the ESA Copernicus Sentinels Scientific Data Hub (ESA 2017c). Image data is in JPEG2000 format. The elementary Sentinel-2 MSI data products are granules of a fixed size depending on the product level. Granules or tiles for Level-1C and Level-2A orthorectified products are 100 x 100 km squared ortho-images in the UTM-WGS84 projected coordinate system (ESA 2015b). Digital Numbers (DNs) for Level-1C images represent top-of-atmosphere (TOA) reflectance values. The Sentinel Core ground segment systematically processes MSI data up to Level-1C (ESA 2015b). Level-2A products can be generated on the user side by applying atmospheric correction using the Sen2Cor algorithm (See section 3.2.1) that can be implemented in ESA's Sentinel Application Platform (SNAP) software. This algorithm converts TOA to bottom-of-atmosphere (BOA) reflectance values (ESA 2015b).

Table 3.2: Sentinel-2 product types (ESA 2015b).

Sentinel-2 Product type	Specification
Level-0	Compressed raw image data & ancillary data to generate the next level products. Tile size: 25 across track x 23 km along track.
Level-1A	Decompressed raw image data; geometric model. Tile size: 25 x 23 km.
Level-1B	Radiometrically corrected imagery in Top-Of-Atmosphere (TOA) radiance values and in sensor geometry & refined geometric model which is used to generate the Level-1C product. Radiometric corrections applied are: dark signal, pixels response non uniformity, crosstalk correction, defective pixels interpolation, high spatial resolution bands restoration (deconvolution plus denoising), binning (spatial filtering) for 60 m bands. Tile size: 25 x 23 km. File size: 27 MB.
Level-1C	The Level-1C product results from using a Digital Elevation Model (DEM) to project the image in cartographic geometry. Per-pixel radiometric measurements are provided in Top Of Atmosphere (TOA) reflectance along with the parameters to transform them into radiance. Level-1C products are resampled with a constant Ground Sampling Distance (GSD) of 10, 20 and 60 m depending on the native resolution of the different spectral bands. Cloud, Land and Water masks are generated. Tile size: 100 x 100 km. File size: 500 MB.
Level-2A	Bottom Of Atmosphere (BOA) corrected reflectance images derived from the associated Level-1C products through atmospheric correction. Level-2A products are not systematically generated at the ground segment but can be generated by the user through the Sentinel-2 toolbox. The final product includes a scene classification image, aerosol optical thickness map and water vapor map together with quality indicators for cloud and snow probabilities at 60 m resolution. Tile size: 100 x 100 km in UTM WGS84 cartographic projection. File size: 600 MB.

3.1.4 Overview of used Sentinel-2 Level-1C datasets

Nine Sentinel-2 (almost) cloud free datasets for South-Central Friesland are available for the growing season of 2016 (Table 3.3). These datasets were downloaded using ESA's Scientific Data Hub (ESA 2017c). The data were unzipped using 7Zip software (Pavlov 2016). The long filenames may cause problems when other unzip software is used. The projected coordinate system for all datasets is WGS84 / UTM zone 31N EPSG:32631.

Table 3.3: Overview of available cloud-free Sentinel-2 datasets for the 2016 growing season. Values for solar zenith and viewing geometry (Mean view zenith angle and Sun zenith angle) were taken from the pixel that represents Itens, Littenseradiel.

Granules	Acquisition Date + Time	Mean view zenith angle	Sun zenith angle	Cloudy pixel %	Degraded MSI data %
S2A_OPER_MSI_L1C_TL_SGS__20160312T181201_A003766_T31UFU_N02.01	12 March 10:50:37	3.48°	57.20°	0.0104	0
S2A_OPER_MSI_L1C_TL_SGS__20160401T163301_A004052_T31UFU_N02.01	1 April 10:50:24	3.46°	49.21°	22.6475	0
S2A_OPER_MSI_L1C_TL_SGS__20160411T150737_A004195_T31UFU_N02.01	11 April 10:50:25	3.47°	45.38°	0	0
S2A_OPER_MSI_L1C_TL_MPS__20160421T130055_A004338_T31UFU_N02.01	21 April 10:50:29	3.51°	41.81°	0.8841	0
S2A_OPER_MSI_L1C_TL_SGS__20160508T163213_A004581_T31UFU_N02.02	8 May 10:40:27	9.77°	37.05°	0.0032	0
S2A_OPER_MSI_L1C_TL_SGS__20160607T162830_A005010_T31UFU_N02.02	7 June 10:40:26	9.80°	31.78°	10.3119	0
S2A_OPER_MSI_L1C_TL_MTI__20160727T121350_A005625_T31UFU_N02.04	20 July 10:55:47	3.54°	33.87°	0	0
S2A_OPER_MSI_L1C_TL_SGS__20160908T161324_A006340_T31UFU_N02.04	8 Sept. 10:54:16	3.56°	48.36°	0	0
S2A_OPER_MSI_L1C_TL_SGS__20160925T161027_A006583_T31UFU_N02.04	25 Sept. 10:41:15	9.88°	54.98°	0	0

3.2 Data processing

3.2.1 Atmospheric correction

To be able to compare Sentinel-2 images from different acquisition dates, sun elevation correction, earth-sun distance correction and atmospheric correction are necessary (Lillesand et al. 2015). Sun elevation correction accounts for differences in seasonal position (elevation angle) of the sun relative to the earth whilst earth-sun distance correction is used to normalize for seasonal changes in earth-sun distance (Lillesand et al. 2015). The sun elevation angle is complementary to the sun zenith angle (Table 3.3). Under extreme view zenith angles, atmospheric path length may vary considerably (Lillesand et al. 2015). View zenith angles taken from the pixel overlying Itens, Littenseradiel, vary between 3.46 and 9.88 degrees (Table 3.3); these small angles will have little effect on atmospheric path length. Also, atmospheric correction compensates for effects of atmospheric scattering and absorption and takes into account differences in atmospheric conditions and solar geometry (Lillesand 2015). Sun elevation and earth-sun distance corrections are applied by the data provider when Level-1C TOA reflectance products are generated (ESA 2017e). Atmospheric correction has to be performed by the data user (ESA 2015b).

Therefore, the first step in data processing was to run the Sen2Cor (V2.3.0) Level-2A processor implemented in SNAP 5.0, at 10 m resolution to generate atmospherically corrected Level-2A surface BOA reflectance products for all downloaded datasets. Default settings were used for Look-up table selection (=rural (continental) aerosol type, mid latitude summer). Figure 3.3 shows the Sen2Cor processing steps. The Sen2Cor processor performs atmospheric, terrain (optional DEM) and cirrus correction and provides a scene classification image (Mueller-Wilm 2016). The Sen2Cor algorithm relies on a database of radiative transfer look-up tables which has been compiled using an atmospheric radiative transfer model based on libRadtran1, this is a library for calculation of solar and thermal radiation in the Earth's atmosphere (Mueller-Wilm 2016). Look-up tables have been generated for different atmospheric conditions, solar geometries and ground elevations (Mueller-Wilm 2016). The Atmospheric Precorrected Differential Absorption (APDA) algorithm is used to retrieve the water vapor content from Level-1C images (Louis et al. 2016). The Aerosol Optical Thickness (AOT) is estimated using the Dark Dense Vegetation (DDV) pixel method; this requires that the image contains areas of known reflectance behavior, dark dense vegetation or dark soil/water bodies (Louis et al. 2016; Mueller-Wilm 2016). Cirrus correction is applied using Sentinel-2 band 10 (Mueller-Wilm 2016).

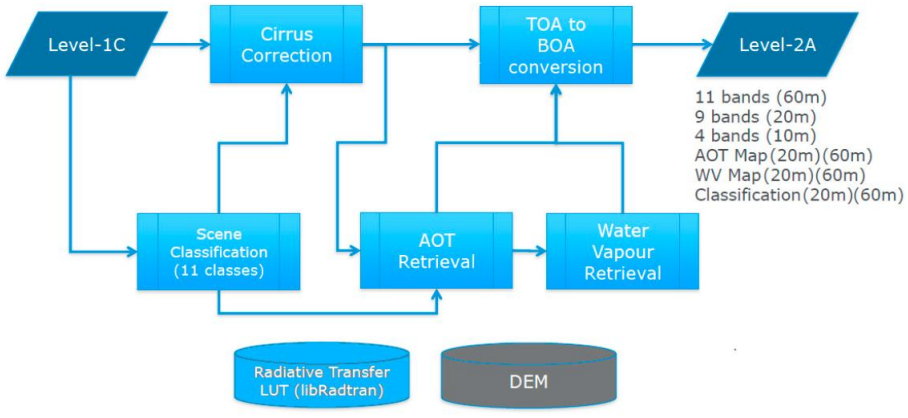

Figure 3.3: Sen2Cor processing steps (Louis et al. 2016).

3.2.2 Creation of data subset

Using SNAP 5.0, data subsets were created for all Level-2A datasets. These subsets show the South-Central Friesland study area, including the Littenseradiel and Grouw field survey areas (Figure 3.4). The extent ranges from top: 5700, left: 4507, right: 10067 and bottom: 342 in pixel numbers. This is top: 5896610, left: 658263, right: 700613 and bottom: 5854960 in WGS1984_UTM_31N coordinates. Creating subsets required resampling of all bands to 10 m resolution.

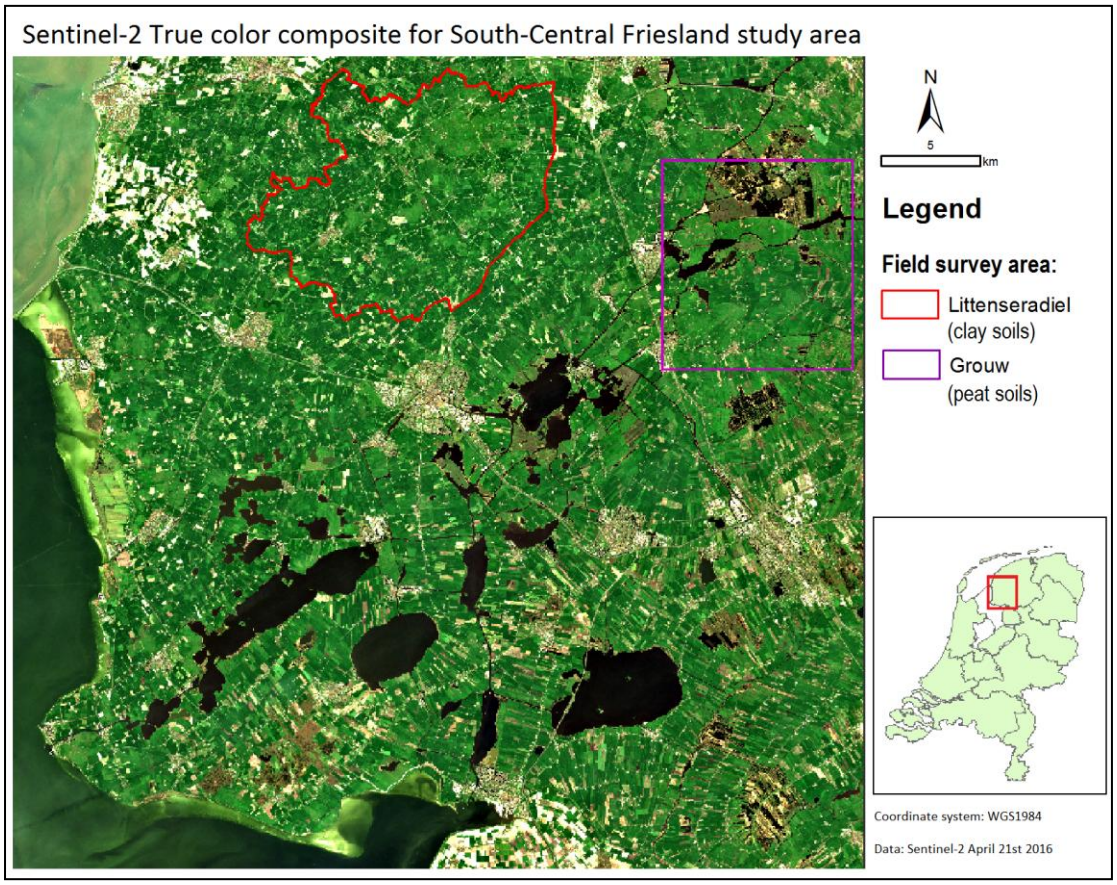

Figure 3.4: True color composite (B4-B3-B2) of Sentinel-2 image of the South-Central Friesland study area for April 21st 2016, with the outlines of Littenseradiel and Grouw field survey areas.

3.3 Ancillary data

Besides Sentinel-2 satellite images, additional data were used and integrated into a Geographic Information System (GIS). In Table 3.4 an overview of these datasets is provided. Whilst QGIS 2.18.1 was used for analysis and classification, ArcGIS 10.3.1 was used to make the maps, since some of the datasets were only available through ArcGIS online.

Selection of extensive grassland areas was based on the dataset of nature management plans (Provincie Fryslân 2016). Selection of clay and peat soil areas was based on the soil map and map of landscape types (Provincie Fryslân 2016). The cropland registration dataset for 2016, '*BRP Gewaspercelen*', was used to create a grassland mask (Nationaal georegister 2017).

GIS point data on distribution of meadow bird nests in Littenseradiel for 2016 (except for Skrok and Skrins), was provided by the Bond Friese Vogelwachten. This data is gathered by volunteers who register the coordinates of each nest using a mobile phone app (BFVW 2017). For Skrok and Skrins, data on the total number of meadow bird territories for 2016 were provided by

Natuurmonumenten (De Boer and De Winter 2016). The nest distribution will be compared with the grassland management intensity maps.

In addition to these datasets, a database of biologic/organic/meadow bird friendly farmers was created, based on data from the *Red de rijke weide* website (Vogelbescherming 2017) and other web-based sources, e.g. websites of biological farmshops. From this database a vector point file was generated in ArcGIS. The database may not be complete; to my knowledge no publicly available official list with addresses of biologic/organic farmers exists.

A vector shapefile was created showing the outlines of relevant (meadow) bird reserves (Appendix A). This was done in ArcGIS by digitizing boundaries of relevant features of the Dutch National Nature Network (EHS), which was available in ArcGIS online (Bodematlas Provincie Fryslân 2016). The biologic farmers shapefile and the EHS shapefile are used as overlay to further validate the grassland management intensity maps.

Table 3.4: Overview of additional ancillary datasets that have been used.

Name	Source	Type	Scale/resolution	Date	Projected coordinate system
Soil map (Groundwater levels)	Alterra Wageningen	Vector	1:50.000	2006	RD New
Administrative boundaries	PDOK	Vector	Variable, 10 m accuracy	2016	RD New
Meadow bird reserves (beheergebieden/natuurbeheerplan)	Provinciaal georegister Provincie Fryslân	Vector	1:10.000	2016 + 2017	RD New
Registration of croplands (BRP-gewaspercelen 2016 definitief)	Nationaal georegister	Vector	1:10.000	2016	RD New
Soil map	Bodematlas Provincie Fryslân (ArcGIS Online)	Vector	Variable	2016	RD New
Dutch Ecological Network/National Nature Network (Natuurnetwerk Nederland, formerly Ecologische Hoofdstructuur (EHS))	Bodematlas Provincie Fryslân (ArcGIS Online)	Vector	Variable	2016	RD New
Agricultural Nature Management Plans (SNL)	Portaal Natuur en Landschap	Vector	Variable	2016	RD New
Nest counts of meadow birds for Littenseradiel	Bond Friese VogelWachten	Vector	Variable	2016	RD New
Territory counts of meadow birds for Skrok and Skrins	Natuurmonumenten	Paper list	-	2016	-
MODIS13Q 16 day EVI time series	USGS	Raster	250 m	2016	Sinusoidal

4.0 Study area

4.1 Study area: South-Central Friesland

The study area comprises South-Central Friesland, an area of ca. 161.000 ha, in the north of the Netherlands (Figure 4.1). It contains (parts of) the municipalities: Fryske Marren, Súdwest Fryslân, Heerenveen, Littenseradiel, Harlingen, Leeuwarden, Franekeradeel, Tytsjerksteradiel, Opsterland and Smallingerland. The population number for these municipalities is 374.687 in total (December 2016) (CBS 2017).

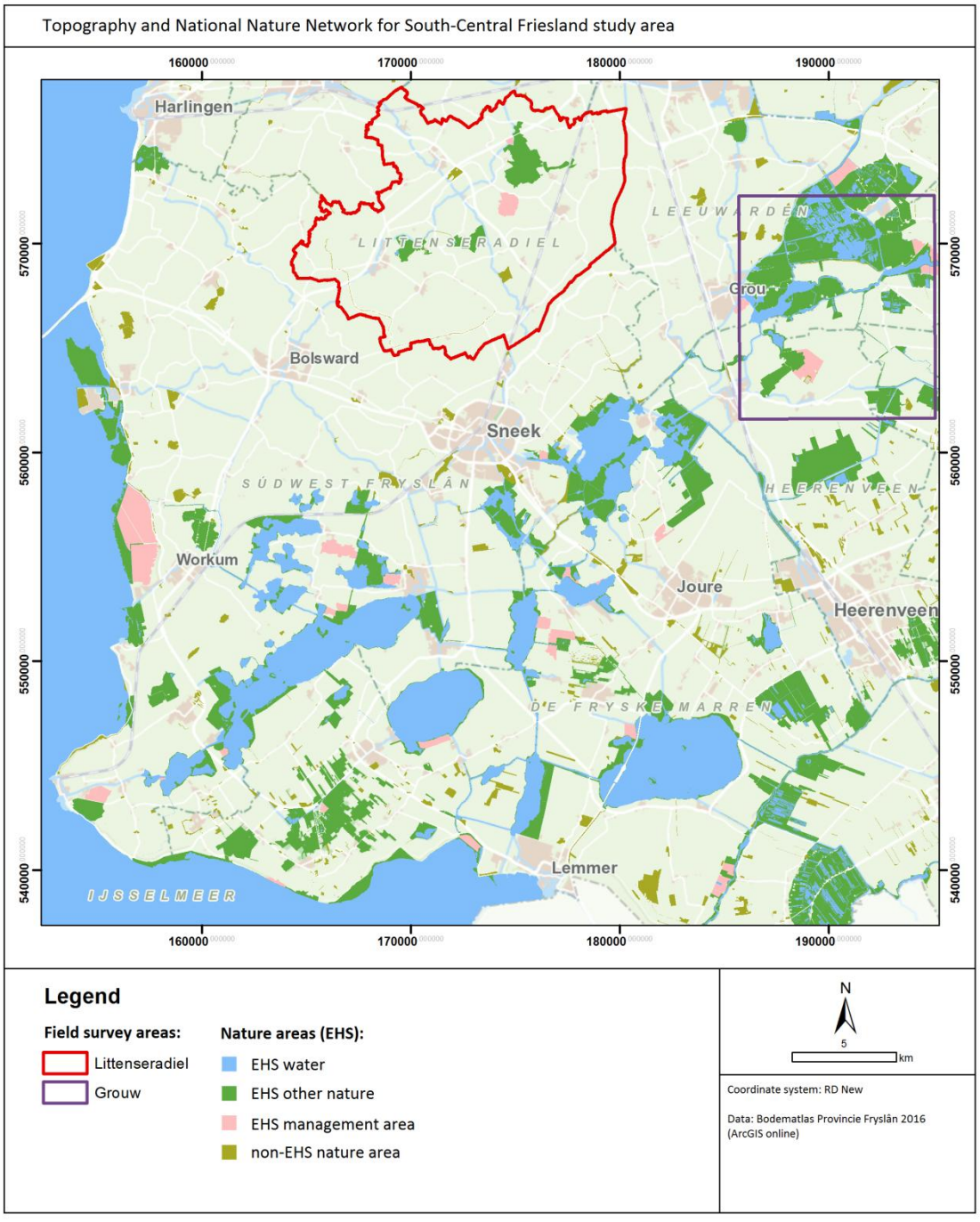

Figure 4.1: South-Central Friesland study area, with Grouw and Littenseradiel field survey areas and the Dutch National Nature Network, formerly known as Ecological Network (EHS); See Appendix A for annotated map showing important (meadow) bird areas (Provincie Fryslân 2016).

The study area contains the region South West Friesland (which lies south-west of Sneek) which was designated one of the twenty national landscapes in the Netherlands in 2005 (Schroor 2012). In this region a relatively large area of grassland is used for biological farming: 1437 ha in 2014, 4.2% of the total surface area of biological grassland in the Netherlands (CBS 2014). Within the study area, there are also numerous smaller nature areas and other protected areas that are part of the Dutch Nature Network, the former ecological network (EHS) (Appendix A). An important nature area is 'De Alde Feanen' National Park near Grouw (See section 4.3). Friesland has a temperate maritime climate with an average temperature of 9.6 to 9.9°C and ca. 850 mm rain per year (KNMI 2017). The majority of the population lives in the main urban areas: Leeuwarden, Harlingen, Heerenveen, Sneek and Lemmer. Small villages and hamlets are scattered throughout the area.

Land cover is dominated by grassland, used for sheep- and cattle farming. Near Harlingen and Franeker, areas with arable land dominate. In Gaasterland and near St. Nicolaasga, some forest cover exists (Provincie Fryslân 2016). A large area of South West Friesland consists of lakes that are interconnected through canals.

To study the influence of soil type on spectral reflectance values, two field survey areas were chosen within the study area: Littenseradiel, representing an area with clay soils and Grouw, an area dominated by peat soils (Figure 4.2).

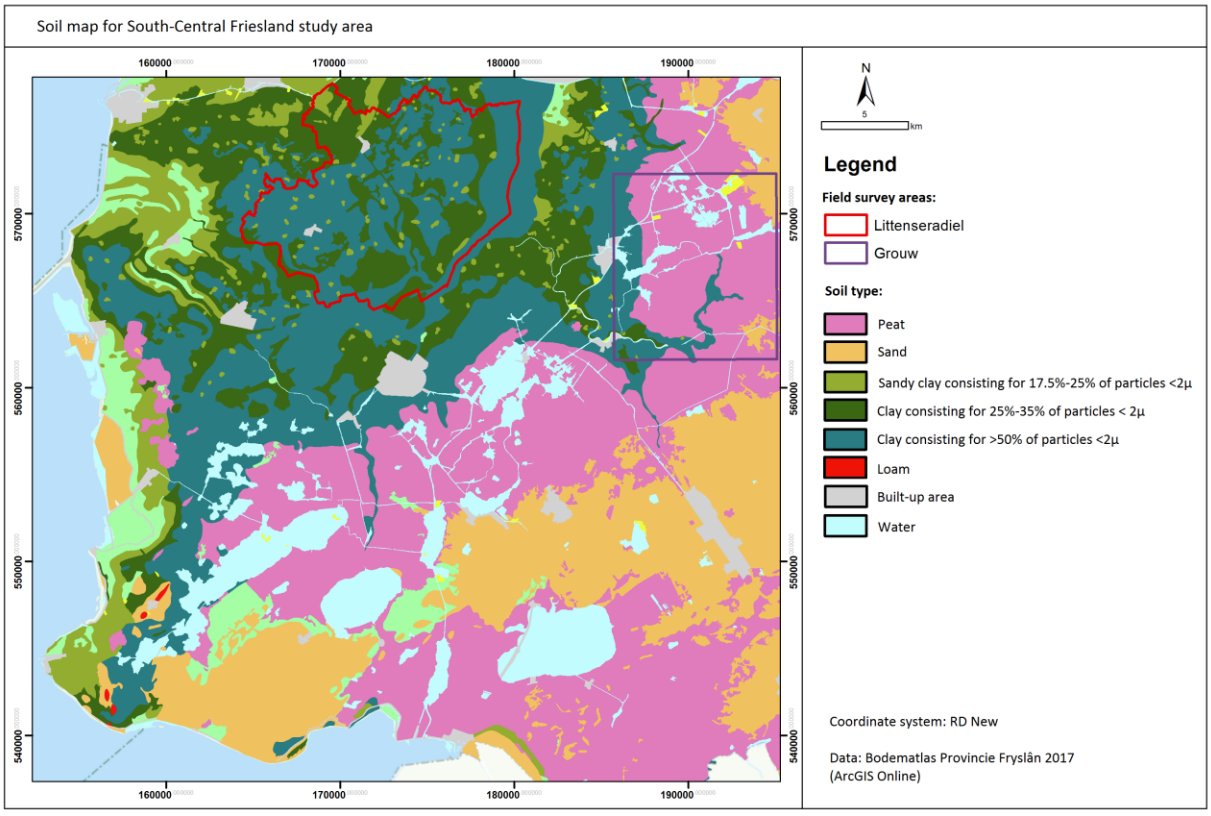

Figure 4.2: Soil map of South-Central Friesland showing the Littenseradiel (clay soils) and Grouw (peat soils) field survey areas (Provincie Fryslân 2017).

Elevation

In rugged areas, topographic (illumination) effects may influence spectral response (Moreira et al. 2016). In South-Central Friesland this will not cause any problems because the landscape is relatively flat; elevation ranges from 3.0 m below mean sea level in polder areas, to 12.7 m above mean sea level on the highest push moraines in Gaasterland (Schroor 2012)(Figure 4.3). Nature areas, including areas with extensive grassland management, are often found in the lower parts of the study area. Here, groundwater levels are usually higher (See Figure 4.9).

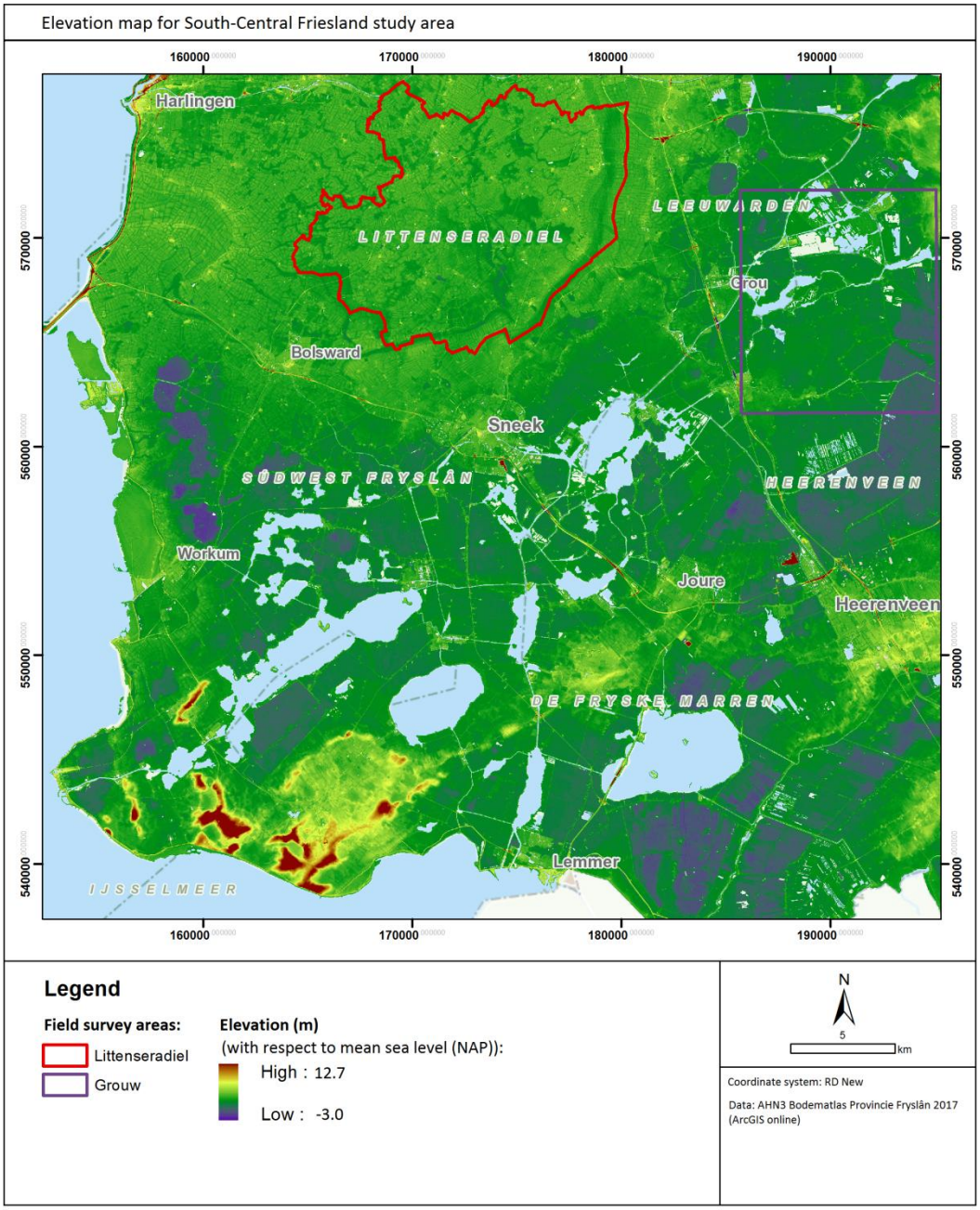

Figure 4.3: Elevation map of study area. AHN3 50x50cm resolution (Provincie Fryslân 2017).

4.2 Field survey area Littenseradiel

The field survey area for clay soils consists of the municipality Littenseradiel (13.200 ha) in the center of Friesland (Figure 4.4). This region was chosen because it is one of the core areas for meadow birds. Another reason for choosing this municipality is the author's knowledge of this area, which is important when validating results of Remote Sensing (ground truthing). Compared to other parts of the Netherlands, Littenseradiel is relatively sparsely populated with a population of 10.740 people (December 2016) (CBS 2017b). Littenseradiel contains three large bird reserves that will be used as areas representing extensively managed grassland: Skrok, Skrins and Lionserpolder (Figure 4.4). The landscape in the field survey area is very open and almost completely covered by grasslands, 10.900 ha in total, mostly used for cattle farming. Of this area, only 3700 ha is occupied by grassland used for biological farming (CBS 2014). Average parcel size in Littenseradiel is 2.4 ha.

An important trend here, as well as in the rest of the Netherlands, is that smaller farms disappear and only a few large intensive farms remain with growing numbers of milking cows (CBS 2016). With this development, grassland use has intensified as well. Many farmers have switched to growing high produce, protein-rich ryegrass types and maize and have installed underground drainage systems to replace foot drains (Groen et al. 2012). In 2014, there were eight registered organic/biodynamic farms in Littenseradiel (CBS 2014).

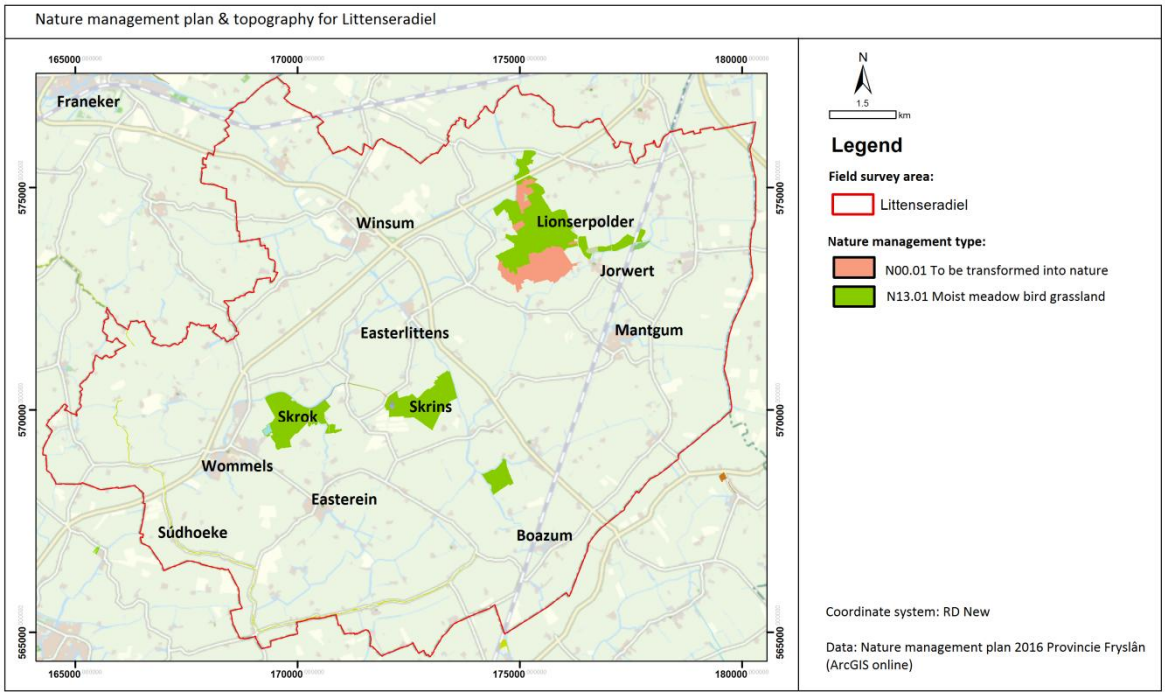

Figure 4.4: Nature management plan 2016 and topography for Littenseradiel (Provincie Fryslân 2016).

Skrok, Skrins and Lionserpolder

The meadow bird reserves, Skrok (105 ha), Skrins (99 ha) and 102 ha of the Lionserpolder (337 ha) are managed by the Dutch association Natuurmonumenten. All three reserves are part of the Dutch National Nature Network. Natuurmonumenten bought their first parcels in Skrok and Skrins in 1983; development of the Lionserpolder started in 1991 (De Boer et al. 2006). These reserves belong to the best meadow bird areas of Friesland; every spring, large numbers of meadow birds use these areas for breeding (Oosterveld & Hoekema 2012). The reserves are not only important for meadow birds, but have high value in terms of cultural history as well. Here, the characteristic allotment structure is

preserved with its irregular parcel shapes and alternating pattern of foot drains and convex strips of grass (De Boer et al. 2006). Traces of the Middelzee delta (from ca. 1500-1200 BC) can still be seen in the landscape. The presence of saline seepage in Skrins and Lionserpolder is a reminder of the time when this area was flooded by the Middelzee. Plant species that tolerate salty soils can be found here (De Boer et al. 2006).

Traditional agricultural methods are used for managing the grasslands. Natuurmonumenten contracts local farmers who can use the parcels for grazing (after May 1st) and production of hay (after June 15th). Alternating between grazing and mowing leads to variation in grassland structure. Every three to four years, dry goat manure is spread out on the parcels. Manure injection or artificial fertilizers are not allowed. Reeds, shrubs and unwanted plants, such as Curly Dock (*Rumex crispus,* Krulzuring), are removed to prevent settling of predators. Within all reserves, small ponds have been created that attract large numbers of migratory birds. Groundwater levels are kept high to preserve water in the ditches and foot drains (De Boer et al. 2006). Optimal groundwater level for godwits lies between 20 to 40 cm below ground level in spring and should not be deeper than 60 cm below ground level in summer (Oosterveld & Hoekema 2012).

According to the nature management plan, moist meadow bird grasslands (N13.01) are found in Skrok, Skrins and Lionserpolder (Figure 4.4). This category comprises wet and moist grasslands with slightly acid to neutral pH and may contain both herb-rich and nutrient rich ryegrass pastures (OBN 2015). However, grassland type in the three reserves is predominantly extensive, herb-rich grassland with Crested Dog's tail (*Cynosurus cristatus,* Kamgras) and Sweet Vernal grass *(Anthaxanthum odoratum,* Reukgras) (De Boer et al. 2006).

Agricultural Nature Management in Littenseradiel

Within Littenseradiel, agricultural nature management is organized by four collectives that fall within one of the seven collectives of Kollektivenberied Fryslân. Unfortunately, only data for individual management packages was available. The dominant management package is nest protection (Figure 4.5). In some parcels, resting periods are applied and there are a few herb-rich parcels. Recently, more moist *'plas-dras'* areas have been created (Figure 4.6).

Skriezekrite rûnom Skrok en Skrins

'Skriezekrite rûnom Skrok en Skrins' was a group that focused on protection of godwits in the area surrounding the Skrok and Skrins meadow bird reserves. Unfortunately, in 2017 the group ceased to exist. It was a joint effort of Natuurmonumenten, wildlife management group 'de Alde Slachte', local groups of the Bond Friese Vogelwachten (BFVW) and Murk Nijdam. Nijdam is a farmer with 42 ha of land in the 'Súdhoeke' near Wommels (See Figure 4.4), who has successfully adapted his management to optimize godwit breeding success. The Skriezekrite tried to stimulate farmers to complete their 1st cuts early in spring, well before godwit chicks have hatched, and to delay further mowing activity until after June 15th. Aim of this measure is to prevent death of chicks that wander from the 'safe' reserves into nearby intensively managed fields (Heitman et al. 2015).

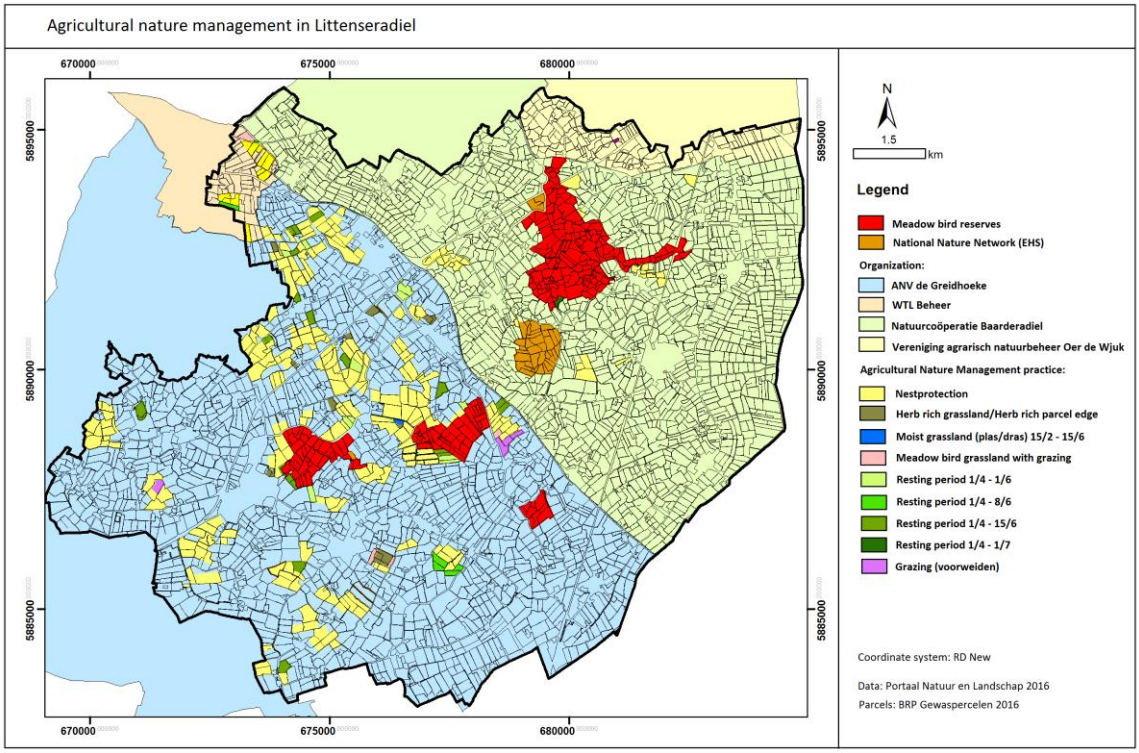

Figure 4.5: Agricultural Nature Management organizations and individual management packages for Littenseradiel 2016 (Portaal Natuur en Landschap 2016).

Figure 4.6: New *'plas-dras'* (shallow pond) on extensive grassland near Itens, Littenseradiel (March 2017).

Biodiversity

The 'Nationale databank flora en fauna' was consulted to acquire data on biodiversity for two 1 km^2 squares in Littenseradiel: Monoculture area: 169-571 (Bonkwerd); extensive area: 175-573 (Lionserpolder) (Figure 4.7). The table reveals that biodiversity of vascular plants *(vaatplanten)* and number of breeding birds *(broedvogels)* is higher for extensive than for monoculture grasslands in Littenseradiel (Nationale databank Flora en Fauna 2017). However, it should be noted that completeness of the species counts is rated as 'bad' *(slecht)* for most categories.

169 - 571	vaatplanten	landzoogdieren	broedvogels	wintervogels	vissen	dagvlinders
Rode-Lijstsoorten			3			
Vogelrichtlijn			7	129		
Habitatrichlijn						
WNB-andere soorten						
Aantal soorten	8	7	7	149	1	
Detaillering 0-0.25/0.251-1	12%/25%	59%/0%	98%/0%	3%/0%	100%/0%	
Volledigheid onderzoek	slecht	slecht	slecht*	redelijk*	slecht	niet
Onderzoeks-periode	1997-2017	2007-2017	2007-2017	2007-2017	2007-2017	2007-2017

175 - 573	vaatplanten	landzoogdieren	broedvogels	wintervogels	vissen	dagvlinders
Rode-Lijstsoorten	1		9			
Vogelrichtlijn			25	17		
Habitatrichlijn						
WNB-andere soorten						
Aantal soorten	37	5	26	32		2
Detaillering 0-0.25/0.251-1	98%/0%	30%/0%	80%/12%	0%/0%		66%/0%
Volledigheid onderzoek	slecht	slecht	goed	redelijk*	niet	goed
Onderzoeks-periode	1997-2017	2007-2017	2007-2017	2007-2017	2007-2017	2007-2017

Figure 4.7: Biodiversity for monoculture and extensive area in Littenseradiel (Nationale databank Flora & Fauna 2017).

4.3 Field survey area Grouw

The field survey area for peat soils is situated in a low-lying peat area of about 10.200 ha in Central Friesland, 'It Lege Midden' near the village Grouw (Figure 4.8). It contains part of the 'De Alde Feanen' National Park with several important meadow bird areas, e.g. 'De Burd' and the 'Wyldlannen' (Fûgelwacht Grouw 2015a; 2015b). The area consists mainly of small lakes, grasslands used for sheep and cattle farming and natural marshlands. Average parcel size is 2.5 ha. Local soil type is dominated by peat soils, but in the most western part of the field survey area including the western tip of De Burd, clay soils are also present (Figure 4.2). Ground cores for the clay soils on the western part of De Burd reveal that a thin layer of clay (ca. 40 cm), which is very rich in humus, lies on top of a thick peat layer (ca. 210 cm); peat layers on the eastern part of De Burd are not covered with clay (Dinoloket 2017). Peat was extracted in De Alde Feanen in the 18th and 19th century, creating a maze of small lakes and ditches interspersed with reedlands and marshes. Parts of the National Park have been protected nature areas since 1934 (De Vries 2017).

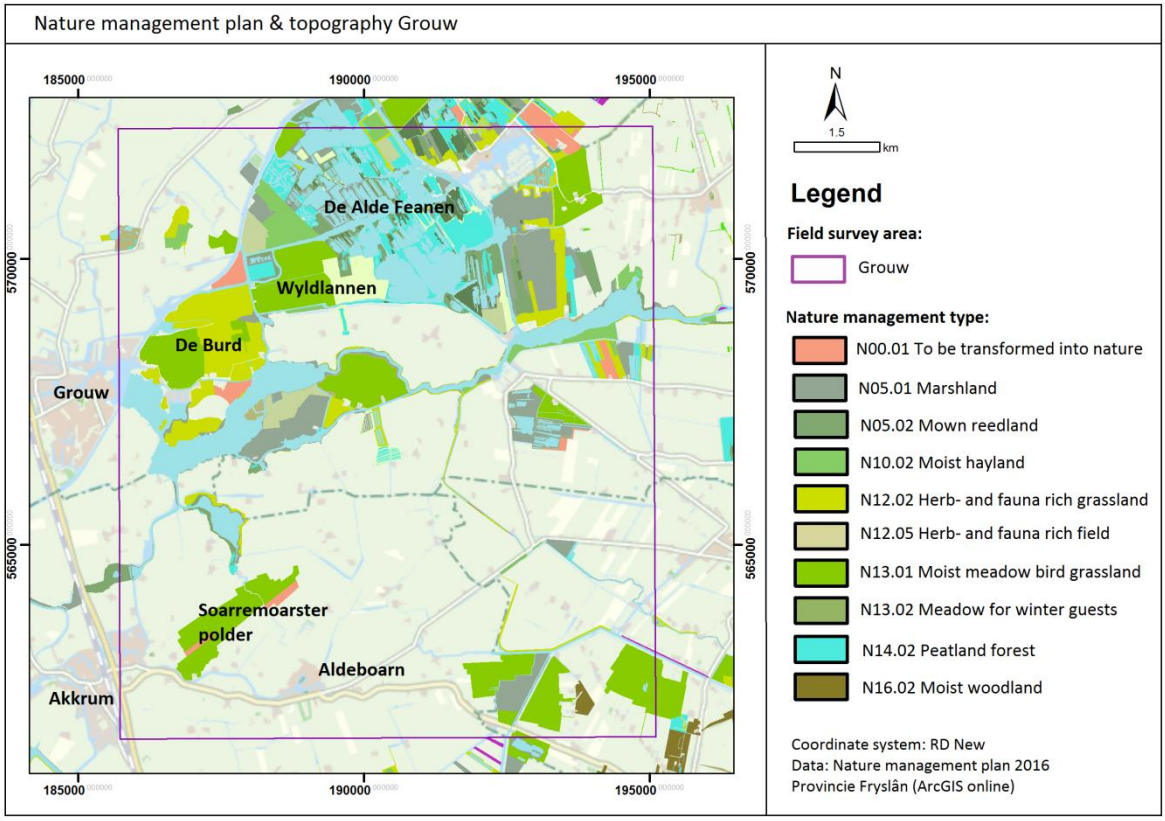

Figure 4.8: Nature management plan 2016 for Grouw area (Provincie Fryslân 2016).

De Burd and Wyldlannen

De Burd is an island to the east of the village Grouw (Figure 4.8). On the southern part of the island numerous holiday homes have been built; the rest of the island consists of grasslands protected by 'It Fryske Gea', a Friesian nature conservation organization. Within the grasslands, moist areas *'plas-dras*' have been created to attract meadow birds (Fûgelwacht Grouw 2015a). According to the nature management plan, grassland types consist of moist meadow bird grassland (N13.01), similar to the type found in Littenseradiel, and also herb-rich grassland (N12.02)(Provincie Fryslân 2017). Vegetation in these herb-rich grasslands can belong to different grassland types, e.g. Crested Dog's tail (*Cynosurus cristatus,* Kamgras) and Tufted grass (*Holcus lanatus,* Gestreepte Witbol). These grasslands are often used for production of hay and extensive grazing. Little to no manure or fertilizer is applied (OBN 2015).

The Wyldlannen area, also owned by It Fryske Gea, is used as resting place by godwits that return to their breeding grounds in early spring. It is a former marshland area that has been drained in the 20th century. During the winter the meadows are inundated (Fûgelwacht Grouw 2015b).

Agricultural Nature management

In the Grouw area there are at least seven biological/organic/meadow bird friendly farmers, of which six are situated close to the village Aldeboarn. In this area, five agricultural nature organizations successfully work together in the cooperation 'It Lege Midden'. They focus on protection of meadow birds and conservation of herb-rich grasslands (KBF 2017).

4.4 Groundwater levels

Besides a difference in soil type, differences in soil moisture may exist for Littenseradiel and Grouw. In the low-lying peat area near Grouw, groundwater levels are usually higher than in Littenseradiel (Figure 4.9). High groundwater levels in springtime slow down grass growth (See section 2.1.3). Soil moisture content also directly influences spectral response. E.g. for bare soils, higher soil moisture content results in decreased reflectance in the visible and NIR regions (Jensen 2007). In the field survey areas, presence of vegetation cover will partly compensate for this effect, but this depends on vegetation density. Also, the clay soils in Littenseradiel have a good capacity of retaining rain water, further reducing differences in soil moisture between clay and peat soils.

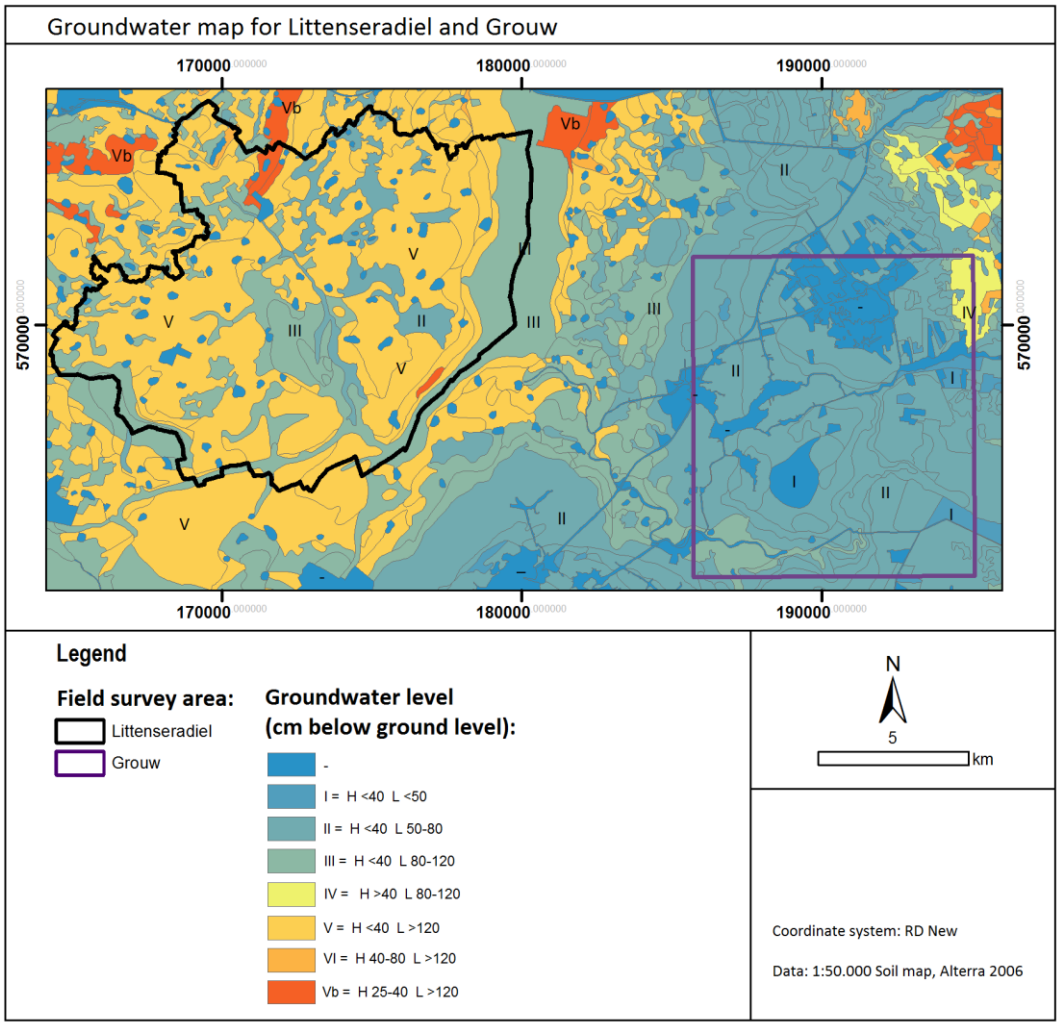

Figure 4.9: Average groundwater levels in Littenseradiel and Grouw (Alterra 2006).

4.5 Local weather and timeline of agricultural activities in 2016

The growing speed of grass is strongly dependent on temperature and precipitation (See section 2.1). These factors will also influence NDVI and S2REP vegetation index time series, causing e.g. seasonal fluctuations. To be able to interpret the vegetation index time series it is essential to have knowledge of the local climate. Therefore, a summary of the weather conditions for Friesland in 2016 is given here in combination with the timeline of agricultural activities.

Compared to other years, January 2016 was relatively mild (Table 4.1). It was also a wet month with more precipitation than usual (Figure 4.11)(KNMI 2016a). February was also mild and wet but with more sunshine than usual. From the second half of February onwards, farmers started with manure injection, continuing with spreading artificial fertilizer and dragging of pastures until the end of March (Hoekstra 2017). March was a lot colder than usual and overall quite dry and sunny but with some very wet days in the beginning and towards the end of the month. April was cold as well, more than 1°C colder than usual, especially during the second half of the month (Figure 4.10). During the first half of the month, there were some warmer days. April was also very wet but from April 18th onwards, there was a short dry period, during which a few farmers already mowed some of their parcels. Despite the rain, April saw more hours of sunshine than usual. Farmers let their cows out to pasture at the end of April, beginning of May (Hoekstra 2017).

May was very warm, sunny and dry, with less precipitation than normal (Figure 4.10). Between May 6th and May 12th, day temperatures reached ca. 25 °C and the nights were also warm. For farmers, this was an excellent opportunity for the first silage harvest. Overall, June was wet and cloudy but with normal temperatures. Many pastures were mown for the 2nd time in the first weeks of June (Hoekstra 2017). July was dry, quite sunny and warm, especially during the second half of the month; between July 18th and July 21st temperatures reached 28-30 °C, a good opportunity for farmers to mow extensive pastures and to produce hay. The first half of August was cooler than normal, but the second half was relatively warm and dry with some very hot days between August 24th and 27th. The amount of precipitation varied strongly per region. September was much warmer than usual and also quite dry. Especially during the first half of the month, temperatures reached 25 °C and higher. After September 19th, temperatures dropped, especially during the night. The first half of September was also a good period to mow both intensive and extensive pastures. Warm conditions in the fall led to continuation of mowing until late October.

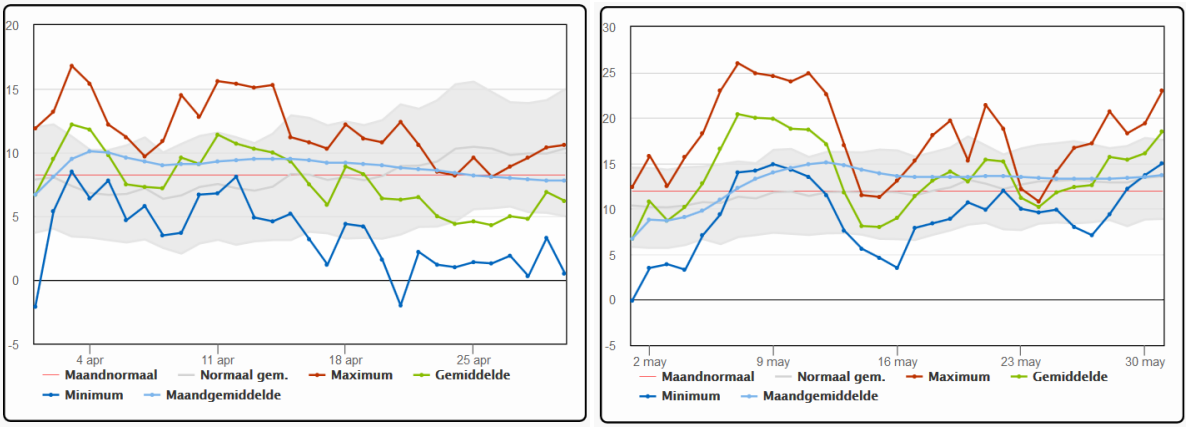

Figure 4.10: Temperatures in April and May 2016 for the KNMI weather station in Leeuwarden (Weerstation Hallum 2016).

Table 4.1: Average temperature per month (°C) (KNMI weather station Leeuwarden).

Month	Normal	2015	2016
January	3.1	3.9	3.3
February	3.3	3.2	4.2
March	6.2	5.8	4.8
April	9.2	7.6	7.8
May	13.1	11.1	13.7
June	15.6	14.0	15.6
July	17.9	17.4	17.5
August	17.5	18.0	17.2
September	14.5	13.3	17.5

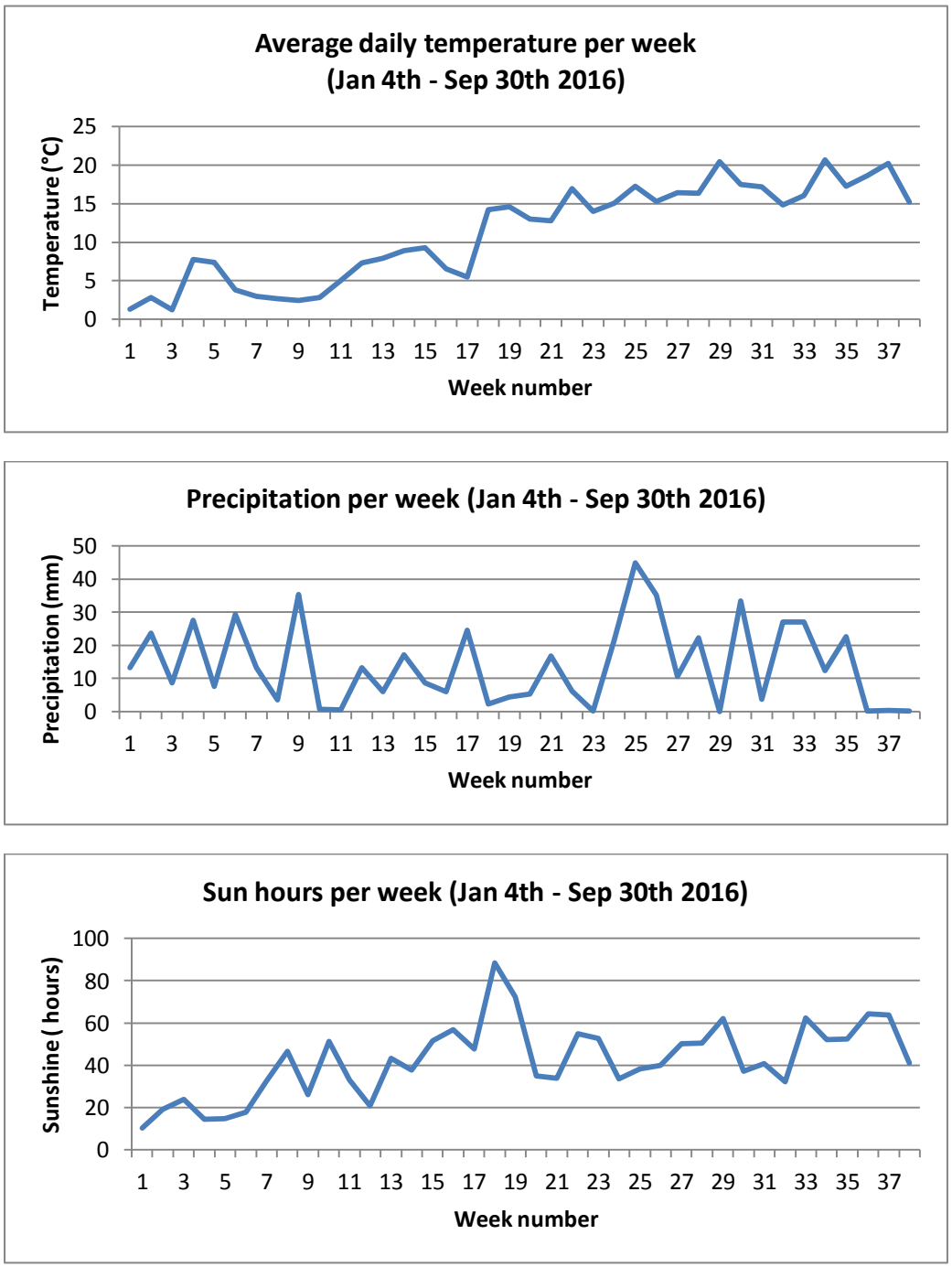

Figure 4.11: Graphs showing average daily temperature, amount of precipitation and sun hours per week (starting at January 4th) for 2016 for the KNMI weather station in Leeuwarden.

5.0 Methods

5.1 Methods workflow

Figure 5.1 summarizes the methodology that was used for this research. Data collection and preparation were already discussed in Chapter 3.0. Field survey methods, data analysis, classification and accuracy assessment will be explained in the next paragraphs.

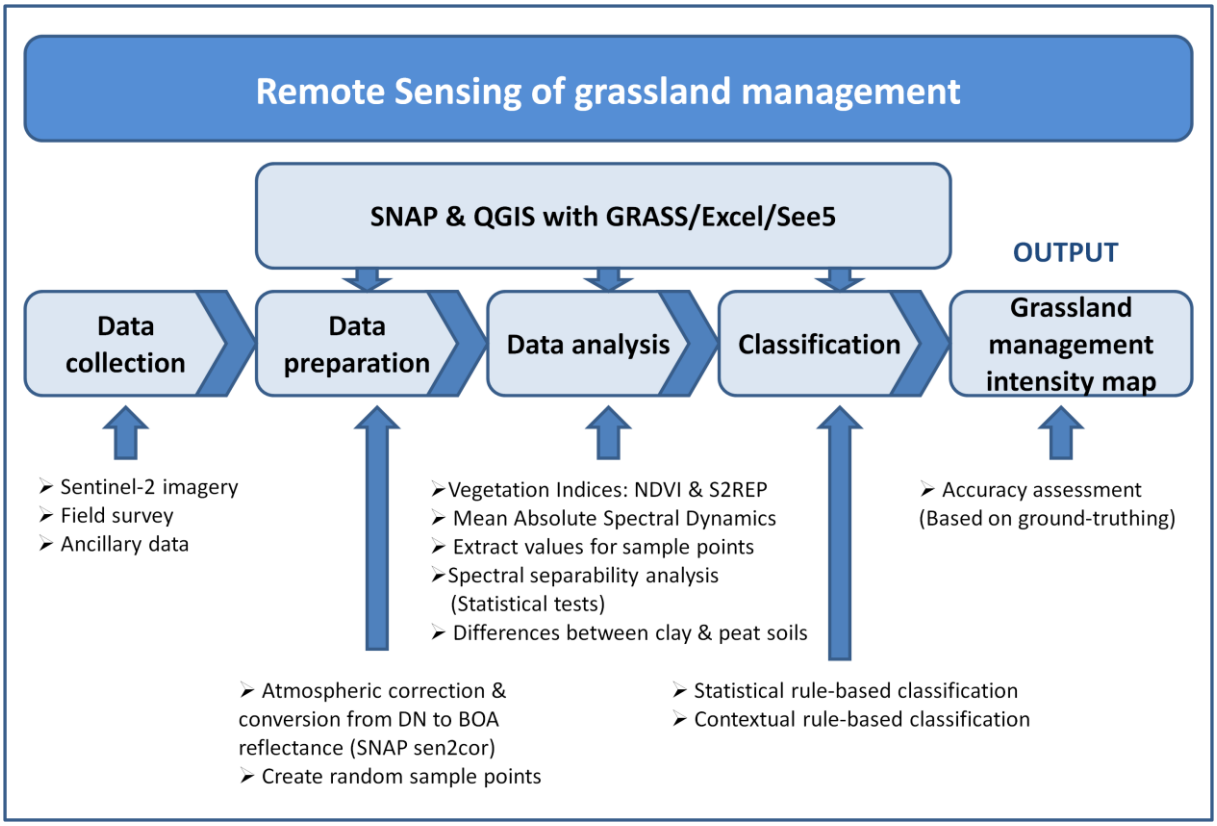

Figure 5.1: Methods workflow.

5.2 Field survey & ground truthing

In October 2016 a field survey was performed by bicycle to roughly identify grassland management at parcel level. Based on this survey, areas with monoculture grassland were selected (Figures 5.2 and 5.3). Known bird reserves, derived from maps of nature management plans (Provincie Fryslân 2016), were chosen to represent areas with extensive management and herb-rich grass. Parcel geometry for grasslands was extracted from the 2016 cropland registration dataset (Nationaal georegister 2017). Surface areas of both grassland categories are comparable (Table 5.1). The field survey was repeated thoroughly in the second half of April 2017 when differences in grassland management intensity are most pronounced, thanks to the presence of flowering herbs. Grassland in Littenseradiel was inspected by bicycle and on foot. To achieve ground truthing for areas that could not be reached, high resolution Google Earth imagery from May 7th 2016 was used. Traces of liquid manure injection, characteristic for monoculture grasslands, are visible on these images. Presence of foot drains is also visible, these are characteristic for extensive grasslands (Groen et al. 2012). A vector map showing the distribution of grassland type for each parcel was created for the whole of Littenseradiel. This map has been used for accuracy assessment. Discrepancies in the ground truth data may arise because the Sentinel-2 satellite imagery dates from 2016 and the field survey was performed in 2017. E.g. re-seeding of grassland may lead to misclassification.

Table 5.1: Surface area of selected sample parcels for monoculture and extensive grassland.

Littenseradiel	Size (m^2)	Nr. of parcels
Monoculture	4830310	153
Extensive (Bird reserves)	4825080	231
Grouw	**Size (m^2)**	**Nr. of parcels**
Monoculture	5223500	250
Extensive (Bird reserves)	5307690	161

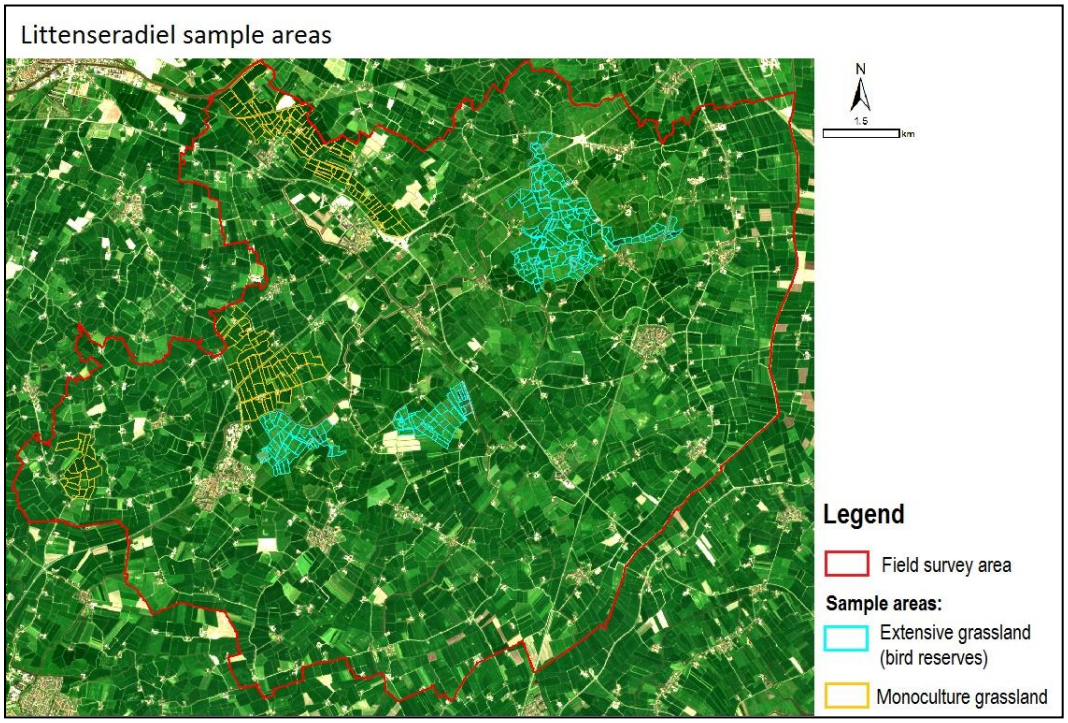

Figure 5.2: True color composite (RGB = B4-B3-B2) of Littenseradiel field survey area on April 21st, 2016, showing the outlines of the extensive and monoculture sample areas (Data source: ESA Sentinel-2).

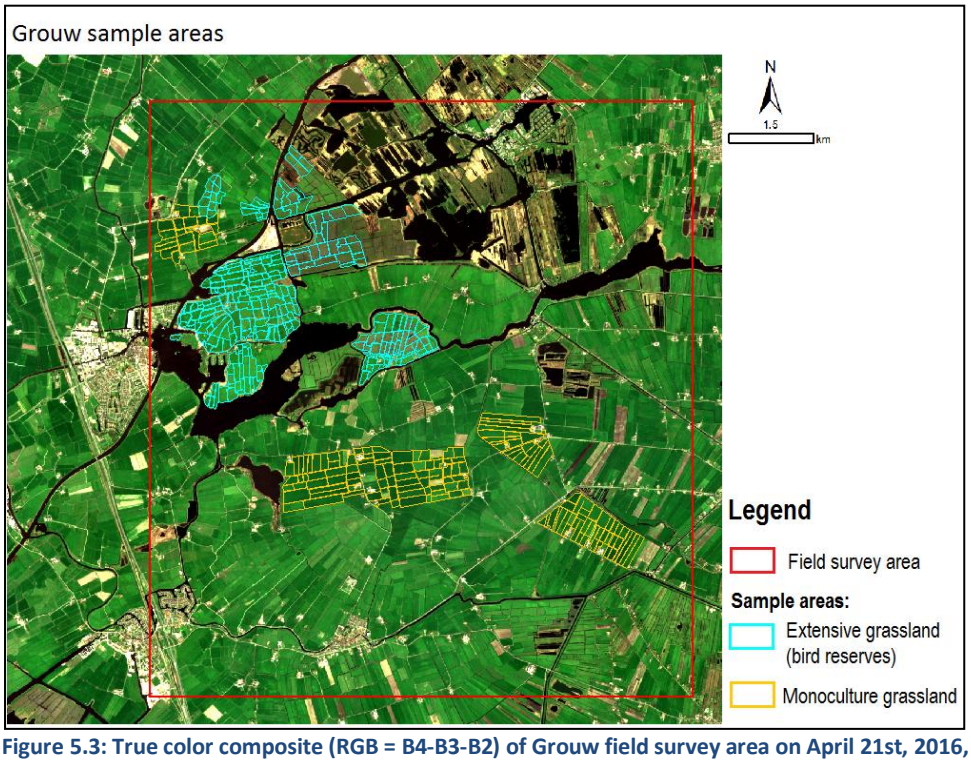

Figure 5.3: True color composite (RGB = B4-B3-B2) of Grouw field survey area on April 21st, 2016, showing the outlines of the extensive and monoculture sample areas (Data source: ESA Sentinel-2).

5.3 Sample points

Using QGIS Desktop 2.18.1 with GRASS 7.0.5, 400 random sample points were created within the polygons of extensive grassland for clay soils (Littenseradiel) and peat soils (Grouw). Because Sentinel-2 images have a spatial resolution of 10 m for bands 2, 3, 4 and 8, a distance of at least 10 m was chosen between the sample points to avoid duplicate samples. The same procedure was applied for polygons of monoculture grassland. All 1600 sample points were imported into SNAP as ESRI shapefiles and used as mask to extract reflectance, NDVI and S2REP values for these points for the whole time series which comprises nine observation dates. Data were saved as a tab delimited text file that could be analyzed in Microsoft Excel. In Excel, sample points affected by cirrus clouds were excluded, this was only necessary for the dataset of June 7th.

5.4 Spectral separability

Spectral separability of extensive and monoculture grassland and differences between clay and peat soils were assessed by analyzing spectral reflectance curves based on mean reflectance values. Also, coincident spectral plots were created (Lillesand et al. 2015). Based on analysis of the spectral response curves (Figure 6.1), it was decided to use the NDVI and the S2REP to discriminate between the four grassland categories. The Mean Absolute Spectral Dynamics (MASD) (Franke et al. 2012), was added to test its usefulness for grassland classification. NDVI and S2REP vegetation indices and MASD were calculated using SNAP 5.0.

5.4.1 Vegetation indices

NDVI

The Normalized Difference Vegetation Index, based on the difference of reflectance in NIR and red spectral bands, was first proposed by Rouse et al. (1974) to identify areas with vegetation. Vegetated areas will yield high NDVI values because vegetation reflects NIR light and chlorophyll absorbs red light. The index has been used in countless studies for vegetation monitoring and assessment (Lillesand et al. 2015; Frampton et al. 2013).

NDVI was calculated for all nine images of the 2016 time series using the NDVI processor in the thematic land processing tools in SNAP 5.0. Sentinel-2 bands 4 (red) and 8 (NIR) were used for the NDVI calculation as advised by ESA in the Sentinel-2 technical guide (ESA 2017f).
NDVI Formula:

$$\mathrm{NDVI} = \frac{\rho_{\mathrm{nir}} - \rho_{\mathrm{red}}}{\rho_{\mathrm{nir}} + \rho_{\mathrm{red}}}$$

S2REP

The Sentinel-2 Red-edge Position (S2REP) vegetation index can be used as an indicator for chlorophyll content (Frampton et al. 2013). S2REP was calculated using the S2REP processor in the thematic land processing tools in SNAP 5.0. It uses the Sentinel-2 red-edge bands 5 and 6, combined with band 7, the edge of the NIR plateau and band 4, the red band. The S2REP results from the following (sensor-dependent) equation (Frampton et al. 2013):

$$\begin{aligned}\mathrm{S2REP} &= 705 + 35 * \frac{\left(\frac{\rho\mathrm{NIR}+\rho R}{2}\right) - \rho\mathrm{RE1}}{\rho\mathrm{RE2} - \rho\mathrm{RE1}} \\ &= 705 + 35 * \frac{\left(\frac{\rho 783+\rho 665}{2}\right) - \rho 705}{\rho 740 - \rho 705}\end{aligned}$$

Translated into Sentinel-2 bands, the formula is: 705 + 35 * ((((B7 + B4)/2) - B5) / (B6 - B5)).
The formula is based on the calculation of the red-edge inflection point developed by Guyot and Baret (1988). In this method it is assumed that the reflectance curve at the red-edge can be simplified into a straight line which is centered around a midpoint between the reflectance minimum (= maximum chlorophyll absorption) located at 665 nm (B4) and the NIR reflectance at 783 nm (B7) on the edge of the NIR plateau (Table 3.1). Reflectance measurements in B7 and B4 are used to estimate reflectance for the red-edge inflection point. A linear interpolation procedure is then applied between 705 nm (B5) and 740 nm (B6) to establish the inflection point wavelength, or Red-edge Position (REP). The constants 705 and 35 are derived from interpolation in the 705 and 740 nm interval (Cho et al. 2008). 740 nm is the maximum value for the Red-Edge Position; the S2REP range for vegetated areas lies between 690 and 740 (ESA Step Forum 2017). Values outside this range were removed as outliers.

Besides atmospheric correction, smoothing of NDVI and S2REP time series through applying e.g. filtering methods was not applied because of the risk of loss of small fluctuations which may represent grazing or mowing (Halabuk et al. 2015).

5.4.2 Mean Absolute Spectral Dynamic

The Mean Absolute Spectral Dynamic (MASD) is an indicator of spectral variability for each pixel over two or more observation dates. It represents vegetation dynamics throughout the growing season and can be used as an indicator for grassland use intensity (Franke et al. 2012). The MASD parameter is calculated as follows:

$$\mathrm{MASD} = \frac{1}{m-1}\sum_{t=1}^{m-1}\left(\frac{1}{n}\sum_{i=b}^{n}|\rho_i^t - \rho_i^{t+1}|\right)$$

Here, *m* is the number of observation dates, *t* is the observation date, *n* is the number of spectral bands, *b* is the spectral band, and *ρ* is the pixel reflectance (Franke et al. 2012). If the MASD is calculated for two observation dates, it gives the mean absolute change between these dates. It should be noted that MASD only describes the magnitude of the spectral response and does not give any information on the spectral shape.

MASD was calculated using Raster Band math in SNAP 5.0. MASD4_spring is based on the images for April 1st, April 11th, April 21st and May 8th, indicating spectral variability before the 1st mowing date of extensive grasslands. MASD7_total (April-September) also includes July 20th, September 8th and September 25th to assess spectral variability during the entire growing season. March 12th and June 7th were excluded because of presence of clouds. Also, MASD between subsequent observation dates was calculated.

5.4.3 Statistical tests

All statistical tests were performed using XLSTAT implemented in Microsoft Excel (Addinsoft 2015a). Data were tested for normality using the Shapiro-Wilk test. Mean values for NDVI, S2REP, MASD and reflectance for monoculture and extensive grasslands on peat and clay soils and values for peat vs. clay soils were compared using the Mann-Whitney U test. This non-parametric test can be used to compare independent samples if data is not normally distributed; the test determines whether samples can be considered identical or not, based on their ranks (Addinsoft 2015b). The non-parametric Kolmogorov-Smirnov test was used to compare distributions for NDVI, S2REP, MASD and reflectance values for all nine observation dates (Addinsoft 2015c).

5.4.4 Spectral heterogeneity

According to the Spectral Variation Hypothesis (SVH), spatial variation in reflectance is correlated to spatial variation in the environment and species richness (Palmer 2000; 2002). Therefore, in herb-rich grasslands with a high variety in species, higher spectral heterogeneity is expected. To assess spectral variability for extensive and monoculture grasslands, variance in reflectance was calculated for all sample points.

Spectral heterogeneity within grassland parcels was assessed based on the calculation of the mean distance to the spectral centroid (Rocchini et al. 2010; 2007; Oldeland et al. 2010)(Figure 5.4). First, principal component analysis (PCA) for the Sentinel-2 image of April 21st was carried out in QGIS to reduce the number of dimensions. Next, using ArcGIS 10.3.1, pixel values for PC1 and PC2 were extracted for 5 sampling units of 1 ha in size (100 pixels) for extensive, herb-rich grassland and 5 sampling units for monoculture grassland. These values were exported to an Excel workbook. In Excel, mean values for PC1 en PC2 were calculated, this represents the spectral centroid which can be plotted in a two-dimensional coordinate system (Figure 5.4). Distance from each (PC1, PC2) coordinate to spectral centroid was calculated using Pythagoras:

Distance to centroid = square root ((value PC1 - mean PC1)^2 + (value PC2 - mean PC2)^2)

Finally, the mean distance was calculated by adding all distances and dividing by 100.

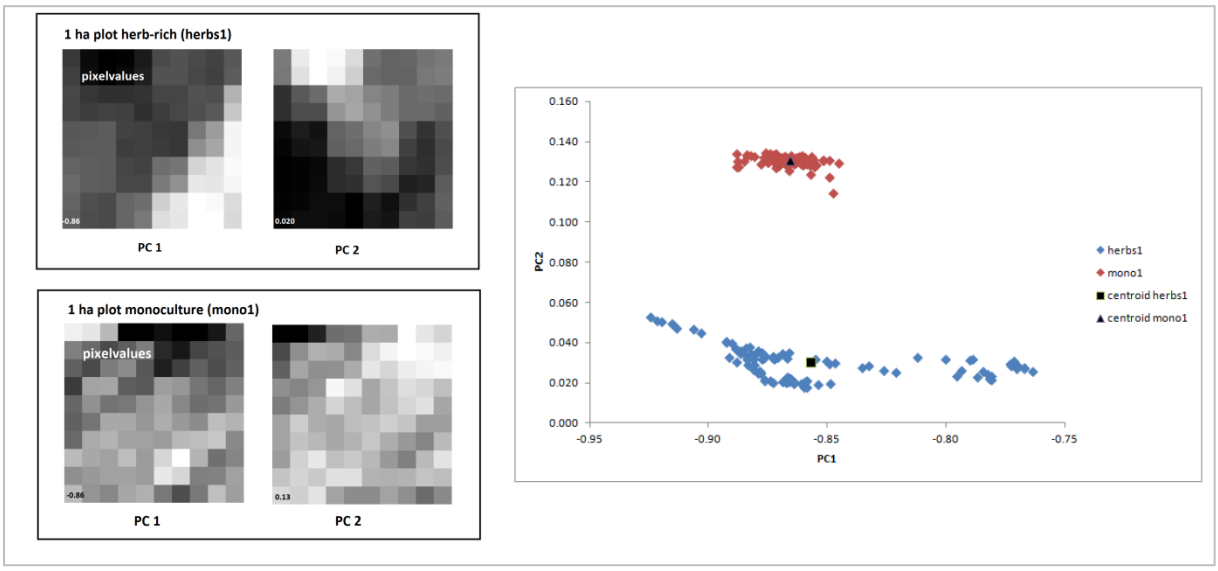

Figure 5.4: Example of calculation of spectral heterogeneity for herb-rich and monoculture plots of 1 ha in size (100 pixels). Values for PC1 and PC2 pixels are plotted in 2D; black square = spectral centroid for herb-rich plot, black triangle = spectral centroid for monoculture plot. SVH predicts the higher the distance from the centroid, the higher the spectral variability and species richness (After: Rocchini et al. 2007).

5.5 Classification

5.5.1 See5 data mining software

See5 is a form of machine learning that aims to discover patterns in data that allow classification into categories (Rulequest Research 2017). See5 uses the univariate decision tree (DT) algorithm See5.0/C5.0, the successor of C4.5 developed by Quinlan in 1993 (Kotsiantis 2007). Univariate means that decision boundaries at each tree node depend on the outcome of a test applied to one feature at a time, in contrast to multivariate DT's that use multiple features simultaneously. An advantage of See5 is that it can handle different data types in one run, e.g. nominal and numerical data, continuous and discrete data (Pal and Mather 2003).

The measure that is used by See5 to partition data into different classes is the normalized information gain (the difference in entropy) (Santini 2015). At each node of the DT, the algorithm aims to decrease the entropy of the dataset by creating subsets that are more homogeneous (Santini 2015). The procedure is recursively repeated, creating new branches on the tree, until all data is classified (Pal and Mather 2003; Kotsiantis 2007). This may lead to very large and complex DT's. If the training data contains noise, e.g. samples that do not belong to the class they are thought to represent, overfitting may occur. Overfitting may lead to poor performance of the classifier when predicting data classes for new datasets. To avoid overfitting, the DT's may be pruned; the number of branches is reduced (Pal and Mather 2003; Kotsiantis 2007).

The demo version of See5 v2.10 (Rulequest Research 2017) was used to establish NDVI and S2REP thresholds that allow classification of monoculture and extensive grasslands on clay and peat soils. The created DT can be used to derive decision rules that can be implemented in QGIS. See5 will also give information on which attributes are the most important for classification.

5.5.2 Statistical rule-based classification

The See5 demo version only allows a maximum of 400 sample points as training input. Therefore, from the original 1600 training sample points, 400 random points were selected as training input for See5: 100 sample points for monoculture grassland on clay soils, 100 for monoculture on peat soils, 100 for extensive grassland on clay soils and 100 for extensive on peat soils. The remaining sample points were used as test data to evaluate the decision rules. Studies have shown that up to a size of 2100 input pixels, classification accuracy increases with the size of the training set. But it was also found that a training data set size of 300 samples per class provided an adequate description of land cover variations (Pal and Mather 2003).

Using SNAP 5.0, pixel values for all sample points were extracted for 27 attributes, NDVI and S2REP for 9 observation dates and MASD4_spring, MASD7_total and the MASD between subsequent observation dates (Table 5.2). In Excel, data was prepared to be used for analysis with See5.
The decision rules that were generated by See5 were implemented in QGIS and classification was performed using the Semi-Automatic Classification Plugin version 5.2.4 (Congedo 2016)(Appendix K). The importance of specific attributes for classification was tested by removing e.g. April 21st values and repeating the See5 analysis.

Table 5.2: Attributes used for Statistical rule-based classification in See5.

Attribute	Data type	Attribute	Data type
grasslandtype.	| the target attribute	S2REP8May:	continuous.
grasslandtype:	extensive, monoculture.	S2REP7June:	continuous.
NDVI12March:	continuous.	S2REP20July:	continuous.
NDVI1April:	continuous.	S2REP8Sep:	continuous.
NDVI11April:	continuous.	S2REP25Sep:	continuous.
NDVI21April:	continuous.	MASD1Apr11Apr:	continuous.
NDVI8May:	continuous.	MASD11Apr21Apr:	continuous.
NDVI7June:	continuous.	MASD21Apr8May:	continuous.
NDVI20July:	continuous.	MASD8May20July:	continuous.
NDVI8Sep:	continuous.	MASD20July8Sep:	continuous.
NDVI25Sep:	continuous.	MASD8Sep25Sep:	continuous.
S2REP12March:	continuous.	MASD4spring:	continuous.
S2REP1April:	continuous.	MASD7total:	continuous.
S2REP11April:	continuous.	ID:	label.
S2REP21April:	continuous.		

5.5.3 Contextual rule-based classification

Contextual rule-based classification aims to test if good classification results can be achieved by implementing simplified decision rules generated by See5 when only MASD4_spring values, S2REP and NDVI for April 21st are used. It also aims to improve the results of the statistical rule-based classification by incorporating knowledge on first mowing date. It uses only two Sentinel-2 scenes, April 11th and April 21st. See5 derived decision rules are combined with a threshold value of -0.1 for the NDVI change between April 11th and April 21st, which is used to identify fields mown before April 21st. This threshold value is based on the mowing model (See sections 5.7 and 7.2.1). If this threshold is not added to the decision rules, mown monoculture fields are misclassified as extensive grasslands. The decision rules were implemented in QGIS using the SCP (Appendix K).

5.6 Accuracy assessment

For accuracy assessment, the ground truthed grassland vector map for the whole of Littenseradiel is used as reference. From a sampling design point of view, one should not use pixels for validation that were already used for training. However, training data for Littenseradiel was based on just 200 pixels compared to the total of 1092409 classified pixels that were used for validation.

Accuracy assessment is performed using the SCP in QGIS (Congeda 2016). The SCP converts the ground truthed grassland vector shapefile into raster and generates error matrices and error raster maps, calculates overall accuracy, producer's and user's accuracy and Kappa statistics. The Kappa coefficient or KHAT statistic can be used to test whether differences between two images are due to chance or real (dis)agreement. This is especially useful when the number of classes is small, because in a two category classification an accuracy of 50% may be reached solely due to random chance (Lillesand et al. 2015). Calculation of the Kappa coefficient or KHAT statistic is based on the error matrix. True agreement will approach 1 and chance agreement approaches 0. It can also be used to compare classification accuracy between the two used methods (Lillesand et al. 2015). A conceptual definition of KHAT is:

$$\hat{K} = \frac{\text{observed accuracy - chance agreement}}{1 - \text{chance agreement}}$$

Overall accuracy is calculated as the total number of correctly categorized pixels divided by the total number of pixels. Producer's accuracy is the number of correctly classified pixels for each class divided by the total number of pixels for that class in the reference raster. User's accuracy is the number of correctly classified pixels for each class divided by the total number of pixels for that class in the classified raster; this measure of commission represents the probability that a pixel that is classified into e.g. monoculture actually represents monoculture grassland on the ground (Lillesand et al. 2015).

5.7 Detection of mowing and grazing

For meadow bird conservation it is important to have an accurate model for detection of 1st mowing dates for individual parcels. It would also be of interest to know whether birds are nesting in parcels that are grazed by cattle or sheep. Mowing will cause a strong, sudden decrease in biomass and crop height; also, patches of bare soil may become visible (Dussaux et al. 2014). Grazing causes a more subtle decrease in biomass and crop height; within a parcel, biomass decrease will vary, depending on stocking densities.

Change in NDVI between two consecutive observation dates was used to create a model that allows detection of mowing. In theory, MASD may be used to detect mowing, however, it is an absolute value, which makes it difficult to discriminate between fast growth and mowing. Change in NDVI has proven useful for detection of mowing in previous research (Courault et al. 2010; Lips 2010). To assess the effect of mowing on NDVI, values from parcels that were not mown, freshly mown and recently mown, were extracted for April 21st and May 7th, using 6 plots of 1 ha in size (200 pixels per category). Based on the results, a mowing threshold was established.

To test the performance of the Sentinel-2 based mowing model, it was compared with the EVI based mowing model of Lips (2010). For this purpose, MODIS13Q 16 day EVI composites were downloaded for the 2016 growing season. The MODIS datasets were projected into WGS84 / UTM zone 31N. Sentinel-2 NDVI and MODIS EVI pixel values were extracted for monoculture and extensive plots in Littenseradiel.

The effect of grazing on Sentinel-2 based NDVI values was assessed by extracting NDVI values for April 21st and May 8th for 2 grazed and 2 non-grazed plots of 1 ha in size (200 pixels for each class).

6.0 Results

6.1 Spectral separability

6.1.1 Spectral response curves

Figure 6.1 shows the spectral response curves for monoculture and extensive grassland on both clay and peat soils, based on mean reflectance values for all observation dates. For each observation date, the response curves for different grassland types appear almost similar in shape but differ in amplitude, especially in spring. Mann-Whitney U tests were performed to compare mean reflectance for all four grassland categories (Appendix J). E.g. for April 21st, mean reflectance for monoculture grasslands is significantly different from that of extensive grasslands on both clay and peat soils ($p < 0.0001$, alpha 0.05). When comparing clay vs. peat soils, reflectance means are also significantly different ($p < 0.0001$, alpha 0.05), with the exception of B6 for clay mono vs. peat mono. For some of the spectral bands, differences between grassland categories are no longer significant after the 1st mowing event.

In general, all response curves display low reflectance for blue visible light (B2), a small peak for green visible light (B3) and low reflectance for red visible light (B4). In April and July, extensive grasslands on clay soils have slightly higher reflectance for visible light. In May and June visible light is reflected more by monoculture grassland on clay soils.

The vegetation red-edge is visible as a steep increase in reflectance between B4 and B7. In early spring, March 12th to April 21st, this increase is least pronounced for extensive grassland on peat soils and most pronounced for monoculture grassland on clay soils. For all grassland types, reflectance increases between B7 and B8, reaching the top of the NIR plateau. Reflectance is highest in B8 between March and May; after May, the reflectance peak shifts to B8A. In spring, monoculture grassland on clay and peat has higher reflectance values for the red-edge and NIR plateau than extensive grassland. Values for monoculture on peat soil lag slightly behind those of monoculture on clay soil, but in May reflectance values for monoculture on peat soil are slightly higher.

Values decrease steeply between B8A and B11 and decrease further for B12. For March 12th and April 1st, reflectance for B11 is lower for extensive grassland on peat soils than for the other grassland categories. On March 12th extensive grassland on peat has low values for B12. In May and June, B12 values are high for monoculture grassland on clay soils. For all categories, difference between mean reflectance values is least pronounced in September.

6.1.2 Interpretation

The overall 'peak-and-valley' configuration of the spectral response curves is typical for healthy grassland vegetation (compare e.g. Figure 2.4). Higher reflectance for visible light between April 11th and April 21st for extensive grasslands may be caused by the presence of flowering red and yellow herbs. In July it may be attributed to vegetation stress due to a period with high temperatures causing drought; probably more brown dry grass is present. Also, mowing may lead to higher influence of soil reflectance because of decreased vegetation density, this will increase reflectance for visible light (Dussaux et al. 2014). This effect also explains higher visible light reflectance for monoculture on clay soils on May 8th.

From March 12th to April 21st, reflectance in the red-edge, NIR and SWIR range for monoculture on peat soils is lower than for monoculture on clay and reflectance for extensive on peat is lower than extensive on clay. This may be caused by differences in soil moisture. Low reflectance in B11 is related to high leaf water content (Table 4.1). Higher average groundwater

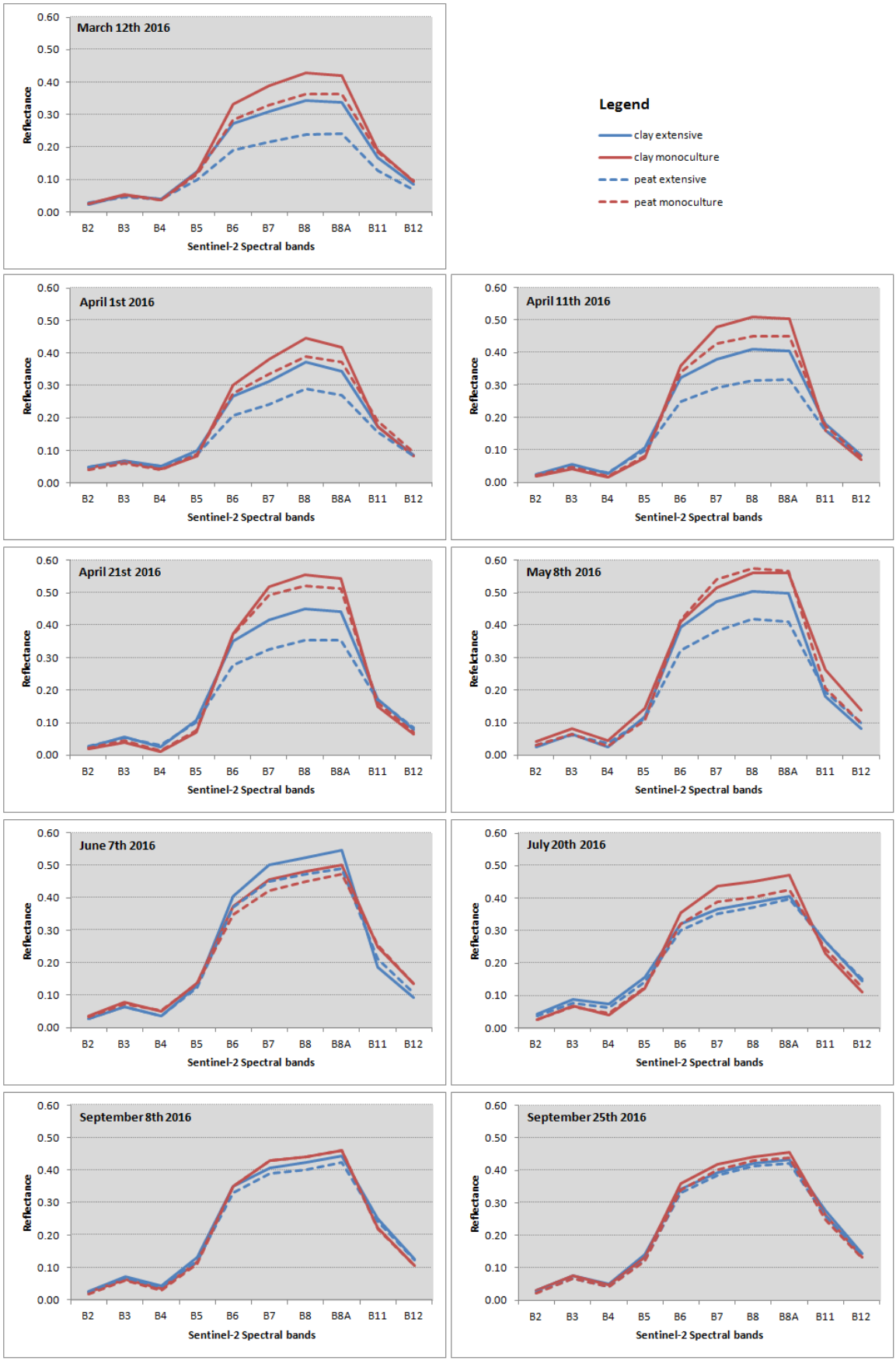

Figure 6.1: Spectral reflectance curves based on mean reflectance values for extensive and monoculture grassland sample points on clay and peat soils.

levels in peat soil areas slow down grass growth (Figure 4.9). In early spring, vegetation cover is less dense on peat soils, especially in extensive grasslands. Because less photosynthetically active vegetation is present, reflectance will be lower than for grassland on clay soils. Also, background effects of soil moisture and the soil itself may directly decrease reflectance. It is known that high organic matter content of peat soils reduces their reflectance (Lillesand et al. 2015). Low reflectance in SWIR bands 11 and 12 for extensive grasslands on peat soils for March 12th and April 1st may be caused by these effects.

On May 8th and June 7th reflectance in B11 is high for monoculture grassland on clay soils, this may be due to reduced leaf water content caused by drought. Temperatures in May were higher than normal and precipitation between May 2nd and June 12th was low (Figure 4.11). The other grassland categories are not affected by drought, probably thanks to higher groundwater levels.

High reflectance values in the red-edge and NIR range for monoculture grassland on clay and peat soils in spring, point to high amounts of total biomass. Fast growing grass types in intensively managed fields produce denser swards than extensive grass types, hence more photosynthetically active biomass. Onset of the growing season is earlier for monoculture grassland on clay soils than on peat soils. Application of manure on peat soils may be delayed in spring due to very wet conditions. Natural fertility of clay soils is also higher than for peat soils.

After the first mowing date for monoculture grassland, around May 8th, red-edge and NIR reflectance values decrease and start to fluctuate for the remaining months of the growing season, due to repeated mowing and re-growth. Mean reflectance values for extensive grassland decrease after June 7th; 1st mowing date for these fields is around June 15th and may be postponed to July if meadow bird chicks are present or if the fields are used for hay production. From July to September, extensive grassland shows similar fluctuations as monoculture grassland which are driven by mowing.

6.1.3 Coincident spectral plots

The coincident spectral plots show the mean spectral response for extensive and monoculture grassland on clay soils for each spectral band (Figure 6.2) (Appendix B). The variance of the distribution is illustrated by the error bars that represent +/- 2 standard deviations. These plots can be used to assess overlap between category response patterns (Lillesand et al. 2015). On September 25th, spectral response shows overlap for all bands for both types of grassland. On April 21st, spectral response pattern shows the least overlap for monoculture and extensive grassland. Relative reversal of spectral response can be seen for e.g. B5 and B7. On September 8th, also relatively little overlap exists between monoculture and extensive grassland, especially for the red-edge bands, NIR and SWIR bands 11 and 12 (Appendix B). The plots give insight into which combination of bands may be useful for discriminating between grassland types.

6.1.4 Variance in reflectance for all sample points

Throughout the growing season, reflectance for bands 6, 7, 8 and 8A shows the highest variability (Figure 6.3). Bands 5 and 11 also show some variability. From March 12th to April 11th, variability for band 11 displays a peak for extensive grassland on peat soils, which may be related to differences in soil moisture. On May 8th, variability for bands 11 and 12 displays a peak for monoculture grassland on clay soil, which may be related to differences in soil moisture and soil background effects due to decreased vegetation density caused by mowing. In general, in springtime, variance for extensive

grassland is much higher than for monoculture grasslands. Variance for extensive grassland on peat soils is twice as high as for extensive grasslands on clay soils. For monoculture grasslands, from April onwards, variance on peat and clay soils is quite similar. After the 1st mowing date, variance for monoculture grasslands strongly increases.

6.1.5 Conclusion

In springtime, for all spectral bands on both clay and peat soils, mean spectral response for extensive grasslands differs significantly from the mean response for monoculture grasslands ($p < 0.0001$, alpha 0.05 for April 21st)(Appendix J). After the 1st mowing event (around May 8th for monoculture and after June 7th for extensive grasslands), spectral response patterns show more overlap; for some of the spectral bands, differences between monoculture and extensive grassland are no longer significant (Appendix J).

Local soil type strongly influences spectral response patterns. When comparing clay vs. peat soils, it was found that in springtime, mean reflectance values for extensive grassland and monoculture grasslands are significantly different ($p < 0.0001$, alpha 0.05 for April 21st).

The spectral response curves reveal that the possibility of discerning extensive and monoculture grasslands on both clay and peat soils is likely to be highest for April 11th and April 21st, when differences in reflectance are most pronounced. This conclusion is supported by the coincident spectral plot for April 21st. Based on the response curves and the coincident spectral plot, it can be concluded that the spectral bands with the least overlap are bands 5, 7, 8 and 8A. Although B6 shows overlap in the coincident plot for monoculture grassland, the mean spectral response curves for peat soils show clear differences in reflectance for B6 between extensive grassland and monoculture grassland. Bands 6, 7, 8 and 8A also show the highest variability on April 21st.

Therefore, the most important bands that allow discrimination of grassland categories are the Sentinel-2 red-edge and NIR bands. This suggests that both the S2REP vegetation index and the NDVI may be important for successful classification, since they are based on these bands.

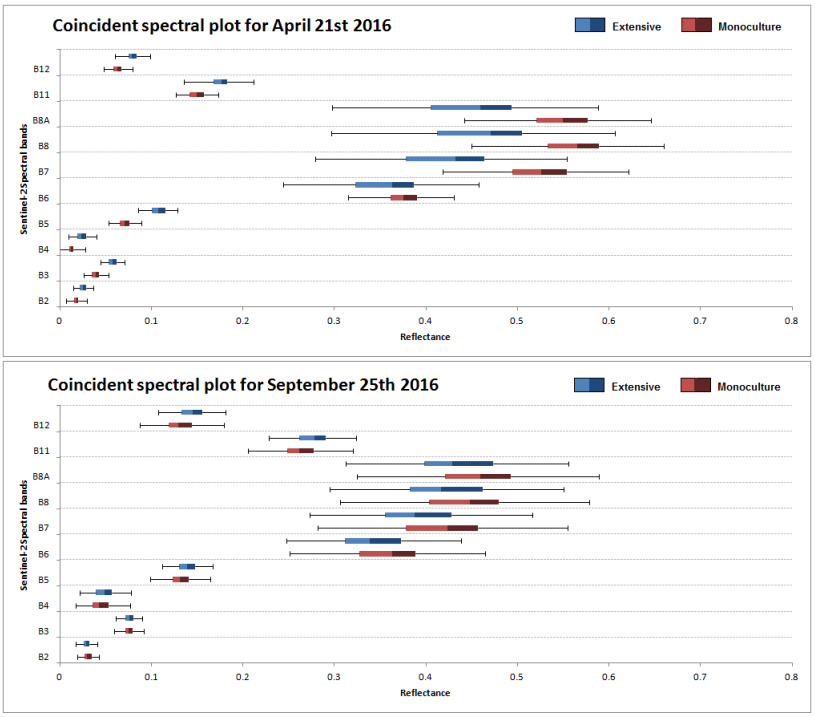

Figure 6.2: Coincident spectral plot for April 21st and September 25th 2016 for Littenseradiel (clay soil) sample points. Boxes show 1st quartile, median, 3rd quartile; Whiskers show 2 x plus and 2 x minus standard deviation (See Appendix B for all coincident spectral plots for Littenseradiel).

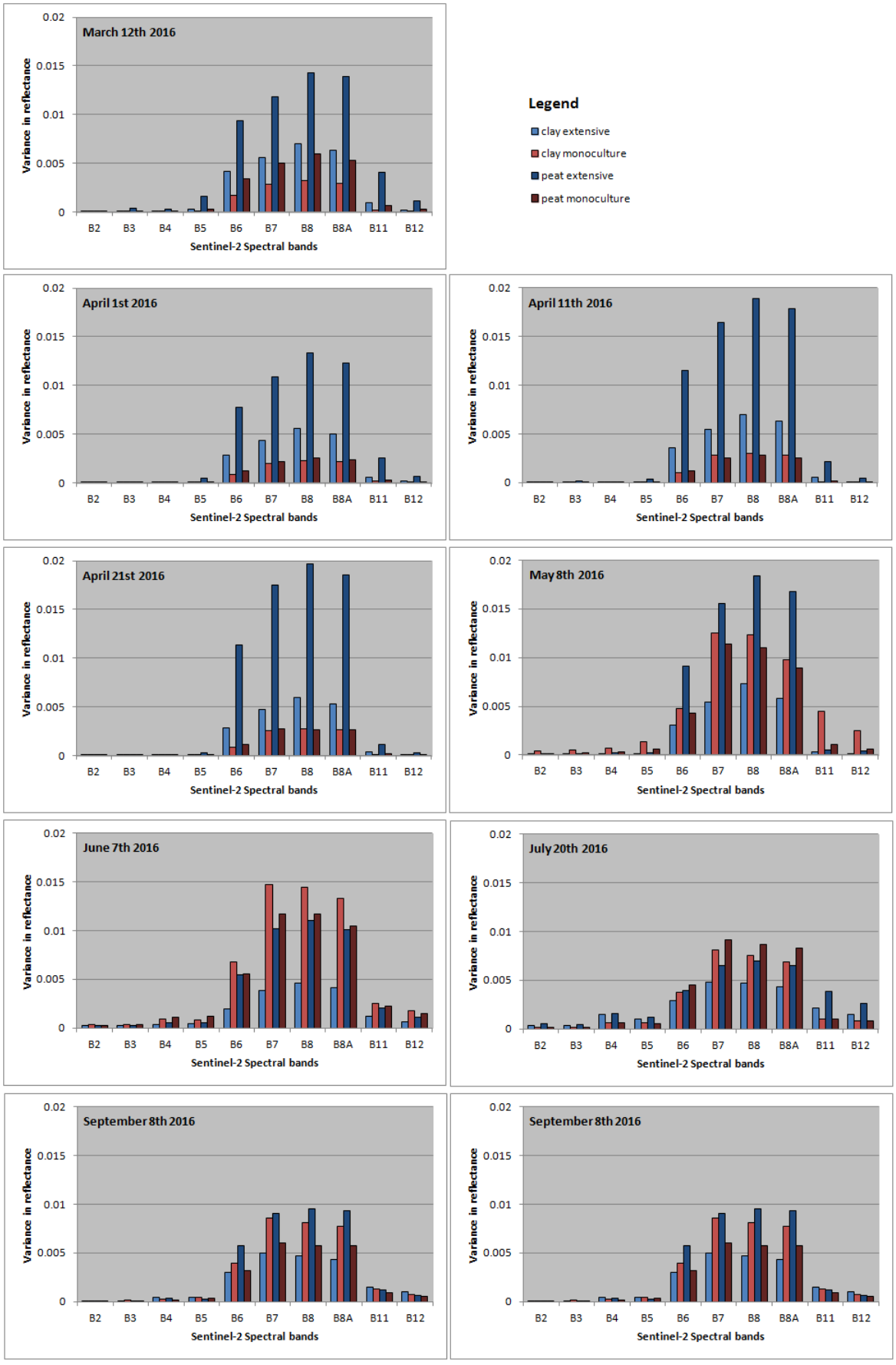

Figure 6.3: Variance in reflectance for all sample points.

6.2 Vegetation indices

6.2.1 NDVI boxplot for Littenseradiel

The NDVI boxplot for Littenseradiel shows differences in NDVI between extensive and monoculture grassland on clay soils (Figure 6.4). In general, monoculture grassland has higher NDVI values than extensive grasslands. NDVI values for both grass types slightly decrease between March 12th and April 1st. Then NDVI increases to a mean maximum of 0.96 on April 21st for monoculture grasslands and 0.89 for extensive grasslands on April 21st and May 8th. After this peak, values decrease and start to fluctuate and display a wider range.

Histograms and statistical tests (Shapiro-Wilk test) have shown that NDVI values for all samples follow a non-normal distribution (Appendix J). The histograms are negatively skewed. Normalization using reflection in combination with log-transformation was not possible. Therefore, non-parametric statistical tests were carried out for all dates to see whether NDVI values are significantly different for extensive and monoculture grassland. The Kolmogorov-Smirnov test revealed that for each date, samples for both grassland types follow a different distribution ($p < 0.0001$, alpha 0.05). The Mann-Whitney U test was used to compare sample means; based on the test results it can be concluded that for all dates sample means are significantly different ($p < 0.0001$, alpha 0.05).

6.2.2 NDVI boxplot for Grouw

The NDVI boxplot for Grouw shows the differences between extensive and monoculture grassland on peat soils (Figure 6.5). For all observation dates, except June 7th, NDVI is higher for monoculture than for extensive grassland. The range in NDVI is wider for extensive grasslands than for monoculture. NDVI values increase to a mean maximum of 0.95 on April 21st for monoculture grasslands and 0.84 for extensive grasslands on June 7th. After this peak, values decrease and start to fluctuate and display a wider range.

Histograms and statistical tests (Shapiro-Wilk test) have shown that NDVI values for all samples follow a non-normal distribution. The histograms are negatively skewed. Normalization using reflection in combination with log-transformation was not possible. Therefore, non-parametric statistical tests were carried out for all dates to see whether NDVI values are significantly different for extensive and monoculture grassland. The Kolmogorov-Smirnov test revealed that for each date, samples for both grassland types follow a different distribution ($p < 0.0001$, alpha 0.05). The Mann-Whitney U test was used to compare sample means; based on the test results it can be concluded that for all dates sample means are significantly different ($p < 0.0001$, for September 25th $p = 0.016$, alpha 0.05).

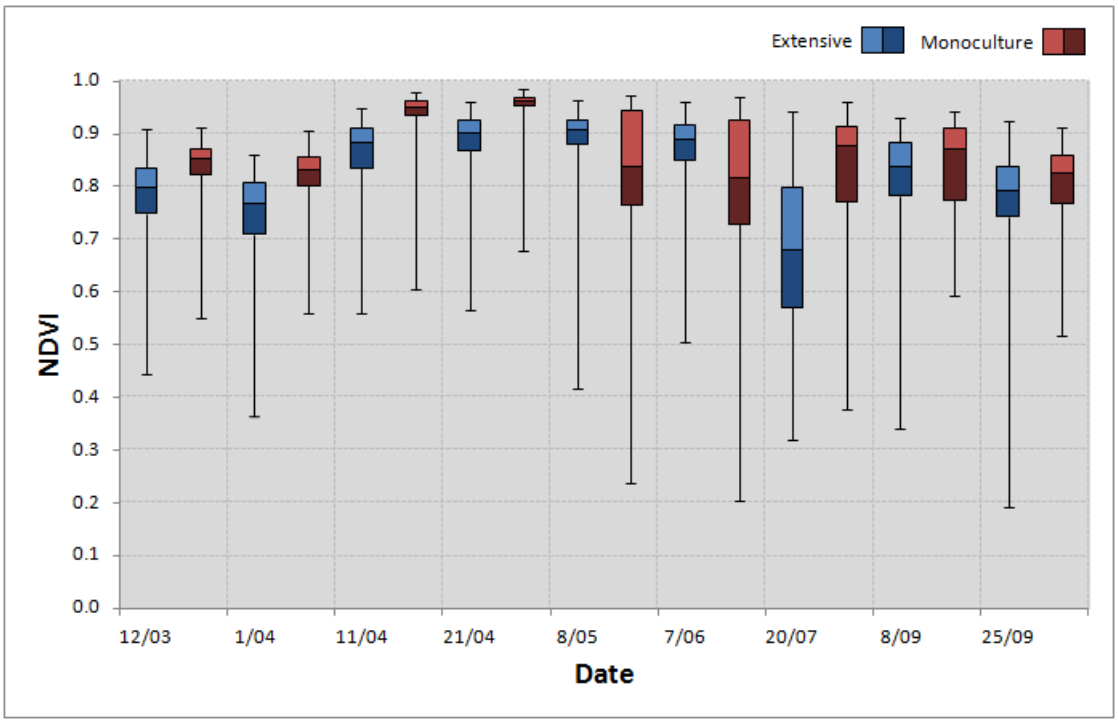

Figure 6.4: NDVI for Littenseradiel (clay soils). The box plots show 1st quartile, median, 3rd quartile, whiskers show minimum and maximum values (See Appendix C for box plot that shows seasonal variability more clear).

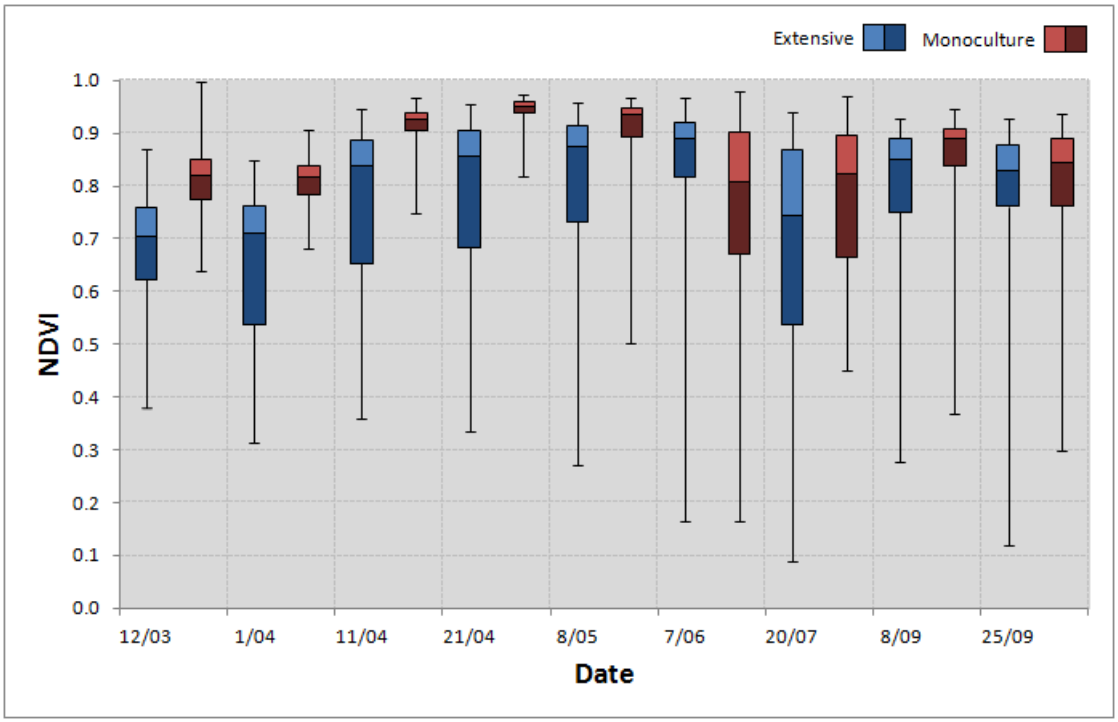

Figure 6.5: NDVI for Grouw (peat soils). The box plots show 1st quartile, median, 3rd quartile, whiskers show minimum and maximum values.

6.2.3 Clay soil vs. peat soil NDVI boxplots

Differences in NDVI between clay soil and peat soil were also assessed (Figure 6.6). In spring, NDVI for monoculture and extensive grasslands on clay soils is higher than for peat soils. Extensive and monoculture grasslands on peat soils display a wider range in NDVI values than on clay soils, except for monoculture grassland on clay soils on May 8th.

Non-parametric statistical tests were carried out for all dates to see whether NDVI values are significantly different for grassland on peat soils and on clay soils. The Kolmogorov-Smirnov test revealed that for all dates, except for extensive grassland on September 8th, samples for both soil types follow a different distribution ($p < 0.0001$, alpha 0.05). The Mann-Whitney U test was used to compare sample means; based on the test results it can be concluded that for almost all dates, sample means are significantly different ($p < 0.0001$, alpha 0.05). Except for two observation dates: On June 7th, the mean is not significantly different for both extensive ($p = 0.630$) and monoculture grassland ($p = 0.225$). For September 8th it is not significantly different for extensive grassland ($p = 0.397$).

6.2.4 Interpretation

Seasonal pattern for NDVI is comparable with the grassland production curve (Figure 2.1). NDVI reaches a first peak in April (monoculture) or May/June (extensive), reflecting high biomass and high photosynthesis activity; then NDVI values decrease in June/July before they reach a second peak in September. For both extensive grassland and intensive monoculture grassland on clay soils, the NDVI drops between March 12th and April 1st (Figure 6.4). This is probably due to the cold weather in the last weeks of March (Figure 4.11). For peat soils, this decrease is not so distinct, probably because onset of grass growth is delayed here due to higher groundwater levels; also, on wet fields, fertilizer cannot be applied as early as on dewatered clay soils.

Until June, NDVI is slightly lower for peat soils than for clay soils for both grassland types. This may be related to the higher natural fertility of clay soils in combination with decreased springtime growth due to higher groundwater levels in peat soils. For March and April, NDVI values show a wider range for extensive grassland than for monoculture grassland, especially for peat soils. The narrow range for monoculture grassland in April is most likely caused by the homogeneous character of fast-growing ryegrass types. From the end of April/beginning of May onwards, monoculture grassland on clay soils shows more variation in NDVI due to mowing. This is consistent with the timeline for agricultural activities in which is stated that 1st cuts were taken between May 6th and May 12th (section 4.1.5). For monoculture on peat soils the NDVI variation increases in June. Visual inspection of the Sentinel-2 true color images reveals that the first mowing activity on monoculture grassland on peat soils did already occur in May, but was limited to relatively few parcels. First cuts for most monoculture parcels on peat soils are taken between May 8th and June 7th.

On July 20th, NDVI strongly drops for extensive grassland for both clay and peat soils. After June 15th, mowing is allowed in the bird reserves; the mowing date may be postponed if meadow birds chicks are present. But, by the end of July, most parcels will have been mown. The NDVI drop in July may also be related to slower grass growth during the flowering season (Figure 2.1).

When comparing these values with the graph from Franke et al. (2012)(Figure 2.5), it is found that overall trends are very similar. NDVI values for extensive grassland in Littenseradiel resemble the values of extensively used grassland in Germany, although mean NDVI is higher in Friesland. The higher values probably reflect the agricultural use of the bird reserves in the South-Central Friesland study area. Monoculture grasslands in Friesland show even higher NDVI values than the intensively used grasslands in Germany. This may also be attributed to application of higher amounts per ha of liquid manure in the Netherlands (section 2.1.3).

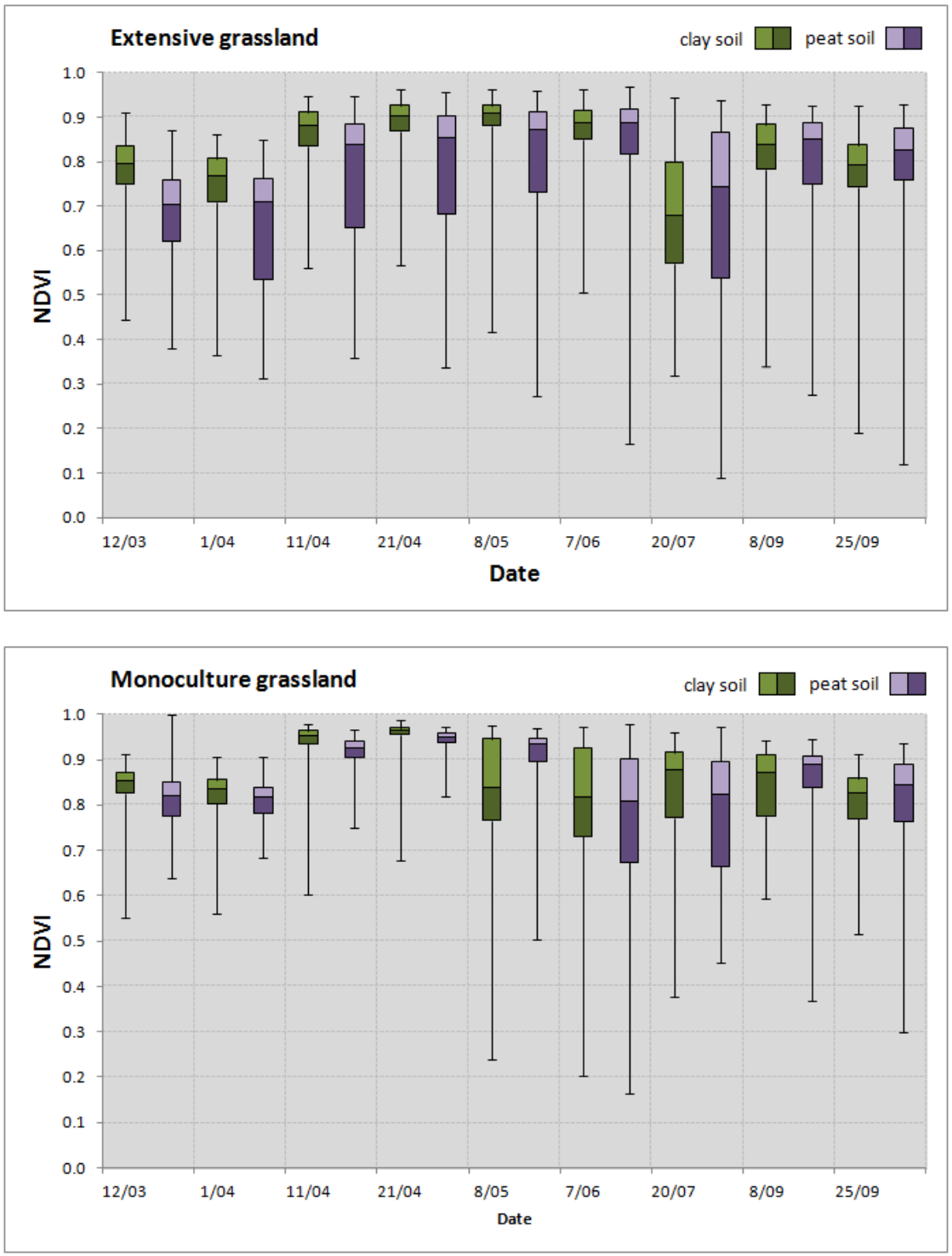

Figure 6.6: Clay soil vs. peat soil NDVI box plots for extensive and monoculture grassland. The box plots show 1st quartile, median, 3rd quartile, whiskers show minimum and maximum values.

6.2.5 S2REP boxplot for Littenseradiel

The S2REP boxplot shows the differences in S2REP value for the sample points for extensive and monoculture grassland on clay soils (Figure 6.7). The value increases between March 12th and April 1st; it continues to increase until April 21st for monoculture grassland, whilst, on April 11th the S2REP shows a slight decrease for extensive grassland. After April 11th, values increase until June 7th for extensive grassland. S2REP fluctuates after June. From May onwards, the range in S2REP increases for monoculture grassland; for extensive grassland the S2REP range shows less variation. Mean values vary between 720 and 727 nm for monoculture and 716 and 722 nm for extensive grasslands.

Histograms and statistical tests (Shapiro-Wilk test) have shown that S2REP values for all samples follow a non-normal distribution. Histograms are slightly skewed to the left. Log transformation of the data was not possible. Therefore, non-parametric statistical tests were carried out for all dates to see whether S2REP values are significantly different for extensive and monoculture grassland. The Kolmogorov-Smirnov test revealed that for each date, samples for both grassland types follow a different distribution ($p < 0.0001$, alpha 0.05). The Mann-Whitney U test was used to compare sample means for both grassland types; based on the test results it can be concluded that for all dates sample means are significantly different ($p < 0.0001$, alpha 0.05).

6.2.6 S2REP boxplot for Grouw

The S2REP boxplot shows the differences in S2REP value for the sample points for extensive and monoculture grassland on peat soils (Figure 6.8). Fluctuations are similar to those of clay soils, including the slight decrease of S2REP for extensive grasslands between April 1st and April 11th. Mean values for monoculture grasslands vary between 719 and 726 nm, and between 714 and 723 nm for extensive grasslands.

Histograms and statistical tests (Shapiro-Wilk test) have shown that S2REP values for all samples follow a non-normal distribution. Histograms are slightly skewed to the left. Log transformation of the data was not possible. Non-parametric statistical tests were carried out for all dates to see whether S2REP values are significantly different for extensive and monoculture grassland. The Kolmogorov-Smirnov test revealed that for each date, samples for both grassland types follow a different distribution ($p < 0.0001$, alpha 0.05). The Mann-Whitney U test was used to compare sample means for both grassland types; based on the test results it can be concluded that for all dates sample means are significantly different ($p < 0.0001$, alpha 0.05).

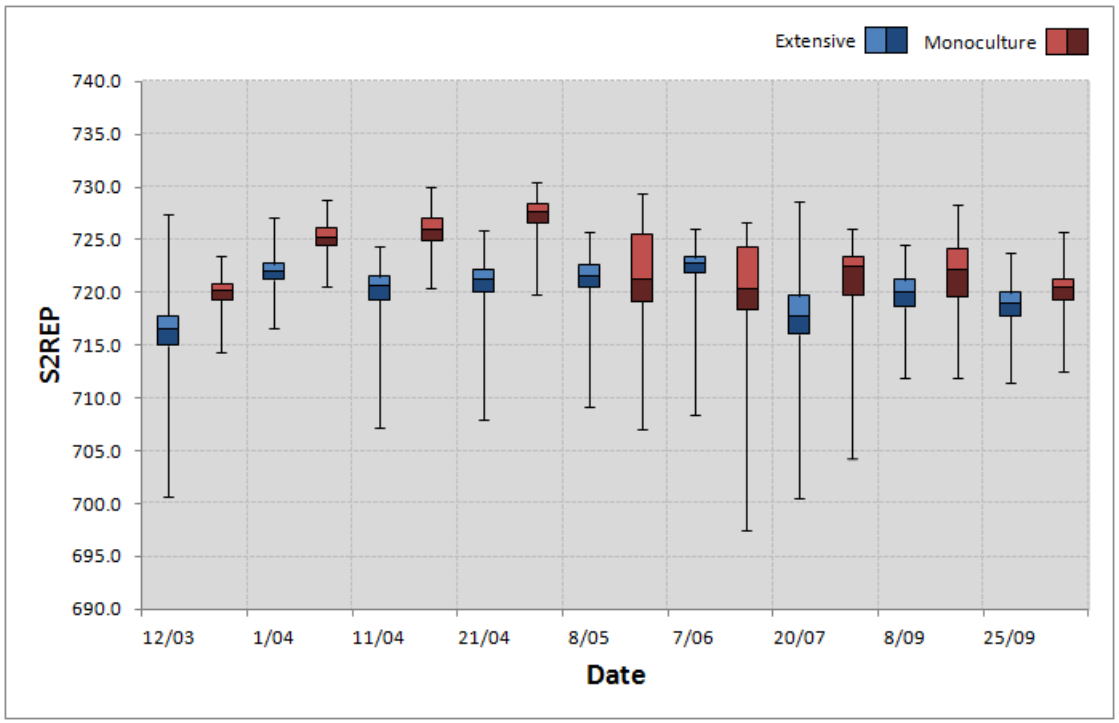

Figure 6.7: S2REP for Littenseradiel, clay soils. The box plots show 1st quartile, median, 3rd quartile, whiskers show minimum and maximum values.

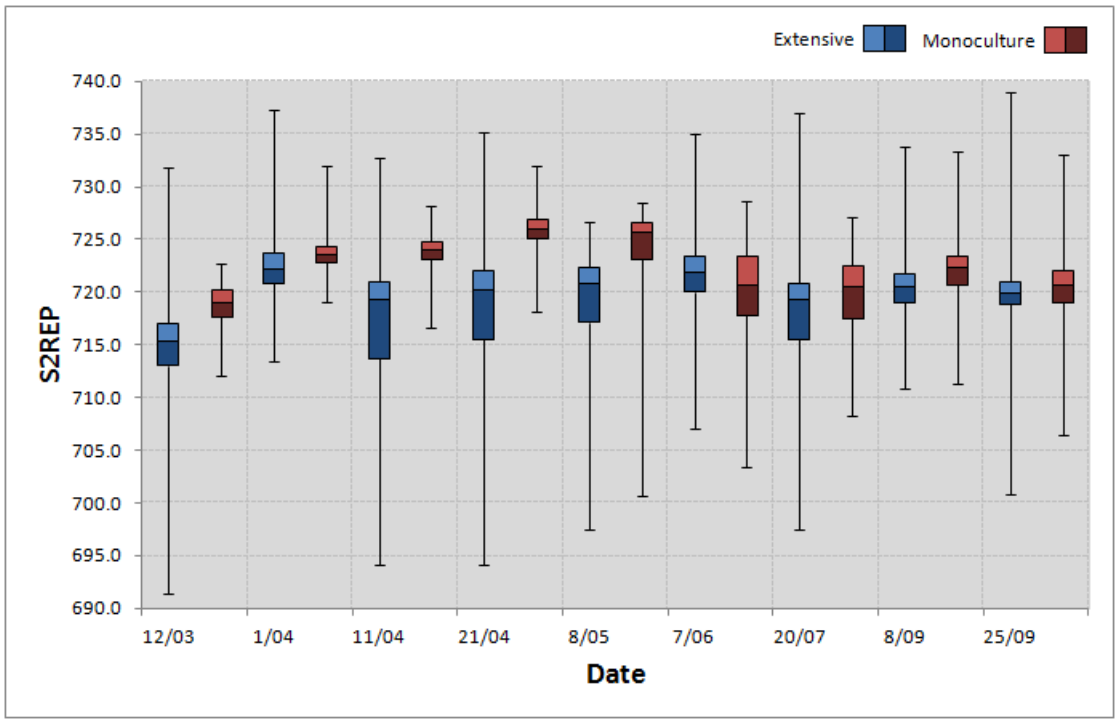

Figure 6.8: S2REP for Grouw, peat soils. The box plots show 1st quartile, median, 3rd quartile, whiskers show minimum and maximum values.

6.2.7 Clay soil vs. Peat soil S2REP boxplots

Differences in S2REP between clay and peat soils were assessed (Figure 6.9). In early spring, mean S2REP values for both grassland types are higher on clay soil than on peat soils. Values show strong overlap for extensive grassland on clay and peat soils; for monoculture grassland on clay and peat soils there is no overlap in early spring. Extensive grassland on peat soils displays a wider range of S2REP than clay soils. For monoculture grassland, this difference is not so pronounced. On April 21st, S2REP is highest for monoculture grassland whilst for extensive grassland values are highest on April 1st.

Non-parametric statistical tests were carried out for all dates to see whether S2REP values are significantly different for grassland on peat soils and on clay soils. The Kolmogorov-Smirnov test revealed that for all dates, except for monoculture grassland on June 7th ($p = 0.099$), samples for both soil types follow a different distribution ($p < 0.0001$, alpha 0.05). The Mann-Whitney U test was used to compare sample means; based on the test results it can be concluded that for almost all dates, sample means are significantly different ($p < 0.0001$, alpha 0.05). Except for April 1st, here the mean is not significantly different for extensive grassland ($p = 0.168$) and also for June 7th ($p = 0.341$), September 8th ($p = 0.788$) and September 25th ($p = 0.062$) not for monoculture grassland.

6.2.8 Interpretation

The overall S2REP seasonal pattern is comparable to the grassland production curve (Figure 2.1), with a peak in April, decrease in summer and a second peak in September. In early spring, March to April 21st, S2REP shows pronounced differences for different types of grassland. Compared to the NDVI time series, there is less overlap between extensive and monoculture grasslands. After 1st mowing dates, the values fluctuate and show more overlap. Monoculture grasslands reach the highest S2REP values on April 21st; for monoculture on clay soils the highest mean is 727 nm compared to 726 nm for peat soils. Highest mean value for extensive grassland on clay soils is 722 nm and 723 nm for peat soils. S2REP for extensive grasslands on clay and peat soils shows a lot of overlap, although the S2REP range is much wider for peat soils.

It is likely that high S2REP values for monoculture grasslands are related to high amounts of chlorophyll and nitrogen in the leaves stimulated by application of liquid manure. Red Edge Position values near 700 nm have been associated with low leaf chlorophyll concentration, whilst Red Edge Position values near 725 nm point to high leaf chlorophyll concentration (Cho and Skidmore 2006). This means that even values for extensive grasslands can be considered quite high, which may be evidence for high nitrogen deposition (eutrophication) through air and water pollution; this is problematic in nature areas where it causes loss of biodiversity (CLO 2016).

For observation dates in March and April, S2REP may be a suitable attribute for discriminating between extensive and intensive grasslands. Because S2REP and NDVI distributions for clay and peat soil are significantly different, successful grassland classification in Friesland has to be based on training areas for both clay and peat soil.

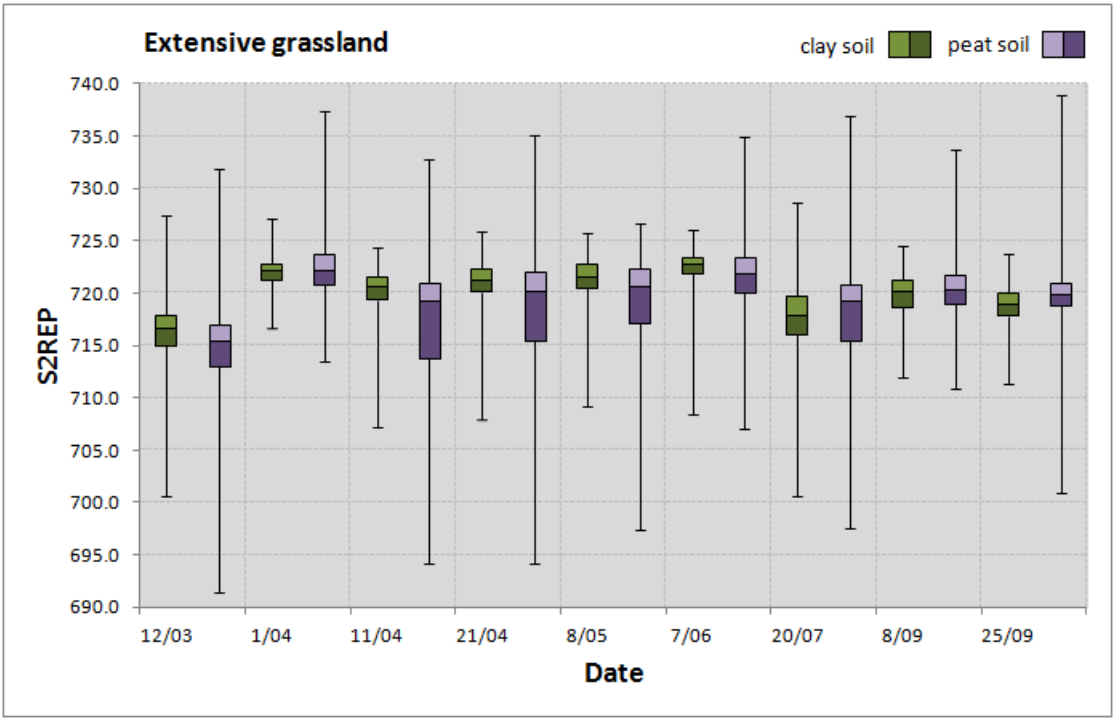

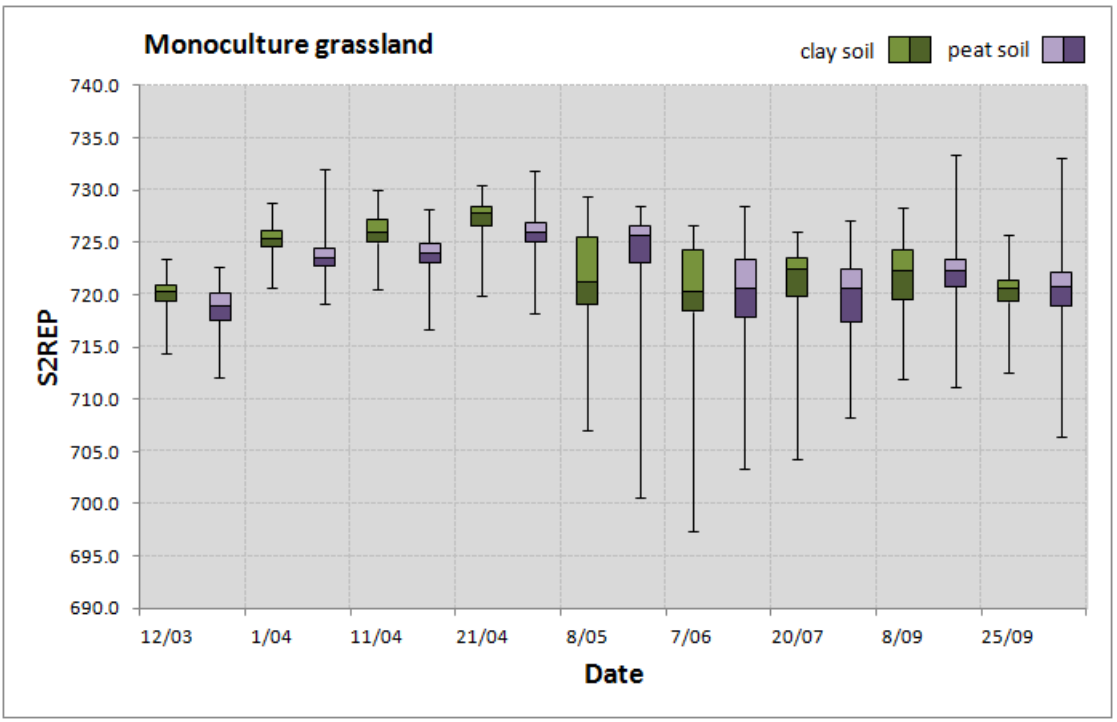

Figure 6.9: S2REP clay soil vs. peat soils. The box plots show 1st quartile, median, 3rd quartile, whiskers show minimum and maximum values.

6.3 MASD

6.3.1 MASD boxplots

Figure 6.10 shows the boxplots for the Mean Absolute Spectral Dynamic parameter. MASD_total is based on 7 observation dates: April 1st, April 11th, April 21st, May 8th, July 20th, September 8th and September 25th; March 12th was excluded because this image contains small clouds and cloud shadows, especially in the Grouw area; June 7th is also excluded due to presence of clouds in the Littenseradiel field survey area. MASD_spring is based on 4 observation dates: April 1st, April 11th, April 21st, May 8th.

Histograms and statistical tests have shown that MASD_total and MASD_spring values follow a non-normal distribution (Appendix J). Non-parametric statistical tests were carried out to see whether MASD values are significantly different for extensive and monoculture grassland in each field survey area, as well as for clay and peat soils. When comparing extensive and monoculture grassland, the Kolmogorov-Smirnov test showed that MASD_total and MASD_spring distributions are significantly different for both clay and peat soils ($p < 0.0001$, alpha 0.05). When comparing clay and peat soils, the MASD_total ($p = 0.372$, alpha 0.05) and MASD_spring ($p = 0.081$, alpha 0.05) distributions are not significantly different for extensive grassland. For monoculture grassland, the MASD_total ($p = 0.005$, alpha 0.05) and MASD_spring ($p < 0.0001$, alpha 0.05) distributions are significantly different. The Mann-Whitney U test was used to compare sample means; based on the test results it can be concluded that for both extensive and monoculture grassland on clay or peat soil, the MASD_total and MASD_spring means are significantly different ($p < 0.0001$, alpha 0.05). When comparing clay vs. peat soil, MASD_total ($p = 0.451$, alpha 0.05) and MASD_spring ($p = 0.573$, alpha 0.05) means do not significantly differ for extensive grassland; for monoculture grassland, the MASD_total ($p = 0.029$, alpha 0.05) and MASD_spring ($p <0.0001$, alpha 0.05) means are significantly different.

MASD_spring may be a suitable variable to use for grassland classification, because the boxes in the boxplots for extensive and intensive grassland show no overlap.

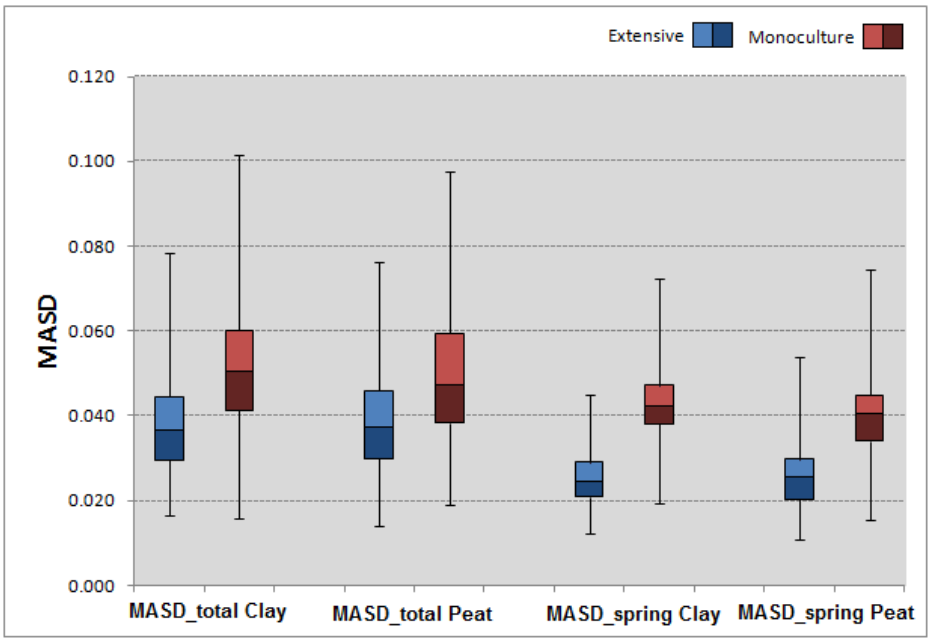

Figure 6.10: MASD box plots for clay and peat soils for the whole season and for spring. The box plots show 1st quartile, median, 3rd quartile, whiskers show minimum and maximum values.

6.3.2 MASD maps

The map below shows MASD4_spring (April 1st-May 8th) for grassland parcels in Littenseradiel, this is after the 1st mowing date for monoculture grassland (end April - beginning of May) and before the first mowing date for extensive grassland (Figure 6.11). Meadow bird reserves and other extensive grassland areas, such as fields of biological/organic farmers, display low spectral dynamics. Monoculture grassland shows high spectral dynamics. This can be attributed to the presence of fast growing ryegrass types and early mowing. Also, small pastures that are grazed intensively by sheep may show high dynamics. In some parcels with low spectral dynamics, irregular areas with high spectral dynamics can be seen, this represents presence of water. In early spring, farmers may create shallow ponds (*'plas-dras'* areas) for the meadow birds in some of their parcels. In case of subsidized agricultural nature management, these areas have to be kept wet from February 15th to June 15th (or longer, depending on the management package). After this date, the ponds dry out (see SWIR composite below; Figure 6.12). Also, straight dark red lines in otherwise blue or light red parcels probably represent ditches with water. Checkerboard and striped patterns may represent "mosaic management", parcels which have been partly mown, so the birds can find refuge in the remaining higher grass. Stripes also represent parcels that are partly mown to harvest fresh grass for feeding cattle that are kept indoors.

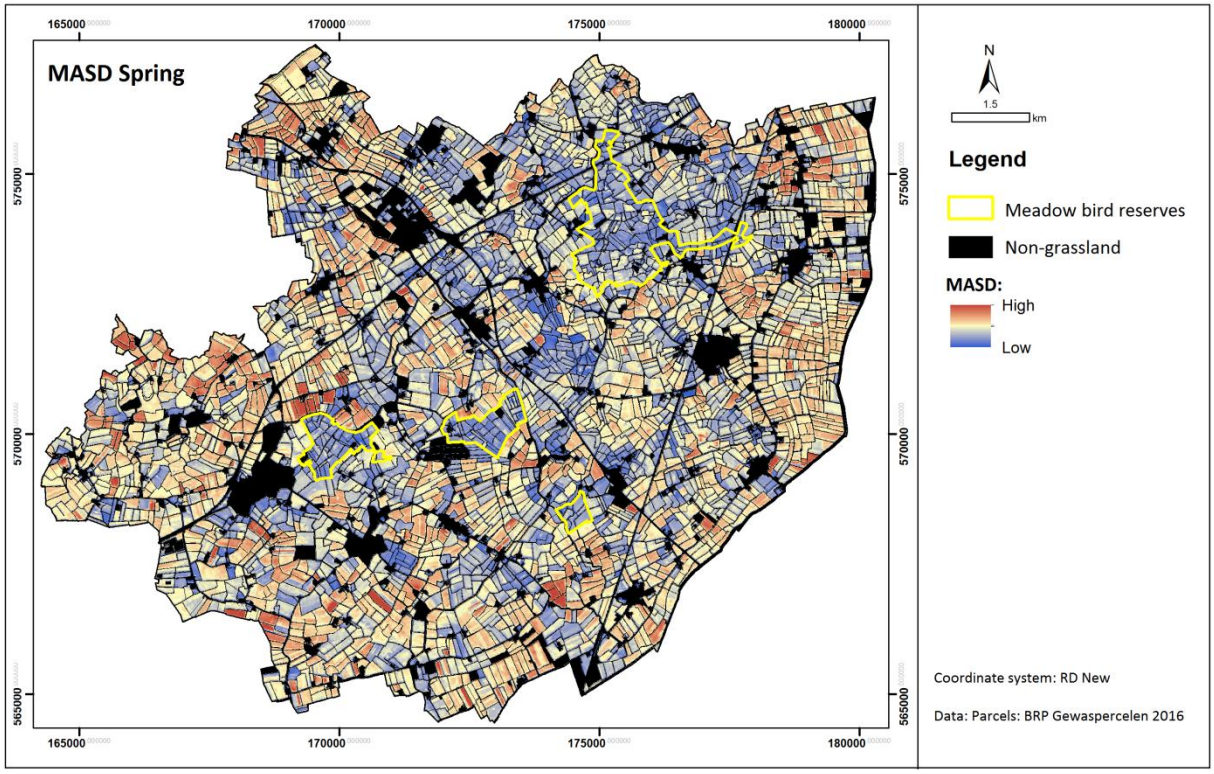

Figure 6.11: MASD4_spring map for Littenseradiel based on observation dates: April 1st, April 11th, April 21st and May 8th. Infrastructure, villages and non-grassland are shown in black.

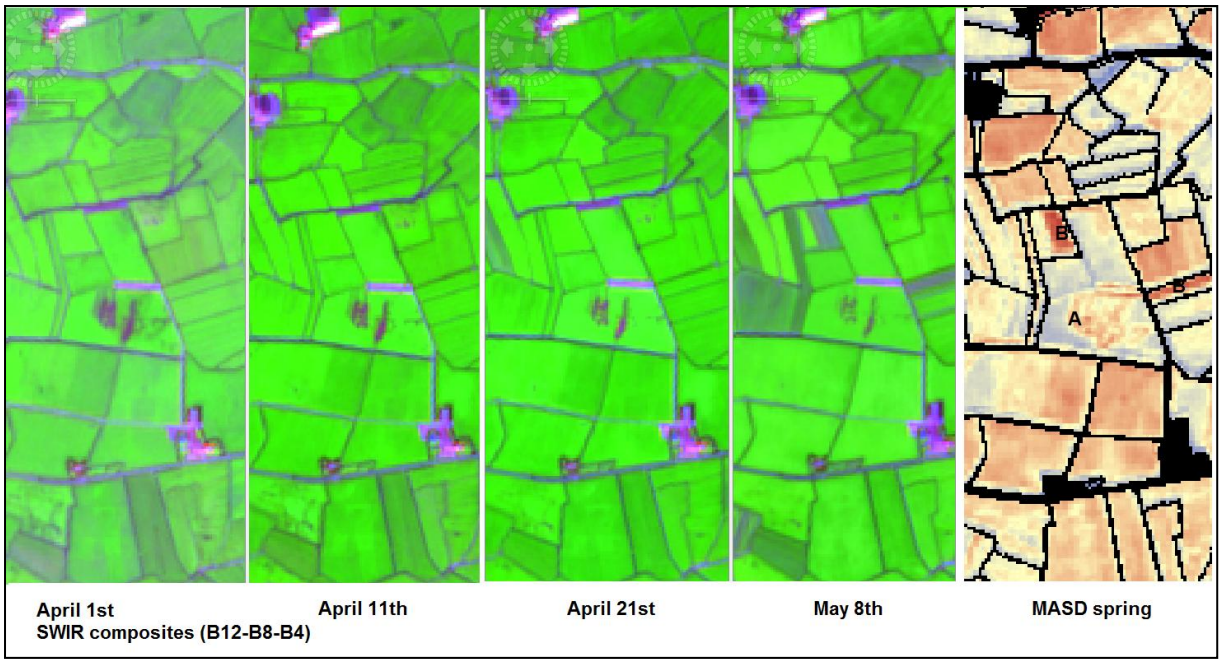

Figure 6.12: Spring time series Sentinel-2 SWIR false color composite for small part of Littenseradiel compared with MASD4_spring map. A = moist area, B = freshly mown fields.

SWIR false color composites can be used to reveal soil moisture. Irregular areas with high MASD values (A) represent moist areas that dry up later in summer. Freshly mown fields (B) show reduced moisture content and high MASD.

Figure 6.13 shows the MASD7_total map for the whole season of 2016. Compared to the MASD4_ spring map, spectral dynamics has slightly increased in bird reserves, due to repeated mowing and grazing from late June until September.

The MASD4_spring map for Grouw displays mostly low spectral dynamics in meadow bird reserves and high spectral dynamics in monoculture grassland (Figure 6.14). High dynamics in monoculture grassland is probably caused by fast growing grass types and early mowing. Irregular areas with high dynamics represent very moist areas that dry out during late spring/early summer. On the MASD7_total map for April-September low spectral dynamics is more clear for bird reserves, especially for De Burd. In general, taking into account all observation dates, the bird reserves in the peat area have lower spectral dynamics than monoculture areas; this is also found for the Littenseradiel area.

Figures 6.15 shows the MASD4_spring map for the South-Central Friesland study area with an overlay of important (meadow) bird areas within the National Nature Network; extensive grasslands that are part of the National Nature Network have low spectral dynamics and appear in dark blue.

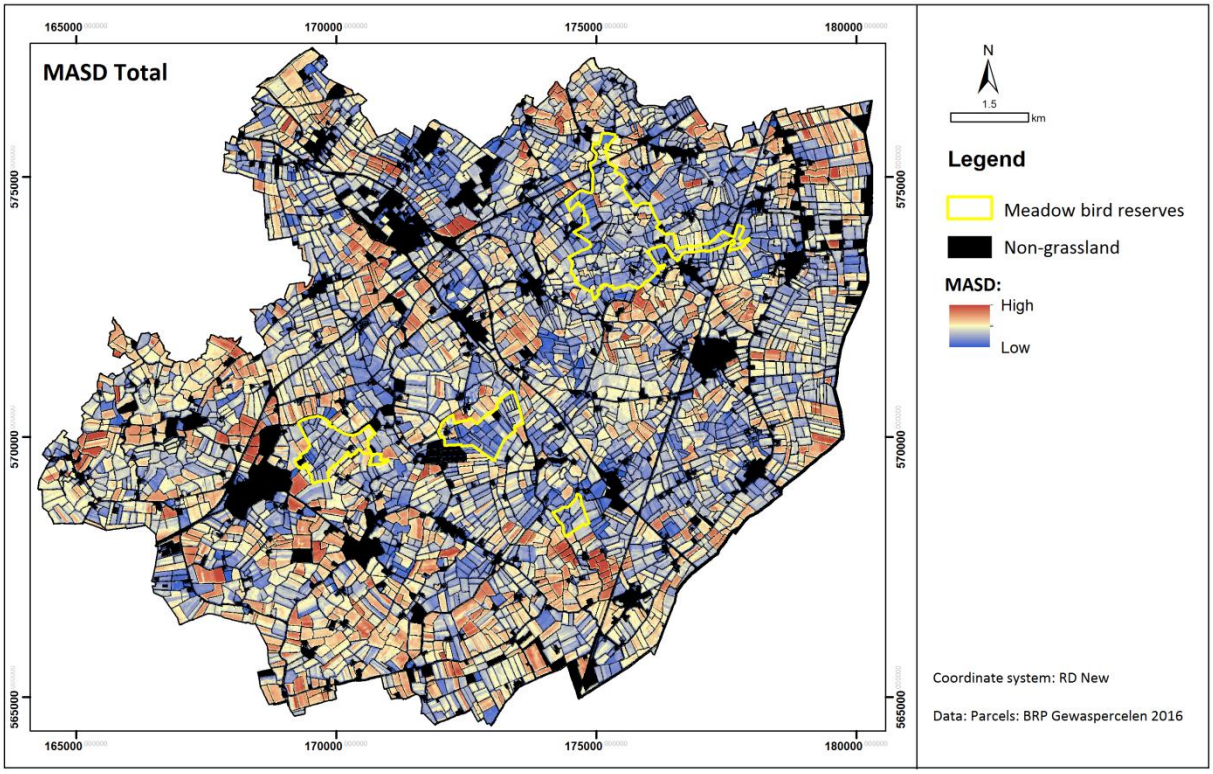

Figure 6.13: MASD7_total (April-September) for Littenseradiel.

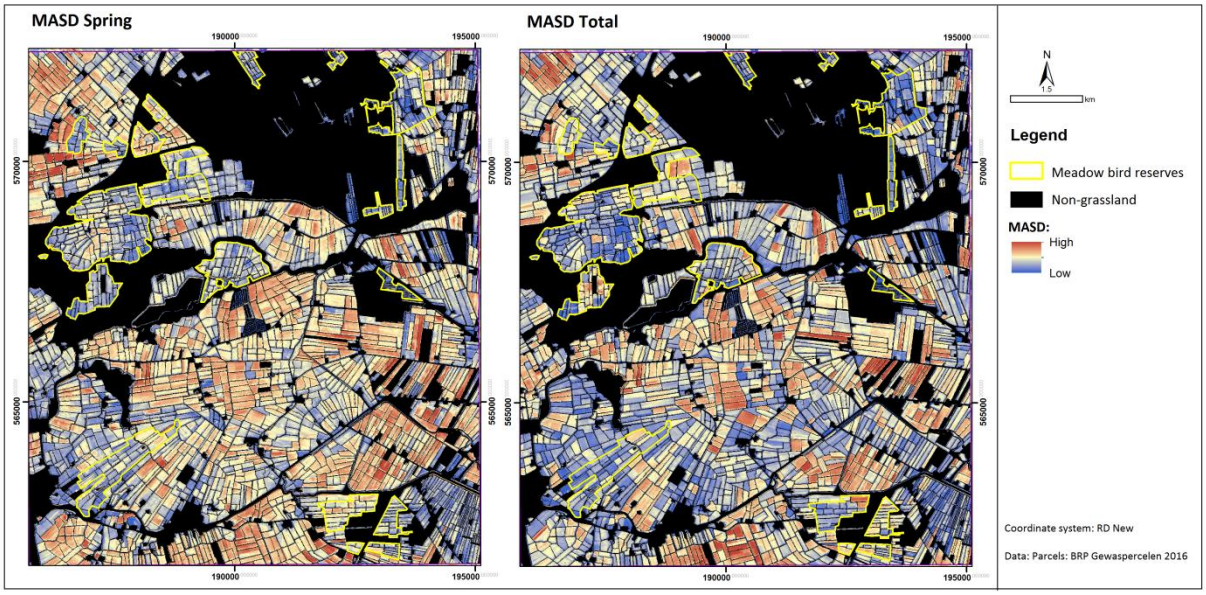

Figure 6.14: MASD maps for Grouw: Right MASD4_spring, left MASD7_total for April-September 2016.

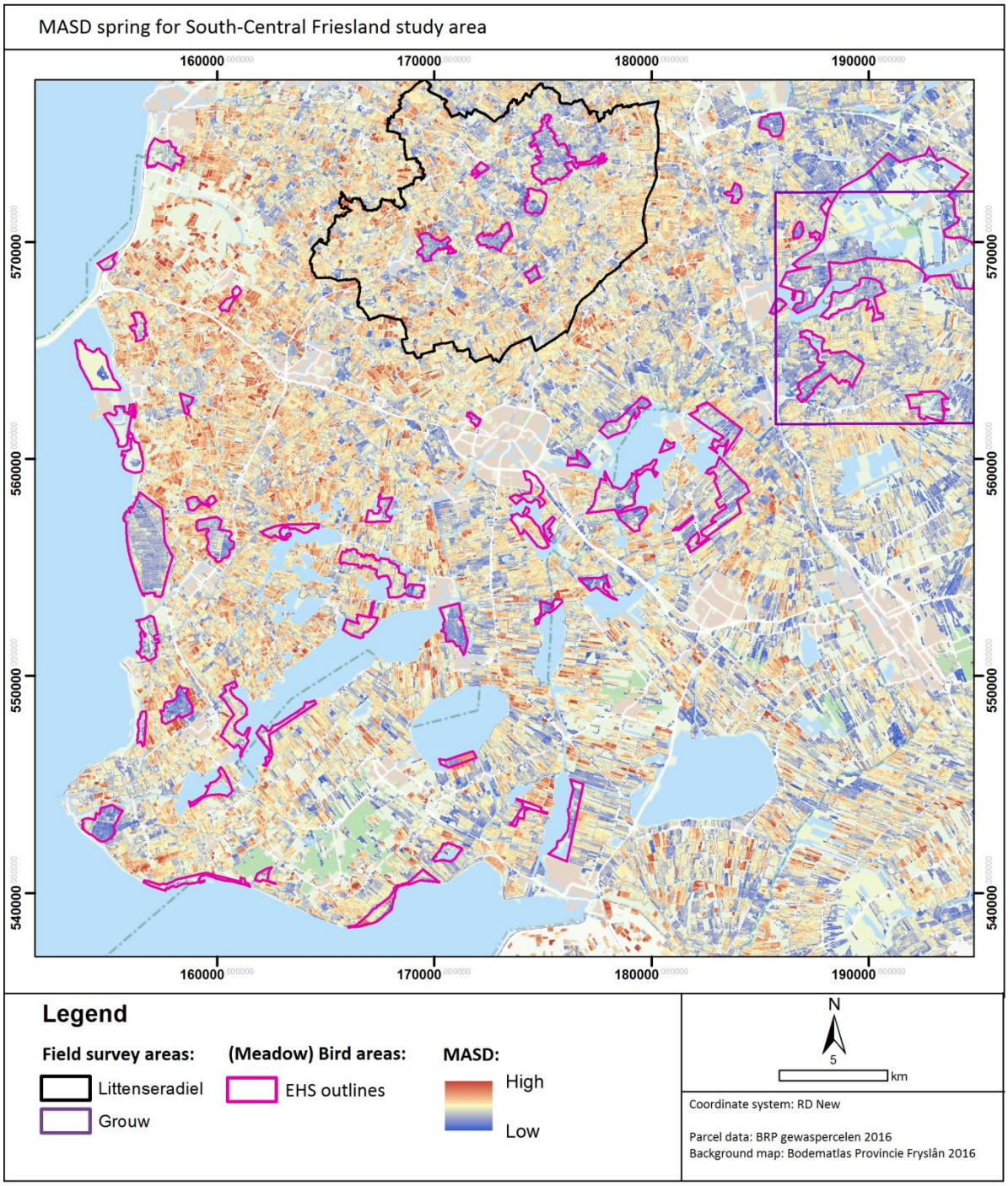

Figure 6.15: MASD4_spring map with the outlines of relevant (meadow) bird areas for the South-Central Friesland study area (Background image from Provincie Fryslân 2017).

6.4 Classification

6.4.1 Statistical rule-based classification

Table 6.1 shows the decision tree that was created with See5, based on analysis of 27 attributes for nine observation dates (See Table 5.3 for used attributes). The evaluation on training data shows that three monoculture sample points were misclassified as extensive, an error of 0.8%. The DT uses five attributes for four observation dates. The S2REP values for April 21st are most important for classification, this attribute is used for all classification decisions (100%). S2REP values for September 8th (51%) and NDVI values for April 21st (50%) are also important to further discriminate between extensive and monoculture grassland. Importance of S2REP and NDVI for April 21st is in accordance with the S2REP and NDVI boxplots. These graphs showed that differences between both grassland types were greatest on April 21st. Importance of the S2REP for September 8th is in accordance with the coincident spectral plot, although it was less expected due to overlap of the S2REP boxplots.

Next, the remaining 1179 sample points were used to evaluate the See5 decision tree; 21 of the original 1600 sample points were removed because of cloud coverage. 54 out of 1179 sample points were misclassified, an error of 4.6%. Higher error percentage in test data compared to training data may be due to overfitting to noise in the training data; it is possible that some training samples may not be members of the class they should represent (Pal and Mather 2003). The decision rules that were created by See5 were implemented in QGIS to generate a classification map (Figure 6.16).

Table 6.1: See5 output based on analysis of 27 attributes.

See5 output: Decision tree, training data evaluation & attribute usage based on 27 attributes

```
See5 [Release 2.10]     Wed May 31 14:16:58 2017

Class specified by attribute `grasslandtype'

Read 400 cases (27 attributes) from grassland.data

Decision tree:

S2REP21April <= 724.0084:
:...S2REP8Sep <= 721.8442: extensive (170/2)
:   S2REP8Sep > 721.8442:
:   :...S2REP21April > 722.8615: monoculture (5)
:       S2REP21April <= 722.8615:
:       :...S2REP25Sep <= 722.9341: extensive (25/1)
:           S2REP25Sep > 722.9341: monoculture (2)
S2REP21April > 724.0084:
:...NDVI21April > 0.9278637: monoculture (176)
    NDVI21April <= 0.9278637:
    :...S2REP21April <= 724.6226: extensive (5)
        S2REP21April > 724.6226:
        :...MASD21Apr8May <= 0.01505: extensive (3)
            MASD21Apr8May > 0.01505: monoculture (14)
```

```
Evaluation on training data (400 cases):

        Decision Tree
      ----------------
      Size      Errors

        8      3( 0.8%)   <<


       (a)   (b)    <-classified as
      ----  ----
       200          (a): class extensive
         3   197    (b): class monoculture


    Attribute usage:

     100%  S2REP21April
      51%  S2REP8Sep
      50%  NDVI21April
       7%  S2REP25Sep
       4%  MASD21Apr8May
```

Evaluation on test data (1197 cases)

```
Evaluation on test data (400 cases):

        Decision Tree
      ----------------
      Size      Errors

        8      13( 3.3%)   <<


       (a)   (b)    <-classified as
      ----  ----
       173     9    (a): class extensive
         4   214    (b): class monoculture
```

```
Evaluation on test data (400 cases):

        Decision Tree
      ----------------
      Size      Errors

        8      15( 3.8%)   <<


       (a)   (b)    <-classified as
      ----  ----
       385    15    (a): class extensive
                    (b): class monoculture
```

```
Evaluation on test data (379 cases):

        Decision Tree
      ----------------
      Size      Errors

        8      26( 6.9%)   <<


       (a)   (b)    <-classified as
      ----  ----
                    (a): class extensive
        26   353    (b): class monoculture
```

6.4.2 The importance of April for classification

See5 was run again to examine which attribute is the most important for classification if S2REP and NDVI for April 21st are excluded. This returns a much more complex DT in which S2REP for April 11th is the most important attribute (100%), followed by MASD4_spring (55%) (which still includes April 21st), S2REP for May 8th and S2REP for March 12th (Table 6.2). S2REP for September 8th is not used. The results illustrate the importance of the S2REP vegetation index for classification and confirms that April is the optimal month to discriminate between extensive and monoculture grassland. This is consistent with findings of Nitze et al. (2015) for grasslands in Ireland.

Table 6.2: See5 output when S2REP and NDVI for April 21st are removed from the dataset.

See5 Decision tree, training data evaluation & attribute usage based on 23 attributes

See5 [Release 2.10] Wed May 31 15:17:03 2017

Class specified by attribute `grasslandtype'

Read 400 cases (25 attributes) from 11april.data

Decision tree:

```
S2REP11April <= 722.0383:
:...S2REP8May <= 724.415: extensive (170/3)
:   S2REP8May > 724.415:
:   :...NDVI12March <= 0.8061701: monoculture (5)
:       NDVI12March > 0.8061701: extensive (4)
S2REP11April > 722.0383:
:...MASD4spring <= 0.03289:
    :...S2REP11April <= 723.4532:
    :   :...NDVI7June <= 0.7463987: monoculture (3)
    :   :   NDVI7June > 0.7463987: extensive (22/2)
    :   S2REP11April > 723.4532:
    :   :...MASD1Apr11Apr <= 0.03072: extensive (5/1)
    :       MASD1Apr11Apr > 0.03072: monoculture (23/1)
    MASD4spring > 0.03289:
    :...S2REP12March > 715.9318: monoculture (159/1)
        S2REP12March <= 715.9318:
        :...NDVI8Sep <= 0.8650235: extensive (3)
            NDVI8Sep > 0.8650235: monoculture (6)
```

Evaluation on training data (400 cases):

Decision Tree

Size	Errors
10	8(2.0%) <<

(a)	(b)	<-classified as
198	2	(a): class extensive
6	194	(b): class monoculture

Attribute usage:

100% S2REP11April
55% MASD4spring
45% S2REP8May
42% S2REP12March
7% MASD1Apr11Apr
6% NDVI7June
2% NDVI12March
2% NDVI8Sep

Evaluation on test data (1197 cases)

Evaluation on test data (400 cases):

Decision Tree

Size	Errors
10	13(3.3%) <<

(a)	(b)	<-classified as
387	13	(a): class extensive
		(b): class monoculture

Evaluation on test data (400 cases):

Decision Tree

Size	Errors
10	14(3.5%) <<

(a)	(b)	<-classified as
173	9	(a): class extensive
5	213	(b): class monoculture

Evaluation on test data (379 cases):

Decision Tree

Size	Errors
10	40(10.6%) <<

(a)	(b)	<-classified as
		(a): class extensive
40	339	(b): class monoculture

6.4.3 Contextual rule-based classification

This is a combination of simplified statistical classification and knowledge of 1st mowing date. The simplified classification is based on three attributes: MASD4_spring, S2REP and NDVI for April 21st. Evaluation on training data returns an error of 3.3%; 3 extensive sample points were misclassified as monoculture sample points and 10 monoculture sample points as extensive (Table 6.3). Again, S2REP for April 21st is the most important attribute used for classification. MASD4_spring is not used.

The remaining sample points were used as test data. Based on the simplified decision rules, 55 out of 1179 sample points are misclassified, an error of 4.6%. Misclassification mainly occurs for monoculture points, of these 46 are misclassified as extensive. The error percentage is similar to that of the complex decision tree (See section 6.4.1).

To avoid misclassification of monoculture fields that were mown before April 21st, an additional decision rule is added before classification. This rule implements a mowing threshold value of -0.01 for the NDVI change image NDVIApril11April21.

The simplified classification rules in combination with the mowing threshold were implemented in the SCP in QGIS to create the contextual rule-based classification map (Figure 6.17).

Table 6.3: See5 output using three attributes, S2REP and NDVI on April 21st and MASD4_spring.

See5 Decision tree, training data evaluation & attribute usage based on 3 attributes

```
See5 [Release 2.10]     Wed May 31 14:54:54 2017

Class specified by attribute `grasslandtype'

Read 400 cases (3 attributes) from three.data

Decision tree:

S2REP21April <= 724.0084: extensive (202/10)
S2REP21April > 724.0084:
:...NDVI21April > 0.9278637: monoculture (176)
    NDVI21April <= 0.9278637:
    :...S2REP21April <= 724.6226: extensive (5)
        S2REP21April > 724.6226: monoculture (17/3)
```

```
Evaluation on training data (400 cases):

        Decision Tree
      ----------------
      Size      Errors

         4     13( 3.3%)   <<


       (a)   (b)    <-classified as
      ----  ----
       197     3    (a): class extensive
        10   190    (b): class monoculture


    Attribute usage:

      100%  S2REP21April
       50%  NDVI21April
```

Evaluation on test data (1197 cases)

```
Evaluation on test data (400 cases):

        Decision Tree
      ----------------
      Size      Errors

         4      7( 1.8%)   <<


       (a)   (b)    <-classified as
      ----  ----
       393     7    (a): class extensive
                    (b): class monoculture
```

```
Evaluation on test data (400 cases):

        Decision Tree
      ----------------
      Size      Errors

         4      8( 2.0%)   <<


       (a)   (b)    <-classified as
      ----  ----
       180     2    (a): class extensive
         6   212    (b): class monoculture
```

```
Evaluation on test data (379 cases):

        Decision Tree
      ----------------
      Size      Errors

         4     40(10.6%)   <<


       (a)   (b)    <-classified as
      ----  ----
                    (a): class extensive
        40   339    (b): class monoculture
```

6.4.4 Classification maps and accuracy assessment

Figures 6.16 and 6.17 show the final classification maps for Littenseradiel. For accuracy assessment, the maps were compared with the ground truthed vector map for all grassland parcels in Littenseradiel using the SCP plugin in QGIS. Results of accuracy assessment are presented in error matrices (Tables 6.6 and 6.8). Maps showing the classification errors are included in Appendix F. Calculation of the Kappa coefficient or KHAT statistic is based on the error matrix; it is used to assess whether difference between images is due to chance or to real (dis)agreements. True agreement will approach 1 and chance agreement approaches 0 (Lillesand et al. 2015). It can also be used to compare classification accuracy between the two used methods. Table 6.4 gives an interpretation of the KHAT value (Bogoliubova and Tymków 2014).

Different measures of accuracy are presented. Overall accuracy is calculated as the total number of correctly categorized pixels divided by the total number of pixels. Producer's accuracy is the number of correctly classified pixels for each class divided by the total number of pixels for that class in the reference raster. User's accuracy is the number of correctly classified pixels for each class divided by the total number of pixels for that class in the classified raster (Lillesand et al. 2015).

Table 6.4: Interpretation of KHAT value (after Bogoliubova and Tymków 2014).

Value of Kappa (hat)	Interpretation of agreement
0.81 ≤ K (hat) ≤ 1	Almost perfect agreement
0.61 ≤ K (hat) ≤ 0.80	Substantial agreement
0.41 ≤ K (hat) ≤ 0.60	Moderate agreement
0.21 ≤ K (hat) ≤ 0.40	Fair agreement
0.0 ≤ K (hat) ≤ 0.20	Slight agreement
K (hat) < 0	Poor agreement

Statistical rule-based classification

Table 6.5 gives the total area for extensive and monoculture grassland for Littenseradiel based on the statistical rule-based classification (4 observation dates, 5 attributes). 69.7% of the pixels are classified as intensively managed, monoculture grassland and 30.3% as extensive grassland. Overall accuracy is 82.5% and KHAT is 0.59 (Table 6.6).

Contextual rule-based classification

Table 6.7 gives the total area for extensive and monoculture grassland for Littenseradiel according to the contextual rule-based classification (2 observation dates, 2 attributes and mowing threshold). 69.3% of the pixels are classified as intensively managed, monoculture grassland and 30.7 as extensive grassland. Overall accuracy is 84.3% and KHAT is 0.65 (Table 6.8).

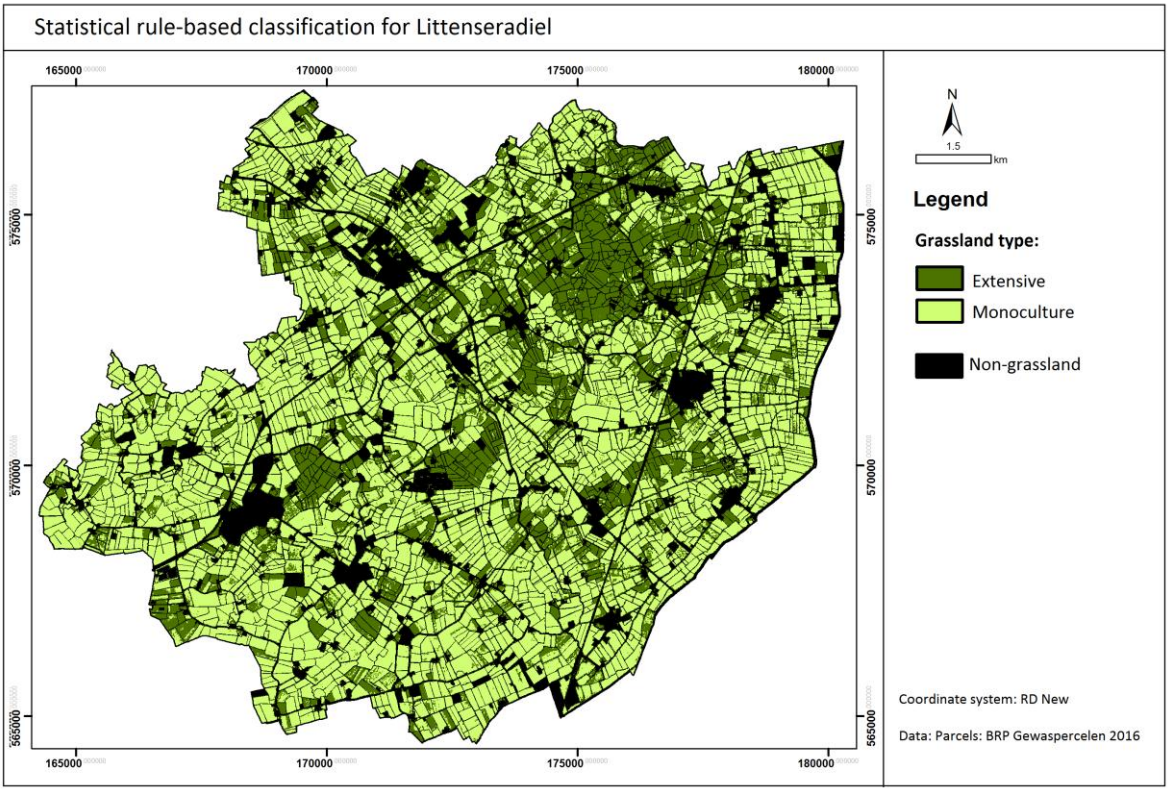

Figure 6.16: Statistical rule-based classification of grassland for Littenseradiel (4 observation dates).

Table 6.5: Total area for extensive and monoculture grassland according to statistical rule-based classification.

Classification	Nr. of pixels	Area (km2)	Percentage
Extensive	330793	33.1	30.3
Monoculture	761616	76.1	69.7
Total	1092409	109.2	100

Table 6.6: Error matrix, KHAT values, producer's and user's accuracy for statistical rule-based classification.

Error matrix	Reference data (columns)		
Classification (rows)	Extensive	Monoculture	Total (nr. of pixels)
Extensive	237757	93036	330793
Monoculture	97804	663812	761616
Total (nr. of pixels)	335561	756848	1092409
Overall accuracy = 82.5% Kappa hat = 0.59			
Class	Producer's accuracy (%)	User's accuracy (%)	Kappa hat
Extensive	70.9	71.9	0.59
Monoculture	87.7	87.2	0.58

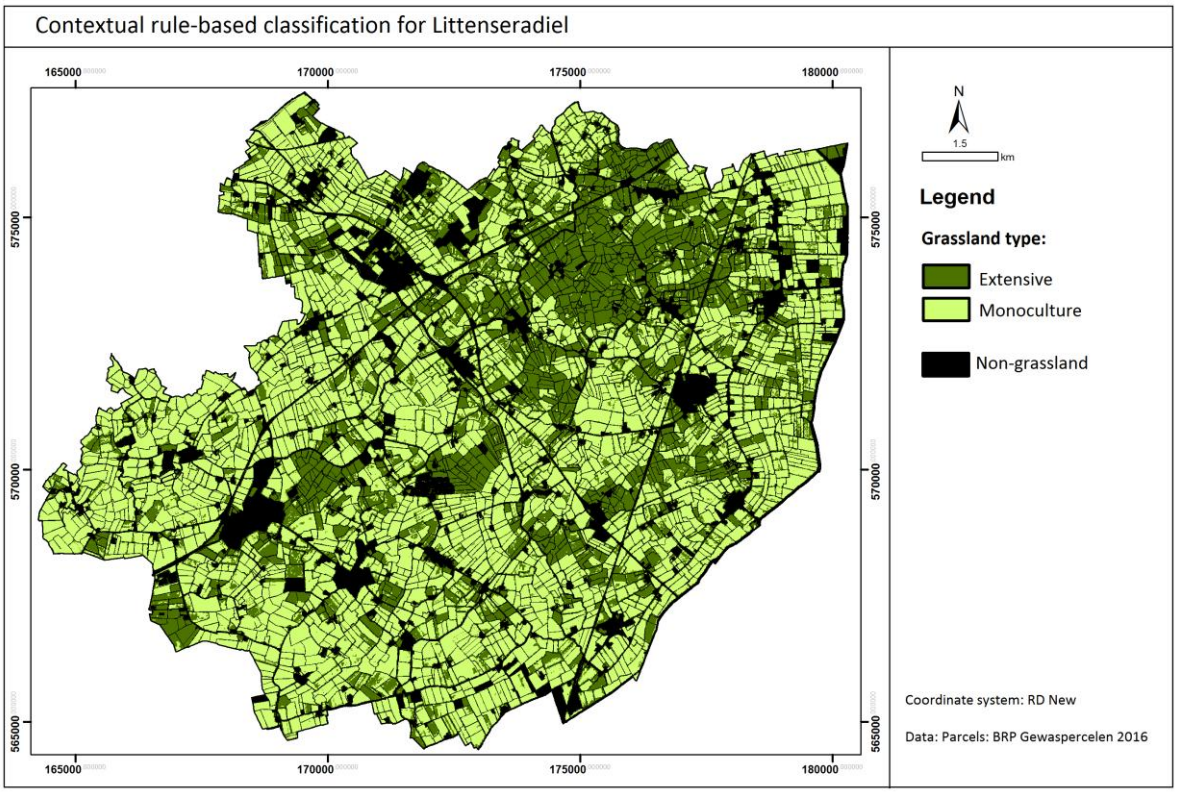

Figure 6.17: Contextual rule-based classification of grassland in Littenseradiel (2 observation dates).

Table 6.7: Area for extensive and monoculture grassland in Littenseradiel.

Classification	Nr. of pixels	Area (km2)	Percentage
Extensive	335561	33.6	30.7
Monoculture	756848	75.7	69.3
Total	1092409	109.2	100

Table 6.8: Error matrix, KHAT, producer's and user's accuracy for contextual rule-based classification (Littenseradiel).

Error matrix	Reference data (columns)		
Classification (rows)	Extensive	Monoculture	Total (nr. of pixels)
Extensive	271900	107306	379206
Monoculture	63661	649542	713203
Total (nr. of pixels)	335561	756848	1092409
Overall accuracy = 84.3% Kappa hat = 0.65			
Class	Producer's accuracy (%)	User's accuracy (%)	Kappa hat
Extensive	81.0	71.7	0.59
Monoculture	85.8	91.1	0.71

Additional validation

Figure 6.18 shows the contextual rule-based classification map for Littenseradiel with the outlines of meadow bird reserves, National Nature Network, agricultural nature management packages and locations of organic/bird-friendly farmers. Nearly all grassland pixels within bird reserves are classified as extensive. Patches of extensive grassland are also found at organic/bird-friendly farmers, for example the parcels of Black-tailed Godwit farmer Murk Nijdam in the 'Súdhoeke' (black arrow) and of the neighboring sheep farm. Fields with nest protection are often classified as monoculture grassland.

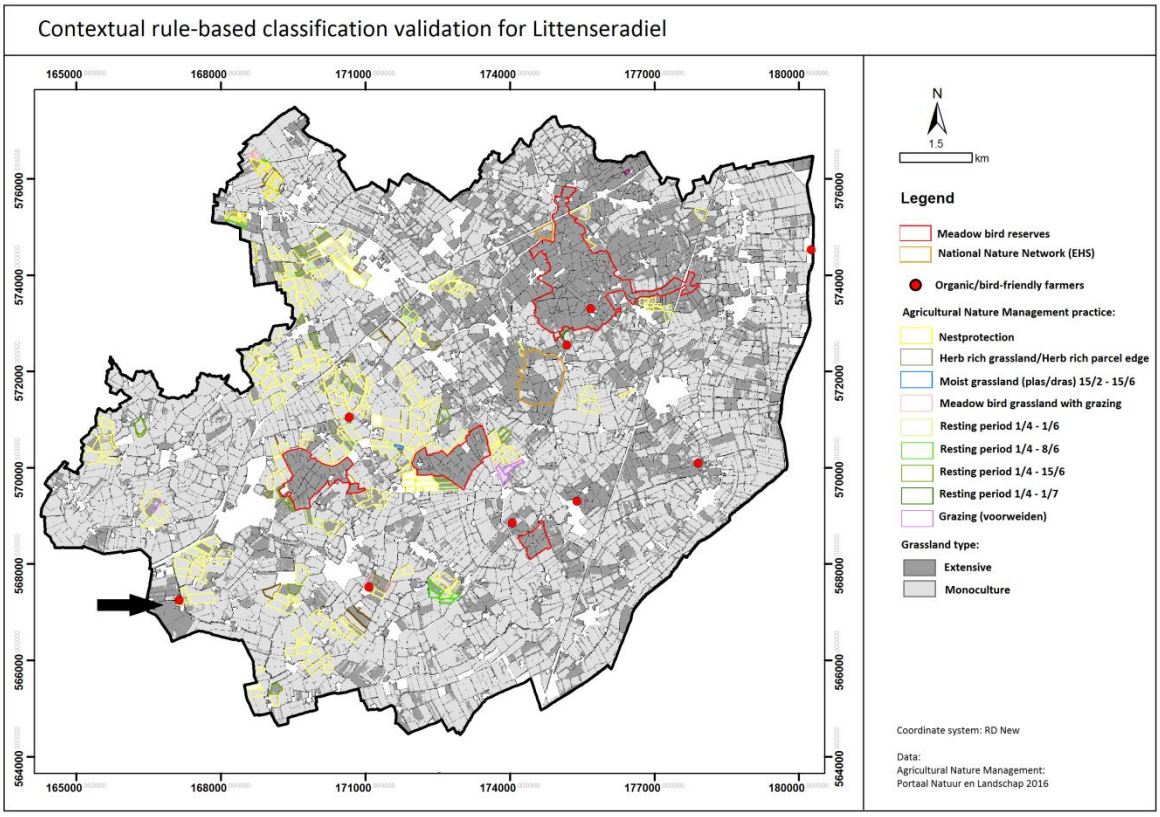

Figure 6.18: Additional validation for contextual rule-based classification (non-grassland shown in white; black arrow = 'Súdhoeke') (Agricultural Nature Management data from: Portaal Natuur en Landschap 2016).

Conclusion

Overall accuracy for contextual rule-based classification (84.3%) is slightly higher than for statistical rule-based classification (82.5%). KHAT is also higher for contextual rule-based classification, 0.65 (=substantial agreement) compared to 0.59 (=moderate agreement). These overall accuracies are comparable to those found by Franke et al. (2012). Overall accuracy for both methods may be underestimated because for many fields, parcel edges are extensively managed, whilst the ground truthed vector map is based on discrete values for the whole parcel.

In the statistical rule-based classification, misclassification is mainly due to failure to recognize monoculture fields that were mown before April 21st. The contextual rule-based classification removes most of these errors by applying a mowing threshold. Nevertheless, misclassification still occurs because not all mown fields are recognized at this threshold (See section 7.2.1). Also, the few fields that were cut before April 11th are not recognized and may be misclassified as extensive.

Misclassification of monoculture as extensive grasslands may also occur for fields that contain areas of bare soil, e.g. due to recent re-seeding. Grasslands that have been used for growing maize crops in previous years may also be misclassified as extensive grasslands because grass growth is slower here. Relatively small fields that are grazed by a large number of animals may also be misclassified as extensive grasslands.

An additional finding for Littenseradiel is that mean parcel size is 2.72 ha (27227 m^2) for monoculture grasslands vs. 1.96 ha (19601 m^2) for extensive grasslands; also, extensive parcels tend to be irregular in shape, whereas monoculture parcels are more symmetrical. It may be an option to incorporate parcel geometry for classification.

6.4.5 Contextual rule-based classification for South-Central Friesland study area

Because contextual rule-based classification yields the highest KHAT value and overall accuracy, this method was used for classification of the South-Central Friesland study area (Figure 6.19). Here, 40.3% of the grassland is classified as extensive and 59.7% as monoculture (Table 6.9).

The map is further validated by comparing the classification with the outlines of important (meadow) bird areas that are part of the National Nature Network (former EHS) as well as the database of organic/bird-friendly farmers (Figure 6.20). From this map can be observed that nearly all grassland in nature areas is classified as extensive grassland and that concentrations of extensive grassland are also found near organic/bird-friendly farmers. Peat soils contain relatively more extensive grassland than clay soils. Reason for this may be that these soils are less suitable for intensive management because their natural fertility is lower and groundwater levels are higher.

Table 6.9: Area and percentage of extensive and monoculture grassland for South-Central Friesland study area.

	Nr. of pixels	Area (km2)	Percentage
Extensive	3968080	396.8	40.3
Monoculture	5880651	588.0	59.7
Total	9848731	984.8	100

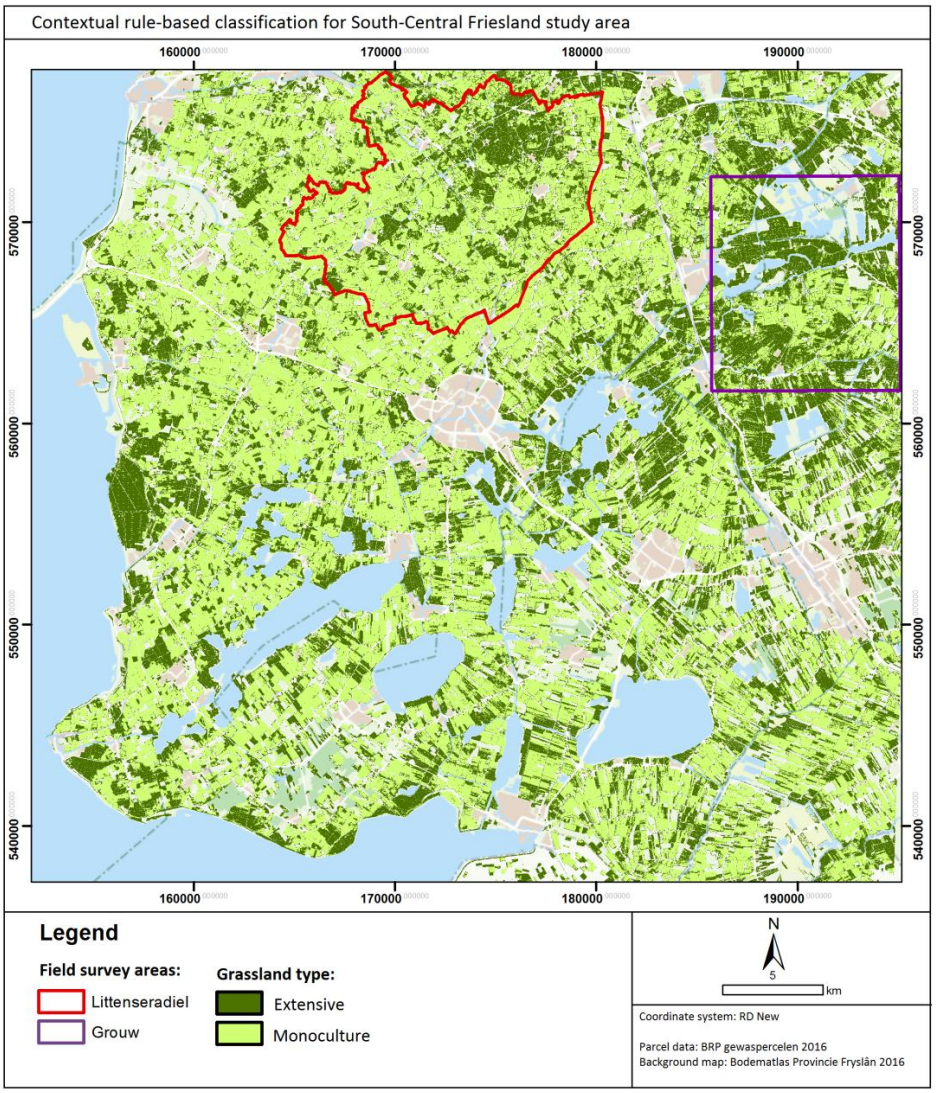

Figure 6.19: Contextual rule-based grassland classification for South-Central Friesland (Background image from Provincie Fryslân 2017).

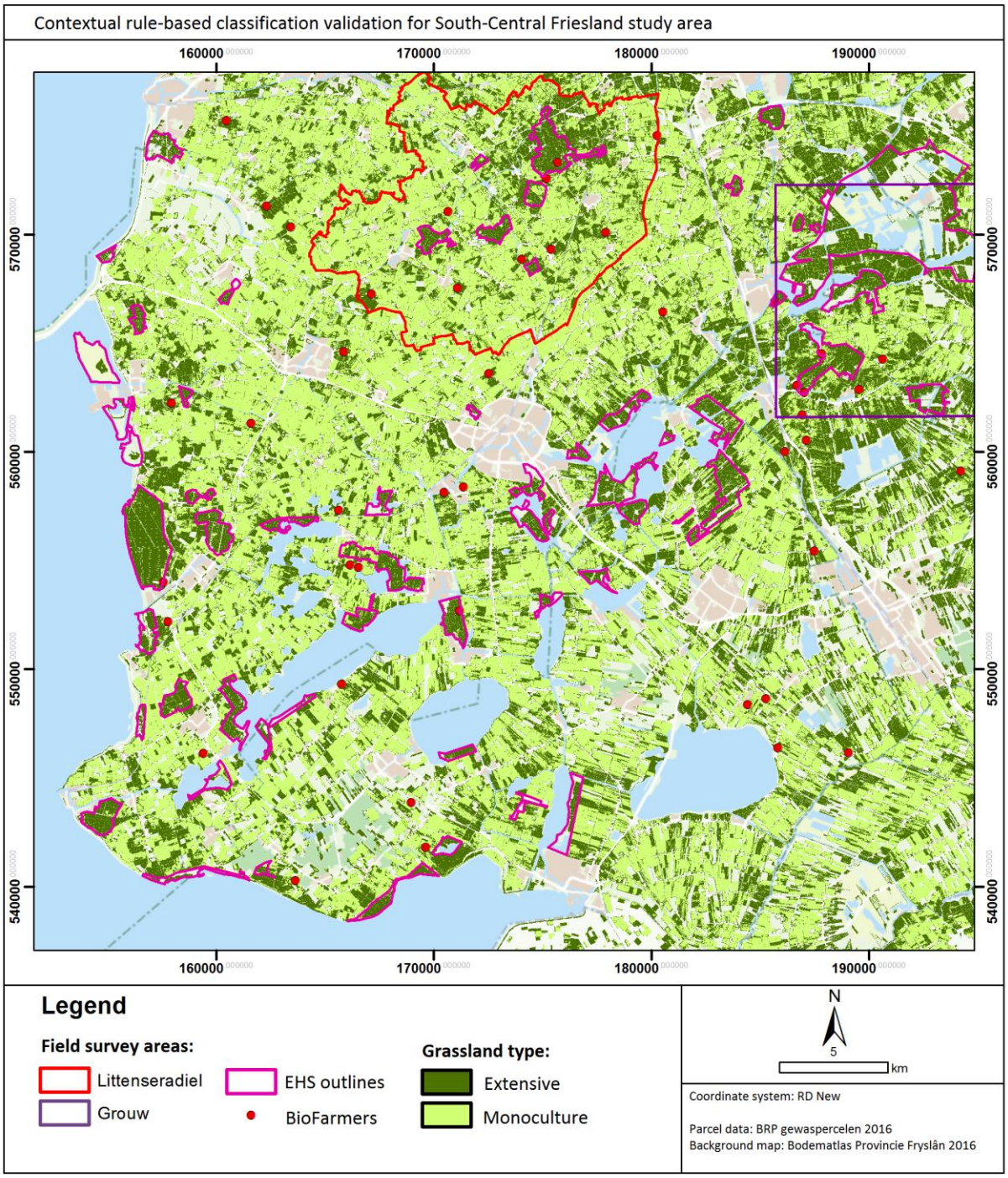

Figure 6.20 Contextual rule-based classification for study area, compared with location of the National Nature Network (EHS) and organic/bird-friendly farmers (Background image from Provincie Fryslân 2016).

6.5 Spectral heterogeneity

To assess spectral heterogeneity for monoculture and extensive grasslands, principal component analysis was carried out for April 21st. The first two principal components explain 98.66% of total variance (Appendix G). PC1 and PC2 were used to calculate the mean distance to the spectral centroid for 5 monoculture and 5 extensive grassland plots of 1 ha in size (Figure 6.21). Plots herbs5 and mono5 correspond to the areas in Littenseradiel for which biodiversity is known from the Nationale databank Flora & Fauna (2017). In mono5, 8 vascular plant species have been counted and herbs5 contained 37 vascular plant species. Mean distance to spectral centroid is almost twice as high for herbs5 than for mono5 (Table 6.10). For these 10 plots, mean distance to centroid is smaller for monoculture than for herb-rich grasslands. But, within the monoculture class as well as within the herb-rich class, mean distance shows a wide range. Further research is necessary to test whether spectral heterogeneity can be used as a measure for herb-richness; vascular species counts for 1 ha plots in extensive grasslands of different categories of herb-richness are required to establish a correlation between spectral heterogeneity and species richness.

Table 6.10: Mean distance to spectral centroid for 10 plots of 1 ha in size (100 pixels).

Spectral variability (April 21st 2016)					
Soil type	Plot (1 ha)	Mean distance	Soil type	Plot (1 ha)	Mean distance
Clay soil	herbs1	0.03445	Peat soil	herbs2	0.02423
	mono1	0.00758		mono2	0.01292
Clay soil	herbs3	0.02180	Peat soil	herbs4	0.04754
	mono3	0.01513		mono4	0.01496
Clay soil	herbs5	0.01766			
	mono5	0.00846			

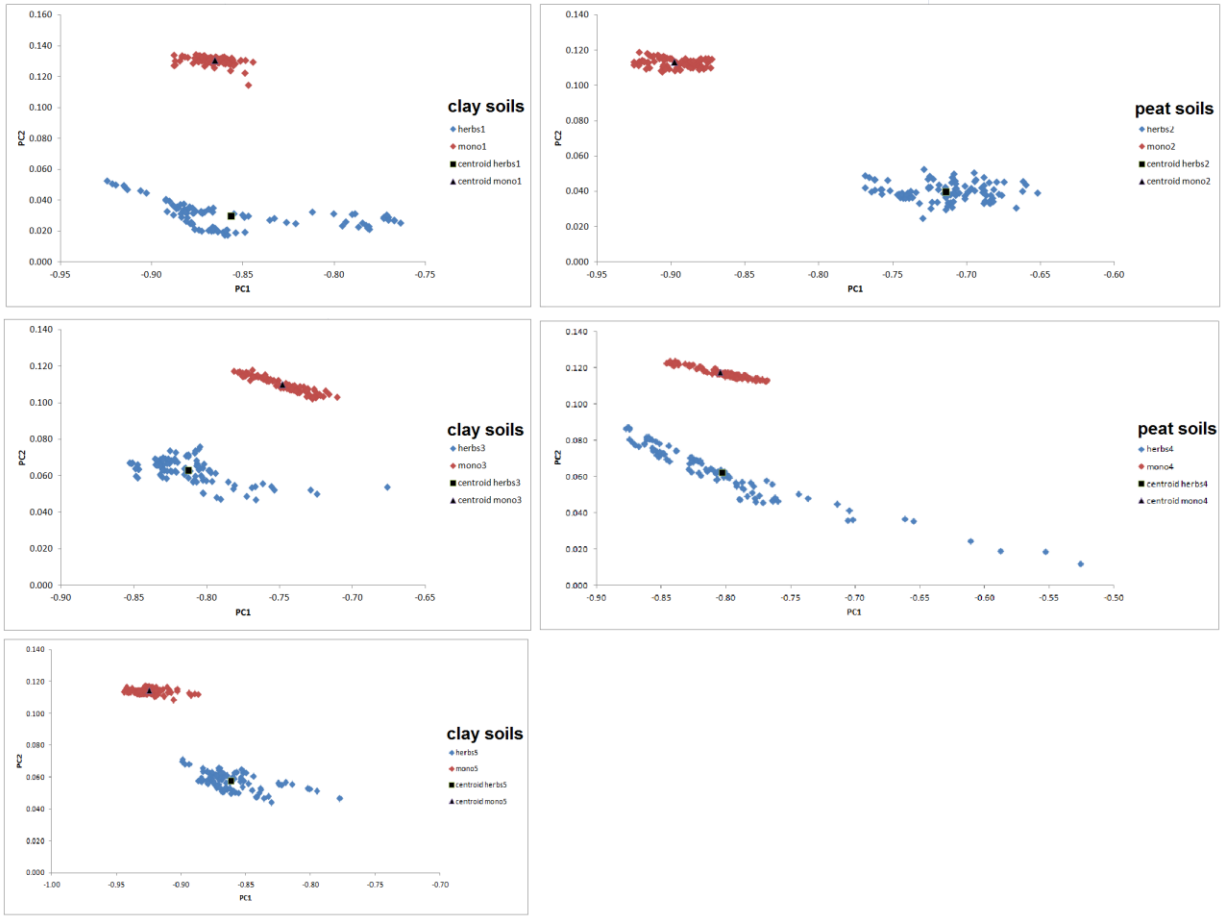

Figure 6.21: Scatterplots showing the mean distance to spectral centroid for 10 different plots of 1 ha.

7.0 Applications for meadow bird conservation

7.1 Grassland types compared to distribution of meadow bird nests

This chapter illustrates the potential use of Sentinel-2 data for meadow bird conservation. First, the grassland management intensity map was used to analyze the distribution of nests of lapwing, redshank, godwit and oystercatcher in Littenseradiel. Figure 7.1 shows the distribution map for godwit nests, larger versions of this map and for the other species are included in Appendix H. Table 7.1 gives the total number of nests for extensive, monoculture and arable land. All four species prefer extensive grassland over monoculture grassland as nesting site. For godwit and redshank, presence of extensive grassland is most important. Lapwings also favor bare lands/croplands over monoculture grassland. Nevertheless, still 20% of the combined species breeds on monoculture lands. Therefore, protection of their nests and chicks remains essential in these parcels.

For all species, it is clearly visible that nests concentrate within bird reserves and on parcels of organic/bird friendly farmers. Lapwing nests also concentrate on bare lands/croplands (See Appendix H).

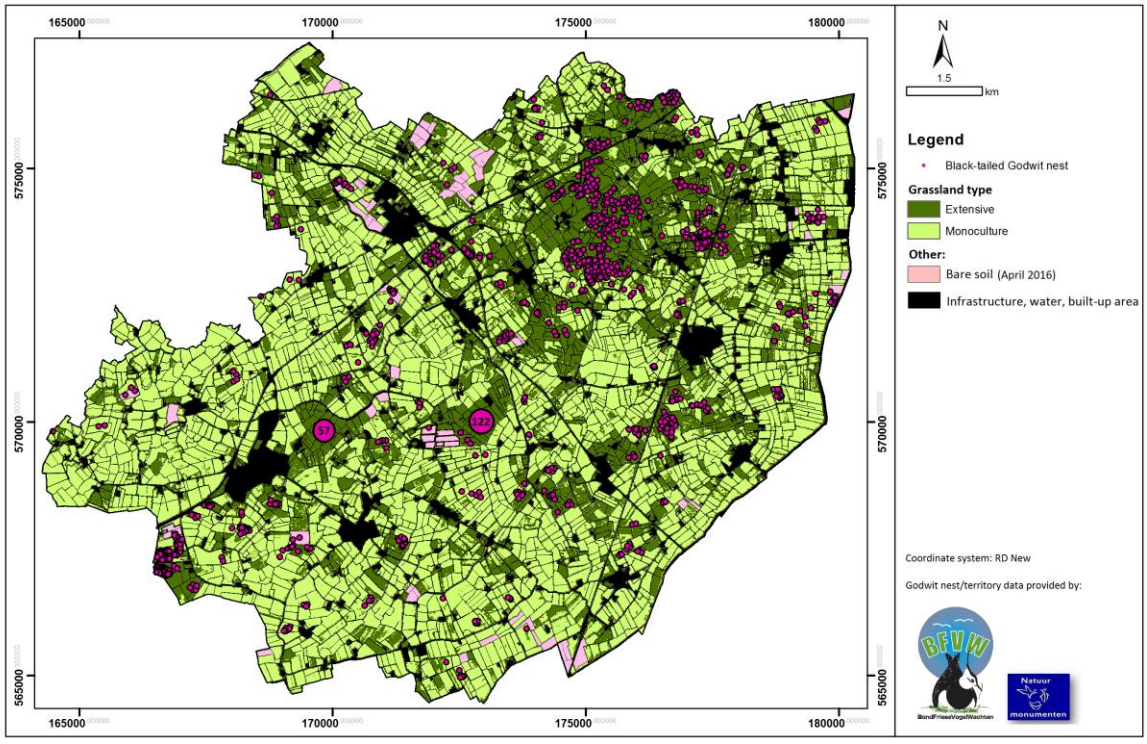

Figure 7.1: Contextual rule-based classification with distribution of Black-tailed Godwit nest sites for Littenseradiel 2016. Total numbers are given for Skrok and Skrins (Nest distribution data for Littenseradiel from: Bond Friese Vogel Wachten 2016; nr. of territories for Skrok and Skrins from: De Boer and De Winter 2016).

Table 7.1: Grassland type vs. distribution of nests in Littenseradiel (2016) for four meadow-bird species.

	Total nr. of nests for 2016	Extensive grassland (33.6 km^2)			Monoculture grassland (75.7 km^2)			Other/Arable land (2.1 km^2)		
		Nr. of nests	%	Nests/km^2	Nr. of nests	%	Nests/km^2	Nr. of nests	%	Nests/km^2
Black-tailed Godwit	1150	891	77	26	237	21	3	22	2	10
Redshank	554	435	79	13	115	21	1	4	0.7	2
Northern Lapwing	1004	607	60	18	141	14	2	256	26	122
Oystercatcher	517	293	57	9	161	31	2	63	12	30
Combined species	3225	2226	69	66	654	20	9	345	11	164

7.2 Detection of mowing and grazing

7.2.1 Detection of mowing

Mowing can be detected on Sentinel-2 true color composites using visual inspection (Figure 7.2). Distinct differences in color can be seen between parcels that were not cut, that were freshly cut and were recently cut (= ca. 7 days before image acquisition date). To be able to create a model that allows fast assessment of 1st mowing dates, the influence of mowing on NDVI values was examined. For the mowing model, NDVI was preferred over MASD because MASD gives the absolute change, making it difficult to discriminate between changes due to mowing or fast grass growth.

NDVI values from not mown, freshly mown and recently mown parcels were extracted for April 21st and May 7th, using 6 plots of 1 ha in size (200 pixels per category). NDVI values for fields that were not cut, show a minimal decrease in NDVI whilst freshly cut fields display a mean drop in NDVI of 0.47 (Figure 7.3). Mean drop in NDVI for recently cut parcels is 0.21; the minimum drop is 0.16. Clearly, under the right weather conditions, the vegetation recovers very fast after mowing. This observation corresponds with research performed in France, where NDVI values increased to 'normal' in ca. 15 days (Courault et al. 2010). Based on this knowledge, it is evident that when the gap between two observation dates is 15 days or longer, mowing may not be detected. Unfortunately, the 2016 Sentinel-2 time series has wide gaps, e.g. 30 days between May 8th and June 7th.

Despite this limitation, a mowing model was developed based on change in NDVI between two consecutive observation dates, using a mowing threshold of -0.1 (Figure 7.4). This threshold was chosen based on trial and error; if -0.16 was used (= the minimum change for recently cut parcels), some fields that had been cut, were misclassified as not cut.

To test the reliability of this mowing model, all fields in Littenseradiel that showed visual evidence of mowing between April 21st and May 8th were counted. In total, 532 fields were mown. The model detected 531 of these mown parcels (=99.8%). Between April 11 and April 21st, visual inspection detected 131 mown parcels of which 97 were correctly classified by the model (=74%). Probably the threshold of -0.1 is too low for this period due to fast grass growth. However, if the threshold is raised to e.g. -0.08, intensively grazed parcels are mistaken for mown parcels.

Figure 7.2: Sentinel-2 true color composite for May 7th 2016 showing the difference in color between parcels that were not mown (dark green), freshly mown (yellow green) and mown ca. 7 days before (light green).

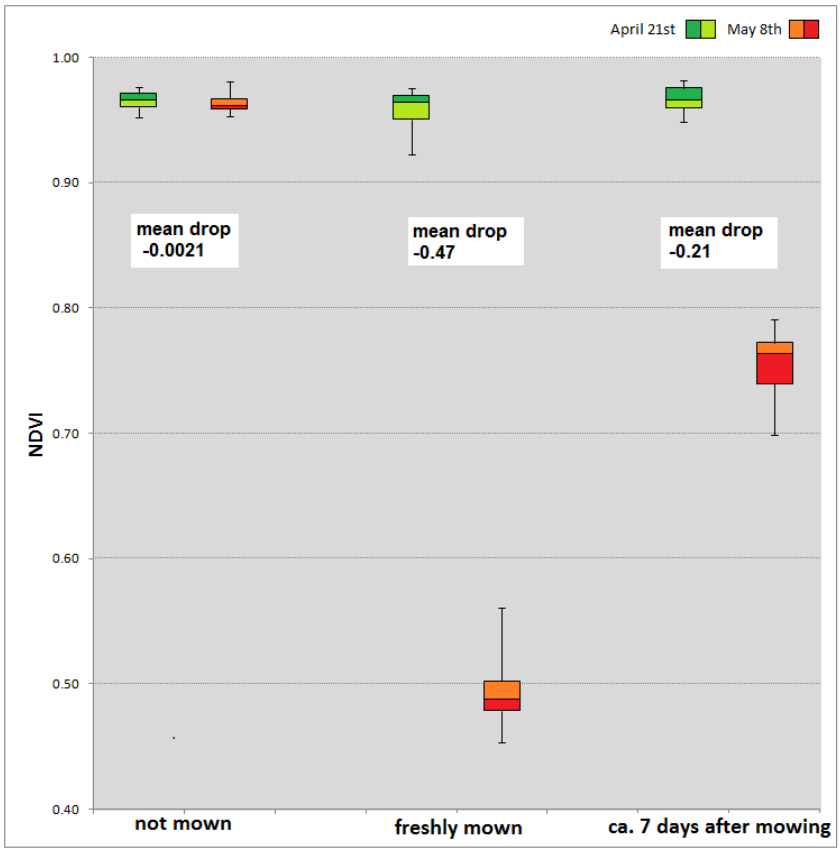

Figure 7.3: Differences in NDVI values between April 21st and May 8th for fields that were not mown, freshly mown or recently mown.

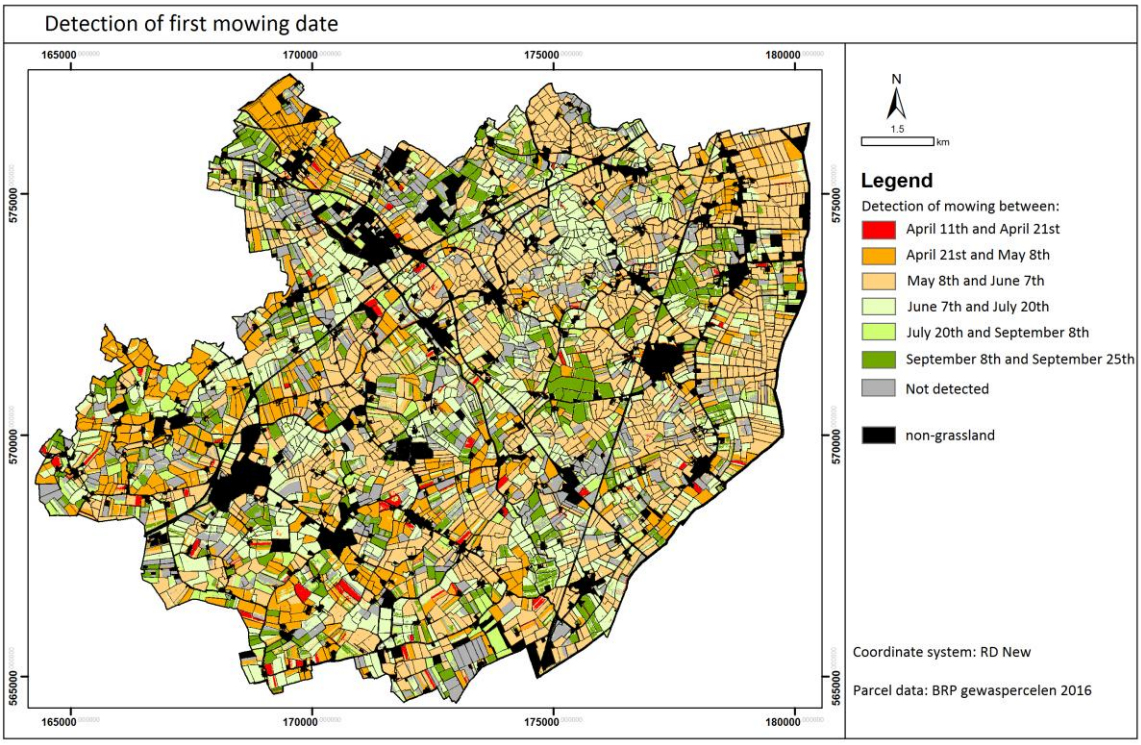

Figure 7.4: Map of Littenseradiel showing detection of mowing based on NDVI change of at least -0.1 between observation dates. Only the 1st detection of mowing for each parcel is shown. Non-grassland is shown in black (See Appendix I for larger version).

MODIS 16 day composite EVI time series were successfully used by Lips (2011) to estimate first mowing dates for grassland. The model is based on the difference in EVI value between two consecutive composites. By applying a mowing threshold of -0.06 a detection accuracy of 71.4% was achieved (Lips 2011).

To compare the results for the Sentinel-2 mowing model with MODIS 16 day composite EVI data, MODIS13Q satellite imagery was downloaded for the 2016 growing season. MODIS 16 day EVI values were extracted for pure grassland pixels of extensive and monoculture parcels, Sentinel-2 NDVI values were extracted for pixels of the same parcels (Figure 7.5).

First detection of mowing for the monoculture parcel is between April 22nd and May 7th (median date is April 29th) for the MODIS EVI time series and between April 21st and May 8th for the Sentinel-2 NDVI time series. For the extensive parcel, mowing is detected between July 11th and July 26th (median date is July 18th) for the MODIS EVI time series and between June 7th and July 20th for the Sentinel-2 NDVI time series. This means that for the monoculture parcel, detection of 1st mowing date based on Sentinel-2 data, is comparable to the MODIS EVI data. For the extensive parcel, the 1st mowing date in ca. half July is also accurately detected, but probably only because mowing took place shortly before July 20th. If this parcel had been cut shortly after June 7th, it would not have been detected. Due to the wide gaps in the current Sentinel-2 time series, it is not yet possible to check precisely whether farmers obey the agreed resting period for parcels under agricultural nature management; e.g. no mowing before June 15th, June 22nd or July 1st. When Sentinel-2B is active, chances of acquiring cloud free datasets at higher temporal resolution (every 5 days) increase, which will improve the model.

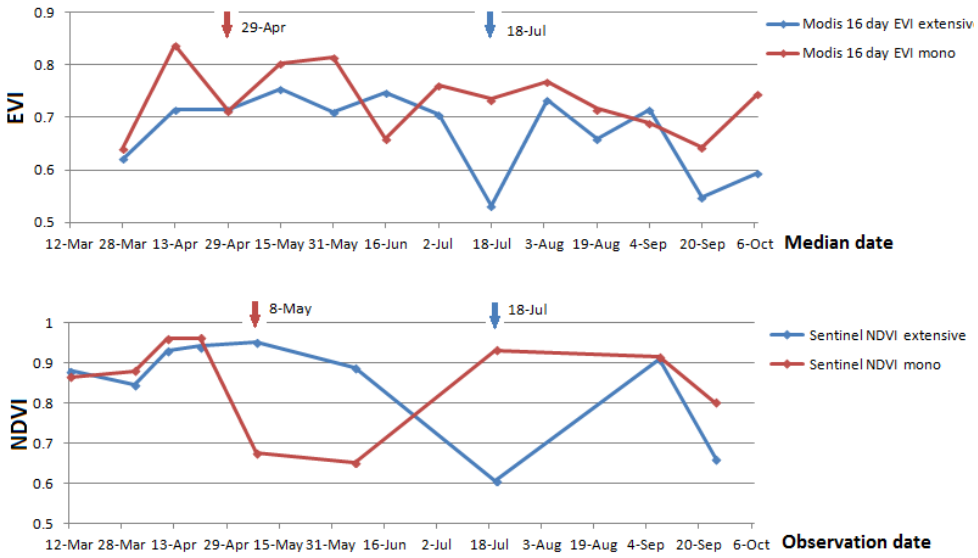

Figure 7.5: Detection of mowing: MODIS EVI 16 day composite time series (median date) vs. Sentinel-2 NDVI time series (observation date) for extensive and monoculture parcels. Red arrows = 1st mowing date monoculture parcel, blue arrows = 1st mowing date extensive parcel.

Figure 7.4 shows the first detection of mowing per parcel for Littenseradiel based on a change in NDVI of at least -0.1 between two consecutive observation dates. Because Sentinel-2 temporal resolution for April to early June is quite good, detection of parcels that were cut for the first time early in spring is reliable. But for monoculture parcels with first detection of mowing in September, it is to be expected that earlier mowing dates have been missed. However, the map clearly shows the difference in mowing dates for monoculture and extensive parcels. Large scale mowing occurred between April 21st and May 8th. First mowing activity in bird reserves is detected between June 7th and July 20th.

Despite its disadvantages, the map does nicely show differences in mowing regime, e.g. cutting of strips of grassland in some parcels (Figure 7.7), or parcels where only the edges have been cut. The map can also be used to (roughly) detect adequate mowing management. Figure 7.6 shows the mowing dates and distribution of meadow bird nests (all 4 species) for some parcels. The white arrow points at a parcel that was cut very early, between April 11th and April 21st. In May, 6 nests were found here. The second cut was in July, giving the chicks enough time to become fully-fledged. Another example of successful mowing management is found at the blue arrow; this is a parcel with several bird nests that was cut in July.

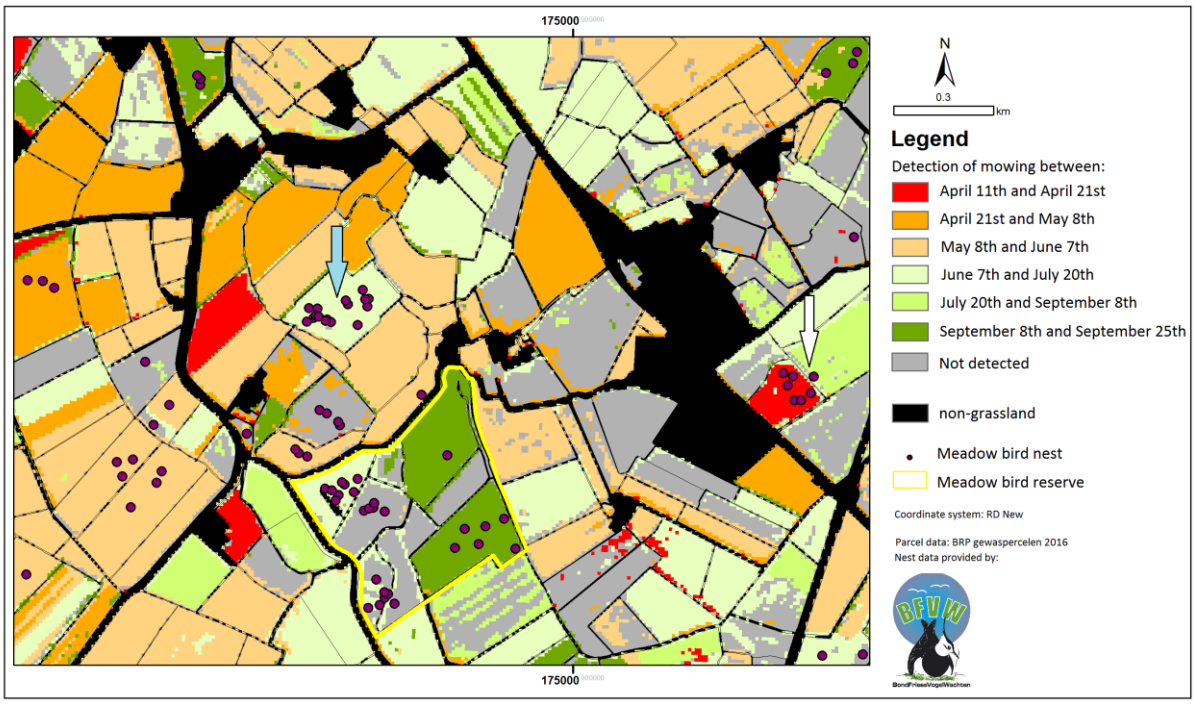

Figure 7.6: Examples of adequate mowing management to support bird conservation (white and blue arrows).

Figure 7.7: Cutting of strips of grassland to feed cattle that are kept indoors, Littenseradiel, April 2017.

7.2.2 Detection of grazing

In the model of Lips (2010), based on MODIS EVI 16 day composites, grazing could not be differentiated from mowing. Sentinel-2 NDVI data was used to see whether it is possible to detect grazing. NDVI values for April 21st and May 8th were extracted for 2 grazed plots and 2 non-grazed plots of 1 ha in size (200 pixels for each class). The grazed plots are intensively grazed by cattle.

Non-grazed plots show a slight increase in NDVI whilst grazed plots show a mean drop in NDVI value of 0.066 (Figure 7.8). The range in NDVI for parcels grazed between April 21st and May 8th is wide, with a maximum drop of 0.16. Unfortunately, in the current mowing detection model based on NDVI decrease of at least 0.1, pixels in intensively grazed parcels will be therefore mistaken for mown parcels. However, upon inspection of the mowing map for Littenseradiel, one can see that grazed parcels often display a mixture of colors opposed to a uniform color for mown parcels (Figure 7.9). In grazed parcels as opposed to cut parcels, grass of irregular length occurs because patches of grass are not grazed (Figure 7.10).

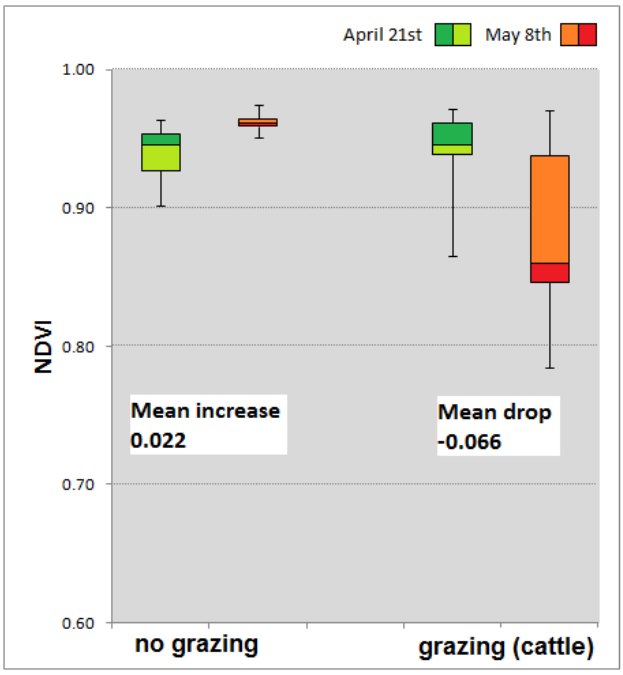

Figure 7.8: Difference in NDVI between April 21st and May 8th for parcels that are grazed by cattle and parcels that were not grazed.

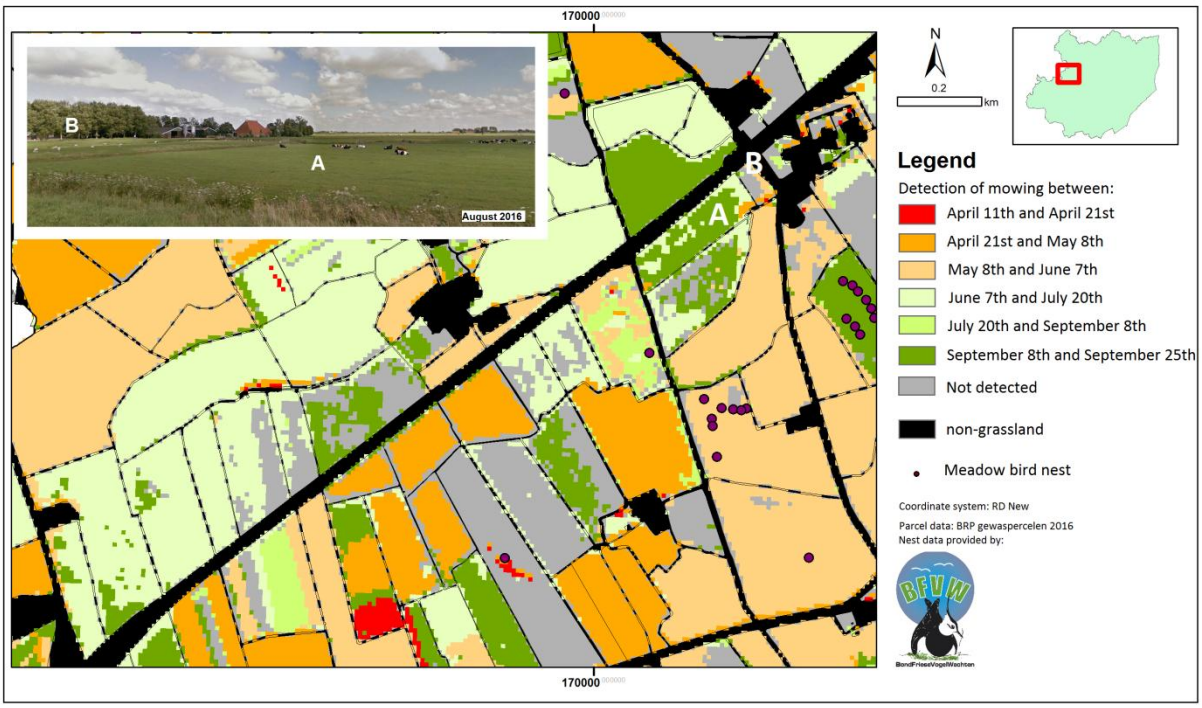

Figure 7.9: Grazed parcels tend to show a irregular mixture of colors on the mowing map: parcel A is grazed by cattle, parcel B by sheep. Inset shows photograph of these parcels from August 2016 (from Google Earth).

Figure 7.10: Monoculture parcel grazed by cattle showing remaining patches of longer grass, Littenseradiel (April 2017).

8.0 Conclusion/Discussion

For areas with known distribution of grassland, Sentinel-2 satellite imagery has shown high potential for detecting management intensity, which includes fertilizing, mowing and grazing. It is possible to create maps that show the extent of intensively managed and extensively managed grasslands at parcel level.

In springtime, for all spectral bands on both clay and peat soils, mean spectral response for extensive grasslands differs significantly from the mean response for monoculture grasslands ($p < 0.0001$, alpha 0.05 for April 21st)(Figure 6.1). After the 1st mowing event (around May 8th for monoculture and after June 7th for extensive grasslands), spectral response patterns show more overlap; for some of the spectral bands, differences between monoculture and extensive grassland are no longer significant (Appendix J).

Local soil type strongly influences spectral response patterns. When comparing clay vs. peat soils, it was found that in springtime, mean reflectance values for extensive grassland and monoculture grasslands are significantly different ($p < 0.0001$, alpha 0.05 for April 21st). For accurate classification of grassland management intensity in a research area with both clay and peat soils it is essential to use training data for both soil types. If only samples for clay soils are used, the threshold for the class monoculture will be set too high, causing misclassification of monoculture grassland on peat soils.

From March 12th to April 21st, reflectance in the red-edge, NIR and SWIR range for monoculture grassland on peat soils is lower than for monoculture on clay and reflectance for extensive grassland on peat is lower than extensive on clay. This may be caused by differences in soil moisture. Low reflectance in B11 is related to high leaf water content (Table 4.1). Higher average groundwater levels in peat soil areas slow down grass growth (Figure 4.9). In early spring, vegetation cover is less dense on peat soils, especially in extensive grasslands. Because less photosynthetically active vegetation is present, reflectance will be lower than for grassland on clay soils. Also, background effects of soil moisture and the soil itself may directly decrease reflectance. It is known that high organic matter content of peat soils reduces their reflectance (Lillesand et al. 2015).

Sentinel-2 spectral bands that display the greatest variability in spectral response for both grassland categories are bands 5, 6, 7, 8 and 8A. In springtime, variance in reflectance for extensive grasslands is higher than for monoculture grasslands; this reflects the heterogeneous character of herb-rich grasslands and the uniform character of intensively managed ryegrass plots. From March 12th to April 11th, variability also shows a small peak for band 11 for extensive grassland on peat soils; this is probably related to differences in soil moisture.

The seasonal pattern of the S2REP and NDVI time series is comparable to the grassland production curve, showing a peak in May, lower values in July and a second peak in September (Appendix C; D). The NDVI time series for extensive grasslands on peat soils shows a delayed onset of grass growth with a peak in June, whilst monoculture grasslands reach their peak on April 21st. This delay is less pronounced on clay soils. Delayed onset of grass growth on peat soils is caused by higher groundwater levels in spring.

S2REP, NDVI time series and MASD values were used as input for See5. S2REP, in which bands 4, 5, 6 and 7 are used, was found to be the most important attribute for classification of grassland management intensity (100%). NDVI was the second most important attribute (50%). An advantage of VI's that incorporate red-edge bands, such as the S2REP, is that they are less susceptible to saturation than the NDVI in areas with dense vegetation cover (Mutanga and Skidmore

2004). Imagery for April 21st was found to be the most important for successful classification. Both the S2REP (100%) and NDVI (50%) attributes for this date were essential in the See5 decision tree. The MASD parameter was not found to be very useful for classification. See5 did not use it at all, unless S2REP and NDVI for April 21st were removed. It should be noted that MASD only describes the magnitude of the spectral response and does not give any information on the spectral shape. Nevertheless, the MASD maps do give a nice impression of spatiotemporal differences in spectral dynamics.

Based on these findings it can be concluded that for classification, availability of springtime imagery is required, preferably from the second half of April. Other European studies have also shown that spectral separability is optimal in April (Nitze et al. 2015) and Franke et al. (2012) concluded that availability of imagery before the 1st mowing date, was essential for successful classification of grassland management intensity.

Two related classification methods were tested: statistical rule-based classification and contextual rule-based classification. Accuracy assessment has shown that both classification methods performed well. Overall accuracy for contextual rule-based classification (84.3%) is slightly higher than for statistical rule-based classification (82.5%). KHAT is also higher for contextual rule-based classification, 0.65 (=substantial agreement) compared to 0.59 (=moderate agreement). These overall accuracies are comparable to those found by Franke et al. (2012). Overall accuracy may be underestimated, because for many fields parcel edges are extensively managed, whilst the ground truthed vector map is based on discrete values for the whole parcel. Differences in overall accuracy and KHAT can be mainly attributed to the addition of the mowing threshold for the contextual rule-based classification, through which misclassification of mown parcels is avoided. Despite adding a mowing threshold, misclassification of monoculture as extensive grasslands may still occur due to recent re-seeding, slower grass growth in fields that have been used for maize crops in previous years, fields that are intensively grazed by sheep or cattle and failure to detect mowing.

Provided that adequate springtime imagery is available, accurate grassland management classification does not necessarily require data for many observation dates. The statistical method uses four scenes and the contextual method two. For the contextual rule-based classification, availability of data from two consecutive observation dates is essential, preferably at an interval of 10-15 days, to be able to detect mowing of intensively managed grasslands.

The current grassland classification model is based mainly on the S2REP; this vegetation index seems to be very useful for detecting grassland management intensity. It is especially sensitive to application of liquid manure, which causes the red-edge position to shift to the right due to increase of chlorophyll content. This effect of fertilizer application was also found in previous research (Sibanda et al. 2017; 2015). Red Edge Position values near 700 nm have been associated with low leaf chlorophyll concentration, whilst Red Edge Position values near 725 nm point to high leaf chlorophyll concentration (Cho and Skidmore 2006). For monoculture on clay soils the highest mean is 727 nm compared to 726 nm for peat soils. Highest mean value for extensive grassland on clay soils is 722 nm compared to 723 nm for peat soils. Here, no liquid manure is used, groundwater levels are high and vegetation grows slower in springtime. Nevertheless these S2REP values can still be considered quite high, which may be evidence for high nitrogen deposition (eutrophication) through air and water pollution; this is problematic in nature areas where it causes loss of biodiversity (CLO 2016).

The current model reflects grassland management intensity more than true difference in species of grasses and herb-richness. It is difficult to separate these parameters because they are

strongly related. The narrow range of S2REP and NDVI for intensively managed grassland compared to extensive grassland does reflect the homogeneous character of ryegrass monocultures on which large amounts of liquid manure are applied. Some fertilized ryegrass fields contain a lot of dandelions; this is not recognized by the current model, probably because it has no influence on total biomass and chlorophyll content.

Differences in herb-richness between extensively managed parcels are not recognized. Most of the extensively managed grasslands in bird reserves and at organic farmers belong to the most herb-rich type (category 3). But, in Littenseradiel, moderate herb-rich grasslands (category 2) also occur. In this thesis, it was investigated whether spectral heterogeneity can be used as a proxy for biodiversity. Mean distance to spectral centroid was calculated as a measure of spectral heterogeneity. It was found that mean distance to centroid is smaller for monoculture grasslands than for herb-rich grasslands. However, it requires further research, preferably in combination with vascular species counts in 1 ha plots for category 2 and category 3 grasslands to assess whether this measure truly correlates to herb-richness and is significantly different for grasslands of each category.

According to the contextual rule-based classification for Littenseradiel, 31% of the total grassland area is classified as extensive vs. 69% as monoculture. For the South-Central Friesland study area, 40.3% of the grassland is classified as extensive and 59.7% as monoculture. The classification method can probably be successfully applied for other grassland areas in the Netherlands, because most meadow bird grasslands lie on clay or peat soils. However, no thorough accuracy assessment was performed for the peat soil area due to lack of time. Therefore, further validation of the model is required.

The grassland management map can be used to analyze distribution of meadow bird nests. The majority of godwits, lapwings, redshanks and oystercatchers prefers extensive grassland over monoculture grassland as nesting site. Especially redshank (79%) and godwit (77%) choose to breed on extensive parcels. The distribution maps may contribute to meadow bird conservation because they can show for which monoculture parcels it may be wise to apply nest protection or resting periods with delayed or very early mowing.

With respect to meadow bird conservation, knowledge of first mowing date is also important. Sentinel-2 data can be used to establish a mowing model. By using change in NDVI between two consecutive observation dates it is possible to detect mowing at parcel level. Advantage of using NDVI over S2REP for detection of mowing, is that data for bands 4 and 8 are acquired at 10 m resolution, whereas data for bands 5, 6, 7 and 8A are acquired at 20 m resolution. Mowing maps based on NDVI will appear more smooth and reveal more detail than maps based on S2REP. For detection of mowing, MASD was found to be less useful than NDVI; its absolute values do not allow discriminating between fast increase or decrease of reflectance, making it difficult to differentiate between mowing, fast grass growth and seasonal differences in moisture content. Unfortunately, temporal resolution of Sentinel-2 imagery for 2016 is too low to detect all mowing events. Grazing causes a mean drop in NDVI of 0.066 but with a maximum drop of 0.16. By applying a mowing threshold of -0.1, grazing may be mistaken for mowing. If Sentinel-2B data is available, chances of acquiring cloud free data at higher temporal resolution increase. This will make it possible to apply a lower mowing threshold of e.g. smaller than -0.16 which will avoid confusion with grazing.

Research recommendations

Eventually the steps used in the current method, from data download to classification, may be combined into a model to automate the classification process. But, before this can be achieved, it is necessary to test the robustness of the model using Sentinel-2 data for the current and coming years. It may well be that the S2REP and NDVI classification thresholds differ from year to year depending on weather conditions. Unfortunately, at the moment of writing no cloud free data was available for April 2017. A cloud free Sentinel-2 image was downloaded for March 27th 2017. Mean spectral response is comparable to that of April 1st 2016 (Figure 8.1). S2REP values for March 27th 2017 are lower than for April 1st 2016 whilst NDVI values are higher. This illustrates that it is important to test the validity of the model for other years.

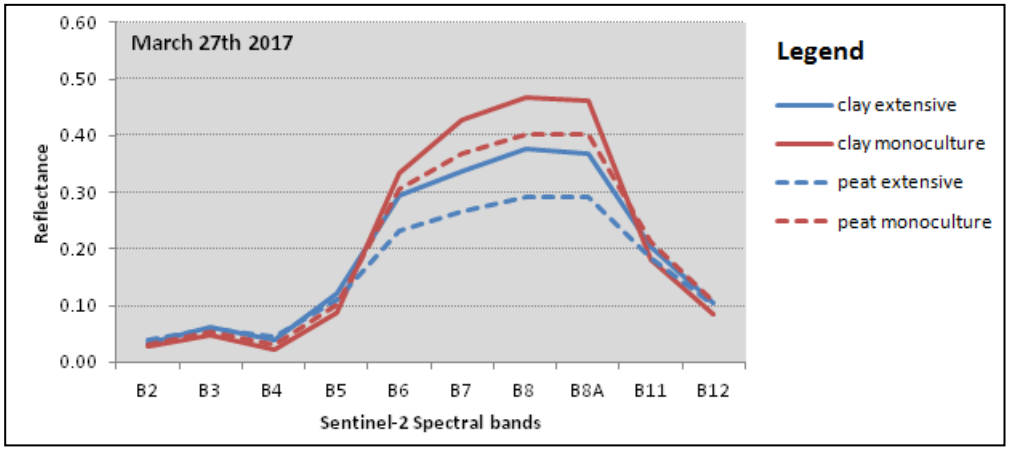

Figure 8.1: Sentinel-2 Spectral response curve for March 27th 2017.

The current method incorporates expert knowledge on local grassland management, especially with regard to mowing. If the method is to be used in an operational process and applied in study areas for which no knowledge of mowing is available, it is essential to have a reliable mowing model. The current mowing model may be improved by using Sentinel-1 data in addition to Sentinel-2 data. Sentinel-1 is a twin satellite constellation which provides Synthetic Aperture Radar (SAR) data; the satellite actively transmits microwave signals and measures the energy that is scattered back by the ground surface; presence of clouds will not affect data collection. The Sentinel-1 signal is affected by the dielectric constant of materials on the ground as well as by soil moisture and ground surface roughness, e.g. vegetation and ploughed fields (ESA 2017g; Wagner et al. 2010). Tamm et al. (2016) have used this data to calculate interferometric coherence in relation to mowing events on agricultural grasslands. It was found that median VH (vertical transmit, horizontal receive) and VV (vertical transmit, vertical receive) polarization coherence values were significantly higher after mowing. However, precipitation caused the coherence to decrease. Also, a 6 day temporal resolution is required to accurately detect all mowing events.

With regard to spectral heterogeneity, further research is necessary to assess if it can be used to detect differences in herb-richness for extensive grasslands. Counts of vascular plant species in 1 ha plots are required to test whether correlations exist between mean distance to spectral centroid and actual number of species.

9.0 References

Addinsoft (2015a). *XLSTAT Software*. [Online] Available at: https://www.xlstat.com/en/ [Accessed 20-2-2017].

Addinsoft (2015b). *The Mann-Whitney U Test in Excel Tutorial*. [Online] Available at: https://help.xlstat.com/customer/en/portal/articles/2062371-running-a-mann-whitney-test-on-two-independent-samples-with-xlstat?b_id=9283 [Accessed 20-2-2017]

Addinsoft (2015c). *The Kolmogorov-Smirnov Test in Excel Tutorial*. [Online] Available at: https://help.xlstat.com/customer/en/portal/articles/2062428 [Accessed 20-2-2017].

Alberda, Th. (1959). *De periodiciteit in de grasproductie*. In: Jaarboek 1959. Instituut voor biologisch en scheikundig onderzoek van landbouwgewassen Wageningen, mededelingen 71-90, pp. 73-81.

Ali, I., Cawkwell, F., Dwyer, E., Barrett, B. and S. Green (2016). Satellite remote sensing of grasslands: from observation to management. *Journal of Plant Ecology* **9**(6), pp. 649-671.

Asam, S., Klein, D. and S. Dech (2015). *Estimation of grassland use intensities based on high spatial resolution LAI time series.* The International Archives of the Photogrammetry, Remote Sensing and Spatial Information Sciences, Volume XL-7/W3, 2015, 36th International Symposium on Remote Sensing of Environment, 11-15 May 2015, Berlin, Germany.

Alterra (2006). *Bodemkaart van Nederland, schaal 1:50.000.* Alterra Wageningen. [Online] Available at: http://geoplaza.vu.nl/data/dataset/bodemkaart-van-nederland [Accessed 14-9-2016].

BFVW (2017). *Bond Friese VogelWachten*. [Online] Available at: http://www.friesevogelwachten.nl/nl/home.html [Accessed 20-2-2017].

Boer, J. de, Tiemersma, K. and H. Dommerholt (2006). Weidevogels bij Natuurmonumenten. *De Levende Natuur* **107** (3), pp. 86-91.

Boer, J. de, and S. de Winter (2016). *Greidhoeke en Lytse Bouhoeke. Vogelinventarisatie 2016*. Natuurmonumenten rapport. 48 p.

Bogoliubova, A. and P. Tymków (2014). Accuracy assessment of automatic image processing for land cover classification of St. Petersburg protected area. *Acta Scientiarum Polonorum - Geodesia et Descriptio Terrarum* **13**, nr.1-2, pp. 5-22.

Brenner, J.C., Christman, Z. and J. Rogan (2012). Segmentation of Landsat Thematic Mapper imagery improves buffelgrass (*Pennisetum ciliare*) pasture mapping in the Sonoran Desert of Mexico. *Applied Geography* **34**, pp. 569-575.

Carlier, L., Rotar, I., Vlahova, M. and R. Vidican (2009). Importance and Functions of Grasslands. *Notulae Botanicae Horti Agrobotanici Cluj-Napoca* **37**(1), pp. 25-30.

CBS (2014). *Biologisch grasland*. [Online] Available at: http://www.boerenbusiness.nl/ondernemen/top5/artikel/10865588/waar-groeit-het-meeste-biologische-grasland [Accessed 26-4-2017].

CBS (2016). *Statline. Grasland, oppervlakte en opbrengst*. [Online] Available at: http://statline.cbs.nl/StatWeb/publication/?VW=T&DM=SLNL&PA=7140gras&LA=NL [Accessed 15-3-2017].

CBS (2017a). *Statline. Landbouw vanaf 1851*. [Online] Available at: https://www.cbs.nl/nl-nl [Accessed 8-3-2017].

CBS (2017b). *Statline. Bevolkingsontwikkeling regio per maand*. [Online] Available at: https://www.cbs.nl/nl-nl [Accessed 20-2-2017].

Cho, M.A. and A.K. Skidmore (2006). A new technique for extracting the red edge position from hyperspectral data: The linear extrapolation method. *Remote Sensing of Environment* **101**, pp. 181-193.

Cho, M.A., Skidmore, A.K. and C. Atzberger (2008). Towards red-edge positions less sensitive to canopy biophysical parameters for leaf chlorophyll estimation using properties optique spectrales des feuilles (PROSPECT) and scattering by arbitrarily inclined leaves (SAILH) simulated data. *International Journal of Remote Sensing* **29**(8), pp. 2241-2255.

Clerici, N., Weissteiner, C.J., Halabuk, A., Hazeu, G., Roerink, G. and S. Mücher (2012). *Phenology related measures and indicators at varying spatial scales. Investigation of phenology information for habitat classification using SPOT VGT and MODIS NDVI data.* Alterra Report 2259, Wageningen. 114 p.

Clevers, J.G.P.W. and A.A. Gitelson (2013). Remote estimation of crop and grass chlorophyll and nitrogen content using red-edge bands on Sentinel-2 and -3. *International Journal of Applied Earth Observation and Geoinformation* **23**, pp. 344-351.

Compendium voor de Leefomgeving, CLO (2015). *Vogels van het boerenland 1990-2014*. [Online] Available at: http://www.clo.nl/indicatoren/nl1479-vogels-van-het-boerenland. [Accessed 14-9-2016].

Compendium voor de Leefomgeving, CLO (2016). *Milieucondities in water en natuurgebieden, 1990-2014.* [Online] Available at: http://www.clo.nl/indicatoren/nl1522-milieudruk-op-natuur [Accessed 8-6-2017].

Compendium voor de Leefomgeving, CLO (2017). *Trend van boerenlandvogels 1990-2015*. [Online] Available at: http://www.clo.nl/indicatoren/nl1479-vogels-van-het-boerenland [Accessed 27-3-2017].

Congedo Luca (2016)**.** *Semi-Automatic Classification Plugin Documentation*. DOI: http://dx.doi.org/10.13140/RG.2.2.29474.02242/1 [Accessed 20-2-2017].

Courault, D., Hadria, R., Ruget, F., Olioso, A., Duchemin, B., Hagolle, O. and G. Dedieu (2010). Combined use of FORMOSAT-2 images with a crop model for biomass and water monitoring of permanent grassland in Mediterranean region. *Hydrology and Earth System Sciences* **14**, pp. 1731-1744.

Delegido, J., Verrelst, J., Meza, C.M., Rivera, J.P., Alonso, L. and J. Moreno (2013). A red-edge spectral index for remote sensing estimation of green LAI over agroecosystems. *European Journal of Agronomy* **46**, pp. 42-52.

Demonceau, D. (2016). *Monitoring crop field soil moisture (NDWI) using Sentinel-2 temporal series*. [Online] Available at: http://www.quadratic.be/en/le-suivi-de-letat-hydrique-ndwi-des-cultures-par-les-series-temporelles-sentinel-2/ [Accessed 7-6-2017]

Dinoloket (2017). *Ondergrondgegevens TNO*. [Online] Available at: https://www.dinoloket.nl/ondergrondgegevens [Accessed 29-5-2017].

Dussaux, P., Vertès, F., Corpetti, T., Corgne, S. and L. Hubert-Moy (2014). Agricultural practices in grasslands detected by spatial remote sensing. *Environmental Monitoring and Assessment* **186**(12), pp. 8249-8265.

Elachi, C. (1987). *Introduction to the Physics and Techniques of Remote Sensing*. Wiley: Chichester. xvii + 413 p.

ESA (2015a). *Space for Copernicus*. Pdf file available at: http://esamultimedia.esa.int/multimedia/publications/sentinels-family/ [Accessed 31-2-2017].

ESA (2015b). *Sentinel-2 User Handbook*. Pdf file available at: https://sentinels.copernicus.eu/web/sentinel/user-guides/document-library/-/asset_publisher/ xlslt4309D5h/ content/ sentinel-2-user-handbook [Accessed 13-2-2017].

ESA (2017a). *Sentinel-2 Satellite Description*. [Online] Available at: https://earth.esa.int/web/sentinel/missions/sentinel-2/satellite-description [Accessed 13-2-2017].

ESA (2017b). *Copernicus website. Overview*. [Online] Available at: http://www.esa.int/Our_Activities/Observing_the_Earth/Copernicus/Overview [Accessed 13-2-2017].

ESA (2017c). *Sentinels Scientific Data Hub*. [Online] Available at: https://scihub.copernicus.eu/ [Accessed 31-2-2017].

ESA (2017d). *Sentinel-2 Document Library. Spectral Responses*. [Online] Available at: https://earth.esa.int/documents/247904/685211/Sentinel-2A+MSI+Spectral+Responses [Accessed 13-2-2017].

ESA (2017e*). Sentinel-2 Technical Guide. Level-1C algorithm.* [Online] Available at: https://sentinel.esa.int/web/sentinel/technical-guides/sentinel-2-msi/level-1c/algorithm [Accessed 6-6-2017].

ESA (2017f). *Sentinel-2 Technical Guide. Level-2A Algorithm Overview*. [Online] Available at: https://sentinel.esa.int/web/sentinel/technical-guides/sentinel-2-msi/level-2a/algorithm [Accessed 20-2-2017].

ESA (2017g). *Sentinel-1. Geophysical measurements.* [Online] Available at: https://sentinel.esa.int/web/sentinel/user-guides/sentinel-1-sar/product-overview/geophysical-measurements [Accessed 8-6-2017].

ESA Step Forum (2017). *S2REP output flag 4.* [Online] Available at: http://forum.step.esa.int/t/s2rep-output-flag-4/4455 [Accessed 27-1-2017].

Frampton, W.J., Dash, J., Watmough, G. and E.J. Milton (2013). Evaluating the capabilities of Sentinel-2 for quantitative estimation of biophysical variables in vegetation. *ISPRS Journal of Photogrammetry and Remote Sensing* **82**, pp. 83-92.

Franke, J., Keuck, V. and F. Siegert (2012). Assessment of grassland use intensity by remote sensing to support conservation schemes. *Journal for Nature Conservation* **20**, p. 125-134.

Fûgelwacht Grou (2015a). *De Burd.* [Online] Available at: http://fugelwachtgrou.nl/landschap/de-burd/ [Accessed 6-3-2017].

Fûgelwacht Grou (2015b). *Wyldlannen*. [Online] Available at: http://fugelwachtgrou.nl/landschap/wyldlannen/ [Accessed 6-3-2017].

Gao, J. (2006). Quantification of grassland properties: how it can benefit from geoinformatic technologies? *International Journal of Remote Sensing* **27**(7), pp. 1351-1365.

Gillespie, T.W. (2005). Predicting woody-plant species richness in tropical dry forests: a case study from South Florida, USA. *Ecological Applications* **15**(1), pp. 27-37.

Gitelson, A.A., Viña, A., Verma, S., Rundquist, D.C., Arkebauer, D.C., Keydan, T.J., Galina, P., Leavitt, B., Ciganda, V., Burba, G.G. and A.E. Suyker (2006). Relationship between gross primary production and chlorophyll content in crops: Implication for the synoptic monitoring of vegetation productivity. *Journal of Geophysical Research* **111**, 13p.

Gollebeek, L. and I. Hoving (2016). *Voorjaarsbemestingsadvies grasland op basis van bodemtemperatuur*. Rapport 1004. Wageningen Livestock Research Wageningen. 29 p.

Gould, W. (2000). Remote Sensing of vegetation, plant species richness and regional biodiversity hotspots. *Ecological Applications* **10**(6), pp. 1861-1870.

Groen, N.M., Kentie, R., Goeij, P. de, Verheijen, B., Piersma, T. and J. Hooijmeijer (2012). A modern landscape ecology of Black-tailed Godwits: Habitat selection in southwest Friesland, The Netherlands. *Ardea* **100**(1), pp. 19-28.

Guyot, G. and F. Baret (1988). Utilisation de la haute resolution spectrale pour suivre l'etat des couverts vegetaux. In: Assois (Ed.): *Proceedings of the 4th International colloquium on spectral signatures of objects in remote sensing*. ESA SP-287. pp. 279-286.

Halabuk, A., Mojses, M., Halabuk, M. and S. David (2015). Towards Detection of Cutting in Hay Meadows by Using of NDVI and EVI Time Series. *Remote Sensing* **7**, pp. 6107-6132.

Heitman, J., Minnema, N., Overdiep, E., Rensema, L. en H. Schmeink (2015). *Natuurvisie De Greidhoeke. Op weg naar het weidevogellandschap van de 21e eeuw.* Vereniging Natuurmonumenten. 64 p.

Hoekstra, M. (2017). *Verslag commissie nazorg BFVW over het jaar 2016*. In: Fûgelwacht ''De Fjouwer Doarpen''. Jierferslach 2016. 48 p.

Hooijboer, A.E.J., Koeijer, T.J. de, Ham, A. van de, Boumans, L.J.M., Prins, H., Daatselaar, C.H.G. and E. Buis (2014). *Agricultural practices and water quality*. RIVM Report 680717038, 150 p.

Hooijmeijer, J., Bruinzeel, L.W., Kamp, J. van der, Piersma, T. and E. Wymenga (2011). Grutto's onderweg. pp. 15-54. In: Teunissen, W.A. and E. Wymenga (Eds.) 2011. *Factoren die van invloed zijn op de ontwikkeling van weidevogelpopulaties. Belangrijke factoren tijdens de trek, de invloed van waterpeil op voedselbeschikbaarheid en graslandstructuur op kuikenoverleving.* SOVON onderzoeksrapport 2011/10. SOVON Vogelonderzoek Nederland, Nijmegen. A&W-rapport 1532. Bureau Altenburg & Wymenga, Veenwouden. Alterra rapport 2187, Alterra, Wageningen.

Huete, A., Didan, K., Miura, T., Rodriguez, E.P., Gao X., and L.G. Ferreira (2002). Overview of the radiometric and biophysical performance of the MODIS vegetation indices. *Remote Sensing of Environment* **83**, pp. 195-213.

Jensen, J. (2007). *Remote Sensing of the Environment: an Earth Resource Perspective*. 2nd Edition. Pearson Prentice Hall, New Jersey. 592p.

Jensen, F.P., Béchet, A. and E. Wymenga (2008). *International Single Species Action Plan for the Conservation of Black-tailed Godwit* (*Limosa limosa*) & *L. l. islandica*. AEWA Technical Series No. 37. AEWA, Bonn, 51 p.

Jönson, P. and L. Eklundh (2004). TIMESAT - a program for analyzing time series of satellite sensor data. *Computers and Geosciences* **30**, pp. 833-845.

KBF (2017). *Kollektivenberied Fryslân*. [Online] Available at: http://www.kbf.frl/ [Accessed 6-3-2017].

Kenniscoalitie (2015). *Dutch national research agenda*. [Online] Available at: http://www.wetenschapsagenda.nl/publicatie/dutch-national-research-agenda-english/ [Accessed 12-9-2016].

Kentie, R., Hooijmeijer, J.C.E.W., Trimbos, K.B., Groen, N.M. and T. Piersma (2013a). Intensified agricultural use of grasslands reduces growth and survival of precocial shorebird chicks. *Journal of Applied Ecology* **50**, pp. 243-251.

Kentie, R., Hooijmeijer, J.C.E.W. and T. Piersma (2013b). *Grutto-demografie in Zuidwest-Friesland vanaf 2004. Update na de doorstart en uitbreiding in 2012*. Rijksuniversiteit Groningen. 78 p.

Kleijn, D., Berendse, F., Smit, R., Gilissen, N., Smit, J., Brak B. and R. Groeneveld (2004). Ecological Effectiveness of Agri-Environment Schemes in Different Agricultural Landscapes in The Netherlands. *Conservation Biology* **18**(3), pp. 775-786.

Kleijn, D., Schekkerman, H., Dimmers, W.J., Kats, R.J.M. van, Melman, D. en W.A. Teunissen (2010). Adverse effects of agricultural intensification and climate change on breeding habitat quality of Blacktailed Godwits *Limosa l. limosa* in the Netherlands. *Ibis, The International Journal of Avian Science* **152**, pp. 475-486.

KNMI (2016a). *January 2016*. [Online] Available at: https://www.knmi.nl/nederland-nu/klimatologie/maand-en-seizoensoverzichten/2016/januari [Accessed 27-2-2017].

KNMI (2016b). *Klimatologie. Daggegevens van het weer in Nederland*. [Online] Available at: http://projects.knmi.nl/klimatologie/daggegevens/selectie.cgi [Accessed 27-2-2017].

KNMI (2017). *Klimaatatlas*. [Online] Available at: http://www.klimaatatlas.nl/klimaatatlas.php [Accessed 20-2-2017].

Koffijberg, K., Foppen, R. and C. van Turnhout (2012). *Vogelbalans 2012. Thema boerenland*. Sovon Vogelonderzoek Nederland, Nijmegen.

Kotsiantis (2007). Supervised Machine Learning: A Review of Classification Techniques. *Informatica* **31**, pp. 249-268.

Kumar, L., Schmidt, K., Dury, S. and A. Skidmore (2001). Imaging spectrometry and vegetation science. In F. van der Meer and S.M. de Jong (Eds.): *Imaging Spectrometry. Basic principles and prospective applications*. Kluwer Academic Press: Dordrecht, pp. 111-155.

LandschappenNL (2015). *Stimuleer kruidenrijke graslanden om afname weidevogels te stoppen.* [Online] Available at: https://www.portaalnatuurenlandschap.nl/themas/vernieuwd-stelsel-agrarisch-natuurbeheer/nieuws/landschappennl-stimuleer-kruidenrijke-graslanden-om-afname-weidevogels-te-stoppen/ [Accessed 14-9-2016].

Liew, S.C. (2001). *Optical Remote Sensing Tutorial*. Center for Imaging Remote Sensing & Processing. [Online] Available at: http://www.crisp.nus.edu.sg/~research/tutorial/optical.htm [Accessed 8-6-2017].

Lillesand, T.M., Kiefer, W.R. and J.W. Chipman (2015). *Remote Sensing and Image Interpretation*. 7th Edition. Wiley: Hoboken. 720 p.

Lips, M. (2011). *Detection of grassland management intensity using MODIS satellite imagery.* Centre for Geo-Information. Thesis Report GIRS-2011-21. Wageningen University and Research Centre. 95 p.

Louis, J., Debaecker, V., Pflug, B., Main-Knorn, M., Bieniarz, J., Mueller-Wilm, U., Cadau, E. and F. Gascon (2106). Sentinel-2 Sen2Cor: L2A Processor for Users. In: *Proceedings Living Planet Symposium 2016*, SP-740, pp. 1-8. Spacebooks Online. ESA Living Planet Symposium 2016, 09 - 13 May 2016, Prague, Czech Republic.

Melman, D., Buij, R., Schotman, A., Vos, C., Verdonschot, R., Sierdsema, H. en B. Vanmeulebrouk (2016). *Kennissysteem agrarisch natuurbeheer. Ondersteuning voor lerend beheer in het agrarisch natuurbeheer*. Alterra Wageningen. Alterra rapport 2702. 114 p.

Möckel, T., Dalmayne, J., Schmid, B.C., Prentice, H.C. and K. Hall (2016). Airborne Hyperspectral Data Predict Fine-Scale Plant Species Diversity in Grazed Dry Grasslands. *Remote Sensing* **8** (2), 133, 19p.

Moreira, E.P., Valeriano, M., Sanches, I. and A.R. Formaggio (2016). Topographic effect on spectral vegetation indices from Landsat TM data: Is topographic correction necessary? *Boletim de Ciências Geodésicas* **22**(1), pp. 95-107.

Mueller-Wilm, U. (2016). *ESA Sentinel-2. Sen2Cor Configuration and User Manual*. S2-PDGS-MPC-L2A-SUM-V2.3, Issue 1, Date 2016-11-25. 47 p.

Mutanga, O. and A.K. Skidmore (2004). Narrow band vegetation indices overcome the saturation problem in biomass estimation. *International Journal of Remote Sensing* **25**(19), pp. 3999-4014.

Nagendra, H., Lucas, R., Honrado, J.P., Jongman, R.H.G., Tarantino, C., Adamo, M. and P. Mairota (2012). Remote sensing for conservation monitoring: Assessing protected areas, habitat extent, habitat condition, species diversity, and threats. *Ecological Indicators* **33**, pp. 45-59.

NASA (2017). *Sentinel-2A launches*. [Online] Available at: https://landsat.gsfc.nasa.gov/sentinel-2a-launches-our-compliments-our-complements/ [Accessed 13-2-2017].

Nationaal georegister (2017). *Basisregistratie gewaspercelen 2016*. [Online] Available at: http://www.nationaalgeoregister.nl/geonetwork/srv/dut/catalog.search#/metadata/%7B25943e6e-bb27-4b7a-b240-150ffeaa582e%7D [Accessed 26-4-2017].

Nationale Databank Flora en Fauna (2017). *Nationale Databank Flora en Fauna.* [Online] Available at: https://www.ndff.nl/ [Accessed 20-3-2017].

Nestola, E., Calfapietra, C., Emmerton, C.A., Wong, C.Y.S., Thayer, D.R. and J.A. Gamon (2016). Monitoring Grassland Seasonal Carbon Dynamics by integrating MODIS NDVI, Proximal Optical Sampling, and Eddy Covariance Measurements. *Remote Sensing* **8**(260), 25 pp.

Nitze, I., Barret, B. and F. Cawkwell (2015). Temporal Optimisation of image acquisition for land cover classification with Random Forest and MODIS time series. *International Journal of Applied Earth Observation and Geoinformation* **34**, pp. 136-146.

OBN (2015). *Ontwikkeling en Beheer. Natuurkennis. Vochtig weidevogelgrasland N13.01.* [Online] Available at: http://www.natuurkennis.nl/index.php?hoofdgroep=2&niveau=2&subgroep=112&subsubgroep=1034 [Accessed 2-3-2017].

Oldeland, J., Wesuls, D., Rocchini, D., Schmidt, M. and N. Jürgens (2010). Does using species abundance data improve estimates of species diversity from remotely sensed spectral heterogeneity? *Ecological Indicators* **10**, pp. 390-396.

Oosterveld, E.B. and F.H. Hoekema (2012). *Naar vitale weidevogellandschappen in Fryslân. Uitwerking van drie voorbeeldgebieden.* A&W rapport 1753. Altenburg & Wymenga ecologisch onderzoek Feanwâlden. 65 pp.

Pal, M. and P.M. Mather (2003). An assessment of the effectiveness of decision tree methods for land cover classification. *Remote Sensing of Environment* **86**, pp. 554-565.

Palmer, M.W., Wohlgemuth, T., Earls, P., Arevalo, J.R. and S.D. Thompson (2000). Opportunities for long-term ecological research at the Tallgrass Prairie Preserve, Oklahoma. pp. 123-128. In Lajtha, K. and K. Vanderbilt (Eds.): *Cooperation in Long Term Ecological Research in Central and Eastern Europe: Proceedings of the ILTER Regional Workshop. 22-25 June, 1999, Budapest, Hungary.* Oregon State University: Corvallis, OR.

Palmer, M.W., Earls, P.G., Hoagland, B.W., White, P.S. and T. Wohlgemuth (2002). Quantitative tools for perfecting species lists. *Environmetrics* **13**, pp. 121-137.

Pavlov, I. (2016). *7Zip Software*. [Online] Available at: http://www.7-zip.org/ [Accessed 13-2-2017].

Portaal Natuur en Landschap (2016). *Collectief beheerplan 2016.* [Online] Available at: http://bron.portaalnatuurenlandschap.nl/CollectiefBeheerPlan?SubsidieJaar=2016 [Accessed 22-2-2017].

Provincie Fryslân (2016). *Bodematlas.* ArcGIS Online. [Online] Available at: http://fryslan.maps.arcgis.com/home/webmap/viewer.html?webmap=913ffee88faa4978b65b0fdbd07a4177 [Accessed 22-2-2017].

Provincie Fryslân (2017). *Natuurbeheerplan 2017.* [Online] Available at: http://www.fryslan.frl/beleidsthemas/natuurbeheerplan-2017_3541/ [Accessed 22-2-2017].

Ramoelo, A., Cho, M., Mathieu, R. and A.K. Skidmore (2015). Potential of Sentinel-2 spectral configuration to assess rangeland quality. *Journal of applied remote sensing* **9**, 12 p.

Rocchini, D., Ricotta, C. and A. Chiarucci (2007). Using satellite imagery to assess plant species richness: The role of multispectral systems. *Applied Vegetation Science* **10**, pp. 325–331.

Rocchini, D. (2007). Effects of spatial and spectral resolution in estimating ecosystem α-diversity by satellite imagery. *Remote Sensing of Environment* **111**, pp. 423-434.

Rocchini, D., Balkenhol, N., Carter, G.A., Foody, G.M., Gillespie, T.W., He, K.S., Kark, S., Levin, N., Lucas, K., Luoto, M., Nagendra, H., Oldeland, J., Ricotta, C., Southworth, J. and M. Neteler (2010). Remotely sensed spectral heterogeneity as a proxy of species diversity: Recent advances and open challenges. *Ecological Informatics* **5**, pp. 318–329.

Rocchini, D., Boyd, D.S., Féret, J., Foody, G.M., He, K.S., Lausch, A., Nagendra, H., Wegmann, M. and N. Pettorelli (2016). Satellite remote sensing to monitor species diversity: potential and pitfalls. *Remote Sensing in Ecology and Conservation* **2**(1), pp. 25-36.

Rouse Jr., J.W., Haas, R.H., Schell, J.A. and D.W. Deering (1974). *Monitoring Vegetation Systems in the Great Plains with ERTS*. Presented at Third Earth Resources Technology Satellite-1 Symposium, NASA, Washington D.C., pp. 309-317.

Rulequest Research (2017). *See5 Data Mining Software*. [Online] Available at: https://www.rulequest.com/see5-info.html [Accessed 20-2-2017].

Sakowska, K., Juszczak, R. and D. Gianelle (2016). Remote Sensing of Grassland Biophysical Parameters in the Context of the Sentinel-2 Satellite Mission. *Journal of Sensors*, Volume 2016, 16 p.

Santini, M. (2015). *Machine learning for language technology 2015. Decision Trees*. Lecture slides [Online] Available at: https://www.slideshare.net/marinasantini1/lecture-4-decision-trees-2-entropy-information-gain-gain-ratio-55241087 [Accessed 7-6-2017].

Schekkerman, H., Teunissen, W. and E. Oosterveld (2005). *Resultaatonderzoek Nederland Gruttoland; broedsucces van grutto's in beheersmozaïeken in vergelijking met gangbaar agrarisch graslandgebruik.* Alterra-report 1291. Alterra, Wageningen. 153 p.

Schils, R. (2012). *30 vragen en antwoorden over bodemvruchtbaarheid*. Alterra Wageningen, 146 p.

Schroor, M. (2012). *Tussen Hemdijk en Klif. Het nationale landschap Zuidwest-Fryslân*. Afúk: Leeuwarden, 104 p.

Schuster, C., Förster, M. and B. Kleinschmit (2012). Testing the red-edge channel for improving land-use classifications based on high-resolution multi-spectral satellite data. *International Journal of Remote Sensing* **33**(17), pp. 5583-5599.

Sibanda, M., Mutanga, O. and M. Rouget (2015). Examining the potential of Sentinel-2 MSI spectral resolution in quantifying above ground biomass across different fertilizer treatments. *ISPRS Journal of Photogrammetry and Remote Sensing* **110**, pp. 55-65.

Sibanda, M., Mutanga, O. and M. Rouget (2017). Testing the capabilities of the new WorldView-3 space-borne sensor's red-edge spectral band in discriminating and mapping complex grassland management treatments. *International Journal of Remote Sensing* **38**(1), pp. 1-22.

Skriezekrite Idzegea (2008). *Skriezekrite Idzegea*. [Online] Available at: http://www.skriezekriteidzegea.nl/ [Accessed 27-2-2017].

Sovon (2017). *Grutto*. [Online] Available at: http://www.sovon.nl/nl/soort/5320 [Accessed 6-4-2017].

Tamm, T., Zalite, K., Voormansik, K. and L. Talgre (2016). Relating Sentinel-1 Interferometric Coherence to Mowing Events on Grasslands. *Remote Sensing* **8**(10), pp. 1-19.

Teunissen, W.A., Schotman, A.G.M., Bruinzeel, L.W., ten Holt, H., Oosterveld, E.O., Sierdsema, H., Wymenga, E. and Th.C.P. Melman (2012). *Op naar kerngebieden voor weidevogels in Nederland. Werkdocument met randvoorwaarden en handreiking*. Wageningen, Alterra, Alterra-rapport 2344. Nijmegen, Sovon Vogelonderzoek Nederland, Sovon-rapport 2012/21, Feanwâlden, Altenburg & Wymenga ecologisch onderzoek, A&W-rapport 1799. 144 p.

Teunissen, W.A. en C. Plate (2011). Weidevogels nog steeds onder druk. Nestbescherming beredeneerd uitvoeren. *Sovon-nieuws* **24**, nr. 1.

Toivonen, T. and M. Luoto (2003). Landsat TM images in mapping of semi-natural grasslands and analysing of habitat pattern in an agricultural landscape in south-west Finland. *Fennia* **181**(1), pp. 49-67.

USGS (2017). *USGS Spectral Characteristics Viewer*. [Online] Available at: https://landsat.usgs.gov/spectral-characteristics-viewer [Accessed 8-3-2017].

Van 't Veer, R., Sierdsema, H., Musters, C.J.M., Groen, N. and W.A. Teunissen (2008). *Weidevogels op landschapsschaal; ruimtelijke en temporele veranderingen*. Directie Kennis, Ministerie van LNV, report DK nr. 2008/dk105. Directie Kennis, Ede. 123 p.

Verhulst, J., Melman, T.C.P., and G.R. de Snoo (2008). *Voedselaanbod voor gruttokuikens in de Hollandse veenweidegebieden*. Alterra-report 1668. Alterra, Wageningen. 50 p.

Vickery, J.A., Tallowin, J.R., Feber, ,R.E., Asteraki, E.J., Atkinson, P.W., Fuller, R.J. and V.K. Brown (2001). The management of lowland neutral grasslands in Britain: effects of agricultural practices on birds and their food resources. *Journal of Applied Ecology* **38**, pp. 647-664.

Viedma, O., Torres, I., Pérez, B. and J.M. Moreno (2012). Modeling plant species richness using reflectance and texture data derived from QuickBird in a recently burned area of Central Spain. *Remote Sensing of Environment* **119**, pp. 208-221.

Visscher, J. (2010). *Verlenging groeiseizoen grasland*. Rapport 301, Lelystad: Wageningen UR Livestock Research, 48 p.

Vogelbescherming (2017). *Red de rijke weide*. [Online] Available at: https://www.redderijkeweide.nl/ [Accessed 27-3-2017].

Vries, G. de (2017). *Landschapsgeschiedenis Lage Midden*. [Online] Available at: http://landschapsgeschiedenis.nl/deelgebieden/2-Lage_Midden.html [Accessed 17-3-2017].

Wagner, W., Sabel, D., Doubkova, M., Bartsch, A. and C. Pathe (2010). The potential of Sentinel-1 for monitoring soil moisture with a high spatial resolution at a global scale. *Proceedings 'Earth Observation and Water Cycle Science'. Frascati, Italy 18-20 November 2009.* ESA SP-674, 5p.

Weerstation Hallum (2016). *Seizoensoverzichten Leeuwarden*. [Online] Available at: http://www.weerstation-hallum.nl/v3/index.php?p=leeuwarden/seizoenoverzicht [Accessed 27-2-2017].

Appendix A: Nature Network: important (meadow) bird areas

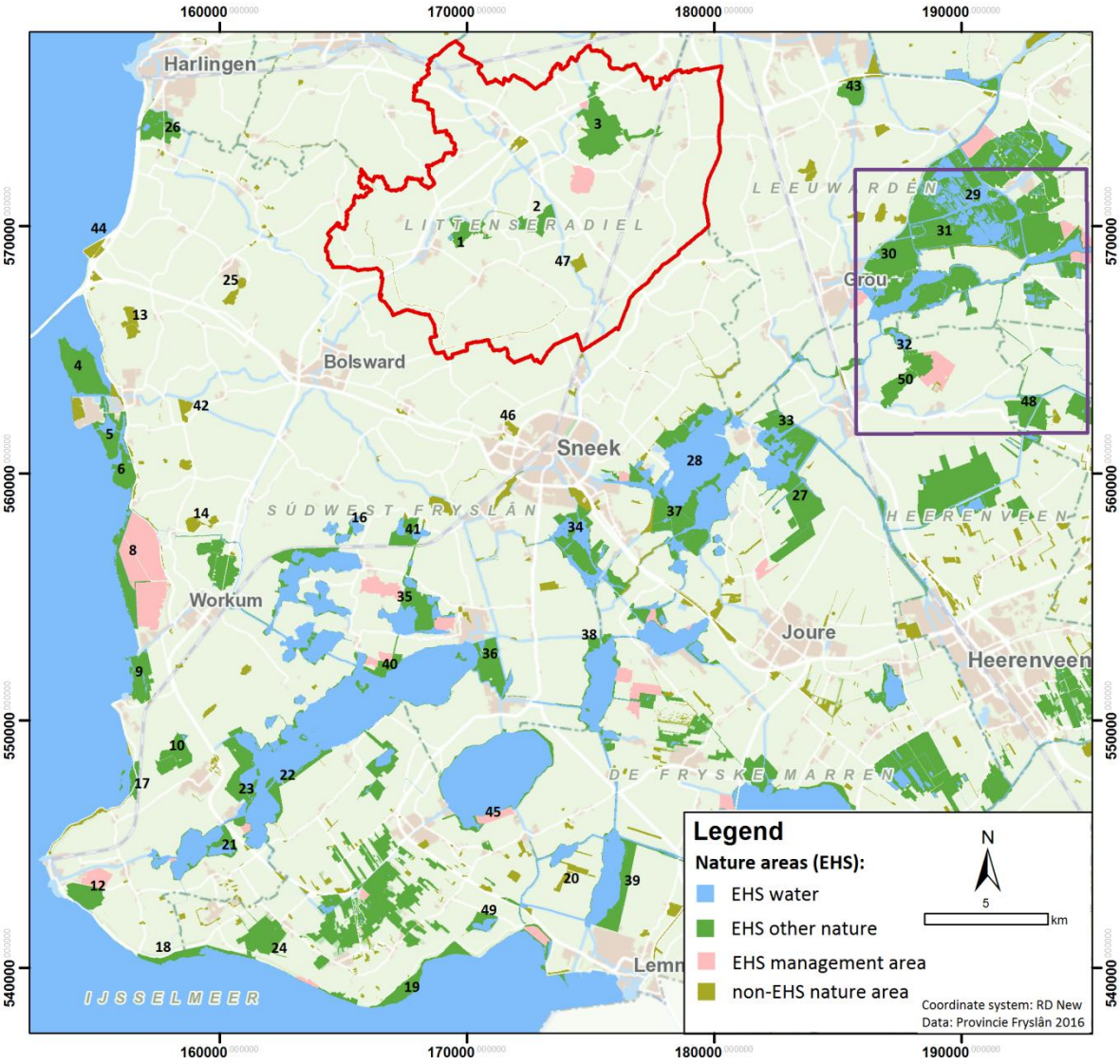

1: Skrok	21: Fûgelhoeke	41: Pikesyl
2: Skrins	22: De Fluezen	42: Allingawier
3: Lionserpolder	23: Polder de Samenvoeging, De Oarden	43: Hempenserpolder
4: Makkumer noordwaard	24: Zuiderfennenspolder	44: Zuricher oord
5: Makkumer zuidwaard	25: Filenspolder	45: Korte Jerden
6: Koaiwaard	26: Hegewiersterfjild	46: Ysbrechtum
7: Workumermar	27: Akmaryp blauwgraslanden	47: Zwarte molen/Swaenwert
8: Workumerwaard	28: Sneekermeer gebied	48: Oosterboorn
9: Workumer Nieuwland	29: De Alde Feanen	49: Sondeler Leijen
10: Haanmeer	30: De Burd	50: Soarremoarster polder
11: Monnikeburenpolder	31: Wyldlannen	
12: Zuidermeerpolder	32: Botmeer	
13: Polders Cornwerd	33: Terherne	
14: Aeltsjemar	34: Witte en Zwarte Brekken	
15: De Ryp	35: Idzegea/De Pine	
16: Blauwhuisterpoelen + Tjesskar	36: Gouden Boaijum	
17: Bocht van Molkwerum	37: Geeuwpolder	
18: Mokkebank	38: Polder Lippenwoude	
19: Huitebuersterbûtenpolder + Steile bank	39: Grutte Brekken	
20: Bancopolder	40: Fiskersbuorren/Lange Hoek	

Appendix B: Coincident spectral plots for Littenseradiel

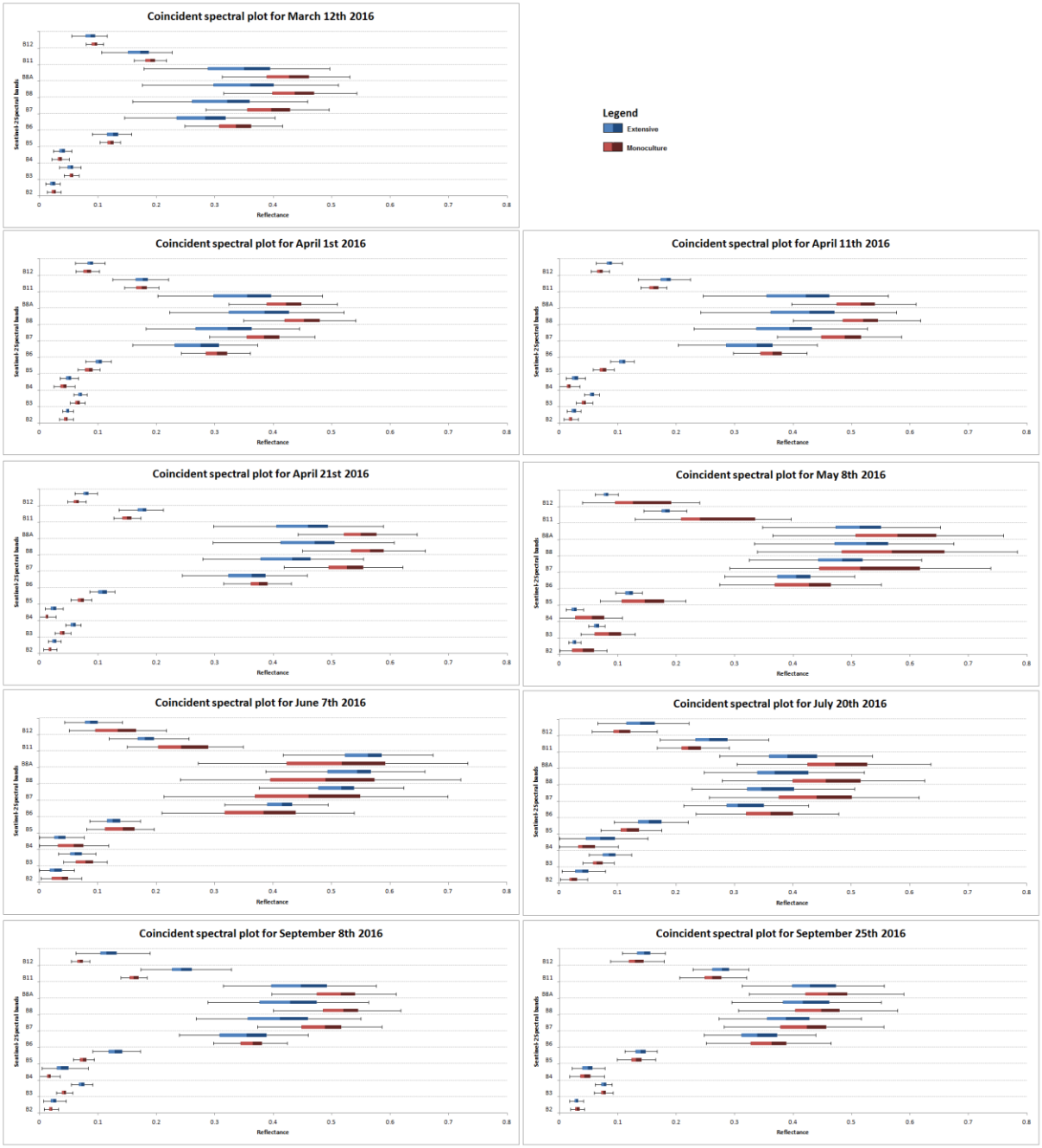

Coincident spectral plot for April 21st and September 25th 2016 for Littenseradiel (clay soil) sample points. Boxes show 1st quartile, median, 3rd quartile; Whiskers show 2 x plus and 2 x minus standard deviation.

Appendix C: NDVI Seasonal variability

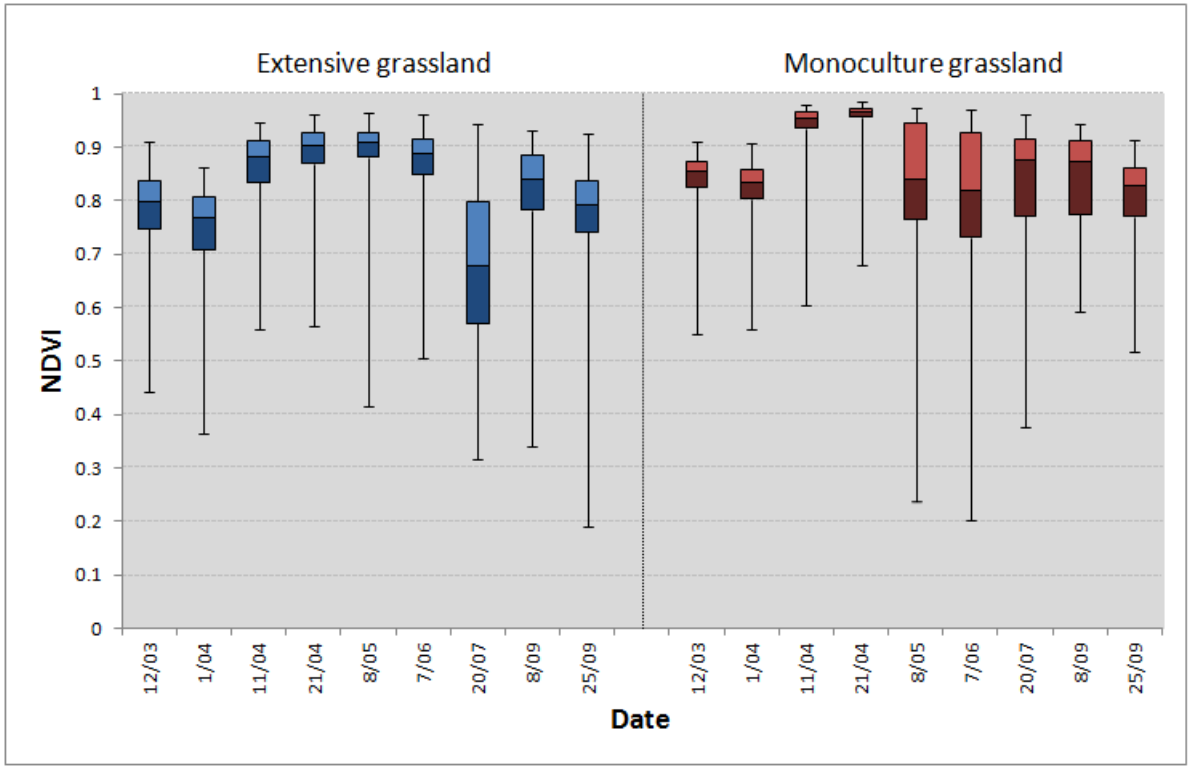

Seasonal variability of NDVI for Littenseradiel (clay soils).

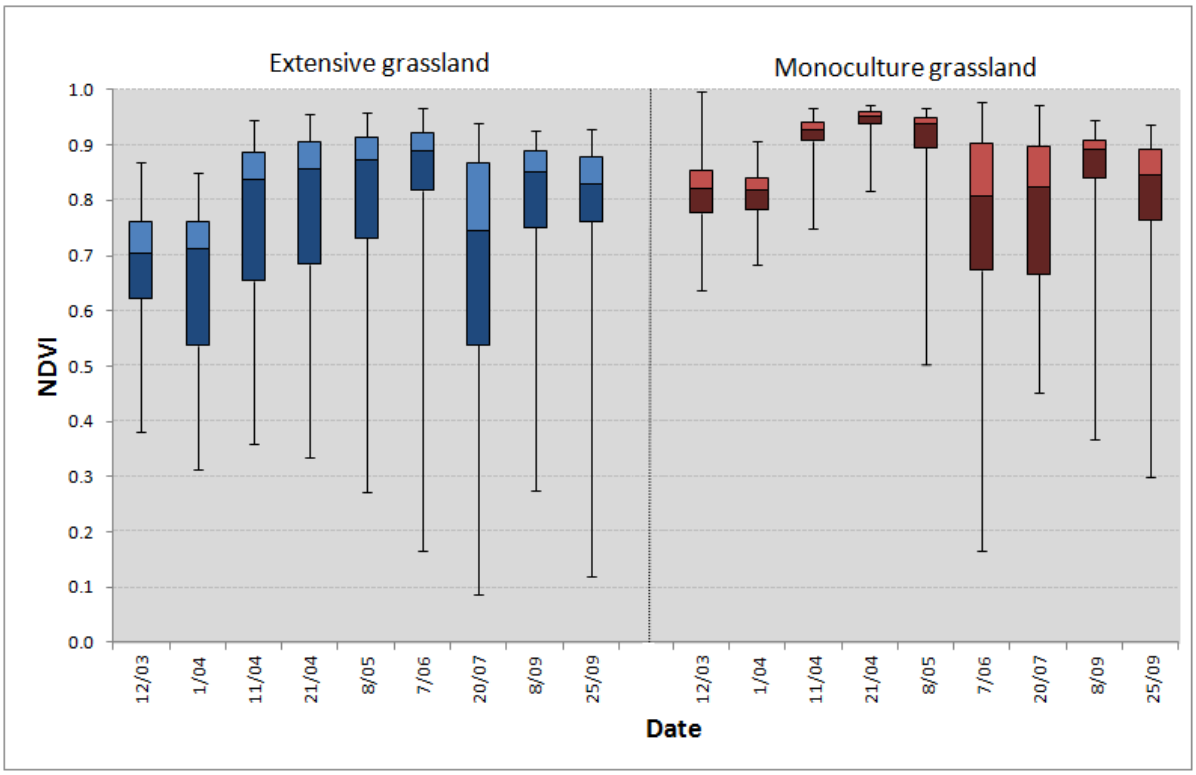

Seasonal variability of NDVI for Grouw (peat soils).

Appendix D: S2REP Seasonal variability

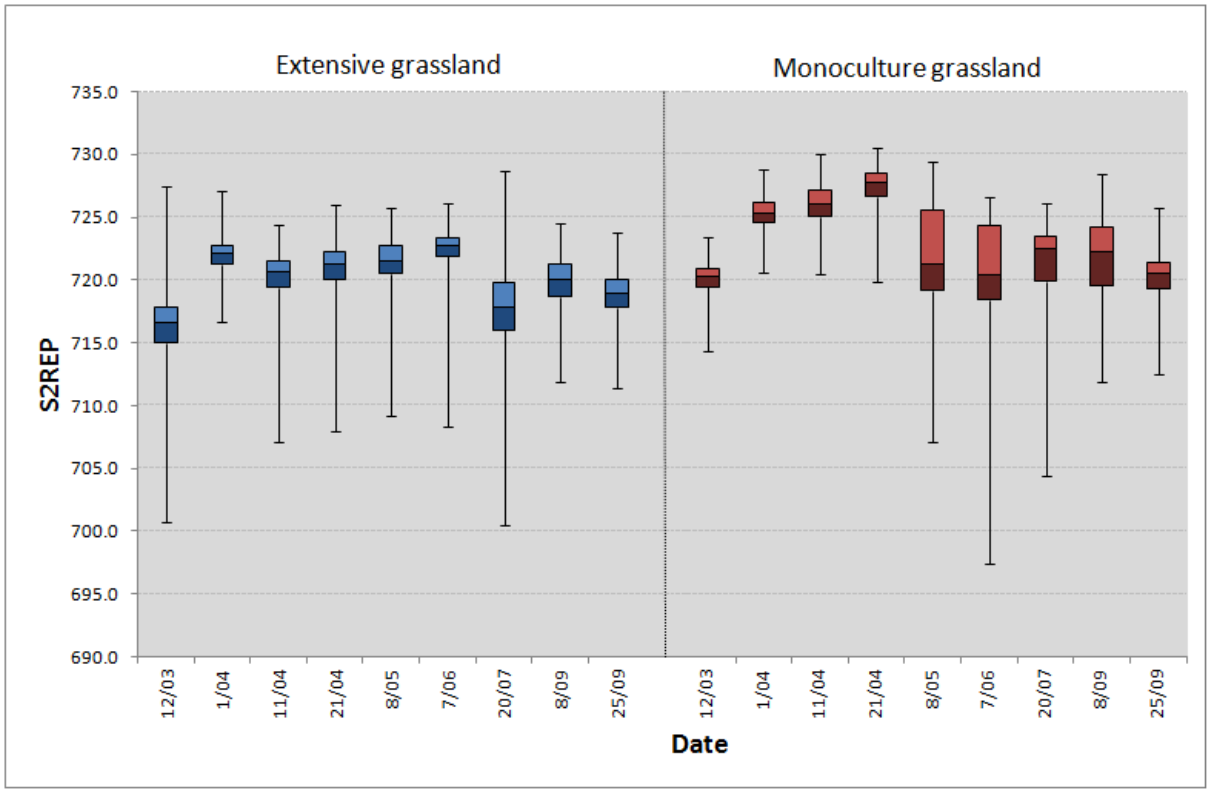

Seasonal variability of S2REP for Littenseradiel (clay soils).

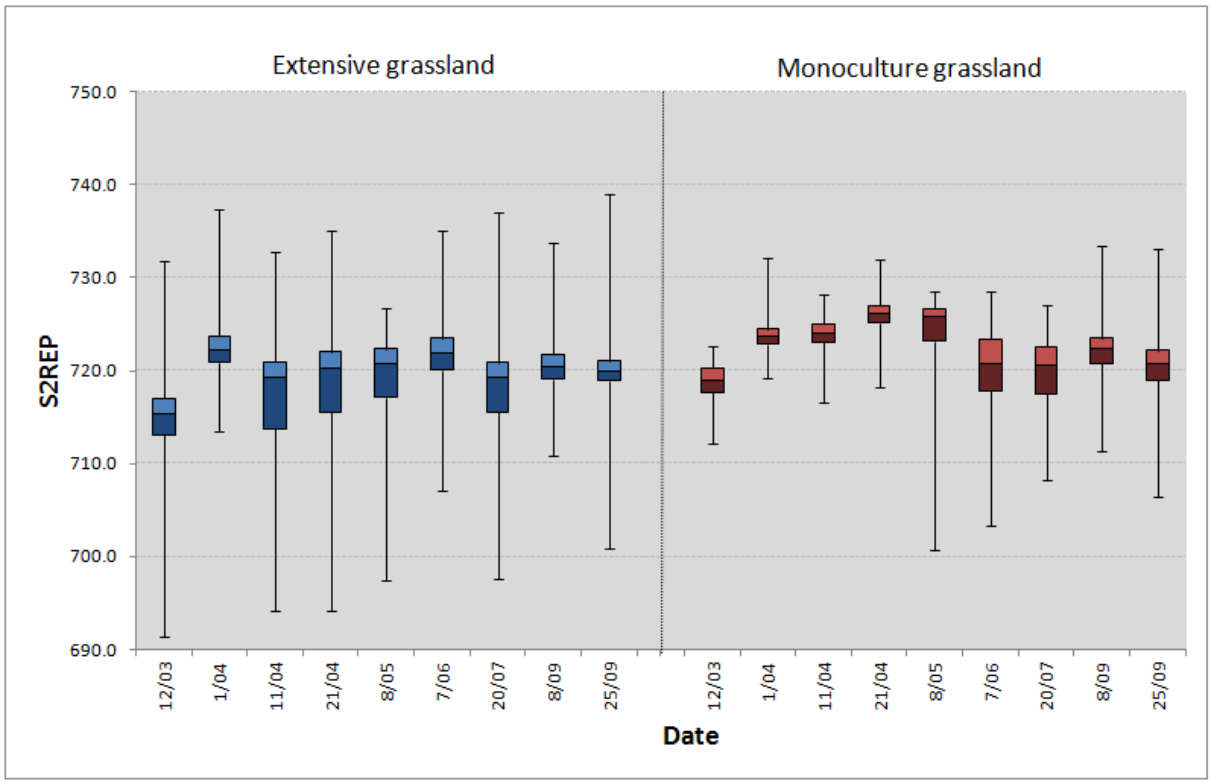

Seasonal variability of S2REP for Grouw (peat soils).

Appendix E: MASD Total (April-September)

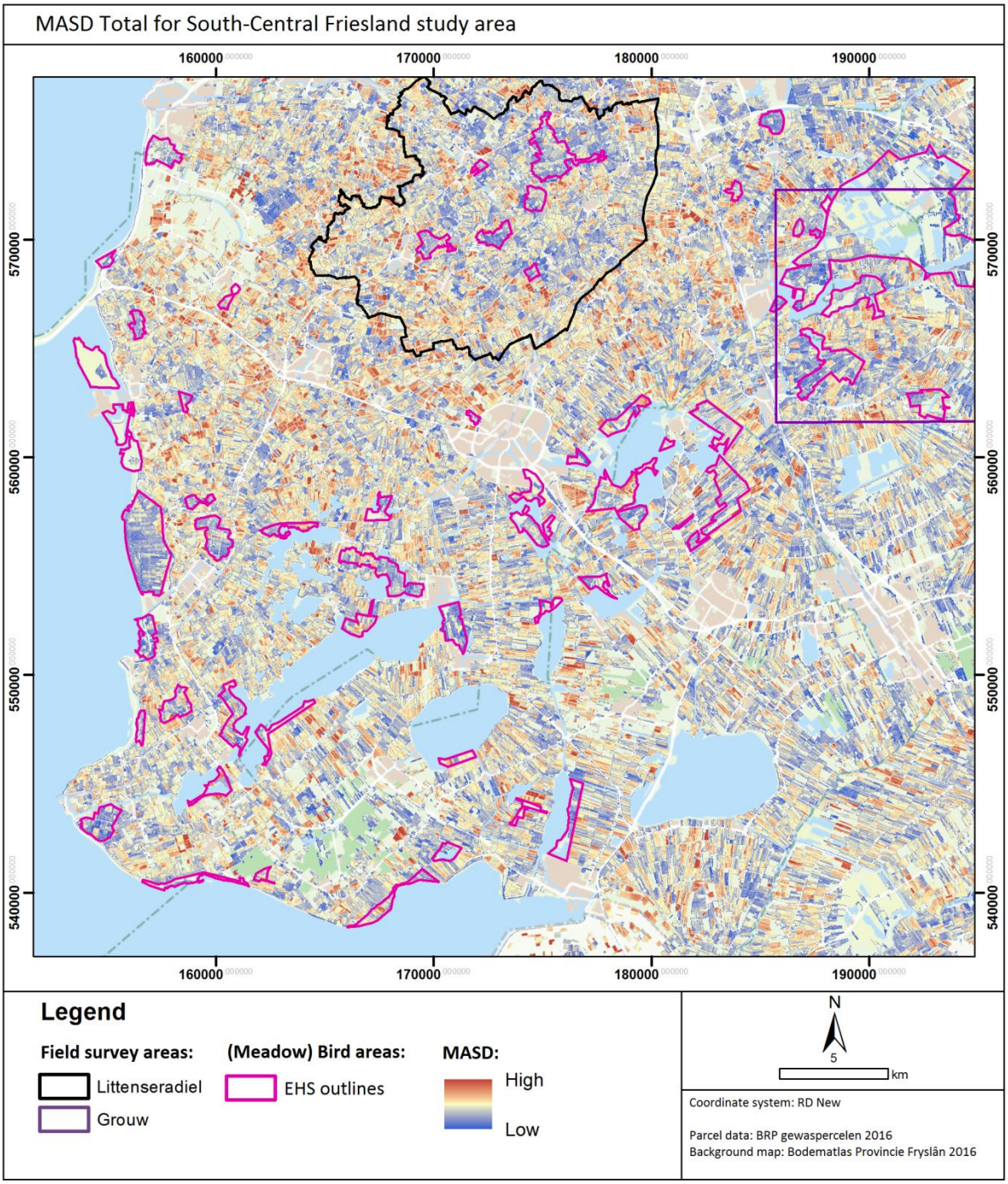

MASD7_total (April - September) for South-Central Friesland study area.

Appendix F: Error maps (accuracy assessment)

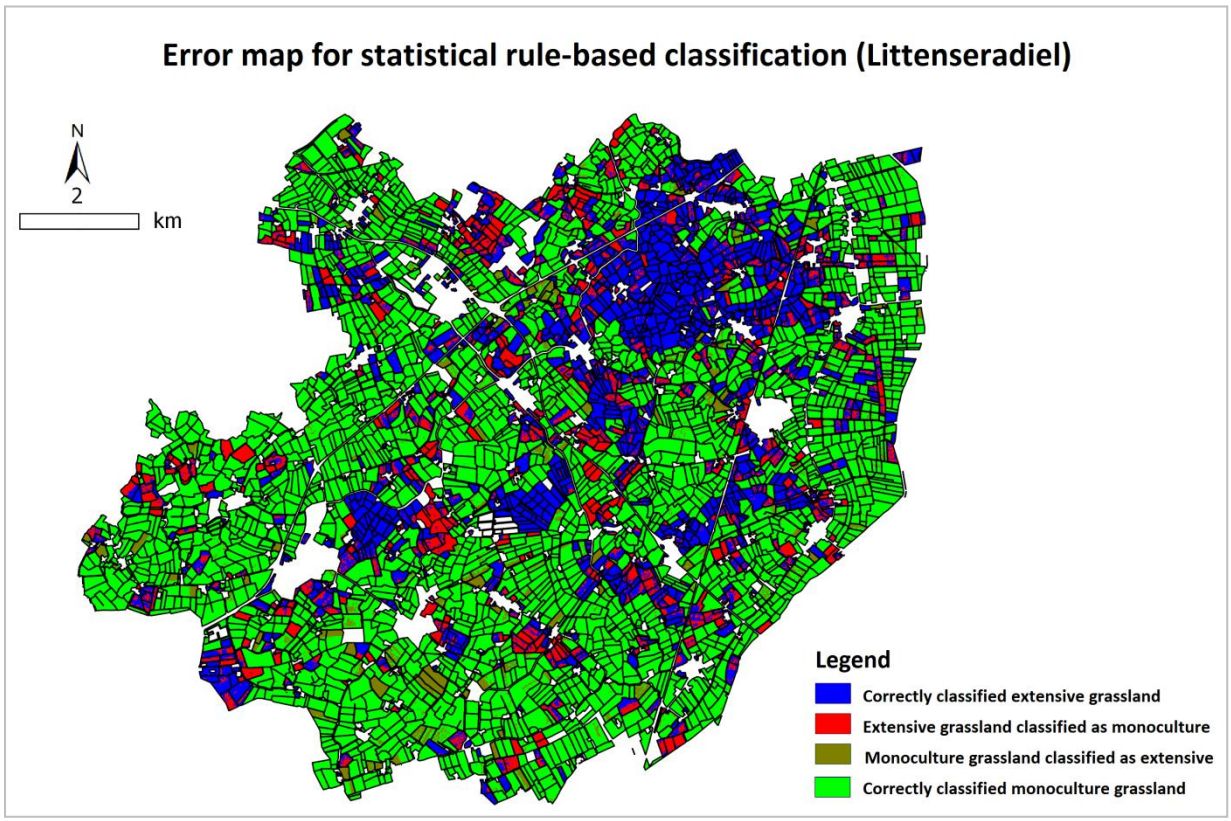

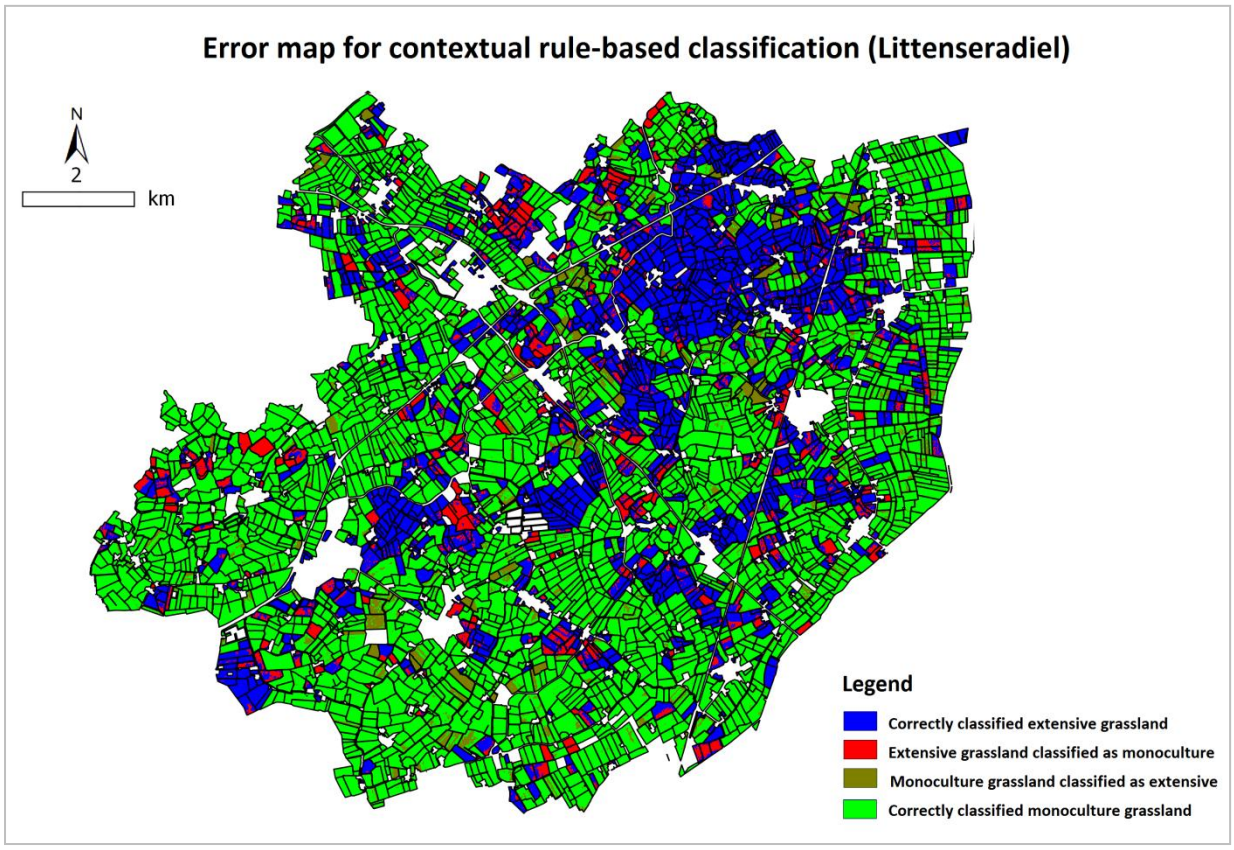

Appendix G: Principal component analysis for April 21st 2016

Principal Component Analysis 21 April 2016										
Covariance matrix										
Bands	**2**	**3**	**4**	**5**	**6**	**7**	**8**	**8A**	**11**	**12**
2	0.000634	0.00064	0.000824	0.000675	-0.00034	-0.00079	-0.00084	-0.00079	0.000772	0.000909
3	0.00064	0.000752	0.000833	0.000908	0.000675	0.000476	0.000567	0.000543	0.001199	0.001075
4	0.000824	0.000833	0.001167	0.000931	-0.00086	-0.00165	-0.00174	-0.00164	0.00108	0.001329
5	0.000675	0.000908	0.000931	0.001539	0.00269	0.002898	0.003148	0.003172	0.002506	0.001805
6	-0.00034	0.000675	-0.00086	0.00269	0.020041	0.026696	0.028332	0.027962	0.007113	0.00232
7	-0.00079	0.000476	-0.00165	0.002898	0.026696	0.036345	0.038447	0.037909	0.008591	0.002316
8	-0.00084	0.000567	-0.00174	0.003148	0.028332	0.038447	0.041764	0.040186	0.009269	0.002574
8A	-0.00079	0.000543	-0.00164	0.003172	0.027962	0.037909	0.040186	0.039701	0.009323	0.002669
11	0.000772	0.001199	0.00108	0.002506	0.007113	0.008591	0.009269	0.009323	0.005271	0.003366
12	0.000909	0.001075	0.001329	0.001805	0.00232	0.002316	0.002574	0.002669	0.003366	0.002786

Correlation matrix										
Bands	**2**	**3**	**4**	**5**	**6**	**7**	**8**	**8A**	**11**	**12**
2	1	0.927338	0.958237	0.684101	-0.09616	-0.16554	-0.16252	-0.15845	0.422476	0.68423
3	0.927338	1	0.889026	0.844248	0.173877	0.091041	0.101184	0.099445	0.602287	0.742989
4	0.958237	0.889026	1	0.694864	-0.17864	-0.25327	-0.24963	-0.24152	0.435596	0.737198
5	0.684101	0.844248	0.694864	1	0.484466	0.387448	0.392663	0.405811	0.87983	0.871774
6	-0.09616	0.173877	-0.17864	0.484466	1	0.989154	0.9793	0.991301	0.692039	0.310479
7	-0.16554	0.091041	-0.25327	0.387448	0.989154	1	0.986804	0.997954	0.620679	0.23017
8	-0.16252	0.101184	-0.24963	0.392663	0.9793	0.986804	1	0.986903	0.624677	0.238663
8A	-0.15845	0.099445	-0.24152	0.405811	0.991301	0.997954	0.986903	1	0.64444	0.253804
11	0.422476	0.602287	0.435596	0.87983	0.692039	0.620679	0.624677	0.64444	1	0.878421
12	0.68423	0.742989	0.737198	0.871774	0.310479	0.23017	0.238663	0.253804	0.878421	1

Eigen vectors										
Bands	**Vector_2**	**Vector_3**	**Vector_4**	**Vector_5**	**Vector_6**	**Vector_7**	**Vector_8**	**Vector_ 8A**	**Vector_ 11**	**Vector_ 12**
2	0.009036	-0.22849	0.397791	-0.19015	0.201618	-0.01661	0.360133	-0.10506	0.122447	0.7461
3	-0.00943	-0.25093	0.453924	-0.19241	-0.05382	-0.07713	0.169003	-0.10831	0.58681	-0.54808
4	0.019892	-0.33271	0.384701	-0.18235	0.252554	-0.09621	-0.01509	0.062297	-0.74056	-0.28651
5	-0.04539	-0.36447	0.161087	-0.12313	-0.47137	-0.16313	-0.69689	0.160048	0.070717	0.242727
6	-0.37672	-0.07439	-0.07312	-0.28916	-0.59929	0.431452	0.404167	0.133682	-0.19071	-0.02634
7	-0.50876	0.102211	-0.04581	-0.34466	0.318917	0.306135	-0.37495	-0.52205	0.035626	-0.00369
8	-0.54324	0.094343	0.418191	0.71797	-0.05788	-0.00197	-0.0024	-0.00071	-0.04347	0.019274
8A	-0.53236	0.055318	-0.21099	-0.26295	0.230928	-0.54014	0.09538	0.484673	0.103892	-0.0004
11	-0.12869	-0.57044	-0.4348	0.218266	-0.10853	-0.34162	0.193471	-0.50167	-0.05844	-0.0184
12	-0.03922	-0.53661	-0.21418	0.209156	0.375714	0.519214	-0.07339	0.413218	0.183012	-0.02276

PC	**Eigen values**	**Accounted variance**	**Cum. variance**	**PC**	**Eigen values**	**Accounted variance**	**Cum. variance**
1	0.13953	93.02001	93.02001	**6**	7.57E-05	0.050487	99.91038
2	0.008457	5.638034	98.65805	**7**	5.94E-05	0.039622	99.95
3	0.000798	0.531954	99.19	**8**	3.64E-05	0.024286	99.97429
4	0.000719	0.47946	99.66946	**9**	2.38E-05	0.015841	99.99013
5	0.000286	0.190434	99.8599	**10**	1.48E-05	0.00987	100

Appendix H: Distribution of 2016 meadow-bird territories/nests vs. grassland management

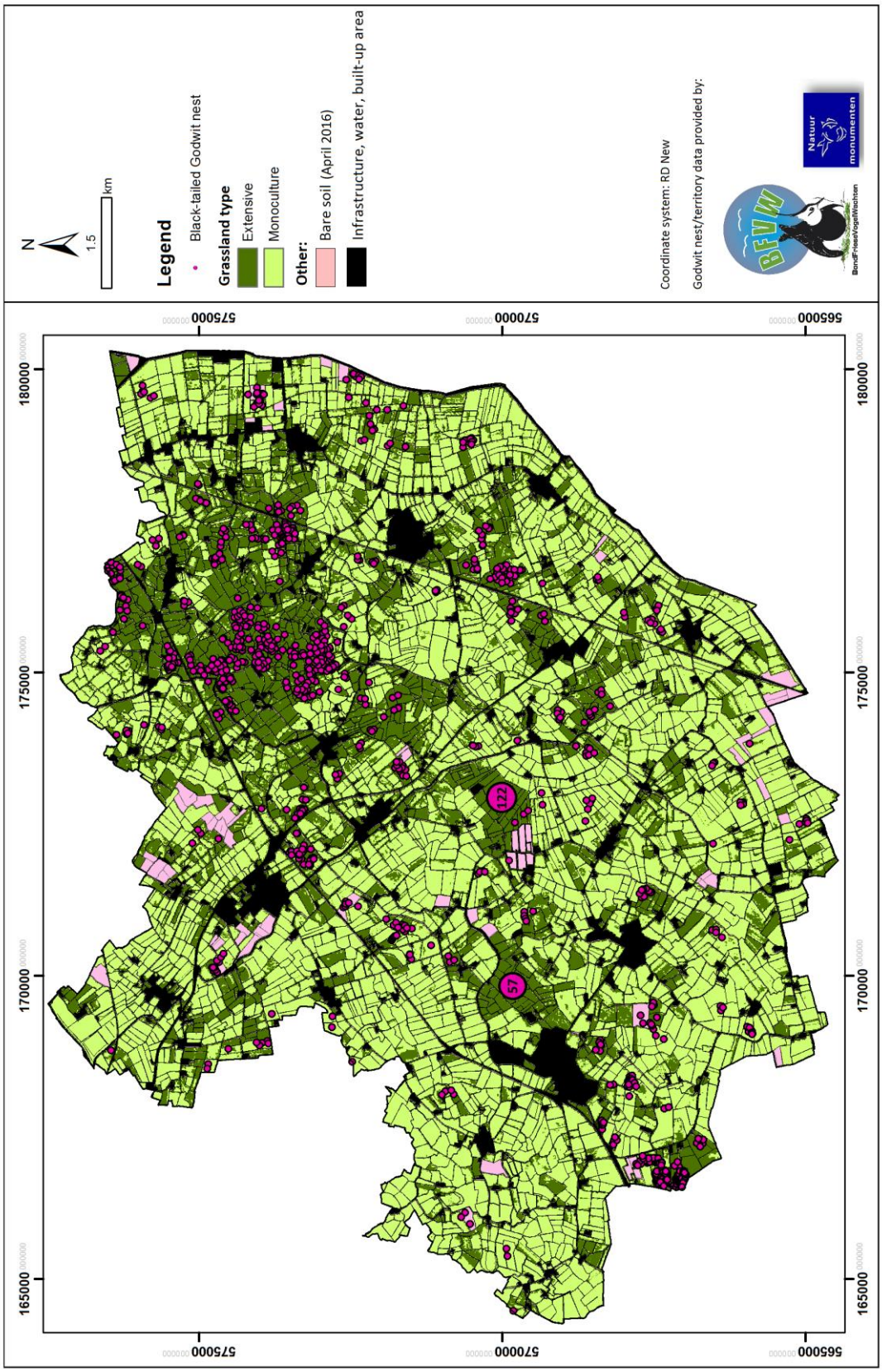

Black-tailed Godwit nest distribution vs. grassland management (Nest distribution data for Littenseradiel from: Bond Friese Vogel Wachten 2016; nr. of territories for Skrok and Skrins from: De Boer and De Winter 2016).

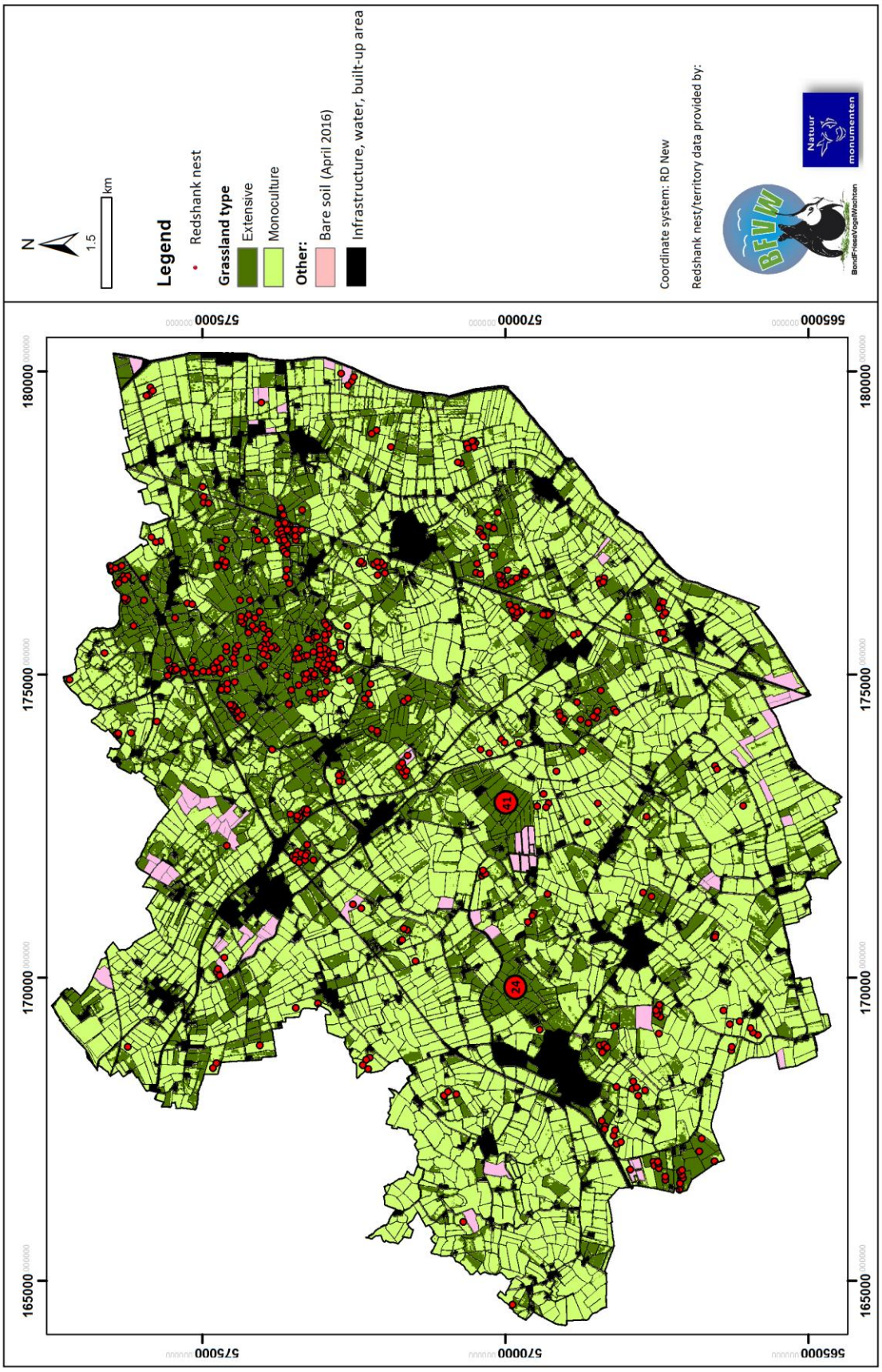

Redshank nest distribution vs. grassland management (Nest distribution data for Littenseradiel from: Bond Friese Vogel Wachten 2016; nr. of territories for Skrok and Skrins from: De Boer and De Winter 2016).

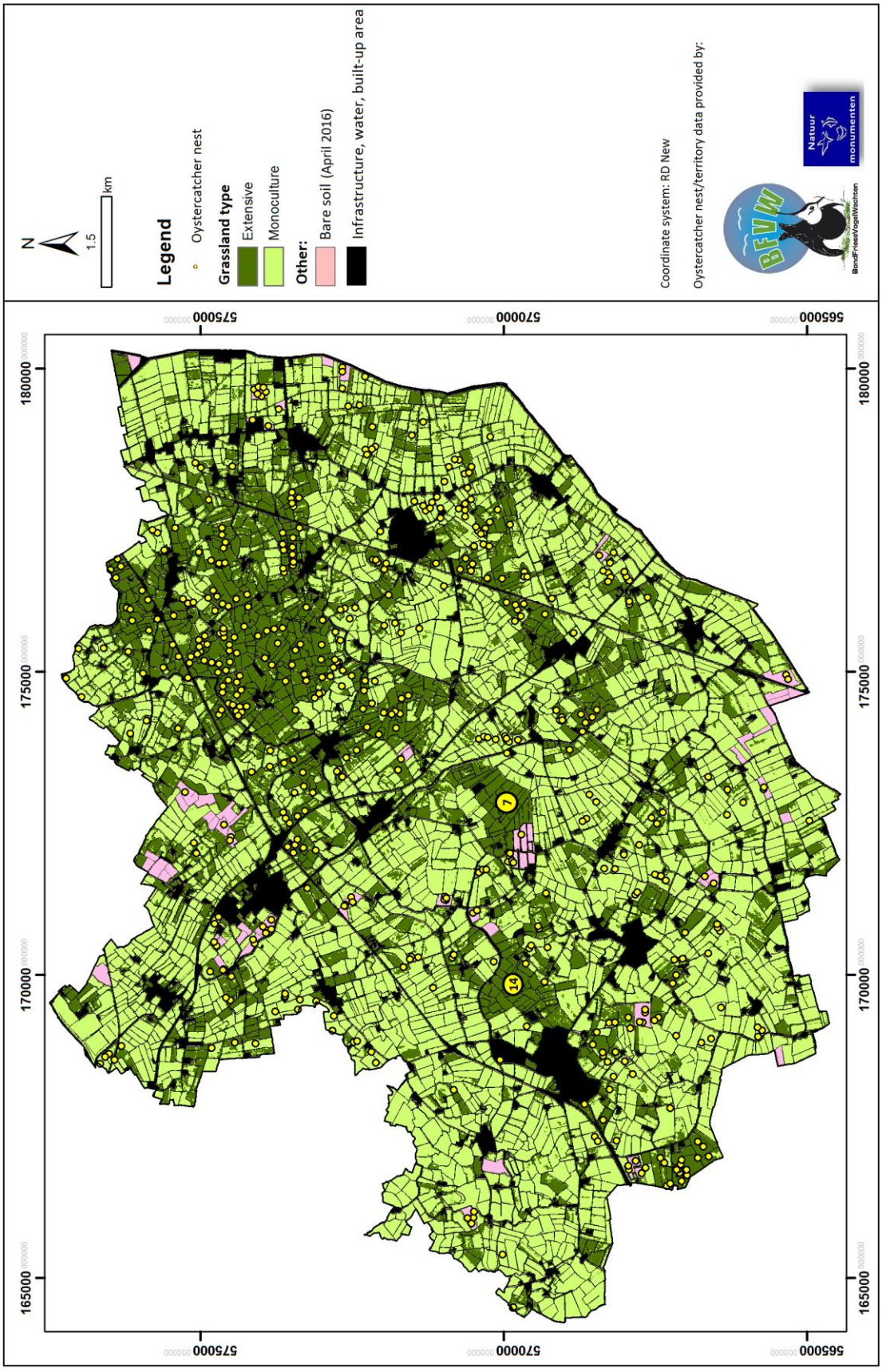

Oystercatcher nest distribution vs. grassland management (Nest distribution data for Littenseradiel from: Bond Friese Vogel Wachten 2016; nr. of territories for Skrok and Skrins from: De Boer and De Winter 2016).

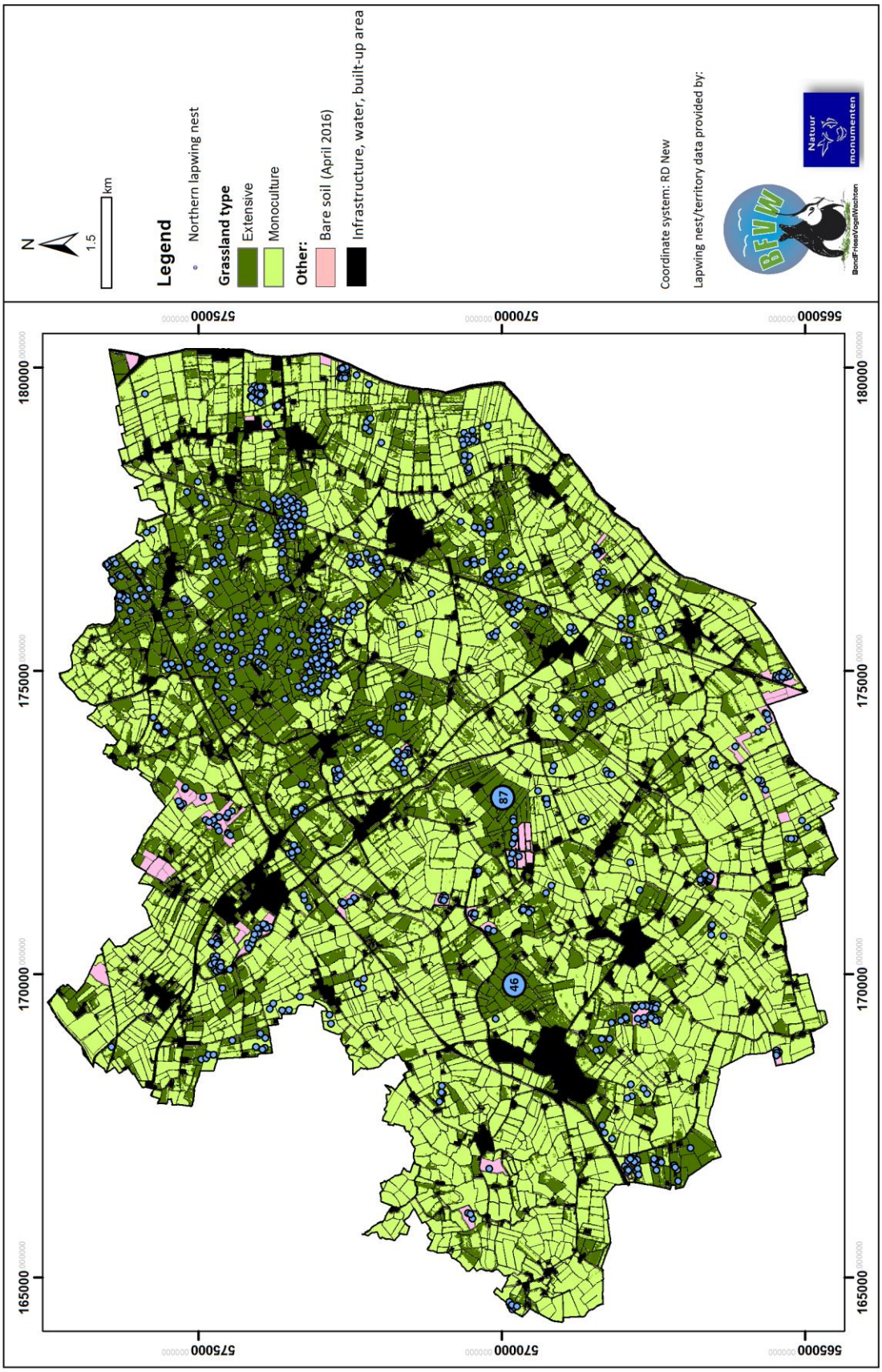

Northern Lapwing nest distribution vs. grassland management (Nest distribution data for Littenseradiel from: Bond Friese Vogel Wachten 2016; nr. of territories for Skrok and Skrins from: De Boer and De Winter 2016).

Appendix I: Mowing map for Littenseradiel

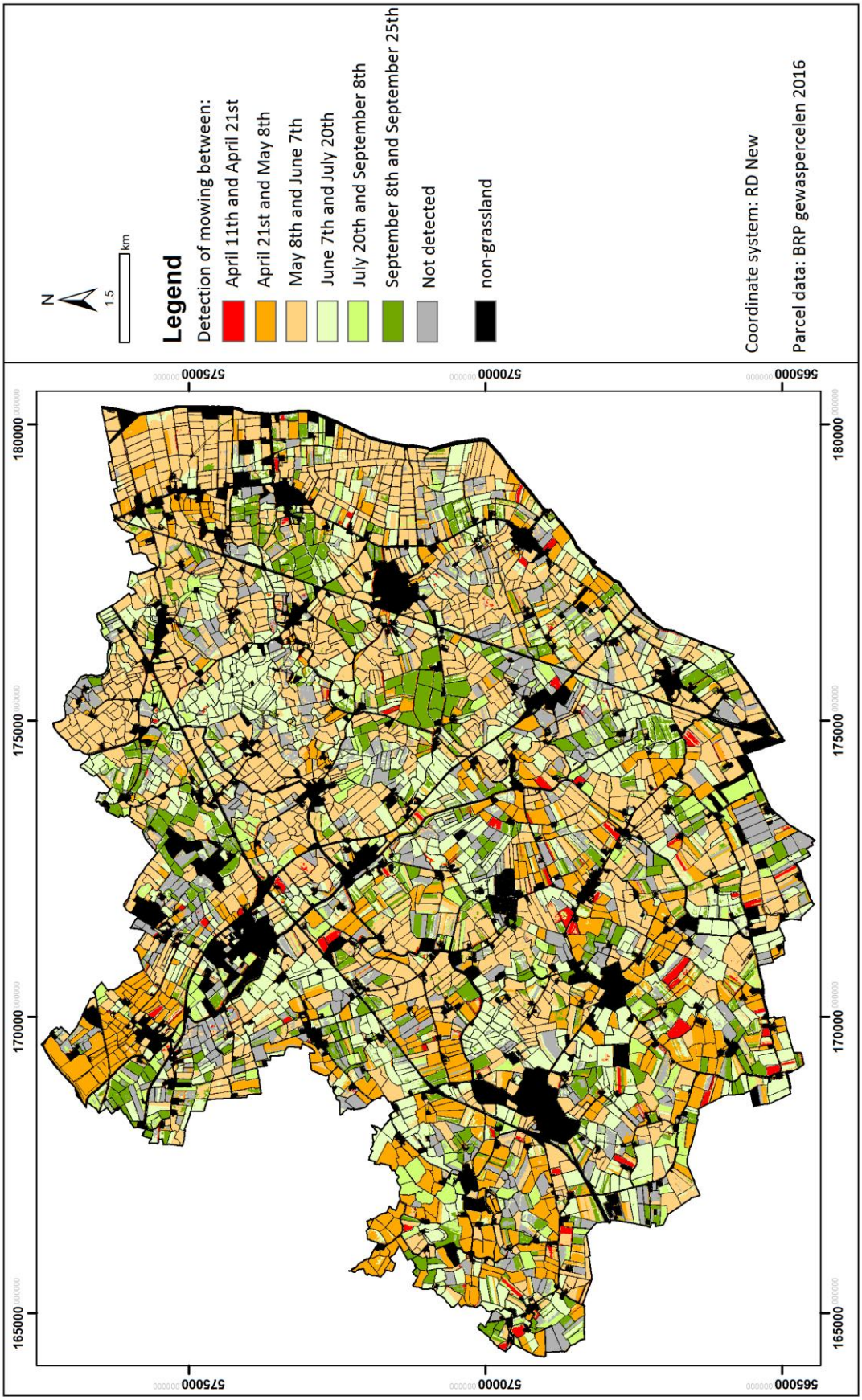

NDVI Statistics for Littenseradiel Clay soils																		
Date	12-Mar		1-Apr		11-Apr		21-Apr		8-May		7-Jun		20-Jul		8-Sep		25-Sep	
Grassland	Ext	Mono	Ext	Mono	Ext	Mono	Ext	Mono	Ext	Mono	Ext	Mono	Ext	Mono	Ext	Mono	Ext	Mono
Min	0.443	0.552	0.365	0.560	0.560	0.604	0.566	0.678	0.415	0.238	0.504	0.203	0.318	0.376	0.340	0.593	0.191	0.516
1st quartile	0.748	0.825	0.709	0.803	0.835	0.936	0.869	0.956	0.881	0.766	0.850	0.731	0.571	0.772	0.782	0.774	0.742	0.770
Median	0.797	0.855	0.769	0.834	0.882	0.953	0.903	0.965	0.908	0.838	0.888	0.818	0.679	0.877	0.839	0.872	0.792	0.827
3d quartile	0.836	0.873	0.807	0.856	0.911	0.964	0.926	0.971	0.927	0.946	0.916	0.926	0.799	0.916	0.884	0.912	0.838	0.859
Max	0.909	0.911	0.861	0.907	0.947	0.979	0.962	0.986	0.964	0.974	0.962	0.971	0.943	0.961	0.930	0.943	0.925	0.912
Mean	0.783	0.842	0.748	0.823	0.864	0.941	0.888	0.956	0.894	0.836	0.868	0.793	0.670	0.822	0.805	0.834	0.782	0.802
SD	0.073	0.047	0.074	0.053	0.065	0.044	0.057	0.033	0.057	0.113	0.078	0.154	0.159	0.132	0.105	0.093	0.078	0.080
Variance	0.0053	0.0022	0.0055	0.0028	0.0042	0.0020	0.0033	0.0011	0.0032	0.0127	0.0061	0.0237	0.0252	0.0173	0.0111	0.0086	0.0062	0.0065
Shapiro-Wilk test (normality test)																		
W	0.912	0.840	0.912	0.877	0.874	0.614	0.829	0.571	0.695	0.897	0.737	0.878	0.969	0.804	0.841	0.867	0.911	0.871
p-value	< 0.0001	< 0.0001	< 0.0001	< 0.0001	< 0.0001	< 0.0001	< 0.0001	< 0.0001	< 0.0001	< 0.0001	< 0.0001	< 0.0001	< 0.0001	< 0.0001	< 0.0001	< 0.0001	< 0.0001	< 0.0001
alpha	0.05	0.05	0.05	0.05	0.05	0.05	0.05	0.05	0.05	0.05	0.05	0.05	0.05	0.05	0.05	0.05	0.05	0.05
Two-sample Kolmogorov-Smirnov test (Compare distributions Ext vs. Mono)																		
D	0.436		0.539		0.745		0.790		0.422		0.369		0.461		0.250		0.201	
p-value	< 0.0001		< 0.0001		< 0.0001		< 0.0001		< 0.0001		< 0.0001		< 0.0001		< 0.0001		< 0.0001	
alpha	0.05		0.05		0.05		0.05		0.05		0.05		0.05		0.05		0.05	
Mann-Whitney U test (Compare mean NDVI Ext vs. Mono)																		
U	34424.500		26927.500		13214.500		10749.000		94222.000		94095.000		34585.000		62099.500		63892.000	
Expected	79600.000		79600.000		79600.000		79600.000		79600.000		75438.000		79600.000		79600.000		79600.000	
Variance	10600066.542		10600066.542		10600066.416		10600066.542		10600066.667		9781794.000		10600066.667		10600066.542		10600066.416	
p-value	< 0.0001		< 0.0001		< 0.0001		< 0.0001		< 0.0001		< 0.0001		< 0.0001		< 0.0001		< 0.0001	
alpha	0.05		0.05		0.05		0.05		0.05		0.05		0.05		0.05		0.05	

NDVI Statistics for Grouw Peat soils																		
Date	12-Mar		1-Apr		11-Apr		21-Apr		8-May		7-Jun		20-Jul		8-Sep		25-Sep	
Grassland	Ext	Mono	Ext	Mono	Ext	Mono	Ext	Mono	Ext	Mono	Ext	Mono	Ext	Mono	Ext	Mono	Ext	Mono
Min	0.380	0.638	0.314	0.683	0.359	0.750	0.336	0.818	0.271	0.503	0.165	0.165	0.088	0.451	0.276	0.368	0.119	0.299
1st quartile	0.623	0.777	0.538	0.784	0.654	0.907	0.684	0.939	0.733	0.896	0.818	0.674	0.538	0.666	0.751	0.841	0.761	0.765
Median	0.704	0.821	0.712	0.819	0.839	0.927	0.856	0.952	0.873	0.937	0.889	0.809	0.745	0.824	0.852	0.892	0.829	0.845
3d quartile	0.761	0.853	0.762	0.840	0.887	0.941	0.906	0.960	0.914	0.948	0.921	0.903	0.867	0.897	0.889	0.909	0.878	0.892
Max	0.870	0.998	0.849	0.906	0.946	0.968	0.956	0.973	0.960	0.968	0.968	0.978	0.939	0.971	0.927	0.945	0.929	0.937
Mean	0.686	0.812	0.654	0.810	0.767	0.921	0.784	0.947	0.810	0.897	0.840	0.775	0.696	0.780	0.798	0.860	0.793	0.813
SD	0.103	0.057	0.138	0.041	0.152	0.029	0.158	0.021	0.144	0.088	0.130	0.163	0.189	0.138	0.131	0.084	0.133	0.102
Variance	0.0105	0.0033	0.0192	0.0017	0.0231	0.0008	0.0249	0.0004	0.0209	0.0077	0.0168	0.0266	0.0357	0.0190	0.0171	0.0070	0.0177	0.0104
Shapiro-Wilk test (normality test)																		
W	0.953	0.973	0.894	0.976	0.861	0.898	0.839	0.810	0.822	0.686	0.746	0.918	0.916	0.911	0.797	0.731	0.727	0.846
p-value	< 0.0001	< 0.0001	< 0.0001	< 0.0001	< 0.0001	< 0.0001	< 0.0001	< 0.0001	< 0.0001	< 0.0001	< 0.0001	< 0.0001	< 0.0001	< 0.0001	< 0.0001	< 0.0001	< 0.0001	< 0.0001
alpha	0.05	0.05	0.05	0.05	0.05	0.05	0.05	0.05	0.05	0.05	0.05	0.05	0.05	0.05	0.05	0.05	0.05	0.05
Two-sample Kolmogorov-Smirnov test (Compare distributions Ext vs. Mono)																		
D	0.575		0.628		0.678		0.790		0.508		0.278		0.200		0.300		0.110	
p-value	< 0.0001		< 0.0001		< 0.0001		< 0.0001		< 0.0001		< 0.0001		< 0.0001		< 0.0001		0.016	
alpha	0.05		0.05		0.05		0.05		0.05		0.05		0.05		0.05		0.05	
Mann-Whitney U test (Compare mean NDVI Ext vs. Mono)																		
U	20374.000		16368.000		13594.000		6072.000		36567.000		98755.500		58764.500		50725.000		71705.000	
Expected	80000.000		80000.000		80000.000		80000.000		80000.000		80000.000		80000.000		80000.000		80000.000	
Variance	10680000.000		10679999.875		10679999.875		10680000.000		10680000.000		10679999.875		10679999.875		10679999.875		10680000.000	
p-value	< 0.0001		< 0.0001		< 0.0001		< 0.0001		< 0.0001		< 0.0001		< 0.0001		< 0.0001		0.011	
alpha	0.05		0.05		0.05		0.05		0.05		0.05		0.05		0.05		0.05	

NDVI Clay soils vs. peat soils Extensive									
Date	12-Mar	1-Apr	11-Apr	21-Apr	8-May	7-Jun	20-Jul	8-Sep	25-Sep
Two-sample Kolmogorov-Smirnov test (Compare distributions Clay vs. Peat) Extensive									
D	0.479	0.295	0.310	0.327	0.314	0.115	0.191	0.076	0.221
p-value	< 0.0001	< 0.0001	< 0.0001	< 0.0001	< 0.0001	0.012	< 0.0001	0.196	< 0.0001
alpha	0.05	0.05	0.05	0.05	0.05	0.05	0.05	0.05	0.05
Mann-Whitney U test (Compare mean NDVI Clay vs. Peat) Extensive									
U	126553.000	112981.000	109960.000	113112.500	107484.500	77719.500	70373.000	76842.000	60560.000
Expected	79600.000	79600.000	79600.000	79600.000	79600.000	76200.000	79600.000	79600.000	79600.000
Variance	10600066.667	10600066.667	10600066.667	10600066.542	10600066.542	9931399.875	10600066.667	10600066.667	10600066.416
p-value	< 0.0001	< 0.0001	< 0.0001	< 0.0001	< 0.0001	0.630	0.005	0.397	< 0.0001
alpha	0.05	0.05	0.05	0.05	0.05	0.05	0.05	0.05	0.05
NDVI Clay soils vs. peat soils Monoculture									
Two-sample Kolmogorov-Smirnov test (Compare distributions Clay vs. Peat) Monoculture									
D	0.290	0.205	0.475	0.423	0.353	0.098	0.183	0.185	0.260
p-value	< 0.0001	< 0.0001	< 0.0001	< 0.0001	< 0.0001	0.044	< 0.0001	< 0.0001	< 0.0001
alpha	0.05	0.05	0.05	0.05	0.05	0.05	0.05	0.05	0.05
Mann-Whitney U test (Compare mean NDVI Clay vs. Peat) Monoculture									
U	108810.000	99275.500	124713.000	119181.000	58912.500	83136.000	94834.000	69288.500	65004.000
Expected	80000.000	80000.000	80000.000	80000.000	80000.000	79200.000	80000.000	80000.000	80000.000
Variance	10680000.000	10679999.750	10679999.750	10679999.625	10679999.875	10520400.000	10680000.000	10679999.750	10680000.000
p-value	< 0.0001	< 0.0001	< 0.0001	< 0.0001	< 0.0001	0.225	< 0.0001	0.001	< 0.0001
alpha	0.05	0.05	0.05	0.05	0.05	0.05	0.05	0.05	0.05

S2REP statistics for Littenseradiel Clay soils																		
Date	12-Mar		1-Apr		11-Apr		21-Apr		8-May		7-Jun		20-Jul		8-Sep		25-Sep	
Grassland	Ext	Mono	Ext	Mono	Ext	Mono	Ext	Mono	Ext	Mono	Ext	Mono	Ext	Mono	Ext	Mono	Ext	Mono
Min	700.678	714.339	716.667	720.619	707.147	720.458	707.962	719.858	709.239	707.081	708.372	697.454	700.540	704.350	711.878	711.904	711.413	712.529
1st quartile	715.010	719.436	721.267	724.595	719.371	725.048	720.077	726.651	720.518	719.145	721.884	718.415	716.032	719.859	718.642	719.607	717.826	719.324
Median	716.560	720.288	722.103	725.297	720.633	726.043	721.268	727.785	721.536	721.280	722.733	720.363	717.849	722.500	720.089	722.287	718.962	720.551
3d quartile	717.789	720.939	722.785	726.186	721.531	727.160	722.237	728.475	722.681	725.587	723.396	724.347	719.736	723.509	721.234	724.258	720.052	721.329
Max	727.434	723.431	727.085	728.849	724.417	730.055	725.929	730.539	725.753	729.362	726.112	726.649	728.706	726.115	724.568	728.389	723.783	725.771
Mean	716.208	720.110	722.043	725.391	720.236	725.957	721.035	727.488	721.389	721.462	722.267	720.204	717.278	721.078	719.521	721.556	718.951	720.186
SD	2.532	1.244	1.334	1.194	2.216	1.481	1.884	1.433	1.851	4.395	2.216	4.597	3.857	4.013	2.548	3.547	1.757	2.155
Variance	6.413	1.548	1.780	1.426	4.911	2.194	3.549	2.055	3.426	19.315	4.911	21.136	14.875	16.103	6.494	12.578	3.086	4.644
Shapiro-Wilk test (normality test)																		
W	0.912	0.960	0.985	0.991	0.853	0.977	0.887	0.923	0.911	0.922	0.721	0.917	0.911	0.829	0.917	0.931	0.989	0.941
p-value	< 0.0001	< 0.0001	0.000	0.015	< 0.0001	< 0.0001	< 0.0001	< 0.0001	< 0.0001	< 0.0001	< 0.0001	< 0.0001	< 0.0001	< 0.0001	< 0.0001	< 0.0001	0.004	< 0.0001
alpha	0.05	0.05	0.05	0.05	0.05	0.05	0.05	0.05	0.05	0.05	0.05	0.05	0.05	0.05	0.05	0.05	0.05	0.05
Two-sample Kolmogorov-Smirnov test (Compare distributions Ext vs. Mono)																		
D	0.769		0.859		0.930		0.972		0.357		0.429		0.604		0.435		0.376	
p-value	< 0.0001		< 0.0001		< 0.0001		< 0.0001		< 0.0001		< 0.0001		< 0.0001		< 0.0001		< 0.0001	
alpha	0.05		0.05		0.05		0.05		0.05		0.05		0.05		0.05		0.05	
Mann-Whitney U test (Compare mean NDVI Ext vs. Mono)																		
U	7806.500		4619.000		1256.000		845.000		75278.000		96309.000		31153.000		46152.000		46142.000	
Expected	79000.000		79400.000		79200.000		79200.000		79000.000		75438.000		79600.000		79600.000		79600.000	
Variance	10480666.166		10560200.000		10520399.625		10520399.499		10480666.542		9781793.500		10600066.667		10600066.542		10600066.416	
p-value	< 0.0001		< 0.0001		< 0.0001		< 0.0001		0.250		< 0.0001		< 0.0001		< 0.0001		< 0.0001	
alpha	0.05		0.05		0.05		0.05		0.05		0.05		0.05		0.05		0.05	

S2REP statistics for Grouw Peat soils																		
Date	12-Mar		1-Apr		11-Apr		21-Apr		8-May		7-Jun		20-Jul		8-Sep		25-Sep	
Grassland	Ext	Mono	Ext	Mono	Ext	Mono	Ext	Mono	Ext	Mono	Ext	Mono	Ext	Mono	Ext	Mono	Ext	Mono
Min	691.360	712.106	713.472	719.106	694.182	716.642	694.114	718.159	697.406	700.683	707.063	703.343	697.542	708.277	710.862	711.257	700.894	706.416
1st quartile	713.060	717.639	720.844	722.821	713.725	723.102	715.546	725.136	717.096	723.144	720.006	717.856	715.549	717.486	719.066	720.773	718.874	719.016
Median	715.406	719.003	722.200	723.664	719.328	724.068	720.235	726.053	720.744	725.725	721.850	720.713	719.269	720.628	720.448	722.343	719.965	720.801
3d quartile	717.029	720.258	723.715	724.442	720.976	724.912	722.017	726.958	722.313	726.645	723.460	723.426	720.832	722.568	721.729	723.448	720.994	722.149
Max	731.833	722.655	737.334	732.021	732.759	728.197	735.116	731.940	726.701	728.450	735.000	728.576	736.945	727.083	733.756	733.404	738.956	733.072
Mean	714.274	718.828	722.971	723.609	717.006	724.017	718.381	725.986	719.535	724.272	721.462	719.972	718.011	719.862	720.188	721.925	719.782	720.331
SD	4.802	1.815	3.764	1.378	6.161	1.448	5.223	1.579	4.012	3.681	3.538	4.417	4.396	3.817	2.185	2.639	2.538	2.829
Variance	23.056	3.293	14.170	1.900	37.955	2.097	27.280	2.494	16.100	13.553	12.514	19.508	19.323	14.569	4.776	6.963	6.441	8.003
Shapiro-Wilk test (normality test)																		
W	0.860	0.978	0.885	0.966	0.863	0.985	0.886	0.978	0.879	0.776	0.932	0.950	0.919	0.960	0.929	0.932	0.759	0.939
p-value	< 0.0001	< 0.0001	< 0.0001	< 0.0001	< 0.0001	0.000	< 0.0001	< 0.0001	< 0.0001	< 0.0001	< 0.0001	< 0.0001	< 0.0001	< 0.0001	< 0.0001	< 0.0001	< 0.0001	< 0.0001
alpha	0.05	0.05	0.05	0.05	0.05	0.05	0.05	0.05	0.05	0.05	0.05	0.05	0.05	0.05	0.05	0.05	0.05	0.05
Two-sample Kolmogorov-Smirnov test (Compare distributions Ext vs. Mono)																		
D	0.583		0.393		0.821		0.875		0.673		0.206		0.247		0.437		0.252	
p-value	< 0.0001		< 0.0001		< 0.0001		< 0.0001		< 0.0001		< 0.0001		< 0.0001		< 0.0001		< 0.0001	
alpha	0.05		0.05		0.05		0.05		0.05		0.05		0.05		0.05		0.05	
Mann-Whitney U test (Compare mean NDVI Ext vs. Mono)																		
U	21370.000		50253.000		7022.000		3381.000		24459.000		93328.000		57940.000		41118.000		63308.000	
Expected	79200.000		79200.000		79200.000		79800.000		80000.000		79600.500		79800.000		79800.000		79800.000	
Variance	10520399.875		10520399.249		10520399.625		10639999.249		10680000.000		10600133.125		10639999.875		10639999.374		10639999.249	
p-value	< 0.0001		< 0.0001		< 0.0001		< 0.0001		< 0.0001		< 0.0001		< 0.0001		< 0.0001		< 0.0001	
alpha	0.05		0.05		0.05		0.05		0.05		0.05		0.05		0.05		0.05	

S2REP Clay soils vs. peat soils Extensive									
Date	12-Mar	1-Apr	11-Apr	21-Apr	8-May	7-Jun	20-Jul	8-Sep	25-Sep
Two-sample Kolmogorov-Smirnov test (Compare distributions Clay vs. Peat) Extensive									
D	0.219	0.187	0.285	0.295	0.256	0.267	0.208	0.105	0.245
p-value	< 0.0001	< 0.0001	< 0.0001	< 0.0001	< 0.0001	< 0.0001	< 0.0001	0.025	< 0.0001
alpha	0.05	0.05	0.05	0.05	0.05	0.05	0.05	0.05	0.05
Mann-Whitney U test (Compare mean S2REP Clay vs. Peat) Extensive									
U	98735.500	74162.500	104051.500	101158.000	98290.000	92050.000	66074.500	68940.000	54582.500
Expected	78210.000	78606.000	78408.000	79002.000	79000.000	76009.500	79401.000	79401.000	79401.000
Variance	10323718.999	10402193.374	10362923.625	10480930.373	10480666.416	9893902.625	10560332.750	10560333.000	10560331.999
p-value	< 0.0001	0.168	< 0.0001	< 0.0001	< 0.0001	< 0.0001	< 0.0001	0.001	< 0.0001
alpha	0.05	0.05	0.05	0.05	0.05	0.05	0.05	0.05	0.05
S2REP Clay soils vs. peat soils Monoculture									
Two-sample Kolmogorov-Smirnov test (Compare distributions Clay vs. Peat) Monoculture									
D	0.360	0.568	0.535	0.450	0.343	0.087	0.248	0.160	0.173
p-value	< 0.0001	< 0.0001	< 0.0001	< 0.0001	< 0.0001	0.099	< 0.0001	< 0.0001	< 0.0001
alpha	0.05	0.05	0.05	0.05	0.05	0.05	0.05	0.05	0.05
Mann-Whitney U test (Compare mean S2REP Clay vs. Peat) Monoculture									
U	114194.000	136515.000	133132.500	124727.000	45512.000	82083.000	100432.500	80880.000	73892.500
Expected	80000.000	80000.000	80000.000	80000.000	80000.000	79002.000	80000.000	80000.000	80000.000
Variance	10679999.875	10679999.750	10679999.374	10679999.750	10679999.625	10480932.000	10679999.875	10679998.373	10679999.499
p-value	< 0.0001	< 0.0001	< 0.0001	< 0.0001	< 0.0001	0.341	< 0.0001	0.788	0.062
alpha	0.05	0.05	0.05	0.05	0.05	0.05	0.05	0.05	0.05

MASD	Littenseradiel (clay soils)				Grouw (peat soils)				Clay vs. Peat				Clay vs. Peat			
Date	MASD4_spring		MASD7_total		MASD_4Spring		MASD7_total		MASD_4spring		MASD_4Spring		MASD7_total		MASD7_total	
Grassland	Ext	Mono	Ext	Mono	Ext	Mono	Ext	Mono	Ext	Ext	Mono	Mono	Ext	Ext	Mono	Mono
Min	0.012	0.019	0.017	0.016	0.011	0.015	0.014	0.019	0.012	0.011	0.019	0.015	0.017	0.014	0.016	0.019
1st quartile	0.045	0.072	0.079	0.101	0.054	0.075	0.076	0.098	0.045	0.054	0.072	0.075	0.079	0.076	0.101	0.098
Median	0.021	0.038	0.030	0.041	0.020	0.034	0.030	0.038	0.021	0.020	0.038	0.034	0.030	0.030	0.041	0.038
3d quartile	0.025	0.042	0.037	0.050	0.025	0.040	0.037	0.047	0.025	0.025	0.042	0.040	0.037	0.037	0.050	0.047
Max	0.029	0.047	0.044	0.060	0.030	0.045	0.046	0.059	0.029	0.030	0.047	0.045	0.044	0.046	0.060	0.059
Mean	0.026	0.043	0.038	0.051	0.026	0.040	0.038	0.050	0.026	0.026	0.043	0.040	0.038	0.038	0.051	0.050
SD	0.006	0.009	0.011	0.014	0.007	0.009	0.012	0.015	0.006	0.007	0.009	0.009	0.011	0.012	0.014	0.015
Variance	0.000	0.000	0.000	0.000	0.000	0.000	0.000	0.000	0.000	0.000	0.000	0.000	0.000	0.000	0.000	0.000
Shapiro-Wilk test (normality test)																
W	0.966	0.953	0.969	0.983	0.976	0.961	0.987	0.978	0.966	0.976	0.953	0.961	0.969	0.987	0.983	0.978
p-value	< 0.0001	< 0.0001	< 0.0001	0.000	< 0.0001	< 0.0001	0.002	< 0.0001	< 0.0001	< 0.0001	< 0.0001	< 0.0001	< 0.0001	0.002	0.000	< 0.0001
alpha	0.05	0.05	0.05	0.05	0.05	0.05	0.05	0.05	0.05	0.05	0.05	0.05	0.05	0.05	0.05	0.05
Two-sample Kolmogorov-Smirnov test (Compare distributions Ext vs. Mono and Ext vs. Ext, Mono vs. Mono)																
D	0.774		0.444		0.648		0.303		0.090		0.198		0.065		0.123	
p-value	< 0.0001		< 0.0001		< 0.0001		< 0.0001		0.081		< 0.0001		0.372		0.005	
alpha	0.05		0.05		0.05		0.05		0.05		0.05		0.05		0.05	
Mann-Whitney U test (Compare means MASD)																
U	8476.000		34239.000		17238.000		45799.000		77764.500		95549.500		77143.000		87140.000	
Expected	79600.000		79600.000		80000.000		80000.000		79600.000		80000.000		79600.000		80000.000	
Variance	10600064.914		10600065.791		10679997.872		10679999.750		10600063.788		10679995.995		10600065.916		10679999.625	
p-value	< 0.0001		< 0.0001		< 0.0001		< 0.0001		0.573		< 0.0001		0.451		0.029	
alpha	0.05		0.05		0.05		0.05		0.05		0.05		0.05		0.05	

Mann-Whitney U test (compare mean reflectance)(alpha=0.05)						
Band nr.	Clay ext vs. Clay mono	Peat ext vs. Peat mono	Clay ext vs. Peat ext	Clay ext vs. Peat mono	Clay mono vs. Peat mono	Clay mono vs. Peat ext
March 12th 2016						
2	< 0.0001	< 0.0001	< 0.0001	< 0.0001	0.354	< 0.0001
3	0.002	0.011	< 0.0001	< 0.0001	< 0.0001	< 0.0001
4	< 0.0001	< 0.0001	0.162	< 0.0001	0.154	< 0.0001
5	< 0.0001	< 0.0001	< 0.0001	< 0.0001	< 0.0001	< 0.0001
6	< 0.0001	< 0.0001	< 0.0001	0.136	< 0.0001	< 0.0001
7	< 0.0001	< 0.0001	< 0.0001	0.000	< 0.0001	< 0.0001
8	< 0.0001	< 0.0001	< 0.0001	0.005	< 0.0001	< 0.0001
8A	< 0.0001	< 0.0001	< 0.0001	< 0.0001	< 0.0001	< 0.0001
11	< 0.0001	< 0.0001	< 0.0001	< 0.0001	< 0.0001	< 0.0001
12	< 0.0001	< 0.0001	< 0.0001	< 0.0001	0.612	< 0.0001
April 1st 2016						
2	< 0.0001	< 0.0001	0.862	< 0.0001	< 0.0001	< 0.0001
3	< 0.0001	< 0.0001	< 0.0001	< 0.0001	< 0.0001	0.028
4	< 0.0001	< 0.0001	0.128	< 0.0001	0.001	< 0.0001
5	< 0.0001	0.014	< 0.0001	< 0.0001	< 0.0001	< 0.0001
6	< 0.0001	< 0.0001	< 0.0001	0.251	< 0.0001	< 0.0001
7	< 0.0001	< 0.0001	< 0.0001	< 0.0001	< 0.0001	< 0.0001
8	< 0.0001	< 0.0001	< 0.0001	0.023	< 0.0001	< 0.0001
8A	< 0.0001	< 0.0001	< 0.0001	< 0.0001	< 0.0001	< 0.0001
11	0.734	< 0.0001	0.325	< 0.0001	< 0.0001	0.331
12	< 0.0001	0.004	0.013	< 0.0001	< 0.0001	< 0.0001
April 11th 2016						
2	< 0.0001	< 0.0001	0.523	< 0.0001	< 0.0001	< 0.0001
3	< 0.0001	< 0.0001	< 0.0001	< 0.0001	< 0.0001	< 0.0001
4	< 0.0001	< 0.0001	< 0.0001	< 0.0001	< 0.0001	< 0.0001
5	< 0.0001	< 0.0001	< 0.0001	< 0.0001	< 0.0001	< 0.0001
6	< 0.0001	< 0.0001	< 0.0001	0.008	< 0.0001	< 0.0001
7	< 0.0001	< 0.0001	< 0.0001	< 0.0001	< 0.0001	< 0.0001
8	< 0.0001	< 0.0001	< 0.0001	< 0.0001	< 0.0001	< 0.0001
8A	< 0.0001	< 0.0001	< 0.0001	< 0.0001	< 0.0001	< 0.0001
11	< 0.0001	0.476	0.005	< 0.0001	< 0.0001	< 0.0001
12	< 0.0001	< 0.0001	0.017	< 0.0001	< 0.0001	< 0.0001
April 21st 2016						
2	< 0.0001	< 0.0001	< 0.0001	< 0.0001	< 0.0001	< 0.0001
3	< 0.0001	< 0.0001	< 0.0001	< 0.0001	< 0.0001	< 0.0001
4	< 0.0001	< 0.0001	< 0.0001	< 0.0001	< 0.0001	< 0.0001
5	< 0.0001	< 0.0001	< 0.0001	< 0.0001	< 0.0001	< 0.0001
6	< 0.0001	< 0.0001	< 0.0001	< 0.0001	0.288	< 0.0001
7	< 0.0001	< 0.0001	< 0.0001	< 0.0001	< 0.0001	< 0.0001
8	< 0.0001	< 0.0001	< 0.0001	< 0.0001	< 0.0001	< 0.0001
8A	< 0.0001	< 0.0001	< 0.0001	< 0.0001	< 0.0001	< 0.0001
11	< 0.0001	< 0.0001	0.001	< 0.0001	< 0.0001	< 0.0001
12	< 0.0001	< 0.0001	< 0.0001	< 0.0001	< 0.0001	< 0.0001
May 8th 2016						
2	< 0.0001	0.304	< 0.0001	< 0.0001	< 0.0001	< 0.0001
3	< 0.0001	0.177	0.058	< 0.0001	< 0.0001	< 0.0001
4	< 0.0001	< 0.0001	< 0.0001	< 0.0001	< 0.0001	0.001
5	< 0.0001	< 0.0001	< 0.0001	< 0.0001	< 0.0001	< 0.0001
6	< 0.0001	< 0.0001	< 0.0001	< 0.0001	0.422	< 0.0001
7	< 0.0001	< 0.0001	< 0.0001	< 0.0001	0.000	< 0.0001
8	< 0.0001	< 0.0001	< 0.0001	< 0.0001	0.088	< 0.0001
8A	< 0.0001	< 0.0001	< 0.0001	< 0.0001	0.416	< 0.0001
11	< 0.0001	< 0.0001	< 0.0001	< 0.0001	< 0.0001	< 0.0001
12	< 0.0001	0.002	< 0.0001	< 0.0001	< 0.0001	< 0.0001

Mann-Whitney U test (compare mean reflectance)(alpha=0.05)						
Band nr.	Clay ext vs. Clay mono	Peat ext vs. Peat mono	Clay ext vs. Peat ext	Clay ext vs. Peat mono	Clay mono vs. Peat mono	Clay mono vs. Peat ext
June 7th 2016						
2	< 0.0001	< 0.0001	0.879	< 0.0001	0.000	< 0.0001
3	< 0.0001	< 0.0001	0.946	< 0.0001	< 0.0001	< 0.0001
4	< 0.0001	< 0.0001	0.111	< 0.0001	0.740	< 0.0001
5	< 0.0001	< 0.0001	< 0.0001	0.004	0.052	< 0.0001
6	< 0.0001	< 0.0001	< 0.0001	< 0.0001	< 0.0001	0.374
7	< 0.0001	0.000	< 0.0001	< 0.0001	< 0.0001	0.478
8	< 0.0001	0.001	< 0.0001	< 0.0001	0.000	0.316
8A	< 0.0001	0.007	< 0.0001	< 0.0001	< 0.0001	0.065
11	< 0.0001	< 0.0001	< 0.0001	< 0.0001	0.059	< 0.0001
12	< 0.0001	< 0.0001	< 0.0001	< 0.0001	0.188	< 0.0001
July 20th 2016						
2	< 0.0001	< 0.0001	< 0.0001	< 0.0001	0.188	< 0.0001
3	< 0.0001	< 0.0001	< 0.0001	< 0.0001	0.801	< 0.0001
4	< 0.0001	< 0.0001	< 0.0001	< 0.0001	0.001	< 0.0001
5	< 0.0001	< 0.0001	< 0.0001	< 0.0001	0.004	< 0.0001
6	< 0.0001	0.001	0.000	0.774	< 0.0001	< 0.0001
7	< 0.0001	< 0.0001	0.032	0.004	< 0.0001	< 0.0001
8	< 0.0001	< 0.0001	0.134	0.013	< 0.0001	< 0.0001
8A	< 0.0001	< 0.0001	0.375	0.001	< 0.0001	< 0.0001
11	< 0.0001	< 0.0001	0.089	< 0.0001	< 0.0001	< 0.0001
12	< 0.0001	< 0.0001	0.857	< 0.0001	< 0.0001	< 0.0001
September 8th 2016						
2	< 0.0001	< 0.0001	0.001	< 0.0001	< 0.0001	0.223
3	< 0.0001	< 0.0001	< 0.0001	< 0.0001	< 0.0001	0.001
4	< 0.0001	< 0.0001	0.003	< 0.0001	< 0.0001	0.001
5	< 0.0001	< 0.0001	< 0.0001	< 0.0001	0.000	< 0.0001
6	0.909	0.001	0.006	0.490	0.537	0.004
7	0.001	< 0.0001	0.043	< 0.0001	0.695	< 0.0001
8	0.005	< 0.0001	0.010	0.003	0.983	< 0.0001
8A	0.001	< 0.0001	0.014	0.000	0.947	< 0.0001
11	< 0.0001	< 0.0001	0.038	< 0.0001	0.691	< 0.0001
12	< 0.0001	< 0.0001	0.043	< 0.0001	0.672	< 0.0001
September 25th 2016						
2	0.003	0.016	< 0.0001	< 0.0001	< 0.0001	< 0.0001
3	0.320	0.407	< 0.0001	< 0.0001	< 0.0001	< 0.0001
4	< 0.0001	0.036	< 0.0001	< 0.0001	< 0.0001	< 0.0001
5	< 0.0001	0.001	< 0.0001	< 0.0001	< 0.0001	< 0.0001
6	< 0.0001	0.272	0.079	0.479	< 0.0001	< 0.0001
7	< 0.0001	0.053	0.575	0.174	0.001	< 0.0001
8	< 0.0001	0.060	0.875	0.088	0.026	< 0.0001
8A	< 0.0001	0.095	0.814	0.172	0.001	< 0.0001
11	< 0.0001	< 0.0001	< 0.0001	< 0.0001	< 0.0001	0.193
12	< 0.0001	< 0.0001	< 0.0001	< 0.0001	< 0.0001	0.000

Appendix K: Decision rules used for classification in QGIS

Statistical rule-based classification:

1;"raster5" <= 724.0084; "raster3" <= 721.8442

2;"raster5" <= 724.0084; "raster3" > 721.8442; "raster5" > 722.8615

1;"raster5" <= 724.0084; "raster3" > 721.8442; "raster5" <= 722.8615; "raster1" <= 722.9341

2;"raster5" <= 724.0084; "raster3" > 721.8442; "raster5" <= 722.8615; "raster1" > 722.9341

2;"raster5" > 724.0084; "raster4" > 0.9278637

1;"raster5" > 724.0084; "raster4" <= 0.9278637; "raster5" <= 724.6226

1;"raster5" > 724.0084; "raster4" <= 0.9278637; "raster5" > 724.6226; "raster2" <= 0.01505

2;"raster5" > 724.0084; "raster4" <= 0.9278637; "raster5" > 724.6226; "raster2" > 0.01505

(class 1 = extensive; class 2 = monoculture; raster 1 = S2REP 25 September; raster 2 = MASD 21 April-8 May; raster 3 = S2REP 8 September; raster 4 = NDVI 21 April; raster 5 = S2REP 21 April)

Contextual rule-based classification:

2;"raster3" <= -0.1

1;"raster2" <= 724.0084

2;"raster1" > 0.9278637

2;"raster2" > 724.6226

1;"raster2" <= 724.6226

(class 1 = extensive; class 2 = monoculture; raster 1 = NDVI 21 April; raster 2 = S2REP 21 April; raster 3 = NDVI 11 April - 21 April)